THE SMALL GTPASE RAC1 IS A NOVEL BINDING PARTNER OF BCL-2 AND STABILIZES ITS ANTI-APOPTOTIC ACTIVITY

KANG JIA

(B.Sc. (Hons) NUS)

A THESIS SUBMITTED

FOR THE DEGREE OF DOCTOR OF PHILOSOPHY

NUS GRADUATE SCHOOL FOR INTEGRATIVE SCIENCES AND ENGINEERING
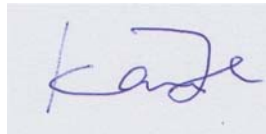
NATIONAL UNIVERSITY OF SINGAPORE

2012

DECLARATION

I hereby declare that the thesis is my original

work and it has been written by me in its

entirety. I have duly acknowledged all the

sources of information which have been used in

the thesis.

This thesis has also not been submitted for any

degree in any university previously.

_____   _____

Kang Jia

24-10-2012

ACKNOWLEDGEMENTS

TABLE OF CONTENTS

SUMMARY

Bcl-2 is best known for its ability to prevent the outer mitochondrial membrane permeabilization through interaction with pro-apoptotic family members leading to inhibition of apoptotic execution. Recently, an alternative paradigm has surfaced that describes Bcl-2 as a redox regulator, conferring survival advantage of cancer cells with Bcl-2 overexpression as compared to their normal counterparts. We have previously demonstrated that a mild but chronic elevation of intracellular O_2^- levels induced by Bcl-2 overexpression in cancer cells would promote a pro-oxidant milieu rendering those cells resistant towards conventional anti-cancer chemotherapies, and a functional involvement of the small GTPase Rac1 was suggested. Here we confirmed that the elevated O_2^- levels at mitochondria are indeed mediated through the activation of Rac1 induced by overexpression of Bcl-2 in chronic myeloid leukaemia cell line model. We also confirmed the existence of a physical interaction between Rac1 and Bcl-2 at the mitochondrial membranes corroborating our previous findings. A further characterization on the binding domains/residues identified five parameters critically required for the interaction, namely 1) the geranylgeranylation of Rac1; 2) the activation of Rac1; 3) the Switch 1 effector loop region (in particular the residue 37) of Rac1; 4) the BH3 domain groove of Bcl-2; 5) the phosphorylation of the flexible loop region (in particular at the residue Ser70) of Bcl-2. In addition, the crosstalk between these parameters where Rac1 activation could induce Bcl-2 phosphorylation at Ser70 through JNK and redox changes, suggests a possible positive feedback loop in enhancing the interaction levels in malignancies with oncogenic Bcl-2. Disruption of the interaction through either the pharmacological inhibitor of Rac1 or siRNA mediated silencing of Rac1 as well as the synthetic Bcl-2 BH3 domain peptides led to a remarkable decrease in O_2^- levels

and sensitized the Bcl-2-overexpressing cancer cells to routine chemotherapeutic agents including etoposide, vincristine and daunorubicin in chronic myeloid leukaemia and cervical cancer models, indicating that this interaction is contributing towards Bcl-2-mediated pro-oxidant state and chemoresistance. Further assessment on the functional relevance of this interaction through computer simulation driven predictive experiments in collaboration with ™CELLWORKS Group Inc., confirmed the pro-oxidant and tumorigenic nature of Rac1-Bcl-2 pathway, corroborating our wet lab experimental data. Interestingly, the transcription factor, STAT3, was identified to positively correlate with the expression levels of Rac1 and Bcl-2. Subsequent preliminary wet lab experiments identified that STAT3 activation as marked by phosphorylation at Tyr705 could be induced by Bcl-2-overexpression, which was mediated through Rac1 activation and O_2^- production, suggesting that STAT3 activation could be a functional readout for Rac1-Bcl-2 interaction leading to transcription of downstream target genes involved in proliferation and survival. These novel findings in understanding the molecular basis for Bcl-2-induced pro-oxidant state has opened a new avenue for future therapeutic design to overcome Bcl-2-mediated chemoresistance, through agents that either disrupt the interaction between Rac1 and Bcl-2 or target their downstream signal transducer STAT3. Indeed, the observations that the Rac1-Bcl-2 interaction was only observed in cancerous cells but not normal tissues lend more weight to the translational relevancy of our study.

LIST OF FIGURES

CHAPTER 3: RESULTS

Figure 36: Combination treatment of Bcl-2 BH3 peptides with conventional chemotherapeutic drugs resulted in a significantly elevated sub-G1 population in Bcl-2-overexpressing cancer cells.

Figure 37: Combination treatment of a pharmacological inhibitor of Rac1 with conventional chemotherapeutic drugs significantly reduced the survival of Bcl-2-overexpressing cancer cells.

Figure 38: siRNA-mediated silencing of Rac1, in combination with conventional chemotherapeutic drugs, significantly reduced the viability of Bcl-2-overexpressing cancer cells.

Figure 39: Combination treatment of Rac1 inhibitor with conventional chemotherapeutic drugs resulted in a significantly elevated sub-G1 population in Bcl-2-overexpressing cancer cells.

Figure 40: Rac1 and/or Bcl-2 overexpression greatly enhanced phenotypic indices on tumourigenesis as predicted by ™CELLWORKS in silico modelling while knocking down of Rac1 or Bcl-2 expression resulted in the opposite.

Figure 41: Rac1 and/or Bcl-2 overexpression greatly enhanced intracellular O_2^- levels as predicted by ™CELLWORKS in silico modelling while knocking down of Rac1 or Bcl-2 expression resulted in the opposite.

Figure 42: Knocking down of Rac1 or Bcl-2 expression greatly elevated the levels of apoptotic markers as predicted by ™CELLWORKS in silico modelling.

Figure 43: Rac1 and/or Bcl-2 overexpression greatly amplified STAT3 protein levels as predicted by ™CELLWORKS in silico modelling while knocking down of Rac1 or Bcl-2 expression resulted in the opposite.

Figure 44: Bcl-2-overexpressing cancer cells have higher phosphorylation levels of mitochondrial STAT3 at Tyr705.

Figure 45: Transient overexpression of Bcl-2 induced STAT3 phosphorylation at Tyr705.

Figure 46: Pharmacological inhibition of Rac1 activity decreased STAT3 phosphorylation levels at Tyr705 in Bcl-2-overexpressing cancer cells.

Figure 47: Pharmacological inhibition of NADPH oxidase activity decreased STAT3 phosphorylation levels at Tyr705 in Bcl-2-overexpressing cancer cells.

Figure 48: Rac1, Bcl-2 and STAT3 co-immunoprecipitated with each other in Bcl-2-overexprssing cancer cells.

Figure 49: Schematic representation of the working model.

LIST OF ABBREVIATIONS

ADP	Adenosine diphosphate
AGER	Receptor for Advanced Glycation End-products
AIF	Apoptosis-inducing factor
AKT	Protein kinase B
ALL	Acute lymphocytic leukaemias
AML	Acute myeloid leukaemia
ANT	Adenine nucleotide translocase
APS	Ammonium persulfate
ATCC	American Type Culture Collection
ATP	Adenosine-5'-triphosphate
Bax	Bcl-2-associated X protein
Bcl-2	B-cell lymphoma 2
Bcl-xL	B-cell lymphoma-extra large
BH	Bcl-2 homology
bp	Base pair
BSA	Bovine serum albumin
CASP	Caspase
Cdc42	Cell division control protein 42 homolog
CDK	Cyclin-dependent kinase
CDKN2A	Cyclin-dependent kinase inhibitor 2A
CLL	Chronic lymphocytic leukaemia
Co-IP	Co-immunoprecipitation
COX	Cytochrome c oxidase
DAB	Diaminobensidine tetrahydrochloride
Dau	Daunorubicin
DMEM	Dulbecco's Modified Eagle's Medium
DMSO	Dimethyl Sulfoxide
DNA	Deoxyribonucleic acid

DTT	Dithiothreitol
DPI	Diphenyleneiodonium Chloride
E.coli	*Escherichia coli*
EDTA	Ethylenediaminetetraacetic acid
EGFR	Epidermal growth factor receptor
EGTA	Ethylene Glycol Tetraacetic Acid
ER	Endoplasmic reticulum
ERK	Extracellular signal-regulated kinase
ETC	Electron transport chain
Eto	Etoposide
FACS	Fluorescence-activated cell sorting
FBS	Fetal Bovine Serum
FITC	Fluorescein isothiocyanate
FKBP	Immunosuppressant FK-506 binding protein
GAP	GTPase-activating protein
GAPDH	Glyceraldehyde-3-phosphate dehydrogenase
GDI	Guanine nucleotide dissociation inhibitor
GDP	Guanosine diphosphate
GEF	Guanine nucleotide exchange factor
GFP	Green fluorescent protein
GGPP	Geranylgeranyl pyrophosphate
GGTase I	Geranylgeranyltransferase I
GGTI	Geranylgeranyltransferase I inhibitor
GMPPNP	Guanosine-5'-($\beta\gamma$-imino) triphosphate
GPX	Glutathione peroxidase
GR	Glutathione reductase
GRX	Glutaredoxin
GSH	Reduced glutathione
GSSG	Oxidised glutathione

GST	Glutathione S-transferase
GTP	Guanosine triphosphate
GTP-γS	Guanosine 5'-O-[gamma-thio] triphosphate
FBS	Fetal bovine serum
HE	Hydroethidine
HEPES	4-(2-hydroxyethyl) piperazine-1-ethanesulfonic acid
HIV	Human Immunodeficiency Virus
HM	Heavy membrane
HRP	Horse radish peroxidase
IB	Immunoblotting
IC_{50}	Inhibitory concentration-50
Ig	Immunoglobulin
IL	Interleukin
JAK	Janus kinase
JNK	c-Jun N-terminal kinase
KD	Knock down
LB	Lysogeny broth
LM	Light membrane
LMW-PTP	Low molecular weight-protein tyrosine phosphatase
MAPK	Mitogen activated protein kinase
MAPKK/MEK	Mitogen activated protein kinase kinase
MAPKKK/MEKK	Mitogen activated protein kinase kinase
MEF	Mouse embryonic fibroblast
MLB	Mg^{2+} Lysis/Wash Buffer
MOMP	Mitochondrial outer membrane permeabilization
mPTP	Mitochondrial permeability transition pore
mRNA	Messenger ribonucleic acid
MTT	3-(4,5-Dimethylthiazol-2-yl)-2,5-diphenyltetrazolium bromide
NADPH	Nicotinamide adenine dinucleotide phosphate

Neo	Neomycin
NF-κB	Nuclear factor κ-light-chain-enhancer of activated B cells
NHE	Na^+/H^+ exchanger
NHL	Non-Hodgkin's lymphoma
NLS	Nuclear localization signal
NMR	Nuclear magnetic resonance
Nox	NADPH oxidase
NSCLC	Non-small cell lung cancer
OD	Optical density
O/E	Overexpression
PAK1 PBD	p21-activated kinase 1 p21-binding domain
PARP	Poly ADP ribose polymerase
PBMC	Peripheral blood mononuclear cell
PBR	Polybasic region
PBS	Phosphate buffered saline
Phox	Phagocyte Nox
PI	Propidium Iodide
PIPES	Piperazine-N,N'-bis (2-ethanesulfonic acid)
PI3K	Phosphoinositide 3-kinase
PKC	Protein kinase C
PLD	Phospholipase D
PMSF	Phenylmethylsulphonyl fluoride
PP2A	Protein phosphatase 2A
PRX	Peroxiredoxin
PS	Penicillin & Streptomycin
PVDF	Polyvinylidene fluoride
Rac1	Ras-related C3 botulinum toxin substrate 1
RFP	Red fluorescent protein
Ras	Rat sarcoma

Rho	Ras homologues
RI	Rac1 inhibitor NSC23766
RIPA	Radioimmunoprecipitation
RISC	RNA-Induced Silencing Complex
ROS	Reactive oxygen species
RNase A	Ribonuclease A
RNS	Reactive nitrogen species
RPMI	Roswell Park Memorial Institute
SCID	Severe combined immunodeficiency
SD	Standard deviation
SDS	Sodium dodecyl sulphate
SDS-PAGE	SDS-polyacrylamide gel electrophoresis
siRNA	small interfering RNA
SO	Superoxide
SOD	Superoxide dismutase
STAT	Signal transducer and activator of transcription
TAT	Trans-activator of transcription
TBB	4,5,6,7-tetrabromobenzotriazole
TBS	Tris-buffered saline
TBST	TBS with Tween-20
TEMED	N,N,N,N-Tetramethyl-Ethylenediamine
TM	Transmembrane domain
TOS	Tocopheryl succinate
TRX	Thioredoxin
TrxR	TRX reductase
TYK	Tyrosine kinase
VDAC	Voltage-dependent anion channel
Vin	Vincristine
WB	Western blotting

Z-VAD-FMK   Benzyloxycarbonyl-Val-Ala-Asp (OMe)-fluoromethylketone

CHAPTER 1: INTRODUCTION

1.1.   Cancer

1.1.1 Cancer Epidemiology: The No.1 Killer in Singapore

Cancer, a group of heterogeneous diseases which result from unregulated expansion of cells, is one of the world's leading causes for deaths. In Singapore, it is the No. 1 killer. Every day, 12 people die from cancer and 28 people are diagnosed with cancer; During 2005-2009, 49,412 incident cancers are diagnosed among the whole resident population; Eventually, 1 in 4 Singaporeans dies of cancer[1]. With such astonishing figures, it is no wonder that research studies aiming at understanding the heterogeneity of cancer at the cellular level, biochemical level, chromosomal level, and molecular level, hoping to find better treatments or even cures for cancer have been increasing exponentially over the past two decades[2-4].

1.1.2 Carcinogenesis: Shifting the Equilibrium

Human bodies are made up of billions of cells. Normal healthy cells grow and multiply at a steady controlled rate and their death is also highly regulated establishing equilibrium between cell proliferation and cell death. Despite the complexity of the various command and control pathways implicated in oncogenic transformation of cells with different origins, the common denominator in all forms of neoplasia is the dysregulated or defective ratio between cell proliferation and cell death[5]. Any disturbance of this ratio due to either enhanced proliferation signals or

defective death circuits would result in an abnormal accumulation of cells leading to carcinogenesis.

1.1.3 Fighting Cancer: Hurdles and Hopes

Conventional chemotherapies for cancer are usually limited to general cytotoxic or cytocidal pharmaceutical agents, which have evolved over half a century to be the major weapon against most forms of cancer[6], including alkaloids[7, 8], taxanes[9, 10], alkylating agents, antibiotics and antimetabolites[11-15], *etc*. Etoposide and vincristine are two forms of alkaloids, the former of which inhibits topoisomerase II and blocks replication of DNA leading to strand breaks[16], while the latter inhibits microtubule assembly and arrests mitosis in metaphase[17, 18]. Vincristine is commonly used in the management of acute lymphocytic and non-lymphocytic leukaemias, Hodgkin's and non-Hodgkin's lymphomas, non-small cell lung cancer, Kaposi's sarcoma and testicular cancer, while etoposide is more restricted to small cell lung cancer and testicular cancer[2]. Another example of drugs is daunorubicin, a member of the antibiotics group, which intercalates into DNA strands resulting in the failure of DNA replication and transcription[19]. However, one of the drawbacks for conventional chemotherapies is a lack of desirable selectivity. A majority of the existing compounds do not distinguish between cancer cells and their rapidly dividing normal counterparts resulting in severe side effects such as myelosuppression[20], haemorrhagic cystitis, acute and chronic cardiotoxicities, gastrointestinal mucositis, renal toxicity[2] and peripheral and central neuropathy[21]. In addition, drug resistance is also a problematic issue, especially when a single agent is used extensively over a sustained period of time[22], although this can be somewhat circumvented by the routine employment of a cocktail of

multiple drugs administered either simultaneously or sequentially in the clinic. The urgent need to develop novel therapeutic agents specifically catered for cancer cells, to be used either alone or in a combination strategy aiming at improved efficacy and reduced toxicity, has always been the stimulus behind research efforts. With our understanding of the genomic aberrations that underlie the malignant transformation of normal cells being greatly improved over the past 5 to 10 years[23], there has been a conceptual revolution in the therapeutic management of this disease. Bearing in mind the heterogeneity and complexity of the disease, a strategy that is aimed at targeting the critical circuit that is common and essential to all cancers irrespective of their origins and types would be a smart choice[2]. One common denominator, as we discussed in the previous section, is the dysregulated or defective ratio between cell proliferation and cell death. The intracellular milieu of cancer cells is non-conducive for efficient death signalling as compared to normal cells and one hypothesis that explains this difference in the process of oncogenic transformation and has been supported by abundant evidence over the past couple of years, places the redox status of cancer cells in the centre of this picture[2, 24-32].

1.2. Role of Reactive Oxygen Species (ROS) in Carcinogenesis

1.2.1 What is ROS?

Reactive oxygen species or ROS in short, are a collective term referring to oxygen derived radicals, which contain one or more unpaired electrons, as well as non-radicals. Superoxide anion (O_2^-), hydroxyl radical ($^{\cdot}OH$), peroxy radical and singlet oxygen are all examples of free oxygen radicals while hydrogen peroxide (H_2O_2) belongs to the category of non-radicals.

1.2.2 Where is ROS Generated?

There are many sources of ROS within a cell, which can be broadly categorized into two types: 1) those biological processes that release ROS as by-products or waste products along with essential biochemical reactions[33]; 2) those that intentionally produce ROS as part of a cell defense mechanism or a signal transduction pathway; although the definition line between these two are not so clear cut .

1.2.2.1 Mitochondria

An example from the first category is the mitochondria, which are among the major intracellular sources of ROS production since about 1-3% of the oxygen consumed by the respiratory chain can be converted to ROS in isolated mitochondria[34]. Partial reduction of molecular oxygen by the unpaired electrons that are generated in the process of oxidative phosphorylation leads to the production of O_2^- which is readily converted to H_2O_2 by magnesium superoxide dismutase (MnSOD) residing in the mitochondria matrix. H_2O_2 can be converted subsequently to the highly reactive oxygen species $\cdot OH$, through the iron-dependent Fenton reaction[35]. $\cdot OH$ is the most reactive among the three species and is the cause for most of the oxidative damage[36]. In addition, O_2^- will react with another freely membrane diffusible radical $\cdot NO$ to form the much more reactive radical species peroxynitrite ($ONOO^-$). Due to its ability to diffuse across the mitochondrial membranes, $ONOO^-$ can result in oxidative damage of critical components throughout the mitochondria via oxidation, nitration and/or nitrosation. The oxidants derived from $\cdot NO$ are collectively named as reactive nitrogen species (RNS)[37], and the detailed description of each species are beyond the scope of this thesis.

4

Although it is well known that ROS can be generated as by-products of oxidative phosphorylation, the question as to the specific site(s) along the electron transport chain (ETC) responsible for ROS generation has always been a hotly debated topic. It is traditionally believed that under physiological conditions, Complex I (NADH dehydrogenase) is the main site for mitochondrial ROS production, where O_2^- is produced on the matrix side and rapidly dismutated to H_2O_2[38, 39]. In addition, Complex III (ubiquinol cytochrome c reductase) has also been reported as a site for O_2^- production[40, 41]. It is demonstrated that under ischemic and apoptotic conditions, O_2^- production is triggered at Complex III. This may happen through inhibition of Complex IV (cytochrome c oxidase or COX) as well as over-reduction of the ETC in the event of mounting hypoxic stress[42]. In a more recent review, the relative contribution of each complex towards O_2^- production has been clearly quantitated with Complex I and Complex III (producing O_2^- to both the matrix and intermembrane space) having the greatest maximum capacities while Complex II having normally negligible rates[43].

Apart from the ETC, several other sites in the mitochondria have also been reported to generate O_2^-, including pyruvate dehydrogenase, α-ketaglutarate dehydrogenase, glycerol-3-phosphate dehydrogenase[44] and fatty acid β-oxidation[43]. Recently, new findings that support the concept of mitochondrial O_2^- flashes have gained much interest and reveal several previously unknown aspects of mitochondrial dynamics. Transient quantal O_2^- flashes were observed in excitable cells such as muscle cells and neurons *in vivo* and they were associated with mitochondrial permeability transition pore (mPTP) opening, which presents a new facet in physiological ROS production[45, 46].

1.2.2.2 NADPH oxidase

The NADPH oxidase (Nox) family proteins belong to the second category, which intentionally produce ROS as part of a cell defense mechanism or a signal transduction pathway. They are membrane-associated, multi-unit enzyme complexes catalysing the electron transfer from NADPH to molecular oxygen, generating O_2^- and H_2O_2. The phagocytic isoform Nox2 (gp91phox where phox stands for phagocytic oxidase), being the one that is firstly identified in the family, robustly produce O_2^- as a defense mechanism in the face of pathogen infection and the O_2^- is converted by superoxide dismutase (SOD) and myeloperoxidase into hypochlorous acid (HOCl) that acts as a potent microbicide. The whole process is known as the phagocytic respiratory burst. Over the past decade, other Nox isoforms have also been characterized in many other cell types although the ROS production is to a lesser extent, which include Nox1[47, 48], Nox3[49, 50], Nox4[51-53], Nox5[54, 55] and Duox1/Duox2[56-58] apart from Nox2[59, 60]. Various stimuli (including angiotensin II, thrombin, platelet-derived growth factor and transforming growth factor β) are known to alter the activity or expression levels of Nox proteins and their subunits, ultimately influencing the amount of ROS generated. Of particular note is the requirement of the small GTPase Rac in a GTP-bound form for Nox1, Nox2 and Nox3 activation while Nox4 is constitutively active when associated with the cytosolic p22phox subunit[59]. Similar to the role of Nox2 in phagocytes, Nox1 and Duox1/Duox2 have also been implicated in the host defense of the colon and the lung, respectively[61]. Apart from host defense mechanisms, Nox family proteins are largely involved in signal transduction pathways as well. Nox-derived O_2^- and H_2O_2 can specifically and reversibly react with proteins, altering parameters such as enzyme activity, subcellular localization and half-life. Although the ROS species produced by

different Nox isoforms are the same (either O_2^- or H_2O_2), they often play distinct roles partly due to the different compartmentalization of different isoforms within the cell. For example, Nox2 is found in phagosomes and on the leading edge of lamellipodia as well as in redoxisomes of nonphagocytic cells[62-64] while Nox4 has been identified in the nucleus[65], the endoplasmic reticulum (ER) [66], the mitochondria[67-70] as well as focal adhesions[71], therefore interacting with distinct kinases, phosphatases and transcription factors involved in discrete signalling pathways.

The relative quantitative contribution of mitochondria and Nox family proteins in cellular ROS production is expected to vary greatly from one cell type to another. In certain cells including the phagocytic neutrophils as well as non-phagocytic fibroblasts, vascular smooth muscle cells and endothelial cells, cellular ROS production is largely contributed by NADPH oxidases[43, 72, 73].

1.2.3 How is ROS Regulated: Their Scavenger System

Since there are a number of intracellular sources of ROS production, it is not surprising that the cells are well equipped with a myriad of antioxidant defence systems to keep the levels of ROS in check. In the mitochondria alone, there are SODs and two major antioxidant systems: the thioredoxin (TRX) system and the glutaredoxin (GRX) system, where the former include TRX, NADPH, TRX reductase (TrxR), TRX-dependent TRX peroxidase and peroxiredoxin (PRX) while the latter include GRX, NADPH, glutathione (GSH), glutathione reductase (GR), and GRX-dependent glutathione peroxidase (GPX)[74-76]. Unlike H_2O_2, O_2^- does not diffuse

that readily across the membrane and thus for O_2^- produced in the mitochondria matrix, the activity of MnSOD is critical to prevent the mitochondrial matrix components from oxidative damage. In certain cell types, the other isoform of the superoxide dismutase Cu/ZnSOD is also present in the mitochondrial intermembrane space apart from its cytosolic residence[77, 78]. The dismutated product H_2O_2 can be either further metabolized by mitochondria isoforms of both the TRX and GRX systems including Trx-2, Grx-2a, Grx-5, Prx III/V and GPX4[76] or diffuse into cytosol where it can be combatted by the cytosolic antioxidant defense machinery.

Although excessive levels of ROS will lead to protein oxidation, lipid peroxidation and DNA damage, lower levels of ROS have been demonstrated to be essential signalling molecules[35, 79, 80]. Indeed, the intracellular redox milieu has a great impact on signal transduction and gene expression and over the past decade, more and more evidences are surfacing to suggest that mild oxidative stress is a contributing factor to carcinogenesis[27, 29, 31, 81].

1.2.4   Pro-oxidant Theory of Carcinogenesis

In a variety of cell types, exposure to low concentrations of ROS, in particular O_2^- and H_2O_2, triggers growth response by stimulating the activation of early growth related genes such as *c-fos* and *c-jun*[82-84]. The mitogenic activity of ROS comes from their ability to alter the activities of a plethora of intracellular signalling targets: activation of transcription factors, oxidative inhibition of phosphatases and modulation of protein kinases[85], which all in turn switch on the downstream

effectors for proliferation. Examples of redox regulated targets include the transcription factors NF-κB and AP-1, tyrosine kinases such as Janus kinase 2 (JAK2) and tyrosine kinase 2 (TYK2)[86, 87], c-Jun N-terminal kinases (JNKs), p38 mitogen-activated protein kinases (MAPKs), phosphatidylinositol 3-kinases (PI3Ks)[88], low molecular weight-protein tyrosine phosphatase (LMW-PTP)[89] and the list goes on[90]. The underlying molecular mechanisms for ROS-induced signalling vary from target to target. For example, NF-κB activation is achieved either by enhanced phosphorylation of IκBα through oxidation or enhanced proteasome-mediated IκB degradation[91, 92]. Inactivation of protein tyrosine phosphatases is achieved through oxidation of their cysteine residues by ROS which renders them unable to counteract the activity of protein tyrosine kinases[93] and results in constant autophosphorylation and activation of the cell-surface receptors such as EGFR (epidermal growth factor receptor) upon ligand induction[94]. Enhanced membrane recruitment of PI3K to the substrate site is achieved through tyrosine phosphorylation of its catalytic subunit by H_2O_2 therefore maximizing its catalytic efficiency enhancing the downstream activation of AKT[88]. In addition to all the targets mentioned above, ROS has also been demonstrated to positively regulate the activity of a number of ion channels[84, 85], in particular Na^+/H^+ exchanger (NHE) which has been shown to influence cell division through the maintenance of an alkaline intracellular milieu[95]. Further evidences to support the notion of ROS being proliferative signals come from the observations that in certain systems, addition of ROS scavengers such as SOD or catalase exogenously led to a reduction in proliferation and an increase in cell death[84].

Low levels of ROS not only serve as mitogenic signals during normal cellular growth and proliferation but also during tumour transformation and progression. The earliest observations that link ROS and carcinogenesis were reviewed in 1985 where increased concentrations of ROS were observed to cause chromosomal damage and promote initiated cells to neoplastic growth in a number of hereditary disorders[96]. It is now well known that a number of cancers exhibit a chronic pro-oxidant intracellular milieu through either constitutive ROS production in substantial amounts or defective antioxidant systems, favouring proliferation and survival as compared to their normal counterparts[82, 83], suggesting a causal relationship between pro-oxidant state and carcinogenesis. Indeed, NIH3T3 fibroblasts with Nox1 overexpression and enhanced O_2^- generation exhibited transformed appearance, anchorage-independent growth and were able to induce tumours in athymic mice providing direct evidence for the hypothesis[47]. Studies in prostate cancers also revealed that ROS generation through the NADPH oxidase system is critical for the migratory/invasive phenotypes observed. Blocking of ROS production reversed cell invasion and increased cell death[97]. In addition, the expression of an important antioxidant enzyme in the mitochondria, MnSOD, has been shown to be down-regulated in a variety of cancer cells, thus creating a constitutive pro-oxidant milieu. The reduction in the MnSOD levels has been demonstrated to enhance the invasiveness of these cells, while reintroduction of MnSOD resulted in a suppression of the malignant phenotypes and favouring of differentiation[98-102]. Further evidence that supports the hypothesis that pro-oxidant cellular status contributes to cancer progression comes from the observation that colon carcinomas showed much greater levels of oxidative damage than colon adenomas and that addition of the antioxidant N-acetylcysteine dramatically impaired the proliferative capacity of the former.

As mentioned in section 1.1.2, carcinogenesis results from the shift in the equilibrium between cell proliferation and cell death. It has been recognized that pro-oxidant state also impairs death signalling pathways while on the contrary, a reduced intracellular milieu facilitate the execution in tumours[24, 47, 103-110]. Two members of the ROS family that are particularly important in this picture and will be the focus of the following section are O_2^- and H_2O_2.

1.2.5 Onco-ROS vs. Onco-suppressor-ROS

Although the prevailing opinions had been that ROS participate in the apoptotic induction and invariably accompany the death execution, more and more pieces of evidence are surfacing to demonstrate that the exact regulatory roles ROS play in cell fate determination depend very much on the concentrations or rather the ratio of respective species involved. It is understood that there are a number of different cell death mechanisms described in the literature such as necrosis, apoptosis, necroptosis, autophagy and most recently ferroptosis[111]. However, detailed discussion on the roles of ROS in other forms of death is beyond the scope of this thesis and apoptosis will be placed as the prime focus here.

Recent findings from our own laboratory as well as other groups demonstrated that a mild increase in the intracellular ROS levels resulted in an inhibition of the apoptotic pathways in cancer cells, irrespective of the triggers[28, 103-105, 107, 110, 112-114]. A closer look at the actual species of ROS led to the identification of O_2^- being the culprit. The first observation on the death inhibitory role of O_2^- was made in a FAS-mediated apoptotic model in human melanoma cells[104]. Subsequently it was

shown by our group that in the absence of cytotoxic amount of H_2O_2 production, an increase in the intracellular O_2^- levels resulted in an inhibition rather than an activation of apoptosis, as opposed to what has been conventionally perceived, while overexpression of the cytosolic O_2^- scavenger Cu/ZnSOD reversed the death inhibitory effect sensitizing the human melanoma M14 cells to chemotherapeutic agents including etoposide and daunorubicin. Inhibition of one major intracellular source of O_2^-, NADPH oxidase, also resulted in a significant increase in the sensitivity to drug-induced apoptosis[104, 107]. Similar observations were made by another group showing that elevated levels of intracellular O_2^- functioned as a pro-survival signal and that death execution could be facilitated by decreasing O_2^- in a virus-induced apoptotic model[115].

Interestingly, on the contrary, another ROS species, H_2O_2, seems to function as a death facilitator in certain systems. Although lower doses of H_2O_2, similar to what O_2^- does, could activate mitogenic signalling as discussed in the previous section, slightly elevated levels of H_2O_2 (lower than the 500 μM threshold that could result in necrosis) lead to a decrease in O_2^- levels, an increase in reduced GSH to oxidized GSSG ratio, a marked drop in intracellular pH, thus creating a reduced intracellular milieu favouring apoptotic execution[28, 105].

The underlying molecular mechanisms that govern the opposing effects of these two ROS species can be attributed to two main aspects: 1) the activity of caspases, the mediators and executioners of apoptosis; 2) intracellular pH. Firstly, the catalytic domain common to the caspase family (QARCG) has a thiol-containing

cysteine residue that is susceptible to oxidative inhibition in an oxidative intracellular milieu[116-119]. Increased levels of O_2^- significantly suppressed the activity of caspase 3 and a decrease in O_2^- restored the activity[107]. On the other hand, H_2O_2 has been demonstrated to directly activate caspase 3 and 9[120]. Secondly, O_2^- production via the NADPH oxidase system results in the oxidation of NADPH to $NADP^+$ and the extrusion of H^+ leading to an increase in the intracellular pH[85]. In addition, it has also been shown that increased levels of O_2^- could induce the promoter activity of the Na^+/H^+ exchanger 1 (NHE-1) gene resulting in an alkaline pH[121]. On the contrary, H_2O_2 has been shown to inhibit the NHE-1 promoter activity and gene expression resulting in an acidic milieu[121, 122].The cytosolic acidification in turn leads to the mitochondrial recruitment of Bax, the pro-apoptotic member of the Bcl-2 family for apoptotic induction[25].

The ratio between these two ROS species, O_2^- and H_2O_2, is therefore critical in cell fate determination. Under homeostatic growth condition, the intracellular ratio between these two is in a tight control by antioxidant systems to keep a balance between cell proliferation and cell death. However, in many cancer cells, this balance is tilted in favour of O_2^- creating a pro-oxidant intracellular milieu that promotes cell proliferation as well as survival indirectly through inhibition of apoptosis, which are two hallmarks for cancer. On the contrary, when the ratio tilts in favour of H_2O_2, this creates a reductive milieu that is permissive for death execution. As such, we term O_2^- as Onco-ROS and H_2O_2 as Onco-suppressor-ROS[123]. In this regard, manipulating the cellular redox status would serve as a promising strategy for enhancing the sensitivity of cancer cells to conventional chemotherapeutic drugs. Over the past decade, our group, with the impetus of identifying the druggable intracellular targets

responsible for redox regulation, have been working intensively on this subject and one of the novel targets that we have discovered is the anti-apoptotic protein Bcl-2.

1.3. Role of Bcl-2 Family in Carcinogenesis

1.3.1 Bcl-2 in the Conventional Picture: Guardians for Mitochondrial Membrane Integrity

1.3.1.1 Bcl-2 portrait: Discovery, structure and localization

Bcl-2 is the acronym for the B-cell lymphoma/leukaemia 2 gene. As its name implies, this gene was first discovered in B-cell malignancies[124] where the Bcl-2 gene, normally localized to chromosome 18q21, was fused with the immunoglobin heavy chain gene promoter and enhancer on chromosome 14q32 [t(14,18) chromosomal breakpoint], thereby its transcription gets excessively deregulated inducing aberrant overexpression[125]. This observation was associated with drug resistance due to the inherent pro-survival function of Bcl-2 through its ability to keep pro-apoptotic proteins at bay and thereby inhibiting mitochondria-dependent apoptotic signalling[126].

Structurally, Bcl-2 possesses four Bcl-2 homology (BH) domains as well as a carboxyl terminal hydrophobic transmembrane domain (TM), which is responsible for its membrane localization. With the use of immunofluorescence and electron microscopic analyses as well as subcellular fractionation studies, Bcl-2 has been identified in the nuclear envelope, ER, and outer mitochondrial membranes[127]. The three-dimensional structure of Bcl-2 contains two central helices that are mostly

hydrophobic, surrounded by four amphipathic α-helices. A hydrophobic groove that consists of BH1, BH2 and BH3 domains is present on the surface of the protein and is essential in its heterodimerization with pro-apoptotic family members[128]. In addition, a putative unstructured loop is also present in Bcl-2 between the first and second helix based on X-ray crystallographic and nuclear magnetic resonance (NMR) spectroscopic studies on Bcl-xL[129], another anti-apoptotic member of the Bcl-2 family, offering ample opportunities for post-translational modifications[130-134].

1.3.1.2 Bcl-2 and its pro- and anti-apoptotic family members

Bcl-2 belongs to the Bcl-2 family of proteins, which can be classified into three sub-groups according to the BH domains that they possess and their regulatory functions on apoptosis. Members that contain all four BH domains (BH1, BH2, BH3 and BH4), which include Bcl-2, Bcl-xL, Bcl-w, Mcl-1 and A1, are classified under anti-apoptotic or pro-survival category[123]. Overexpression of each of these members has protective effects against apoptosis, while genetic knocking down of them shows that they are essential for cell survival. Members that contain BH1, BH2 and BH3 domains but not BH4 domain such as Bax, Bak and Bok are classified under pro-apoptotic category. Bax and Bak are ubiquitously expressed in various tissues while Bok is mainly present in reproductive organs. There is a third divergent class of pro-apoptotic members which only share sequence homology in the BH3 domain. These proteins are called BH3-only proteins, which consist of Bad, Bid, Bim, Bmf, BNIP3, Hrk, Noxa and PUMA[135, 136].

Being regulators of apoptosis, the balance between the pro- and anti-apoptotic members of the Bcl-2 family clearly governs the yes or no answer in the death execution pathways, as their name implies. In response to stress signals, such as exposure to radiation, hypoxia, deprivation of nutrients, heat shock, viral infection and DNA damage, the pro-apoptotic members are activated, resulting in their localization to the mitochondria where they form oligomers and induce mitochondrial outer membrane permeabilization (MOMP), thereby facilitating the release of apoptogenic factors such as cytochrome C, Smac/DIABLO and apoptosis-inducing factor (AIF) from the mitochondria, activating downstream effector caspases. This is the classical type II or the intrinsic pathway of apoptosis, a genetically programmed process with an orchestrated series of events leading to the death of a cell in the end. However, in the event where the anti-apoptotic proteins are overexpressed, which is invariably observed in drug-resistant cancers, they can antagonize the effect of pro-apoptotic Bax, Bak and/or Bok by forming homo- and heterodimers and preventing oligomerization of these pro-apoptotic members[137]. The BH3-only proteins, on the other hand, can act as either antagonists of anti-apoptotic members or direct activators of pro-apoptotic members.

The first elucidation of the three dimensional (3D) structure of human Bcl-xL revealed that it is reminiscent of pore forming proteins[129] and subsequently other members in the family such as Bcl-2 and Bax as well as Bcl-xL itself are all found to be capable of forming pores in artificial membranes[138-140]. It was not until 2001 that the 3D structure of Bcl-2 was resolved with its unstructured loop region being replaced by that of Bcl-xL. Although they share a similar overall helical fold and function, they differ in the highly flexible unstructured loop region, which contributed

to the different solubilities of these two proteins[128]. Another key structural difference lies in the amino acid residues and the size of the hydrophobic groove formed by the BH1, BH2 and BH3 domain, which is the important interaction site with pro-apoptotic members such as Bax and Bak[141] and this probably explains the different binding affinities observed between Bcl-2 and Bcl-xL towards them. The BH3 domain is critical in the functions of the Bcl-2 family proteins, because not only is this domain of Bcl-2 responsible for interacting with and antagonizing the pro-apoptotic members but also is the domain used by the pro-apoptotic Bax and Bak to antagonize Bcl-2 mediated protection against apoptosis. Deletion of this domain from Bax and Bak results in impairment of their pro-apoptotic property and binding towards Bcl-2 and Bcl-xL while transfection of this domain alone can lead to apoptosis acting similarly to BH3-only proteins.

A few mechanistic models have been proposed as in how exactly the pro- and anti-apoptotic Bcl-2 family proteins regulate MOMP. The pro-apoptotic Bax and Bak are capable of forming pore-like channels upon oligomerization[142] or alternatively they are also able to regulate the adenine nucleotide translocase (ANT)[143] and voltage-dependent anion channel (VDAC) causing the former to open and the latter to close resulting in matrix swelling and outer mitochondrial membrane disruption[144]. The anti-apoptotic Bcl-2 and Bcl-xL, on the other hand, in addition to their ability to bind and sequester the pro-apoptotic members, have been shown to directly interact with VDAC1[145] or alternatively function as an ionophore dissipating the electrical transmembrane potential[146], both of which prevent the closure of this channel and maintaining the exchange of ATP/ADP therefore inhibiting the hyperpolarisation, swelling and rupture of the mitochondria[147, 148].

As to the third class of the Bcl-2 family, the BH3-only proteins, they act upstream of the pro-apoptotic Bax and Bak since they cannot induce cell death in Bax-/-Bak-/- double knockout mice[149]. They function as sensors or mediators of apoptosis and different individual BH3-only protein responds to different stimuli. For example, PUMA and Noxa can be transcriptionally induced by p53 upon sensing DNA damage[150, 151]. Another BH3-only protein Bad is regulated through phosphorylation/dephosphorylation. Upon cytokine withdrawal, Bad is dephosphorylated and released from the sequestration by the scaffold protein 14-3-3. It can then bind and neutralize Bcl-2, Bcl-xL and Bcl-w and activates Bax and Bak[152]. Similarly, Bim and Bmf are also kept in sequestration by cytoskeleton proteins without stimuli[153, 154]. The proposed mechanisms of action for the BH3-only proteins can be classified into: 1) Direct activation model; 2) Indirect activation model. Bim and tBid (the truncated form of Bid cleaved by caspase 8 upon apoptotic stimuli), which directly activate Bax and Bak, can be classified into the first category. Apart from these two direct activators, Bad and Bmf are also classified under the first category and they are called sensitizers since they bind to and displace the sequestered Bim and tBid from pro-survival Bcl-2, Bcl-xL and Bcl-w leading to activation of Bax and Bak[155, 156]. However, recent evidences have challenged this model and suggest that this needs not to be a necessary physiological event since Bax is not able to bind Bim or Bid in physiological conditions[157] and also Noxa and Bad BH3 peptides have been found to induce apoptosis even in the absence of Bim, Bid and PUMA[158]. In the indirect activation model, it is suggested that all BH3-only proteins will bind to pro-survival members thus indirectly liberating Bax or Bak from their sequestration, promoting their homo-oligomerization. However, BH3-only proteins are selective in their pairing with pro-survival members. Bim and PUMA

have been shown to be able to bind Bcl-2, Bcl-xL, Bcl-w, Mcl-1 and A1, while Bad and Bmf bind to Bcl-2, Bcl-xL and Bcl-w as mentioned above, and Noxa binds only Mcl-1 and A1[159].

1.3.1.3 Post-translational modifications of Bcl-2 and their implications on apoptosis

Bcl-2 is frequently regulated through post-translational modifications including proteolytic cleavage, ubiquitination, proteosomal degradation and in particular phosphorylation through its interaction with kinases and phosphatases. These modifications alter its folding and conformation, stability and half-life, subcellular localization, protein-protein interactions as well as activity[160, 161]. In this section, phosphorylation/dephosphorylation will be the prime focus. As mentioned in earlier section, Bcl-2 possesses a non-structured loop that lies in-between its BH3 and BH4 domains and certain residues within that flexible loop, to be specific Thr56, Thr69, Thr74, Ser70 as well as Ser87, are subjective to phosphorylation in response to a variety of stimuli. The significance of Bcl-2 phosphorylation on its anti-apoptotic activity is controversial, depending very much on 1) the extent of phosphorylation: single site or multi-site phosphorylation; 2) the exact subcellular localization where the phosphorylation takes place[131, 162, 163].

There are two opposing models of Bcl-2 phosphorylation initially proposed: "Taxol-induced" model and "Interleukin-3 (IL-3)-induced" model. In the first model, microtubule-active drugs including Vinca alkaloids and paclitaxel (Taxol) that lead to mitotic arrest[164] are found to induce Bcl-2 phosphorylation and inhibit its anti-apoptotic function[165-167]. However, phosphorylation of Bcl-2 and initiation of the

apoptotic program are only observed following drug treatment in the cycling cancer cells but not in Bcl-2-overexpressing chronic lymphocytic leukaemia cells that are blocked at G_0-G_1 phase[168] indicating the significance of cellular context (mitotic cells or interphase cells). In addition, Bcl-2 phosphorylation is also observed in normal mitosis therefore it probably functions as a guardian of chromosome segregation[167-170]. On the contrary, in the "IL-3-induced" model, Bcl-2 phosphorylation leads to an enhancement of its anti-apoptotic function in IL-3-depedent hematopoietic cell lines. It might seem to be a paradox at first glance; however, a closer examination on the specific residues in the loop region being phosphorylated revealed that multi-site phosphorylation (including Thr69, Ser70 and Ser87) occurs in the "Taxol-induced" model[171] while only single site phosphorylation on Ser70 accounts for the "IL-3-induced" model[172, 173]. Indeed, a non-phosphorylatable mutant of Bcl-2, S70A, has been shown to be unable to support prolonged cell survival whereas the mutant S70E that mimics a phosphate group by having the negative charge suppressed apoptosis much more potently than the wild type Bcl-2[172]. Taken together, this indicates that single site phosphorylation on Ser70 enhances Bcl-2's anti-apoptotic function while multi-site phosphorylation on Thr69, Ser70 and Ser87 leads to inactivation of Bcl-2. However, a study based on a series of serine/threonine (S/T) to glutamate/alanine (E/A) mutants, that mimic or abrogate either single site or multi-site phosphorylation, clearly demonstrated that all of the phosphomimetic E mutants potently enhanced cell survival upon apoptotic stress induced by paclitaxel and retarded G_1/S cell cycle transition after IL-3 addition or treatment with paclitaxel in the presence of IL-3 with the T69E/S70E/S87E (EEE) triple mutant being the most potent as compared to non-phosphorylatable A mutants

stressing the importance of cellular context when deciphering the functions of Bcl-2 phosphorylation[174].

Multiple kinases have been implicated in phosphorylating Bcl-2, including cyclin-dependent kinase 1 (CDK1)[175], JNK[171, 176], mTOR[177], PKA[178] and Raf-1[167] in "Taxol-induced" model and MEK/MAPK kinase, extracellular signal-regulated kinase (ERK)/MAPK[179] and protein kinase C (PKC)[172, 173, 180, 181] in "IL-3-induced" model. In addition to these two models, mitochondria PKCα is also implicated in other studies to be responsible for phosphorylating Bcl-2 at Ser70 and enhances its anti-apoptotic activity in drug-treated myeloid cells[180-182]. Interestingly, JNK is repeatedly indicated by various groups as a Bcl-2 kinase and has been shown to phosphorylate four sites within the flexible loop region including Ser70 that is common to both models (the rest three residues would be Thr56, Thr74 and Ser87)[171, 176, 183-185]. Since so many kinases are implicated, it is very likely that there are certain levels of redundancy and their activation would depend on specific cellular context. As always emphasized, phosphorylation event is determined not only by kinases but also by phosphatases and sometimes it is the inhibition of phosphatases, as what happens during mitotic arrest, that results in the increased phosphorylation and kinases are not necessarily activated[162]. Indeed the serine/threonine phosphatase, protein phosphatase 2A (PP2A), has been shown to dephosphorylate Bcl-2 on Ser70 leading to an increase in apoptotic cell death[186-189].

Clearly, apart from the residue site of phosphorylation, the role of phosphorylated Bcl-2 also differs in different subcellular localizations. Phosphorylated Bcl-2 is found to be localized to nuclear structures during mitosis[169] while in mitotic arrested cells following paclitaxel treatment it is the mitochondrial Bcl-2 that is phosphorylated by JNK[190]. PKCα-induced Bcl-2 phosphorylation on Ser70 that enhances its anti-apoptotic activity and PP2A-induced dephosphorylation of Bcl-2 that inhibits its activity are also at the mitochondria. Interestingly in one study on the "IL-3-induced" model a minor but distinct cytosolic pool rather than the more predominant mitochondrial pool of Bcl-2 is phosphorylated[191]. In addition, multi-site phosphorylation of Bcl-2 in the ER renders it unable to bind to pro-apoptotic BH3-only proteins and inhibits its protective role against Ca^{2+}-dependent death stimuli[130].

1.3.1.4 Bcl-2 and its interaction network with non-homologous proteins: Modulation of its anti-apoptotic function

We have discussed in the earlier section for the interaction of Bcl-2 with its homologous family members in the mitochondria. In fact, there is a whole list of other non-homologous proteins that also interact with Bcl-2 in a wider variety of cellular pathways modulating its anti-apoptotic property and a few examples from the overwhelming list would be illustrated here in this section including Ras, Raf-1, FKBP38, p53, PP2A and Nur77.

1.3.1.4.1   Interaction to synergise Bcl-2's anti-apoptotic property: Ras, Raf-1 and FKBP38

Ras -- The oncogene Ras, whose mutation has been witnessed in 30% of cancers, is well known to interact with Bcl-2[192]. The mutagenic Ras will activate survival pathways in the cancer cells; however under certain conditions, Ras can also trigger apoptosis[193]. In lymphocytes, activated Ras can trigger Fas mediated apoptosis and when Bcl-2 is overexpressed, this form of apoptosis is inhibited through the association of the BH4 domain of Bcl-2 with mitochondrial Ras. The CAAX motif required for farnesylation at the C-terminus of Ras is demonstrated to be essential for its apoptotic signalling and Bcl-2 association[194].

Raf-1 – Raf-1, a signal transducing serine/threonine kinase in the Ras pathway, has been shown to interact with Bcl-2 as well leading to apoptotic inhibition[195]. Upon phosphorylation by p21-activated kinase 1 (PAK1), Raf-1 is targeted to the mitochondria through its interaction with the BH4 domain of Bcl-2. Mitochondrial Raf-1 then phosphorylates Bad and releases Bcl-2 from Bad-Bcl-2 complex, promoting cell survival[196].

FKBP38 – Another protein that is known to regulate Bcl-2's anti-apoptotic function is the immunosuppressant FK-506 binding protein 38 (FKBP38). Once bound to calcium and calmodulin, FKBP38 becomes active and chaperones Bcl-2 to the mitochondria, where it probably interferes with Bcl-2's ability to bind to its targets by physically interacting with the BH2 domain as well as the loop region of Bcl-2. As discussed in the previous section on post-translational modifications, the loop region

of Bcl-2 offers ample opportunities for phosphorylation whose status is critically linked to its anti-apoptotic property. Indeed, from deletional mutant analysis, sites in the flexible loop region of Bcl-2 that contain or surround Ser70 and Ser87 appear to be critical for the physical interaction with FKBP38 where phosphorylated Bcl-2 showed a significant reduction in its binding affinity towards FKBP38. Therefore FKBP38 is likely to play a role in regulating apoptosis through modulating the phosphorylation status of Bcl-2 although there are controversies in whether it exerts pro- or anti-apoptotic functions[197-199].

1.3.1.4.2   *Interaction to abrogate Bcl-2's anti-apoptotic property: p53, PP2A and Nur77*

P53 – The tumour suppressor activity of p53 is primarily explained by its ability to induce cell cycle arrest, repair of the genome and apoptosis under genotoxic stress through its transcriptional activities. Apart from that, a non-transcriptional mechanism of p53 induced apoptosis was also elucidated. Studies showed that p53 is able to localize to mitochondria upon DNA damage in cancer cells and directly bind to Bcl-2 thus displacing bound Bax and inducing MOMP and cytochrome c release[200]. In addition, upon binding to p53, a conformational change of Bcl-2 occurs and the BH3 domain is exposed correlating with the abrogation of its anti-apoptotic property[201]. Both a negative and a positive regulatory region exist at the flexible loop of Bcl-2 where deletion of the negative regulatory region (amino acid residues 32-68) disrupted the interaction with p53 enhancing Bcl-2's anti-apoptotic property. On the contrary, the multi-site phosphorylation on Thr69, Ser70 and Ser87, as mimicked by the triple mutant T69E/S70E/S87E (EEE), at the positive regulatory region (amino acid residues 69-87) resulted in reduced interaction levels.

PP2A– The serine/threonine phosphatase, PP2A, as mentioned earlier, has been shown to dephosphorylate Bcl-2 on Ser70 leading to an increase in apoptotic cell death[186-189]. It has been demonstrated that it is the BH4 domain of Bcl-2 that PP2A directly binds to and utilizes as a docking site to potentially reach out to the target residue Ser70 located at the adjacent flexible loop region. The inhibitory effects of PP2A on Bcl-2 not only come from the dephosphorylation of Bcl-2 itself but also from an enhanced binding between p53 and dephosphorylated Bcl-2[186].

Nur77 – Although Bcl-2 is well known as an anti-apoptotic protein, recently it has been shown to be able to induce programmed cell death as well. The loop region of Bcl-2 mediates its interaction with orphan nuclear receptor Nur77 and targets it to the mitochondria. The interaction results in a conformational change in Bcl-2 leading to exposure of its otherwise hidden BH3 domain. The exposed BH3 domain, in turn, blocks the function of Bcl-xL, thus converting Bcl-2 from a protector to a killer[202].

As discussed above, it is well known that Bcl-2 serves as a guardian for the mitochondria membrane integrity and its anti-apoptotic function can be modulated through post-translational modifications especially phosphorylation and interaction with both homologous Bcl-2 family members and other non-homologous proteins. However, recent evidences have been accumulating to indicate that the anti-apoptotic property of Bcl-2 can be attributed to its role in redox regulation as well, shedding light on a new facet of Bcl-2 biology.

1.3.2   Bcl-2 as a Non-canonical Redox Regulator

Instead of being mere by-products, mitochondrial ROS production is likely to be highly regulated as a part of physiological functions or even pathological conditions and the underlying molecular mechanisms are being gradually uncovered[35]. One of the proteins identified by our laboratory and other groups over the past couple of years to function as a redox regulator particularly in the mitochondria is Bcl-2[26, 70, 123, 203, 204].

1.3.2.1 Bcl-2: An anti-oxidant or pro-oxidant?

The involvement of Bcl-2 in redox regulation was first demonstrated by Hockenbery *et al*. that Bcl-2 overexpression protected against ROS-induced apoptosis. This is attributed to Bcl-2's function as an anti-oxidant by the group since overexpression of Bcl-2 completely suppressed the lipid peroxidation induced by H_2O_2 and menadione (a quinone that transfers electrons to oxygen leading to production of free radicals) [112]. Soon after other studies also revealed the protective capacity of Bcl-2 against various ROS triggers[205-209] including prevention of oxidant-mediated lipid peroxidation[210, 211] as well as inhibition of NO_2^- production and carbonyl formation[212]. In addition, phenotypes with increased oxidative stress were also observed in Bcl-2-deficient mice[213, 214]. However, Bcl-2 itself was later found out to possess no intrinsic antioxidant ability[215] implying that rather its overexpression indirectly induces an enhancement in antioxidant capacity of the cells when they undergo overt oxidative stress[123, 216]. This is supported by the findings that Bcl-2-mediated protection is associated with up-regulation of the cellular enzymatic and non-enzymatic antioxidant defense machineries including the glutathione system, NAD(P)H, catalase and

Cu/ZuSOD[212, 215, 217-221]. The enhanced glutathione system has been attributed to the increase in the transcription of γ-glutamylcysteine ligase induced by elevated levels of NF-κB in Bcl-2-overexpressing cells, which leads to an increase in GSH levels protecting cells from H_2O_2-induced death[222]. In addition, recent evidence has demonstrated that Bcl-2 is able to regulate the mitochondrial GSH pool as well[223].

A direct physical interaction has been shown between Bcl-2 and GSH-conjugated agarose *in vitro*, which could be disrupted by the Bcl-2 inhibitor, HA14-1, that binds to the BH3 domain groove of Bcl-2, and by another structurally distinct BH3 mimetic as well as a recombinant BH3-only protein, Bim-L. The availability of the BH3 domain groove is clearly essential for Bcl-2 to interact with GSH and the physical tethering probably serves as a means to sustain the mitochondrial pool of GSH by Bcl-2. Supporting this further, GSH was displaced from the mitochondria in intact neurons when its interaction with Bcl-2 was abolished with the use of BH3 mimetics[223]. However, there is no evidence that Bcl-2 has active transport properties for GSH; thus how the physically tethered GSH contributes to the mitochondrial antioxidant capacity remains elusive, but at least physically tethered GSH would likely decrease the susceptibility of oxidation of the proteins at the mitochondrial membranes[224]. Nonetheless, these observations provide further evidence that Bcl-2 is able to counteract excessive oxidative stress in the mitochondria through regulation of the GSH pool, thereby serving as a safety valve in the face of overwhelming ROS insults.

However, all these evidences only supported the notion that Bcl-2 confers protection against oxidative stress without elucidating its intrinsic property until the study highlighted by Steinmann's group where they examined the physiological intracellular milieu upon Bcl-2 overexpression and realized that Bcl-2 was inducing basal levels of oxidative stress that led to increased oxidative damage as measured by 8-hydroxyguanine and a subsequent boost in the antioxidant system such as catalase providing the first piece of evidence that Bcl-2 is functioning as a pro-oxidant[225]. Indeed, subsequently more and more studies all pointed out and established that Bcl-2 serves as a definite pro-oxidant under normal physiological states[114, 203, 218, 226, 227]. Based on this pro-oxidant property of Bcl-2, it implies that the enhanced antioxidant capacity that was observed with Bcl-2 overexpression could be an adaptive response to the chronic but mild oxidative intracellular milieu[206, 215, 217, 220, 227] and this serves as a first-line defense in the event of acute oxidative insults maintaining the ROS levels within a threshold optimal for cell survival[123, 203, 204, 216].

1.3.2.2 Molecular mechanisms of Bcl-2-induced pro-oxidant state

The underlying mechanisms on how Bcl-2 exerts its pro-oxidant activity, however, have not been fully elucidated. It was first hypothesized that the pro-oxidant milieu in Bcl-2-overexpressing mitochondria resulted from altered dynamics of the oxidative phosphorylation. An increase in the mitochondrial size and associated matrix content was observed with Bcl-2 overexpression and this indicates an increase in the number of electron donors and a subsequent increase in the electrons leaking out of the ETC to form O_2^-[218, 228]. However, the exact mechanism linking Bcl-2 expression levels to the mitochondrial size and matrix content was not addressed in

the above mentioned studies. More recently, our group has discovered that one of the mechanisms for Bcl-2 to generate intra-mitochondrial O_2^- is through the engagement of mitochondrial respiration in cancer cells.

1.3.2.2.1   *Interaction with COX*

An increased mitochondrial oxygen consumption rate and Complex IV activity was observed in Bcl-2-overexpressing cancer cells[114, 203, 204, 229]. It is plausible that the increased mitochondrial respiration rate results in an increased electron flux across the ETC and an increased probability of leakage of electrons onto molecular oxygen thus leading to an increase in the by-production of O_2^-. Indeed, either silencing of Bcl-2 with siRNA or functional inhibition of Bcl-2 with the BH3 mimetic, HA14-1, in those cells, reversed both the oxygen consumption rate as well as the O_2^- levels[203]. This is further supported by the observation that mitochondrial respiratory rate and O_2^- levels both correlated with Bcl-2 expression levels across different cancer cell lines with varying amounts of endogenous Bcl-2[204]. Subsequently, it was revealed that Bcl-2 overexpression promoted the mitochondrial localization of COX Va and Vb, the nuclear encoded subunits of Complex IV, which could explain for the significantly increased Complex IV activity in these cells[204] since it has been previously shown that mitochondrial level of COX Vb correlated with the COX holoenzyme activity[230]. In addition, evidence was presented to demonstrate a physical interaction between COX Va and Bcl-2 through the BH2 domain of Bcl-2. In the events of early oxidative stress induced through either serum withdrawal, glucose deprivation or hypoxia, Bcl-2 could function as a redox regulator by decreasing the COX activity accordingly, through adjustment of the COX subunits, thereby maintaining the ROS levels within a non-detrimental threshold[203, 204].

Of particular note, the increased O_2^- release as induced by increased oxygen consumption observed with Bcl-2 overexpression might seem contradictory to the notion that inhibition of ETC also results in O_2^- release. However, as explained earlier, the former occurs as a result of increased electron flux across the ETC and an increased probability of leakage of electrons onto molecular oxygen while the latter is the result of inhibition of the reduction steps along ETC leading to promotion of the reaction of oxygen with accumulated reductants[231].

1.3.2.2.2   *Potential involvement of Rac1*

Apart from COX, an additional functional player in Bcl-2-mediated pro-oxidant state has been identified by our group, which is the small GTPase Rac1. The first evidence indicating the involvement of Rac1 comes from the study that a dominant negative form of Rac1, N17, decreased the levels of O_2^- in Bcl-2-overexpressing cancer cells sensitizing them to either receptor or drug-induced apoptosis[114]. Indeed, preliminary results from our laboratory suggested a direct physical interaction between Bcl-2 and Rac1. This leads us to hypothesize that Rac1 could be a critical regulator in Bcl-2 mediated pro-oxidant state and the work presented in this thesis provide evidences in support of this hypothesis. In the next proceeding section, the physiological roles of Rac1 and its contribution to carcinogenesis with a focus on redox regulation would be discussed in details.

1.4. Role of Small GTPase Rac1 in Carcinogenesis

1.4.1 The Small GTPase Rac1: A Molecular Switch

Ras-related C3 botulinum toxin substrate 1, or commonly known as Rac1, belongs to the Rho (Ras homologues) subfamily of the Ras superfamily, which are monomeric G proteins with molecular mass ranging from 20 to 30 KDa comprising of more than 100 members identified so far[232]. Rho subfamily can be classified into six groups including: 1) the Rho proteins (RhoA, RhoB and RhoC); 2) the Rac proteins (Rac1, Rac2, Rac3 and the splice variant Rac1b); 3) the Cdc42-like proteins (Cdc42, TC10, TCL, Wrch1 and Chp); 4) the Rnd proteins (Rnd1, Rnd2 and Rnd3/RhoE); 5) the RhoBTB proteins (RhoBTB1, RhoBTB2 and RhoBTB3); 6) the Miro proteins (Miro1 and Miro2)[233, 234]. Among them, RhoA, Rac1 and Cdc42 are the most extensively studied and their first identified functions are involved in actin cytoskeleton regulation: RhoA induces stress fibres and focal adhesions; Cdc42 regulates filopodia formation; Rac1 mediates lamellipodia formation and membrane ruffles[235]. In addition, Rac1 is known to function in a variety of other cellular functions including gene transcription, regulation of cell cycle and survival as well as ROS production[236].

Rac1, was first identified together with Rac2 in 1989, which bears 58% homology to Rho proteins and 20-30% homology to Ras proteins[237]. Subsequently, other forms of Rac proteins, namely Rac3 and Rac1b were discovered. The tissue distributions vary among different forms, with Rac1 ubiquitously found all over the body, Rac2 mainly in hematopoietic cells, Rac3 highly enriched in the brain but expressed in other tissues as well at lower levels and the splice variant Rac1b

minimally expressed in normal cells but highly enriched in cancers such as breast and colorectal cancers[238-241].

1.4.1.1 Structure of Rac1

Rac1, being a small GTPase, its activity is tightly regulated through GTP/GDP cycling. In order to better understand the structure-function relationship, the 3D structure of Rac1 complexed with a non-hydrolysable analogue of GTP, guanosine-5'-(βγ-imino) triphosphate (GMPPNP) was resolved through X-ray crystallography [242]. Rac1 contains a central β-sheet made up of six strands (denoted as β1- β6), six α-helices and two short 3_{10}- helices.

There are two effector regions in Rac1, named as Switch 1 (resides 29-40) and Switch 2 (resides 59-74) which are critical regulatory sites for GTP/GDP cycling. The nucleotide binding pocket consists of: 1) the two guanine recognition loops (including residues 116-119 which is the NKXD motif, and residues 158-160); 2) the two phosphate-binding loops (including residues 10-17 which is called the P-loop, and residues 57-61 containing part of the Switch 2); 3) the Switch 1 effector loop region that interacts with the ribose and the magnesium ion (Mg^{2+}). The Mg^{2+} stabilizes not only the binding of guanine nucleotides but also the intrinsic GTPase activity within Rac1, therefore the Switch 1 effector loop is of particular importance since it is involved in the hydrolysis of GTP, the binding of GTPase-activating proteins (GAP) and downstream signal transduction. In addition, if compared with other members of the Rho family, there are several hydrophobic to charged substitutions as underlined in the following sequence: [28]P<u>G</u>EY<u>I</u>PTV<u>F</u>, which render the exposed chain of Switch

1 less stable and possibly more flexible and this is reflected in the density map of the X-ray crystal structure as well with residues [32]YIPTV being poorly defined. Since Rac1's interaction with the guanine nucleotide exchange factors (GEFs) is mapped to a groove formed by Switch 1, Switch 2 and β1- β3 strands, the flexibility of the Switch 1 effector loop is probably important for specificity towards different GEFs to signal distinct downstream functions. In addition, flexible loop also offers greater opportunities for interaction with other proteins and in turn alters the conformation of Rac1 and modulates its activity[242, 243].

The conserved polybasic region (PBR) comprised of multiple lysines or arginines that immediately precedes the C-terminal CAAX sequence motif common to many small GTPases, is important for their subcellular targeting and interaction with other proteins. A unique PBR sequence is the main distinguishing feature of some small GTPases, including the three isoforms of Rac, Rac1, Rac2 and Rac3, stressing the importance of PBR in signalling, subcellular localization and tissue distribution. Nuclear localization signal (NLS) sequence is found in the PBR of Rac1 that directs it to the nucleus where it participates in signalling pathways and is ultimately targeted for degradation[244, 245]. In addition, the basic residues in the PBR have been demonstrated to interact electrostatically with the acidic phospholipids in the plasma membrane promoting the membrane localization of Rac1. Rac1 mutants with mutated or deleted PBR showed reduced interactions with membranes[246, 247]. Furthermore, the trafficking of Rac1 to different membrane compartments is also dependent on the post-translational modifications of the C-terminus. The CAAX motif (where C denotes cysteine, A represents any aliphatic amino acid and X may be any amino acid) is a substrate for post-translational

modification with the covalent attachment of a non-sterol isoprenoid. In the case of Rac1, it is the addition of geranylgeranyl pyrophosphate (GGPP) to the cysteine residue catalysed by geranylgeranyltransferase I (GGTase I) and the whole process is named as geranylgeranylation. This targets Rac1 to the ER where it undergoes further modifications with the three terminal amino-acid residues removed and the carboxyl group of the terminal cysteine methyl esterified. Rac1 then binds to Rho guanine nucleotide dissociation inhibitor (GDI) which keeps it in a soluble state (through recognition of the geranylgeranyl moiety) in the cytosol for shuttling to various membrane compartments to exert its functions[248]. Apart from geranylgeranylation, Rac1 can also be palmitoylated with the reversible addition of fatty acid palmitate at cysteine residue upstream of CAAX motif, which regulates its oligomerization state and activity as well as the partitioning and stabilization into ordered cholesterol-rich membrane microdomains[249].

1.4.1.2 Regulation of the small GTPase Rac1 through GTP/GDP cycling

Being a guanosine triphosphatase, the activation status of Rac1 depends on the binding status of nucleotide, regulated by the joint activities of a series of GEFs, GAPs and RhoGDI. Upon triggers from diverse signals that are sensed by cell surface receptors[250, 251], Rac1 dissociates from RhoGDI in cytosol and translocates to membranes where the GEFs promote its activation by stimulating the release of GDP thus allowing the binding of GTP[252]. The interaction of GEFs with Rac1 destabilizes the binding of nucleotide and Mg^{2+} resulting in the formation of a nucleotide free intermediate. GTP is present in a much higher intracellular concentration as compared to GDP, thus it gets bound by Rac1 much more easily. GEFs function as a catalyst here to promote the equilibrium between GDP- and GTP-

bound Rac1. The change in bound nucleotide from GDP to GTP alters the conformation in the Switch 1 and Switch 2 allowing Rac1 to bind downstream effector proteins including scaffold proteins (such as p67phox and IQGAPs), serine/threonine kinases (such as MEKKs: mitogen activated protein kinase kinase kinase and PAKs), lipid kinases (such as PI3K) and lipases (such as PLD: phospholipase D and PLC-β2), *etc.*[253]. After the transient activation to signal downstream pathways, GTP is hydrolysed to GDP with the stimulation from GAPs since the intrinsic GTPase activity is slow. The inactive GDP-bound Rac1 is then extracted from the membranes and sequestered in cytosol by RhoGDI[251].

The signalling specificity (i.e. activation of which Rho GTPase pathway) is governed in part by GEFs since the specificity of GEFs towards the GTPases varies. For example, Tiam1 is a specific activator of Rac1[254] while Vav promiscuously bind RhoA, RhoG, Rac1 and Cdc42[255]. The structure mapping of Rac1 complexed with its GEFs showed that the groove formed by Switch 1, Switch 2 and β1-3 strands of Rac1 is important in binding with GEFs[256], as mentioned earlier. In particular, the residue Trp56 in β3 region is critical in discriminating the binding of GEFs including Trio and Tiam1[243, 257, 258].

1.4.2   Implications of Rac1 in Carcinogenesis: Redox Regulation

Deregulation of Rac1 functions has been implicated in various disorders, one of which that is of particular interest here in this thesis is carcinogenesis. Many of the cellular processes that Rac1 regulates as mentioned above, including proliferation and apoptosis[259], cell migration and invasion[260] as well as redox regulation, are all

pertinent to malignant tumour initiation and progression[261]. This has been attributed to Rac1-induced enhancement of mitogenic signals such as activation of ERK1/2, JNK, PI3K and AKT as well as transactivation of genes mediated by AP-1, NF-κB, CRE and STAT3, *etc.*[259, 261]. From the perspective of "Pro-oxidant theory of carcinogenesis", the ability of Rac1 to activate NADPH oxidase for ROS production will be an indispensable contributing factor for carcinogenesis. Indeed, as a downstream target for Ras oncogenes, Rac1 activation and ROS production have been demonstrated to contribute to Ras-induced mitogenic signalling in fibroblasts[262, 263]. Therefore, a detailed discussion on the mechanisms of Rac1-induced ROS production would be necessary here.

One of the first effector proteins of Rac1 identified was p67phox, a subunit of the NADPH oxidase complex[264]. Upon trigger, Rac1 gets activated in GTP-bound form, binds to cytosolic p67phox associated with p47phox and p40phox and then recruits them to the membranes where they bind to the integral membrane components gp91phox (Nox2) and p22phox for the assembly and activation of the multimolecular NADPH oxidase complex for O_2^- production through one electron reduction using NADPH as a substrate[265-267]. In addition to the binding of Rac1 to its effector p67phox, direct binding between Rac1 and gp91phox at the membranes has also been demonstrated to be essential in activation of electron transport through the heterodimeric flavocytochrome b_{558} comprised of gp91phox and p22phox[268]. Based on site-directed/deletional mutagenesis and peptide walking studies, regions in Rac1 that have been demonstrated to be critical in NADPH oxidase activation lie in the Switch 1 effector loop, the insert domain as well as the C-terminal basic motif[242, 264, 269-271]. As discussed in earlier section, although this activation model was first

described for phagocytic isoform Nox2-based NADPH oxidase, Rac1 has been shown to activate Nox1 and Nox3-based complexes in non-phagocytic cells as well[272, 273] and the modulatory activity is achieved through Rac1-binding proteins Noxa1 (homolog of p67phox) and Noxo1 (homolog of p47phox)[274, 275].

1.4.3 Preliminary Evidences from Our Laboratory: Involvement of Rac1 in Bcl-2 Mediated Pro-oxidant State and Apoptotic Resistance

The oncogenic potential of Rac1 mediated through ROS production in cancer cells was further demonstrated by our laboratory where we showed constitutively active mutant of Rac1, V12, increased intracellular O_2^- production in human melanoma M14 cells leading to their resistance towards various chemotherapeutic drugs while transient introduction of the dominant negative mutant N17 decreased O_2^- levels and greatly enhanced the sensitivity of those cells. In addition, inhibition of Rac1 in T24 bladder carcinoma cells with mutant Ras also significantly decreased O_2^- levels and increased their sensitivity to both receptor and drug mediated apoptosis. On the contrary, the effect could be reversed with inhibition of the cytosolic O_2^- scavenger Cu/ZnSOD indicating that the apoptotic resistance of oncogenic Ras-expressing cancer cells could be associated with increase in the steady state levels of intracellular O_2^- mediated through Rac1 activation[103].

As discussed in earlier section that Bcl-2 overexpression leads to a pro-oxidant intracellular milieu conferring resistance to apoptotic execution, interestingly, transient transfection of the dominant negative mutant Rac1N17 compromised the pro-oxidant status thus bypassing the resistance. This resulted in a remarkable

increase in the sensitivity of Bcl-2-overexpressing CEM (chronic myeloid leukaemia) cells to receptor or drug-induced apoptosis[114]. Intrigued by these findings, we set out to investigate the possibility of a physical interaction between these two proteins which could explain their functional relevance. Indeed, preliminary results from our laboratory showed that Rac1 and Bcl-2 interacted at the mitochondria providing hint that this interaction might possibly contribute towards the pro-oxidant state and apoptotic resistance induced by Bcl-2 overexpression. Interestingly, although Rac1 is found to be associated with membranes, its predominant membrane residence reported in the literature is plasma membrane and little is known about its mitochondrial membrane association except for a few reports published so far. Boivin and Beliveau reported in 1995 that Rac1 was found in the pure mitochondria from rat kidney cortex using sucrose gradient centrifugation[276]. Another group also reported in 2003 that Rac1 co-localized with Mitotracker, a mitochondrial marker, by confocal microscopic analysis. In addition, Rac1 was observed in the mitochondria-enriched fractions obtained through differential centrifugation[277]. More recently, Heather *et al.* reported the presence of Rac1 in the intermembrane space of mitochondria where the fraction was obtained following digitonin treatment of mitochondria fractions[278]. Indeed, previous results from our group also demonstrated the existence of Rac1 in the mitochondria through: 1) electron microscopic analysis[70]; 2) confocal microscopic analysis on the co-localization of Rac1 with Mitotracker (data not shown); 3) western blot analysis of mitochondria-enriched fractions through differential centrifugation[70]. As such, in view of the mitochondrial localization of Rac1 and its interaction with Bcl-2, further investigations in establishing the interaction and characterizing the binding domains as well as elucidating the functional relevance of the complex in the mitochondrial redox status from a cancer context would be of great

significance for therapeutic management of cancers where Bcl-2 overexpression presents a major hindrance in the clinic.

1.5. Therapeutic Targeting of Bcl-2 in Cancers

1.5.1 Clinical Significance of Targeting Oncogenic Bcl-2

The carcinogenic potential of Bcl-2 was first demonstrated in 1988 where mice injected subcutaneously with the NIH3T3 cells having a stably transfected Bcl-2 resulted in tumour formation[126]. This was supported later by another group where they showed that transgenic mice with stable Bcl-2 overexpression led to massive lymphadenopathy as compared to their normal counterparts due to delayed apoptosis of B-cell lymphocytes resulting in the expansion of those cells in the follicular centre[279]. Further understanding of the oncogenic role of Bcl-2 came from the study in 1991 where genetically engineered Bcl-2-knockout mice demonstrated the importance of Bcl-2 for the survival of T-lymphocytes through protection against radiation-induced cell death[280]. These earlier findings laid the foundation for the subsequent studies to identify Bcl-2's role in apoptotic inhibition through the prevention of MOMP and more recently the new facet of Bcl-2 biology in redox regulation that also contributes to its anti-apoptotic property, is being gradually revealed. The pro-oxidant state induced by Bcl-2 overexpression not only creates an intracellular milieu non-permissive for death execution and stimulates proliferative signals but also promotes genomic instability due to the mild but chronic oxidative stress leading to carcinogenesis[281].

It is now well established that overexpression of Bcl-2 is one of the intrinsic or acquired mechanisms for chemoresistance in a great number of cancers, which has been associated with poor disease prognosis[123]. The list of Bcl-2 dysregulation includes hematologic cancers such as B-cell chronic lymphocytic leukaemia (CLL), acute myeloid leukaemia (AML), follicular lymphoma and multiple myeloma[282] as well as solid tumours such as melanoma[283], head and neck cancers[284], breast[285], lung[286], pancreatic[287], colon[288] and prostate cancers[289], which stress the significance of targeting Bcl-2 therapeutically in the clinical settings. However, conventional strategies which aim at counteracting Bcl-2 by either antisense oligonucleotides to reduce its expression or BH3 mimetics that sit in the BH3 domain groove and inhibit its activity, have showed limited success to be used as a single agent based on experimental and clinical evidences. The emerging role of Bcl-2 as a redox regulator as well as the significance of ROS in cell fate decision have highlighted the potential of a novel approach that combines the targeting of pro-oxidant Bcl-2 with conventional chemotherapies[123, 290].

1.5.2   Current Strategies in Overcoming Bcl-2 Mediated Apoptotic Resistance

1.5.2.1 Antisense oligonucleotides

Since Bcl-2 is overexpressed in many cancers, the first strategy that is logical to think of would be to target it through down-regulation of its expression levels. This could be achieved through antisense strategy which utilizes short stretches of chemically modified oligodeoxynucleotides (18-21-mer) that are complementary to specific regions of the target mRNA. DNA binding to the sequence specific mRNA

results in the inhibition of gene expression by blocking the translation of the mRNA or targeting the mRNA for RNase H mediated degradation.

G3139, an 18-mer oligonucleotide named as oblimersen (Genasense™), targets the first six codons of Bcl-2 mRNA. The phosphothiorate modification renders the oligonucleotide more stable *in vitro* and can efficiently down-regulate Bcl-2 expression, for example, by more than 80% in human breast cancer cells and the reduction in protein levels was associated with 80-95% loss of cell viability due to induction of MOMP and caspases. The breast cancer cells with down-regulated Bcl-2 expression were also observed to be more sensitive towards cytotoxic drugs[291]. Furthermore, Bcl-2 down-regulation by Genasense, followed by the administration of rituximab is an efficient anti-tumour strategy associated with improved survival in lymphoma-bearing severe combined immunodeficiency (SCID) mice, corroborating the *in vitro* data[292]. In another mouse xenograft model of B-cell lymphoma, the treatment of Genasense before addition of the proteosomal inhibitor bortezomib and cyclophosphamide enabled the eradication of B-cell lymphoma from the mice[293]. Genasense was first used in clinical trial to treat Non-Hodgkin's lymphomas (NHL) which mostly overexpress Bcl-2[294]. Although only modest results were observed, due to its limited toxicity, Genasense has been approved for evaluation of its effectiveness in several other cancers such as small cell lung cancer, prostate cancer[295] and renal cell carcinoma[296]. Genasense has also been used with a variety of conventional anticancer treatments as a combination approach, some of which have been very promising. A phase II trial combining Genasense with rituximab in NHL was completed in 2010 and the results demonstrated the safety of the combination treatment and it seems to be most beneficial in patients with indolent

NHL[297]. A Phase III trial involving the combination of Genasense with fludarabine plus cyclophosphamide for the treatment of patients with refractory or relapsed CLL increased the complete response rate as compared to fludarabine/cyclophosphamide alone[298]. Results from another phase III clinical trial on the combination of Genasense with dacarbazine for patients with advanced melanoma also showed significantly improved multiple clinical outcomes and increased overall survival[299]. However, the results from myeloma and AML patients have not been too successful. This could be due to the overexpression of other pro-survival Bcl-2 family members and also the hindrance can come from the lack of efficient delivery and stability *in vivo*[300].

Interestingly, the phosphorylation status of Bcl-2 at the flexible loop region, in particular, on the residue Ser70 is critical in the Bcl-2 antisense sensitization model. Non-phosphorylatable mutant S70A showed greater sensitivity towards the combined treatment of a Bcl-2 antisense oligodeoxynucleotide (although the exact target site was not revealed) and vitamin E analogue α-tocopheryl succinate (α-TOS) whereas the phosphomimetic S70E was remarkably resistant to apoptosis in human acute lymphocytic leukaemia Jurkat cells. Computational modelling revealed that a unique hairpin conformation that resembles a BH3 mimetic was adopted by α-TOS to dock onto the hydrophobic BH3 domain groove of Bcl-2[301].

1.5.2.2 BH3 domain peptides

Apart from down-regulating the expression levels of Bcl-2, another approach is to interfere with Bcl-2's function by blocking its activity. Based on the BH3

domains of Bax and Bad, Shangary and group synthesized peptides that bind to the hydrophobic groove of Bcl-2 and displace pro-apoptotic members and they showed that these peptides were able to induce cytochrome c release and thus apoptosis in Bcl-2-overexpressing cells indicating the potential of BH3 domain peptides to be used as anti-cancer therapeutics[155, 302]. BH3 peptides have also been shown to trigger oligomerization of Bax and Bak resulting in MOMP[156]. However, the use of BH3 peptides as therapeutics is limited due to their poor solubility, metabolic stability, bioavailability and cell permeability *in vivo*. Nonetheless, several approaches have been taken to address these problems, such as tagging the peptides with protein transduction domain from Drosophila antannepedia protein or alternatively from HIV TAT (Human Immunodeficiency Virus trans-activator of transcription) protein as well as chemical modification by synthesizing hydrocarbon stapled BH3 helices to improve cell permeability and resistance to protease digestion[303]. These approaches have enabled several groups to use BH3 peptidomimetics to trigger apoptosis in several cancers including leukaemia[304], neuroblastoma[305] and head and neck cancer[306].

1.5.2.3 BH3 mimetics

More recently, based on computational modelling, structure-based design or high throughput screening, several groups have discovered small molecule compounds that mimic the action of pro-apoptotic BH3 proteins by binding specifically to the BH3 domain groove of pro-survival Bcl-2 family proteins. As such, they are named as BH3 mimetics. For cancer cells that overexpress the pro-survival members of the Bcl-2 family, they tend to be more sensitive towards BH3 mimetics as compared to their normal counterparts.

One of the first *bona fide* BH3 mimetics is a benzenesulfonyl derivative designed on the structure basis of a naturally occurring cottonseeds-derived Bcl-2 inhibitor, gossypol, which is named as TW-37[307]. It has been shown to induce apoptosis in many malignancies including diffuse large B-cell lymphoma, ALL, mantle cell lymphoma[308, 309] and pancreatic cancer[310]. In addition, TW-37 has been demonstrated to increase sensitization of the cancer cells to a range of conventional drugs[311]. Interestingly, synergistic effects were also observed combining TW-37 with the MEK inhibitor U0126 in melanoma cells. The killing effects were mediated through selective p53 activation which was induced by ROS production sparing normal cells. The intrinsic vulnerability of the melanoma cells with dysregulated redox buffering capacity to handle ROS suggests the potential use of this combination regimen in the clinical management of this disease.

ABT-737 is another extensively studied BH3 mimetic, which is also derived from gossypol as an analogue by Abbott (Abbott Laboratories, Abbott Park, IL, USA). As compared to previously reported compounds, it has a significantly enhanced potency with two to three orders of magnitude higher binding affinity towards Bcl-2[312]. Konopleva and group showed that ABT-737 acts as a Bad BH3-only molecule which binds to Bcl-2 displacing Bax and in addition, Bak is also required for efficient killing in mouse embryonic fibroblast (MEF) cells[313]. Enhanced sensitivity to chemotherapeutic agents has also been observed with ABT-737. Numerous studies have demonstrated that primary cells from patients were extremely sensitive to ABT-737 in the nanomolar range, including ALL, lymphocytic leukaemia[314-316], follicular lymphoma and marginal zone lymphoma[313]. The drug is now in the phase II clinical trial[311]. A modified version of ABT-737, ABT-263, with higher oral

availability, is now in the phase I/II clinical trial as well to treat various malignancies including CLL, lymphoma and small cell lung cancer[311, 317-319]. The extremely high binding affinity to Bcl-2 (less than 100 picomolar) makes ABT-737/ABT-263 much more promising therapeutic candidates as compared to other small molecules discussed above[320].

However, ABT-737 only binds Bcl-2, Bcl-xL and Bcl-w but not Mcl-1, thus it is inactive in those cancer cells with Mcl-1 overexpression unless a combination treatment is used which reduces the expression levels or inhibits the activity of Mcl-1. In addition, the phosphorylation status of Bcl-2 also affects the efficacy of this compound. Inhibition of Bcl-2 phosphorylation either by using a MEK1 inhibitor or introduction of a non-phosphorylatable mutant on the three phosphorylation sites within the flexible loop region of Bcl-2 has been demonstrated to restore the sensitivity *in vitro*[312, 314]. Interestingly, inhibition of Bcl-2 function with ABT-737 resulted in a significant depletion of cellular GSH levels in human cervical cancer HeLa cells and Jurkat cells. This has been accounted for the subsequent increase in intracellular ROS levels, caspase activation and finally apoptosis[321] stressing the significance of Bcl-2 as a redox regulator to maintain the ROS levels within an optimal threshold and suggesting the potential of combination treatment with Bcl-2 targeting and ROS-inducing agents[123].

In that regard, further understanding of Bcl-2 function in redox regulation and elucidation of other players involved that could serve as potential druggable targets

would pave the way for future therapeutic design, which forms the basis of the aims in this thesis.

1.6. Aims

This work originated from the attempts to elucidate the source(s) of O_2^- induced by Bcl-2 overexpression, and how this contributes to its carcinogenic property from a novel perspective. Preliminary results indicated the involvement of Rac1 in this pathway probably through a physical interaction as mentioned in earlier section. Intrigued by these findings, this thesis aims to confirm and establish the functional involvement of Rac1 in pro-oxidant status induced by Bcl-2, to confirm and establish the physical interaction, to characterize the binding domains involved and to elucidate the functional relevance and potential downstream players of this interacting complex in the cancer context with specific focus on redox regulation and chemoresistance.

1.6.1   Establishing the Regulatory Role of Rac1 in Bcl-2 Mediated Pro-oxidant State

- To test the hypothesis that Bcl-2 (but not another pro-survival Bcl-2 family member Bcl-xL) is able to induce a pro-oxidant status in cancer cells with a specific focus on mitochondria O_2^- levels.

- To assess the functional involvement of Rac1 in Bcl-2 mediated pro-oxidant state through 1) measurement of Rac1 activation status across cancer cell lines with differential Bcl-2 expression levels as well as upon transient Bcl-2 overexpression; 2) measurement of mitochondrial O_2^- levels upon pharmacological inhibition of Rac1.

1.6.2   Establishing the Physical Interaction between Rac1 and Bcl-2

- To assess the co-localization of Rac1 and Bcl-2 through fluorescence microscopic analysis in cancer cells transiently transfected with both mCherry-Rac1 and GFP-Bcl-2.

- To assess the physical interaction of Rac1 and Bcl-2 through co-immunoprecipitation assay across cancer cell lines with different Bcl-2 expression levels.

- To assess the cancer specificity of the interaction through checking the presence of the interaction by co-immunoprecipitation assay in peripheral blood mononuclear cells (PBMCs) obtained from normal healthy donors.

1.6.3   Establishing the Localization of the Interacting Complex

- To assess the mitochondrial localization of Rac1 through subcellular fractionation studies in cancer cell lines as well as human fibroblast cell lines, which differ in Bcl-2 expression levels.

- To check for the requirement of post-translational geranylgeranylation in the mitochondria targeting of Rac1 (through subcellular fractionation study) as well as its involvement in Rac1-Bcl-2 interaction (through co-immunoprecipitation assay) upon pharmacological inhibition of the geranylgeranyltransferase I.

1.6.4   Identifying the Critical Functional Elements and Binding Domains/Residues for the Interaction

- To investigate whether the activation status of Rac1 is essential for its interaction with Bcl-2 through co-immunoprecipitation assay upon: 1) crude *in vitro* loading of either the non-hydrolysable GTP analogue GTP-γS or GDP to manipulate its activation status; 2) transient transfection of either the constitutively active Rac1V12 or the dominant negative Rac1N17 mutants; 3) pharmacological inhibition of Rac1 activity.

- To investigate whether Nox family proteins are involved in the interaction through:1) checking the interaction levels upon general pharmacological inhibition of Nox proteins followed by co-immunoprecipitation analysis; 2) identifying the presence of Nox subunits in mitochondria through subcellular fractionation study.

- To identify the specific residue(s) of Rac1 involved in the interaction preliminarily through transient transfection of different Rac1 point mutants followed by co-immunoprecipitation analysis.

- To identify the specific domain(s)/region(s) of Bcl-2 critical for its interaction with Rac1 through co-immunoprecipitation analysis upon 1) blocking of its BH3 domain with Bcl-2 BH3 peptides; 2) blocking of its BH4 domain with Bcl-2 BH4 peptides; 3) transient transfection of either non-phosphorylatable or phosphomimetic mutants in the flexible loop region that connects BH3 and BH4 domains.

1.6.5   Establishing the Link between Two of the Parameters Critical for the

Interaction: Rac1 Activation and Bcl-2 Phosphorylation Status

- To investigate whether active Rac1 can induce Bcl-2 phosphorylation on the particular residue Ser70 located at the flexible loop region through 1) transient introduction of Bcl-2 into cancer cells with stably transfected constitutively active Rac1V12 or dominant negative Rac1N17; 2) transient transfection of Rac1V12 or Rac1N17; 3) pharmacological inhibition of Rac1.

- To identify the kinase(s) involved in active Rac1-induced Bcl-2 phosphorylation at residue Ser70 as well as to further confirm its/their involvement in the interaction through pharmacological inhibition of the kinase(s).

1.6.6   Studying the Functional Implication(s) of the Interaction

- To investigate the redox regulatory ability of Rac1-Bcl-2 interaction through measurement of mitochondrial O_2^- levels upon disruption of the interaction through 1) Bcl-2 BH3 peptides; 2) pharmacological inhibition of Rac1.

- To investigate whether disruption of this interaction, through 1) Bcl-2 BH3 peptides; 2) pharmacological inhibition of Rac1; 3) siRNA-mediated silencing of Rac1 expression levels, can sensitize Bcl-2-overexpressing cancer cells to conventional chemotherapeutic drugs based on assessment of the cell proliferation/viability as well as cell cycle profile analysis.

1.6.7 Identifying Additional Downstream Players Involved in the Rac1-Bcl-2 Interaction Pathway through ™CELLWORKS In Silico Modelling

- To confirm the tumorigenic properties of Rac1 and Bcl-2 through manipulation of their expression levels in the modelled HCT116 human colorectal carcinoma cells based on phenotypic indexes such as angiogenesis, proliferation, viability, metastasis and tumour volume as well as O_2^- levels and apoptotic markers.

- To identify the downstream players whose protein levels are affected upon virtual manipulation of Rac1 and/or Bcl-2 expression levels.

- To investigate through wet lab experiments whether STAT3 is a downstream target of Rac1-Bcl-2 interaction pathway as predicted by 1) checking the mitochondrial localization of STAT3; 2) studying whether Bcl-2 overexpression can induce STAT3 activation as marked by the phosphorylation on Tyr705; 3) investigating whether Bcl-2-induced STAT3 activation is dependent on Rac1 activity with the use of the pharmacological inhibitor of Rac1; 4) investigating whether Bcl-2-induced STAT3 activation is redox regualted with the use of the general Nox inhibitor; 5) investigating whether there are physical interactions between each of these three proteins: Rac1, Bcl-2 and STAT3 based on co-immunoprecipitation analysis.

CHAPTER 2: MATERIALS AND MATHODS

2.1. Chemicals

Acrylamide/bis-acrylamide (30% solution), Coomassie Plus Protein Assay Reagent, Stable Peroxide Solution and SuperSignal West Pico Luminol/Enhancer Solution were obtained from Pierce, IL, USA.

Ammonium persulfate (APS), bovine serum albumin (BSA), daunorubicin hydrochloride, 3-(4,5-dimethylthiazol-2-yl)-2,5-diphenyltetrazolium bromide (MTT), diphenyleneiodonium chloride (DPI), dithiothreitol (DTT), ethylenediaminetetraacetic acid (EDTA), ethylene glycol tetraacetic acid (EGTA), 4-(2-hydroxyethyl) piperazine-1-ethanesulfonic acid (HEPES), isopropanol, leupeptin, magnesium chloride ($MgCl_2$), Nickel-enhanced 3, 3 diaminobensidine tetrahydrochloride (DAB) solution, pepstatin A, phenylmethanesulfonyl fluoride (PMSF), potassium chloride, propidium iodide (PI), sodium chloride (NaCl) and SP600125 were obtained from Sigma-Aldrich, LO, USA.

Benzyloxycarbonyl-Val-Ala-Asp (OMe)-fluoromethylketone (Z-VAD-FMK) was obtained from ALEXIS, San Diego, USA.

Dimethyl sulfoxide (DMSO) was obtained from MPBiomedicals, OH, USA.

Dulbecco's Modified Eagle's Medium (DMEM), fetal bovine serum (FBS), L-glutamine, penicillin & streptomycin (PS), phosphate buffered saline (PBS) and Roswell Park Memorial Institute Medium (RPMI 1640) were obtained from HyClone, UT, USA.

EHT1864 was obtained from Tocris Bioscience, Bristol, United Kingdom.

GGTI-2147 and NSC23766 were obtained from Calbiochem, CA, USA.

100X Guanosine 5'-O-[gamma-thio] triphosphate (GTP-γS), 100X guanosine diphosphate (GDP) and p21-activated kinase 1 p21-binding domain (PAK1 PBD) conjugated with agarose were obtained from Millipore, MA, USA.

G418 and hygromycin B were obtained from Roche Diagnostics Corporation, IN, USA.

Hoechst 33342, MitoSox, and N,N,N,N-tetramethylethylenediamine (TEMED) were obtained from Invitrogen, CA, USA.

Lucigenin and etoposide were purchased from Sigma Chemical Co, MO, USA.

Methanol, ribonuclease A (RNase A), and sodium dodecyl sulphate (SDS) were obtained from AppliChem, Darmstadt, Germany.

MitoTracker was obtained from Molecular Probes, Eugene, OR, USA.

Precision Plus Protein Standards and Tween-20 were obtained from Bio-Rad, CA, USA.

Protein A agarose and glutathione agarose were obtained from Santa Cruz Biotechnology, CA, USA.

SuperFect Transfection Reagent was obtained from QIAGEN, Hilden, Germany.

Triton X-100 was obtained from USB, OH, USA.

Vincristine was from ICN Pharmaceuticals Inc., OH, USA.

2.2. Antibodies

Alexa Fluor® 488 goat anti-mouse IgG and Alexa Fluor® 568 goat anti-rabbit IgG were obtained from Molecular probes Invitrogen, CA, USA.

Biotinylated secondary mouse and rabbit secondary antibodies were obtained from Vector Laboratories, Burlingame, CA, USA.

Clean-Blot IP Detection Reagents were obtained from Thermo Scientific, IL, USA.

Goat anti-mouse IgG horseradish peroxidase (HRP) and goat anti-rabbit IgG HRP were obtained from Pierce, IL, USA.

Goat polyclonal anti-Flotillin, rabbit polyclonal anti-Nox2 and rabbit polyclonal anti-Nox4 were obtained from Abcam, Cambridge, UK.

Goat polyclonal anti-p22phox, goat polyclonal anti-VDAC, mouse monoclonal anti-myc-tag, mouse monoclonal anti-p-JNK (Thr183/Tyr185), mouse monoclonal anti-STAT3, rabbit monoclonal anti-PARP, rabbit monoclonal anti-p-Bcl-2 (Ser70), rabbit monoclonal anti-p47phox, rabbit polyclonal anti-c-Jun, rabbit polyclonal anti-Cu/Zn SOD, rabbit polyclonal anti-p-c-Jun (Ser63) and rabbit

polyclonal anti-p-STAT3 (Tyr705) antibodies were obtained from Cell Signalling Technology, MA, USA.

Mouse control IgG, mouse monoclonal anti-β-actin, mouse monoclonal anti-Bax, mouse monoclonal anti-Bcl-2, mouse monoclonal anti-Bcl-xL, mouse monoclonal anti-pan-Ras, rabbit polyclonal anti-Bcl-2, rabbit polyclonal anti-Rac1 and rabbit polyclonal anti-STAT3 antibodies were obtained from Santa Cruz Biotechnology, CA, USA.

Mouse monoclonal anti-Rac1 antibody was obtained from Upstate, NY, USA.

Rabbit control IgG was obtained from ProSci Incorporated, CA, USA.

2.3.   Chemical Synthesis of Peptides

The Bcl-2 BH3 (PVVHLTLRQAGDDFSR), Bcl-2 BH4 (TGYDNREIVMKYIHYKLSQRGYEW) and control peptides with no homology to human protein sequence (ALILTLV) were fused with an internal sequence of HIV TAT (Human Immunodeficiency Virus trans-activator of transcription) protein (KKKRRQRRR) to ensure cell permeability. The peptides were synthesized by 1st BASE (Science Park II, Singapore), dissolved in sterile distilled H_2O and kept as 10 mM stocks in the -80˚C freezer.

2.4. cDNA Plasmids

Bcl-2 and its control vector pcDNA3, Bcl-xL and its control vector pBabe plasmids were a kind gift from Dr. Elizabeth Yang (Vanderbilt University, USA). Bcl-2 single non-phosphorylatable mutant S70A and phosphomimetic mutant S70E were generated by our laboratory using QuikChange®Site-Directed Mutagenesis Kit (Stratagene, CA, USA). Bcl-2 triple non-phosphorylatable mutant T69A/S70A/S87A (AAA) was obtained from Addgene, MA, USA. Green fluorescent protein (GFP) tagged Bcl-2 and GFP tagged Bcl-xL plasmids were kindly provided by Dr. Victor Yu (Institute of Molecular and Cell Biology, Singapore). The empty vector GFP-C1 was a kind gift from Dr. Tang Bor Luen (National University of Singapore, Singapore). mCherry tagged Rac1 plasmid (cloned in SacI and NotI sites of pCAG vector backbone) was constructed by Quek Shuwen Alan from our laboratory and the control mCherry plasmid was kindly provided by Dr. Tapan (Genome Institute of Singapore, Singapore). The constitutively active Rac1 mutant V12, dominant negative Rac1 mutant N17 and control vector pIRES plasmids were a kind gift from Dr. Clément Marie-Veronique (National University of Singapore, Singapore). The red fluorescent protein tagged Rac1 (RFP-Rac1) and control RFP plasmids were kindly provided by Dr. Edward Manser (Institute of Medical Biology, Singapore).

2.5. Buffers

2.5.1 Buffers for Western Blot Analysis

RIPA lysis buffer for total cell lysate preparation: 50 mM Tris HCl (pH 7.5), 150 mM NaCl, 1% Nonidet P40, 1 mM EDTA. Protease and phosphatases inhibitors

(10 µg/ml aprotinin, 10 µg/ml leupeptin, 20 µg/ml pepstatin A, 1 mM NaF, 1 mM Na$_3$VO$_4$, 1 mM PMSF) were added fresh before each lysis.

1X Lammeli loading buffer: 50 mM Tris-HCl (pH 6.8), 50 mM DTT, 2% SDS, 0.1% bromophenol blue, 10% glycerol.

12% Resolving gel for SDS-PAGE (polyacrylamide gel electrophoresis): 30% acrylamide/bis-acrylamide, 1.5 M Tris (pH8.8), 10% SDS, 10% APS, TEMED.

5% Stacking gel for SDS-PAGE: 30% acrylamide/bis-acrylamide, 1.0 M Tris (pH 6.8), 10% SDS, 10% APS, TEMED.

Running buffer for SDS-PAGE: 25 mM Tris base (pH 8.3), 250 mM glycine, 0.1% SDS.

Wet transfer buffer: 39 mM glycine, 48 mM Tris base, 20% methanol.

Tris-buffered saline with Tween20 (TBST): 137 mM NaCl, 20 mM Tris-HCl (pH 7.6), 0.1% Tween-20.

Blocking buffer: 5% non-fat milk in TBST.

2.5.2　Mg^{2+} Lysis/Wash Buffer (MLB) for Rac1 Activation Assay

5X MLB: 125 mM HEPES (pH 7.5), 750 mM NaCl, 5% Igepal CA-630, 5 mM EDTA, 50 mM MgCl$_2$, 10% glycerol. Dilute to 1X by adding 4 mL sterile, distilled water containing 10% glycerol to each ml of 5X MLB used. Protease inhibitors (10 mg/mL Leupeptin, 10 mg/mL aprotinin) and phosphatase inhibitors (1 mM NaF, 1 mM Na$_3$VO$_4$) were added fresh before each lysis.

2.5.3　Buffer for Co-immunoprecipitation (Co-IP)

50 mM Tris (pH 7.6), 150 mM NaCl, 0.5% Nonidet P-40, 1 mM EDTA. Protease and phosphatase inhibitors (10 μg/ml aprotinin, 10 μg/ml leupeptin, 20 μg/ml pepstatin A, 1 mM NaF, 1 mM Na$_3$VO$_4$, 1 mM PMSF) were added fresh before each lysis.

2.5.4　Buffers for Subcellular Fractionation

Extraction buffer A for mitochondrial fractionation: 50 mM PIPES-KOH (pH 7.4), 50 mM KCl, 220 mM mannitol, 68 mM sucrose, 5 mM EGTA, 1mM DTT, 2 mM MgCl$_2$. Protease and phosphatase inhibitors (10 μg/ml aprotinin, 10 μg/ml leupeptin, 20 μg/ml pepstatin A, 1 mM NaF, 1 mM Na$_3$VO$_4$, 1 mM PMSF) were added fresh before each use.

Buffer for subcellular fractionation of heavy membrane (HM), light membrane (LM) and cytosol: 25 mM HEPES KOH (pH 7.6), 0.5 M KCl, 0.5 mM EDTA, 1 mM DTT, 5 mM $MgCl_2$, 10% glycerol, 0.5% Tween-20. Protease and phosphatase inhibitors (10 μg/ml aprotinin, 10 μg/ml leupeptin, 20 μg/ml pepstatin A, 1 mM NaF, 1 mM Na_3VO_4, 1 mM PMSF) were added fresh before each use.

2.6.   Cell Lines and Culturing of Cells

The human chronic myeloid leukaemia CEM cells stably transfected with pcDNA3 vector containing either the neomycin gene (CEM/Neo) or the human Bcl-2 gene (CEM/Bcl-2) were generously provided by Dr. Roberta A Gottlieb (Scripps Cancer Centre, USA). CEM cells were cultured in RPMI 1640 medium supplemented with 5% FBS, 1% L-glutamine and 1% PS at 37°C in a humidified incubator with 5% CO_2. The stable clones were maintained in 20 μg/ml of selective antibiotics G418.

The human cervical carcinoma HeLa cells were obtained from American Type Culture Collection (ATCC, MD, USA). HeLa stably transfected with pcDNA3 vector containing either the neomycin gene (HeLa/Neo) or the human Bcl-2 gene (HeLa/Bcl-2) as well as HeLa (ATCC) cells were cultured in DMEM medium supplemented with 10% FBS, 1% L-glutamine and 1% PS. The stable clones were maintained in 20 μg/ml of selective antibiotics G418.

The human B cell lymphoma Raji and human T cell lymphoma Jurkat cells obtained from ATCC were cultured in RPMI 1640 medium supplemented with 10% FBS, 1% L-glutamine and 1% PS.

The human lung fibroblast MRC5 and IMR90 cells were kindly provided by Dr. Manoor Prakash Hande (National University of Singapore, Singapore).

The human melanoma M14 cells stably transfected with pIRES vector containing the hygromycin gene or the constitutively active mutant of human Rac1 gene (V12) or the dominant negative Rac1N17 gene were cultured in DMEM medium supplemented with 5% FBS, 1% L-glutamine and 1% PS. The stable clones were maintained in 0.5% of selective antibiotics hygromycin B.

Trypsin (0.25%) was used to detach adherent cells from culture flasks and the cells were then pelleted by centrifugation at 1200 rpm for 5 mins at 22°C followed by resuspension in DMEM medium. The number of cells was counted by a haemocytometer before seeding of cells onto culture well plates followed by overnight incubation to allow for attachment prior to start of treatment.

2.7. Clinical Human Samples

Peripheral blood mononuclear cells (PBMCs) were isolated from whole blood using Ficoll-Paque^TM kit (GE Healthcare Bio-Sciences, Singapore) and kindly provided by Dr. Wang Binbin (National University of Singapore, Singapore).

2.8. Amplification and Purification of Plasmids

Plasmids (1 μg each) were mixed gently with 100 μl of competent *E. coli* cells and the mixture was incubated on ice for half an hour. After that, the mixture was incubated at 37°C in a water bath for 45 secs for a heat shock and was then transferred back to ice for 2 mins followed by transfer to 0.9 ml lysogeny broth (LB) with either ampicillin or kanamycin and incubated in a shaker at 200 rpm, 37°C for half an hour. After the incubation, the bacteria broth culture was spread on an LB plate (with either ampicillin or kanamycin) and kept in a bacteria incubator for 16 hrs at 37°C. On the following day, one colony was picked from each bacteria agar plate by a sterile pipette tip and thrown into LB broth (with either ampicillin or kanamycin) in a miniculture tube for incubation in a shaker at 200 rpm, 37°C for 16 hrs. After that, 1ml of each miniculture was added into 250 ml LB broth (with either ampicillin or kanamycin) and again incubated in a shaker at 200 rpm, 37°C for 16 hrs to get a maxiculture.

After amplification of plasmids, they were then purified with PureYield^TM Plasmid Maxiprep System (Promega, WI, USA). The transformed *E. coli* cells were first centrifuged at 5,000 g for 10 mins and the pellet was resuspended in 12 ml Cell Resuspension Solution followed by addition of 12 ml Cell Lysis Solution. The

mixture was then inverted 3-5 times gently and incubated for 3 mins at room temperature followed by addition of 12 ml Neutralization Solution and again inverted for 10-15 times to mix. The bacteria cell lysate was then centrifuged at 14,000 g for 20 mins and the supernatant was passed through the PureYield^{TM} Clearing Column and Maxi Binding Column on a vacuum manifold. After that, 5 ml of Endotoxin Removal Wash was added to the PureYieldTM Maxi Binding Column followed by another 20 ml of Column Wash. The column membrane was then dried for 5 mins by applying vacuum followed by addition of 1.5 ml of Nuclease-Free Water and centrifugation at 2,000 g for 5 mins at room temperature. The eluate that contained the DNA was then collected. In order to increase the DNA concentration, ethanol precipitation was carried out by adding 1/10 volume of 3 M sodium acetate (pH 5.2) and 2.5 volumes of 95% ethanol followed by incubation on ice for 15 mins. The DNA was then pelleted at 14,000 g for 10 mins, washed with 70% ethanol, mixed well and again centrifuged at 14,000 g for 2-5mins. Finally the pelleted DNA was resuspended in water and kept in -20°C.

2.9. Transient Transfection

HeLa cells (0.25×10^6 cells/well/2ml of DMEM medium for 6-well plates) were seeded one day prior to transfection. On the day of transfection, 2 μg plasmid was mixed with 200 μl of plain DMEM medium and 8 μl of SuperFect reagent. The mixture was vortexed for 10 secs and incubated at 37°C for 10 mins. The mixture was then topped up with 300 μl of DMEM medium and added drop by drop into the wells and incubated at 37°C for 3 hrs. The cells were then washed three times with 1X PBS and incubated in fresh DMEM medium for 48 hrs at 37°C.

2.10. siRNA Mediated Silencing

siRNA for endogenous Rac1 was purchased from Ambion, CA, USA. As a negative control, the scrambled siRNA, a perfectly unique sequence which does not match to any sequence in the human genome, was used as recommended by the manufacturer. Transient transfections were carried out using siPORT™ NeoFX™ Transfection Agent (Ambion, CA, USA) and 30nM of Rac1 siRNA. The expression levels of Rac1 were analysed by western blot using anti-Rac1 antibody 48 hrs after the transfection.

2.11. Protein Assay

Protein concentration of cell lysate was determined using Coomassie Plus Protein Assay Reagent. 5 µl of lysate was added to 150 µl of the reagent and loaded into a 96-well plate. Absorbance was measured at 595 nm using a microplate reader (GENios Plus, Tecan, Männedorf, Switzerland). BSA of different concentrations was used as protein standards.

2.12. Western Blot Analysis

Cells were lysed using RIPA lysis buffer containing protease and phosphatase inhibitors. After boiling at 100°C for 5 mins on a heat block, an average of 60 µg of total protein per sample was subjected to 12% SDS-PAGE at 120 V for 1 hr. Precision Plus Protein Standards were used as molecular weight markers for the resolved protein bands. Following wet transfer of the resolved proteins, the polyvinylidene fluoride (PVDF) membrane was incubated with blocking buffer for 1hr on a shaker. After that, the membrane was washed with TBST three times (10 mins each) and

probed with desired primary antibody in TBST overnight on a shaker at 4°C. On the following day, the membrane was again washed three times and incubated with the respective secondary antibody in TBST with 1% non-fat milk on a shaker for 1 hr. Finally, after three washes the membrane was exposed to SuperSignal West Pico Luminol/Enhancer Solution and Stable Peroxide Solution for the protein bands to be visualized (Medical X-ray Processor, Kodak, NY, USA).

2.13. Measurement of Mitochondrial Superoxide Anion Levels

MitoSox is a live-cell permeable dye with hydroethidine (HE) covalently linked to a triphosphonium cation through a hexyl carbon chain and is selectively targeted to mitochondria due to the positive charge on the phosphonium group. The dye exhibits red fluorescence once it is oxidized by superoxide anion (O_2^-).

CEM cells (1.0×10^6 cells per sample) were washed once with 1X PBS and spun at 1200 rpm at 22°C for 5 mins. Pellet was then resuspended in 100 μl plain RPMI medium with 10 μM MitoSox dye and incubated in dark at 37°C for 15 mins. Excess dye was then washed away twice with 1X PBS and the pellet was resuspended in 500 μl plain RPMI medium. At least 10,000 events were analysed by flow cytometry (Epics Elite EPS, Beckman Coulter, FL, USA) and data was further analysed using WINMDI software.

2.14. Measurement of Intracellular Superoxide Anion Levels

The cells were lysed with 400 µl of 1X somatic cell ATP releasing reagent (Sigma-Aldrich, MO, USA). Next 100 µl of 850 µM lucigenin solution was injected automatically before the reading. Chemiluminescence was measured using a Berthold Sirius Luminometer (Berthold detection systems GmbH, Pforzheim, Germany) for 20 secs.

2.15. Quantification of Rac1 Activation Levels

2.15.1 Rac1 G-LISA™ Kit

The kit (Cytoskeleton Inc., CO, USA) contains a Rac-GTP-binding protein linked to the wells of a 96-well plate and only active, GTP-bound Rac1 in cell lysate will bind to the wells while inactive GDP-bound Rac1 is removed during washing steps. The bound active Rac1 is then detected with a Rac1 specific antibody by luminescence.

CEM cells were seeded onto 6-well plates (2.0 x 10^6 cells/well). After treatment, the cells were washed with ice old 1X PBS, lysed in 100 µl of ice cold Cell Lysis Buffer and immediately clarified by centrifugation at 14,000 rpm, 4°C for 2 mins. The cell lysate was then diluted with Lysis Buffer to equalize protein concentration in each sample (not higher than 2.0 mg/ml or below 0.3 mg/ml). The powder in the 96-well plate was dissolved with 100 µl ice cold water and the solution was completely removed just before the addition of cell lysate (25 µl lysate + 25 µl cold Binding Buffer) or blank control (25 µl Lysis Buffer + 25 µl cold Binding Buffer)

or positive control (5 μl Rac1 Control Protein + 45 μl cold Binding Buffer), accordingly. The plate was immediately placed on an orbital microplate shaker (400 rpm) at 4°C for exactly 30 mins. After 30 mins, the solution was flicked out and washed twice with 200 μl Wash Buffer at room temperature. Room temperature Antigen Presenting Buffer (200 μl) was immediately added into each well and incubated at room temperature for exactly 2 mins and washed three times with 200 μl each of room temperature Wash Buffer. Diluted anti-Rac1 primary antibody (50 μl) wash then added to each well and the plate was placed on the orbital microplate shaker (400 rpm) at room temperature for 45 mins and washed again three times with 200 μl each of room temperature Wash Buffer. Diluted secondary antibody (50 μl) was added after that to each well and the plate was placed on the orbital microplate shaker (400 rpm) at room temperature for 45 mins and washed again three times with 200 μl each of room temperature Wash Buffer. After the wash, 50 μl of HRP Detection Reagent was added and the luminescence signal was detected using a microplate reader (GENios Plus, Tecan, Männedorf, Switzerland).

2.15.2 Rac1 Activation Assay through Immunoprecipitation with PAK-1 PBD Agarose

Cell culture and extract preparation: Cells were pelleted by gentle centrifugation (500 g) and then rinsed twice with ice-cold TBS. Ice-cold MLB was added to the cell pellet (0.5-1 ml per 1.0×10^7 cells) to lyse cells by repeated (4-5 times) pipetting. If nuclear lysis occurs, the extract may be very viscous (and difficult to pipette) due to released genomic DNA. In that case, DNA may be sheared by passing the lysate through a 26-gauge syringe needle 3-4 times. The cell lysate was then precleared by adding 100 ml of glutathione agarose per 1 ml of lysate and

rocking for 10 mins at 4°C. The agarose beads were collected by pulsing for 5 secs in the microcentrifuge at 14,000 g. The supernatant was removed and aliquots were stored on ice (for immediate use) or snap frozen in liquid nitrogen and stored at -80°C (for long term).

In vitro GTP-γS/GDP loading for positive and negative controls: 0.5 ml of each cell extract was aliquoted to two microfuge tubes. To each tube, 20 ml of 0.5 M EDTA (to 10 mM final concentration) was added. For the positive control tube, 5 ml of 100X GTP-γS (to 100 mM final concentration) was added while 5 ml of 100X GDP (to 1 mM final concentration) was added to the negative control tube. The tubes were incubated at 30°C for 15 mins with agitation.

Rac1 pull-down assay: 10 ml (10 mg) of PAK-1 PBD agarose (Millipore, MA, USA) was immediately added per 0.5 mL of cell lysate. The reaction mixture was then gently rocked at 4°C for 60 mins (30 mins for GTP-γS and GDP loaded lysates). The agarose beads were collected by pulsing for 5 secs in the microcentrifuge at 14,000 g followed by 3 washes with 0.5 ml of MLB. After that, the agarose beads were resuspended in 40 ml of 2X laemmli reducing sample buffer, boiled for 5 mins and loaded onto SDS-PAGE for western blot analysis.

2.16. Cell Viability Assay

MTT can be reduced to a purple formazan by an active mitochondrial reductase, which only takes place in living cells. Since this conversion reaction is a

direct readout for the number of viable cells, the MTT reduction assay is commonly utilized to determine cell viability.

CEM cells were plated onto 12-well plates (1.0×10^6 cells/well) and after drug exposure, 50 μl of MTT (3 mg/ml in plain RPMI) was added to 50 μl of cells and followed by incubation for 2 hrs at 37°C in the dark. After that, the plate was spun at 3000 rpm for 5 mins. The supernatant was then removed and the crystal in each well was dissolved in 200 μl DMSO and 10 μl Sorenson's glycine buffer (0.1 M Glycine, 0.1 M NaCl, pH 10.5). Cell viability was assessed by dye absorbance measured at 570 nm with the microplate reader (GENios Plus, Tecan, Männedorf, Switzerland).

2.17. Immunofluorescence Microscopic Analysis

HeLa cells transfected with fluorescent protein tagged Bcl-2 or Rac1 plasmids were washed once with 1X PBS, fixed with paraformaldehyde (4% w/v) for 20 mins and permeabilized with 0.5% Triton X-100 for 5 mins. Washing with 1X PBS was done after fixing and permeabilization, respectively, for three times (5 mins each). Cells were then incubated with 10 μM Hoechst 33342 for 10 mins and washed three times with 1X PBS, after which cells were mounted onto slides and examined with a fluorescence microscope. The fluorescence of GFP was excited with 488nm laser line and fluorescence of mCherry was excited with 568-nm laser line. Pictures were taken with the same exposure settings analysed by FluoView 2.0 (Olympus, Hamburg, Germany).

For HeLa cells that were not transfected with fluorescent protein fusion plasmids, after fixing and permeabilization, they were blocked with 1% BSA (in 1X PBS) for 1 hr to prevent non-specific binding followed by incubation with respective primary antibodies for 2 hrs at room temperature. The cells were washed three times with 1X PBS (5 mins) and incubated with Alexa-fluo-conjugated IgG based secondary antibodies for fluorescent labelling followed by another three washes of 1X PBS (5 mins) before mounting onto glass slides for fluorescence microscopic analysis.

2.18. Co-immunoprecipitation

Cells (10×10^6) were pelleted, washed in 1 X PBS and incubated on ice with Co-IP lysis buffer for 20 mins. Subsequently, 4 μg of anti-Rac1 or anti-Bcl-2 or anti-STAT3 antibodies were added to 1000 μg of cell lysate and the mixture was incubated on a rotator overnight at 4˚C where interacting proteins could be co-immunoprecipitated. 40 µl of either protein A or protein G agarose beads were then added to the mixture rotating for 4 hrs at 4˚C to capture the immunocomplexes. The beads were washed three times with 1 ml of Co-IP lysis buffer, resuspended in 30µl of laemmli loading buffer and boiled for 15 mins to release the immunocomplexes. After that, the mixture was centrifuged at 14,000 g and the supernatant that contained the released immunocomplexes were loaded onto a 12% SDS-PAGE gel. Clean-Blot IP Detection Reagents were used in the follow-up western blot analysis to minimize the interference from IgG heavy and light chains.

For co-immunoprecipitation done on subcellular fractions, 60×10^6 cells were used for fractionation followed by subsequent incubation of different fractions with Co-IP lysis buffer.

2.19. Subcellular Fractionation by Differential Centrifugation

2.19.1 Mitochondrial Fractionation

20×10^6 cells were washed with ice-chilled 1 x PBS at 1200 g. Cell pellets were resuspended in 500 µl of extraction buffer A and incubated at 4°C for 20 mins, followed by Dounce homogenization. The homogenate was centrifuged at 300 g for 10 mins at 4°C. The supernatant was additionally centrifuged at 20000 g for 30 mins (fractions enriched with intact mitochondria). The supernatant from the last centrifugation was spun again at 100000g for 45 mins to get the cytosolic fraction. Immunoblotting with VDAC and Cu/Zn SOD antibodies was carried out to show the purity of mitochondria and cytosolic fractions, respectively.

2.19.2 Subcellular Fractionation of HM, LM and Cytosol

20×10^6 cells were washed with ice-chilled 1 x PBS at 1200 g. Cell pellets were resuspended in 600 µl of fractionation buffer and incubated at 4°C for 20 mins, followed by Dounce homogenization (20 strokes). The homogenate was centrifuged at 1000 g for 10 mins at 4°C. The supernatant was additionally centrifuged at 20,000 g for 20 mins to get the HM pellet (fractions enriched with intact mitochondria). The supernatant from the last centrifugation was spun again at 100,000 g for 1 hr to get the LM (pellet) and cytosolic fractions (supernatant). The HM purity was shown by

immunoblotting with VDAC antibody. The purity of LM and cytosolic fractions were checked by probing for Flotillin and Cu/ZnSOD, respectively.

2.20. Immunohistochemical staining and Transmission Electron Microscopy

HeLa/Neo and HeLa/Bcl-2 cells were washed with 1X PBS twice. The cells were then fixed with 0.2% glutaraldehyde in 2% paraformaldehyde in phosphate buffer, pH 7.4 solution for 1 hr. For immunostaining, the fixed cells were blocked with 5% BSA to block nonspecific binding for 1 hr. Cells were then incubated with anti-Rac1 and anti-Bcl-2 respectively for 2 hrs. After 3 washes with 1 X PBS, biotinylated secondary mouse and rabbit secondary antibodies were used to stain the cells for 1 hr. Following 1 hr incubation with Avidin-Biotin Peroxidase complex and 2 washes with 1 X PBS, the peroxidase activity was demonstrated by Nickel-enhanced 3, 3 DAB solution in Tris buffer containing 0.05% hydrogen peroxide. The chemical reaction was stopped with several washes of Tris buffer and then the samples were post-fixed in 1% osmium tetroxide in 0.1M PBS, pH7.4, for 1 hr at room temperature and dehydrated in graded series of ethanol. The samples were then embedded in araldite mixture. Ultra thin sections were stained in lead citrate and viewed in an EM208S electron microscope. Some sections were treated simultaneously with omission of primary antibodies to rule out non-specific binding.

2.21. Cell Cycle Profile Analysis by Flow Cytometry

Cell cycle profile was determined using PI staining by measuring the DNA content of the cells. PI (0.5 mg) was reconstituted in 1ml 38mM sodium citrate buffer (pH 7.0) to give a 50X stock solution while RNase A (10mg) was reconstituted in 1 ml of 10 mM Tris-HCl buffer (pH 7.5) with 15 mM NaCl, boiled for 15min, and cooled to room temperature (40X stock solution). Following treatment, CEM cells (1.0 x 10^6 cells/well) were harvested by washing with 2 ml of 1X PBS with 1% FBS, then spinning at 1200 rpm for 5 mins at 22°C and the pellet was resuspended in 1ml of 1X PBS with 1% FBS, then immediately fixed with 70% ethanol and incubated on ice for 30 mins. After incubation, the cells were again washed twice with 1X PBS with 1% FBS and the pellet was resuspended with 0.5 ml of 1X PI : RNase A (10 μg PI and 250 μg RNase A) in sodium citrate solution and incubated for 30 mins at 37°C in the dark. At least 10,000 events were analysed by flow cytometry using an excitation wavelength of 488 nm and emission wavelength of 610 nm (Epics Elite EPS, Beckman Coulter, FL, USA). Data was further analysed using WINMDI software.

2.22. ™CELLWORKS In Silico Modelling

In an attempt to study the functional implication(s) of Rac1-Bcl-2 interaction, computer simulation driven virtual predictive experiments were carried out based on the protein pathway dynamic network created by ™Cellworks Group Inc., CA, USA. The ™Cellworks Oncology Platform was customized to create a system aligned to HCT116 human colorectal cancer cell line with K-Ras mutation, PI3K overexpression (OE), CDKN2A deletion, β-catenin OE and an additional Bcl-2 OE. A variant cell

line was also created with Rac1 OE based on the above baseline and either Rac1 or Bcl-2 down-regulation (target expression inhibition by 70%) was then tested on the above two modelled cell lines to study the effects on phenotypic indices and key bio markers on tumorigenesis.

2.23. Statistical Analysis

The statistical analysis for the data obtained was performed by Student's t-test assuming equal variances with SPSS software. Means were only considered significantly different when p-value is less than 0.05.

CHAPTER 3: RESULTS

3.1. Bcl-2 Induces a Slight Pro-oxidant Intra-mitochondrial Milieu in Cancer Cells

3.1.1 Overexpression of Bcl-2 in Cancer Cells Increased Mitochondrial O_2^- Levels

Previous results from other groups[225] as well as our group demonstrated a pro-oxidant nature of the anti-apoptotic protein Bcl-2 where its overexpression led to a slightly but constitutively elevated O_2^- levels both intracellularly as well as intra-mitochondrially[70, 114, 203, 322]. In order to confirm this point and establish a working model of Bcl-2-induced pro-oxidant status with the focus on mitochondria for the subsequent experiments in this thesis, the basal levels of mitochondrial O_2^- from two cell lines: the stable Bcl-2-overexpressing human chronic myeloid leukaemia CEM cells (CEM/Bcl-2) and the control vector matched CEM/Neo cells, were measured using MitoSox dye as described in Materials and Methods. MitoSox red, being a live-cell-permeable dye with hydroethidine (HE) covalently linked to a triphosphonium cation, is selectively targeted to mitochondria due to the significantly lower trans-mitochondrial membrane potential as compared to trans-plasma membrane potential. The redox sensitive dye is then oxidized by O_2^- produced in the mitochondria of living cells and the oxidation product exhibits red fluorescence upon binding to nucleic acids, which can be detected by Fluorescence-activated cell sorting (FACS) using a flow cytometry. The specificity of this mitochondria-targeted probe for O_2^- but not other ROS or reactive nitrogen species (RNS) makes it a reliable measurement for live O_2^- production from the mitochondria. Indeed, CEM/Bcl-2 cells

exhibited moderately higher mitochondrial O_2^- levels when comparing to CEM/Neo cells as shown by the right shift in the histogram **(Figure 1)**.
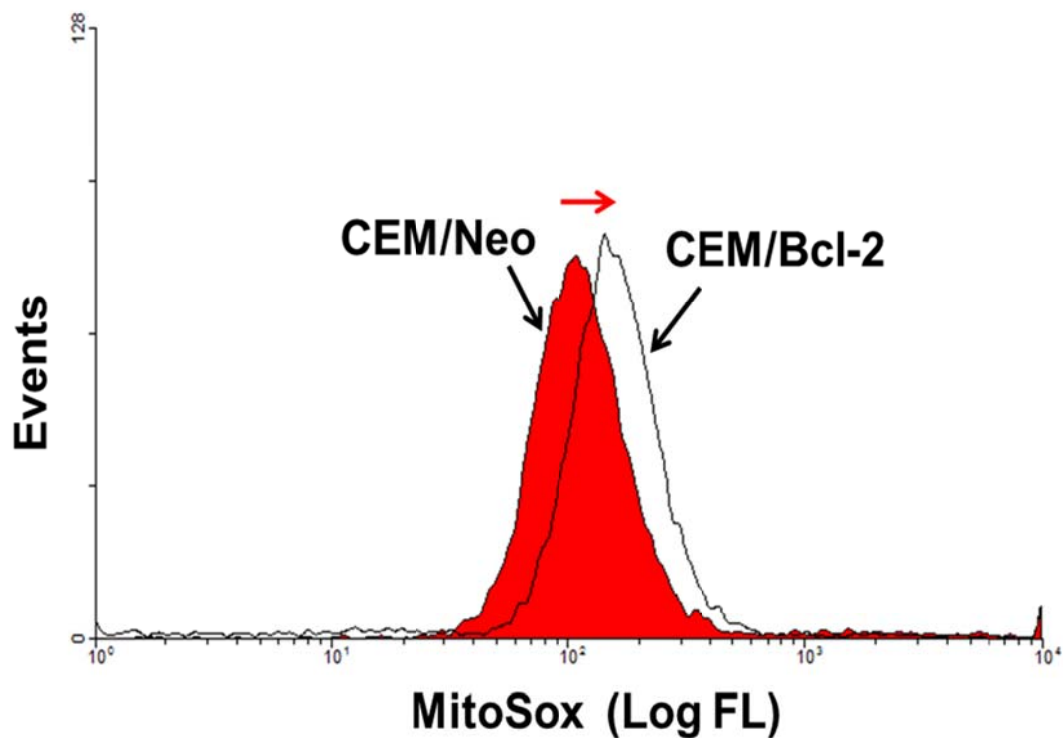
Figure 1: Overexpression of Bcl-2 in cancer cells increased mitochondrial O_2^- levels. Mitochondrial O_2^- levels of human chronic myeloid leukaemia CEM cells were detected by MitoSox staining and analysed through flow cytometry. At least 10,000 events were analysed by WINMDI software. Histograms shown were representative of at least three independent experiments. CEM/Bcl-2: CEM cells stably overexpressing Bcl-2; CEM/Neo: CEM cells stably overexpressing the control vector containing neomycin.

3.1.2 Transient Overexpression of Bcl-xL in Cancer Cells Did not Affect Intracellular O_2^- Levels

In order to explore whether the pro-oxidant property is specific to Bcl-2 only but not other pro-survival Bcl-2 family member such as Bcl-xL, the intracellular O_2^- levels were examined upon transient Bcl-xL overexpression in human cervical cancer HeLa/Neo cells. The intracellular O_2^- levels were determined using a lucigenin-based chemiluminescence assay as described in Materials and Methods. The lucigenin is first reduced by one electron to lucigenin cation radical (probably by the same biological system(s) that produce(s) O_2^-) that can then react with O_2^- to yield the unstable dioxetane intermediate, followed by decomposition and relaxation to the ground state emitting a photon which can be sensitively captured[323]. Indeed, 48 hrs post transient introduction of the Bcl-xL plasmid into HeLa/Neo cells, there was no change observed in the intracellular O_2^- levels **(Figure 2B)**, unlike Bcl-2, which has been reported previously by our group to induce a constitutively elevated production of intracellular O_2^- upon overexpression, be it transiently or stably in HeLa cells[114, 203]. The transfection efficiency of Bcl-xL was confirmed by western blot analysis where β-actin served as an internal control for equal loading **(Figure 2A)**.
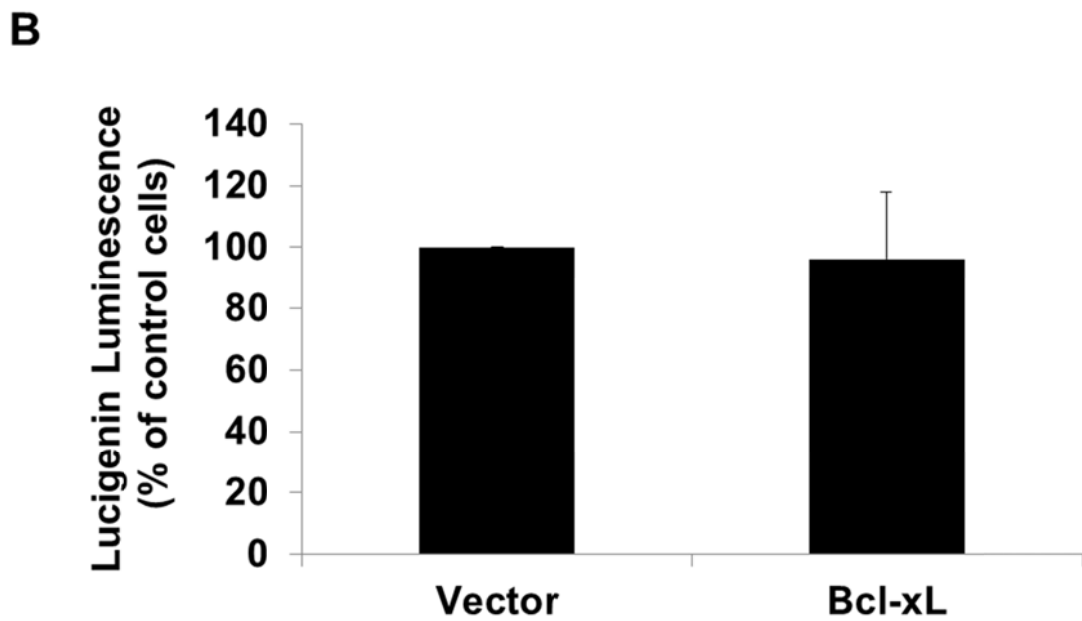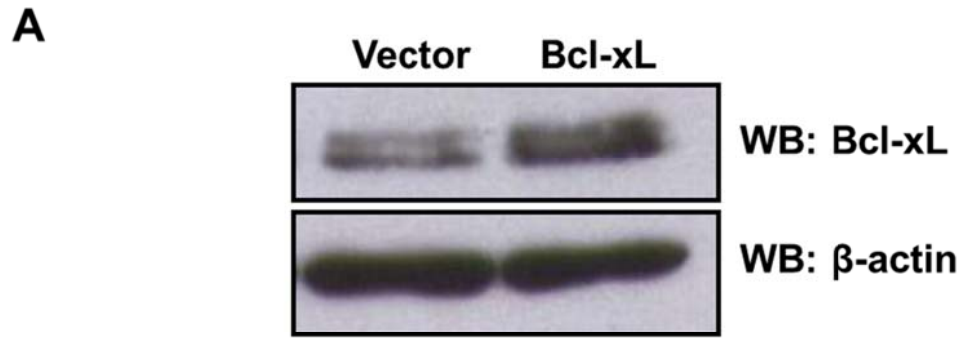
Figure 2: Transient overexpression of Bcl-xL in cancer cells did not affect intracellular O_2^- levels. (A) Western blot analysis of Bcl-xL and β-actin expression in human cervical cancer HeLa/Neo cells transiently transfected with control vector or Bcl-xL plasmid for 48 hrs. (B) Intracellular O_2^- levels were determined in HeLa/Neo cells 48 hrs post transient transfection with control vector or Bcl-xL plasmid using lucigenin-based chemiluminescence assay. The error bars represent means ± SD of at least 3 independent experiments.

3.2.   Bcl-2 Overexpression Induces Rac1 Activation in Cancer Cells

3.2.1   Cancer Cells with Higher Bcl-2 Expression Levels Have Higher Rac1 Activation Levels

Since the discovery of the pro-oxidant property of Bcl-2, extensive studies have been carried out in our laboratory to identify the exact source(s) for the elevated O_2^- production as observed upon Bcl-2 overexpression. One hypothesis is that Bcl-2 engages mitochondrial respiration and this is supported by the evidences that activity of the rate limiting enzyme of the mitochondrial electron transport chain (ETC), cytochrome c oxidase (COX or Complex IV), got enhanced upon Bcl-2 overexpression, which led to increased oxygen consumption rate and an overall increased probability of electron leakage onto molecular oxygen producing O_2^-[203, 204]. In addition, preliminary results suggested an involvement of Rac1 as well, which is known to activate NADPH oxidases for O_2^- production upon GTP loading[264, 272, 273]. Transient transfection of the dominant negative mutant Rac1N17 significantly decreased the intracellular O_2^- levels in CEM/Bcl-2 cells[114]. Intrigued by this finding, the activation levels of Rac1 were examined across four cancer cell lines with differential Bcl-2 expression levels including Raji (the human B cell lymphoma), Jurkat (the human T cell leukemia) as well as CEM/Neo and CEM/Bcl-2, using an affinity precipitation method as described in Materials and Methods. GST-agarose beads bound to PBD (p21 binding domain), the N-terminal regulatory region of Rac1's downstream effector protein PAK1 (p21-activated kinase 1) were used to pull down GTP-loaded Rac1 only and thus the levels of active Rac1 can be quantitatively assessed through subsequent western blot analysis. Indeed, cancer cells with relatively higher Bcl-2 expression levels such as Jurkat and CEM/Bcl-2 as shown in the input **(Figure 3B)**, showed significantly higher Rac1

activation levels indicating a direct correlation between Bcl-2 expression and Rac1 activation levels. Cells loaded with either a non-hydrolysable GTP analog GTP-γS or GDP followed by PAK-1 PBD pull downs served as a positive or negative control, respectively **(Figure 3A)**.
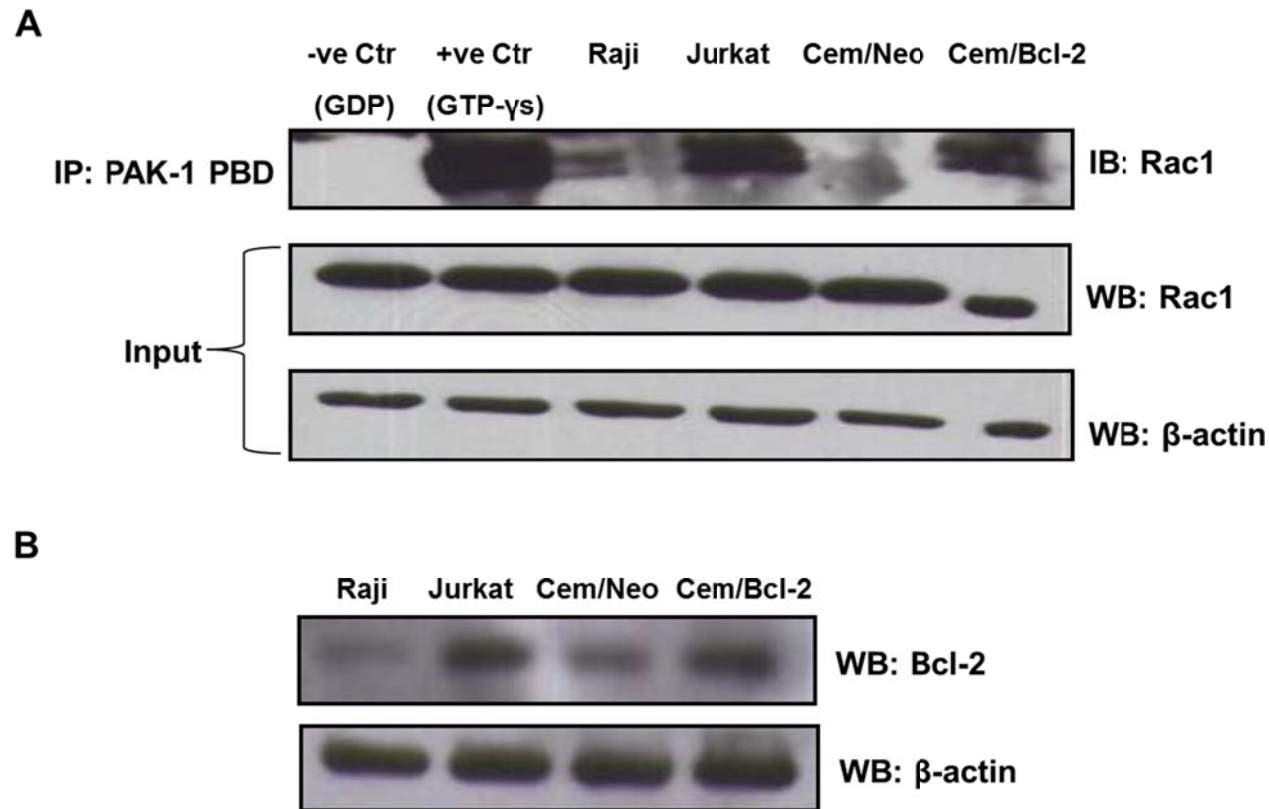
Figure 3: Cancer cells with higher endogenous Bcl-2 expression levels harbour higher Rac1 activation levels. (A) Cancer cells from different origins as labeled were lysed and immunoprecipitated with the p21 binding domain (PBD) of p21-activated protein kinase (PAK-1) fused with GST and coupled to agarose beads. After precipitation, immunoblot analysis was performed with Rac1 antibody for detection of activated Rac1. Western blot analysis of Rac1 and β-actin were shown as internal loading controls at the lower panel (input). GDP or GTP-γS loading was used as a negative or positive control, respectively. (B) Western blot analysis of Bcl-2 and β-actin across different cancer cell lines. Raji: human B cell lymphoma cells; Jurkat: human T cell lymphoma cells; CEM/Bcl-2: human chronic myeloid leukaemia CEM cells stably overexpressing Bcl-2; CEM/Neo: CEM cells stably overexpressing the control vector containing neomycin.

3.2.2 Transient Bcl-2 Overexpression in Cancer Cells Induced Rac1 Activation

In order to study whether there is a direct causal relationship between Bcl-2 expression and Rac1 activation levels, the amount of active Rac1 was assessed upon transient manipulation of Bcl-2 expression levels, using the same affinity precipitation method mentioned in the previous section. Upon transient overexpression of green fluorescent protein tagged Bcl-2 (GFP-Bcl-2) in HeLa cells with relatively low endogenous expression of Bcl-2 **(Figure 4B)**, there was a significant increase in the amount of active Rac1 compared to the control vector GFP-C1 transfected cells **(Figure 4A)** suggesting the transiently introduced Bcl-2 probably either directly or indirectly activated the endogenous Rac1. Interestingly, this was not observed with transient transfection of GFP tagged Bcl-xL (GFP-Bcl-xL) **(Figure 4A)** corroborating with the previously discussed data in section 3.1.2 that overexpression of Bcl-xL in cancer cells did not affect intracellular O_2^- levels (**Figure 2**) and suggesting that Rac1 activation could possibly explain the elevated levels of O_2^- in Bcl-2-overexpressing cancer cells.
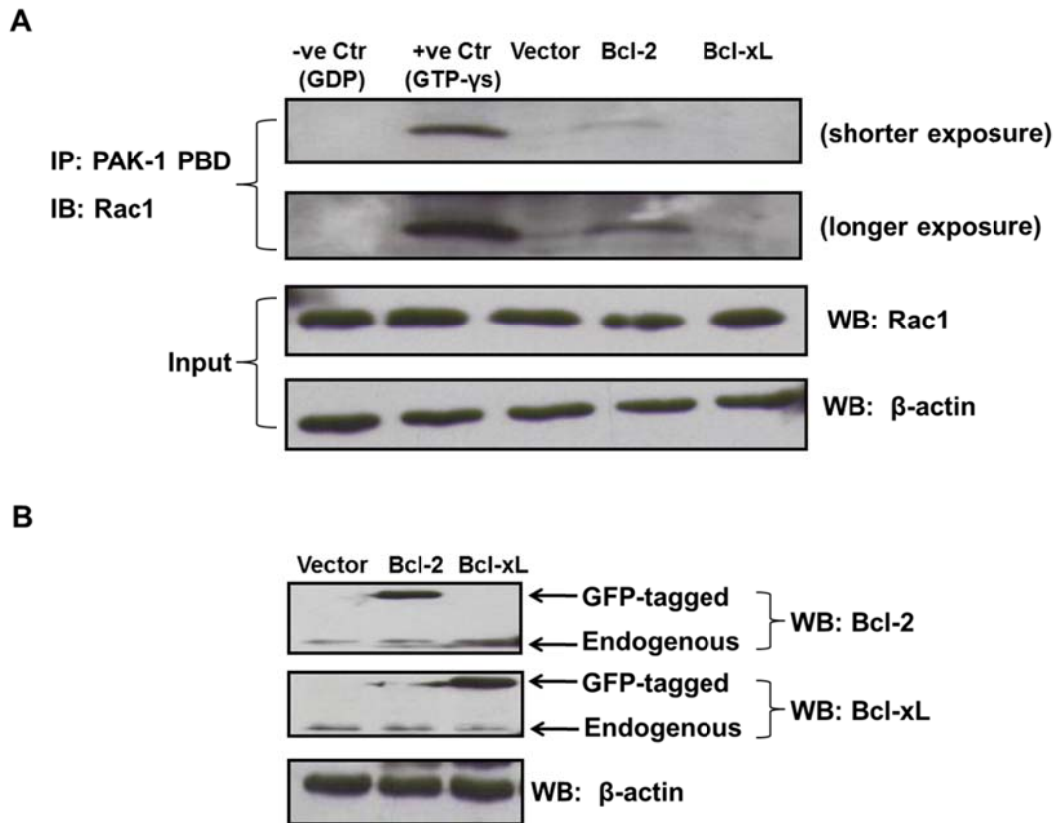
Figure 4: Transient Bcl-2 overexpression in cancer cells induced Rac1 activation. (A) Human cervical cancer HeLa cells transiently transfected with either GFP-C1 control vector, GFP-Bcl-2 or GFP-Bcl-xL plasmids for 48 hrs were lysed and immunoprecipitated with the p21 binding domain (PBD) of p21-activated protein kinase (PAK-1) fused with GST and coupled to agarose beads. After precipitation, immunoblot analysis was performed with Rac1 antibody for detection of activated Rac1. Western blot analysis of Rac1 and β-actin were shown as internal loading controls at the lower panel (input). GDP or GTP-γS loading was used as a negative or positive control, respectively. (B) Western blot analysis of Bcl-2, Bcl-xL and β-actin in HeLa cells transiently transfected with either GFP-C1 control vector, GFP-Bcl-2 or GFP-Bcl-xL plasmids for 48 hrs.

3.3. Rac1 Regulates Mitochondrial O_2^- Levels in Bcl-2-overexpressing Cancer Cells

For a better justification of the direct involvement of Rac1 in Bcl-2-induced pro-oxidant state, the mitochondrial O_2^- levels were measured using MitoSox following the inhibition of Rac1 activity upon exposure to a cell permeable pharmacological inhibitor NSC23766. This is a first generation small molecule inhibitor that specifically targets Rac, identified through a computer based Virtual Screening on over 140,000 small chemical compounds available in the National Cancer Institute database. It was found based on the criteria to interact with residue Trp56 and to be able to dock onto the pocket created by Lys5, Val7, Trp56 and Ser71 of Rac1 according to the structure of Rac1-Tiam1 monomer complex[256]. Trp56 has been demonstrated to be the critical determinant of Rac1 for its ability to discriminate within a subset of Rac1-specific GEFs (guanine nucleotide exchange factors) such as Tiam1 and Trio. As such, any molecule that interacts with Trp56 and occupies the pocket could potentially inhibit the interaction between Rac1 and its GEFs thus blocking its activation[257]. Indeed, the inhibitory effect of NSC23766 was determined using a complex formation assay where it specifically inhibited the binding of TrioN to Rac1 in a competitive manner with an inhibitory concentration-50 (IC_{50}) of about 50 μM *in vitro* but not with Intersectin to Cdc42 (where Intersectin is a Cdc42-specific GEF)[243, 258]. Further investigation revealed that NSC23766 could inhibit Tiam1 binding to Rac1 as well thus inhibiting Rac1 activation but had no detectable inhibitory effect on RhoA. There is also no inhibitory effect observed with Rac1 binding to its effector such as PAK1 or to GAP (GTPase-activating protein) such as BcrGAP indicating that NSC23766 is a specific inhibitor for Rac1-GEF interaction. In the computer simulated model, NSC23766 is able to bind to a surface

cleft that is formed by residues Lys5, Asp38, Asn39, Trp56, Thr58, Leu70 and Ser71 which correspond to the groove between β1-β3 regions, Switch 1 and Switch 2. The inhibitory effect could result from: 1) steric hindrance so that GEFs can no longer bind to Rac1; 2) prevention of the conformational change of loop L4, that is formed with residues 60-64; 3) prevention of the displacing of the Mg^{2+} ion by Ala59. Both 2) and 3) prevent the switch from GDP-bound conformation to a nucleotide free open conformation to allow the loading of GTP onto Rac1[243].

The inhibitory effect of NSC23766 was further validated in our model of CEM/Bcl-2 cells using the Rac1 G-LISA™ Kit as described in Materials and Methods. Only active Rac1 will be captured by the Rac-GTP affinity wells and probed with Rac1 antibody that can be detected with a 96-well plate luminometer. Indeed, dose-dependent inhibitory effect on Rac1 activity was observed upon exposure to increasing doses of NSC23766 with IC_{50} of about 50 μM **(Figure 5A)** which corroborates with previously published results based on *in vitro* complex formation assay mentioned above. The constitutively activated Rac1 recombinant protein was used as a positive control while the blank that contained only the buffers was used as a negative control **(Figure 5B)**. Upon 2 hrs exposure of NSC23766 that blocks the interaction of Rac1-GEFs, mitochondrial O_2^- levels were measured in both CEM/Neo and CEM/Bcl-2 cells. As shown in **Figure 6A**, significant dose-dependent reduction in mitochondrial O_2^- levels was observed with Rac1 activity inhibited in Bcl-2-overexpressing CEM cells compromising its pro-oxidant state as compared to the basal levels without any drug exposure. Minimum effect was observed in CEM/Neo cells with relatively lower Bcl-2 expression levels. In order to confirm that the reduction of O_2^- levels in CEM/Bcl-2 cells comes from the mitochondria, both

whole cells as well as isolated mitochondria were measured for their mitochondrial O_2^- levels upon inhibition of Rac1 activity. Indeed, similar reduction was observed in both whole cells and isolated mitochondria **(Figure 6B)** indicating that mitochondria is a significant contributing organelle site to the pro-oxidant state in CEM/Bcl-2 cells.

To provide evidences that the reduction in mitochondrial O_2^- levels upon NSC23766 treatment in CEM/Bcl-2 cells was due to inhibition of Rac1 activity but not other effects, changes in cell viability and protein expression levels of Rac1 and Bcl-2 were determined, if there are any, using MTT cell viability assay and western blotting, respectively, as described in Materials and Methods. Only viable cells harbor the reductase enzymes which can reduce MTT to formazan dyes, giving a purple color that can be captured by spectrophotometer[324]. Although it is not a direct measurement for cell death, any changes in the proliferation or cell death or even metabolic activity of cells can affect the end products which could be used as a means to assess the toxicity of a certain agent, in this case the pharmacological inhibitor of Rac1, to the cells. No significant changes in cell viability were observed with 5 and 15 μM of NSC23766 **(Figure 7)** that caused a decrease in the mitochondrial O_2^- levels as shown earlier in **Figure 6A & B**. Similarly, no changes in protein levels of Rac1 and Bcl-2 were observed with NSC23766 exposure even at the highest dose of 50 μM tested **(Figure 8)**.
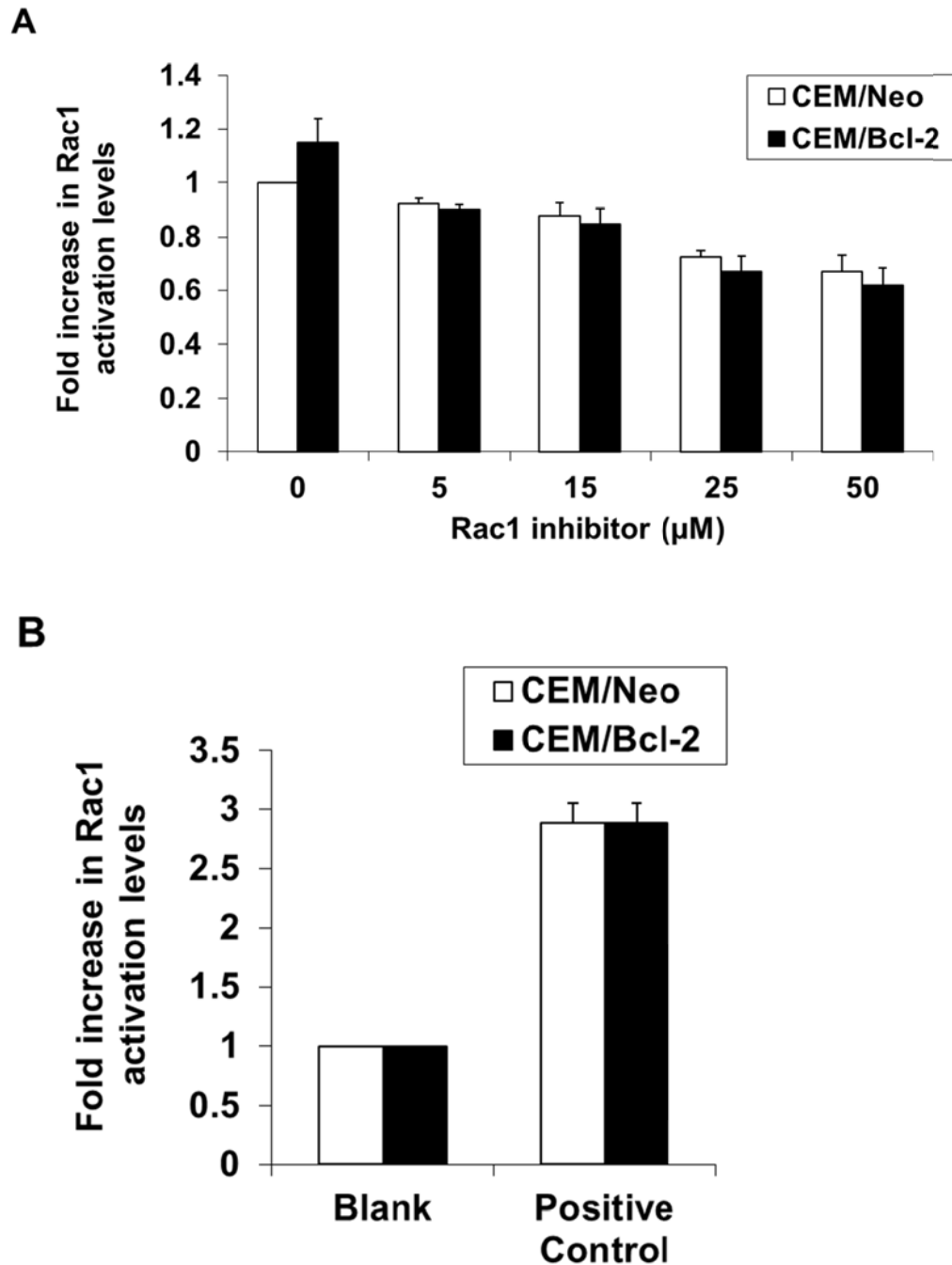
Figure 5: Rac1 activation levels decreased with increasing doses of the pharmacological inhibitor of Rac1, NSC23766. (A) CEM/Neo and CEM/Bcl-2 cells were treated with various doses of Rac1 inhibitor NSC23766 for 24 hrs and Rac1 activation levels were determined by the Rac1 G-LISA^{TM} kit. (B) The constitutively activated Rac1 recombinant protein was used as a positive control while the blank that contained only the buffers was used as a negative control. Data shown are means ± SD of at least 3 independent experiments performed in duplicate. CEM/Bcl-2: human chronic myeloid leukaemia CEM cells stably overexpressing Bcl-2; CEM/Neo: CEM cells stably overexpressing the control vector containing neomycin.
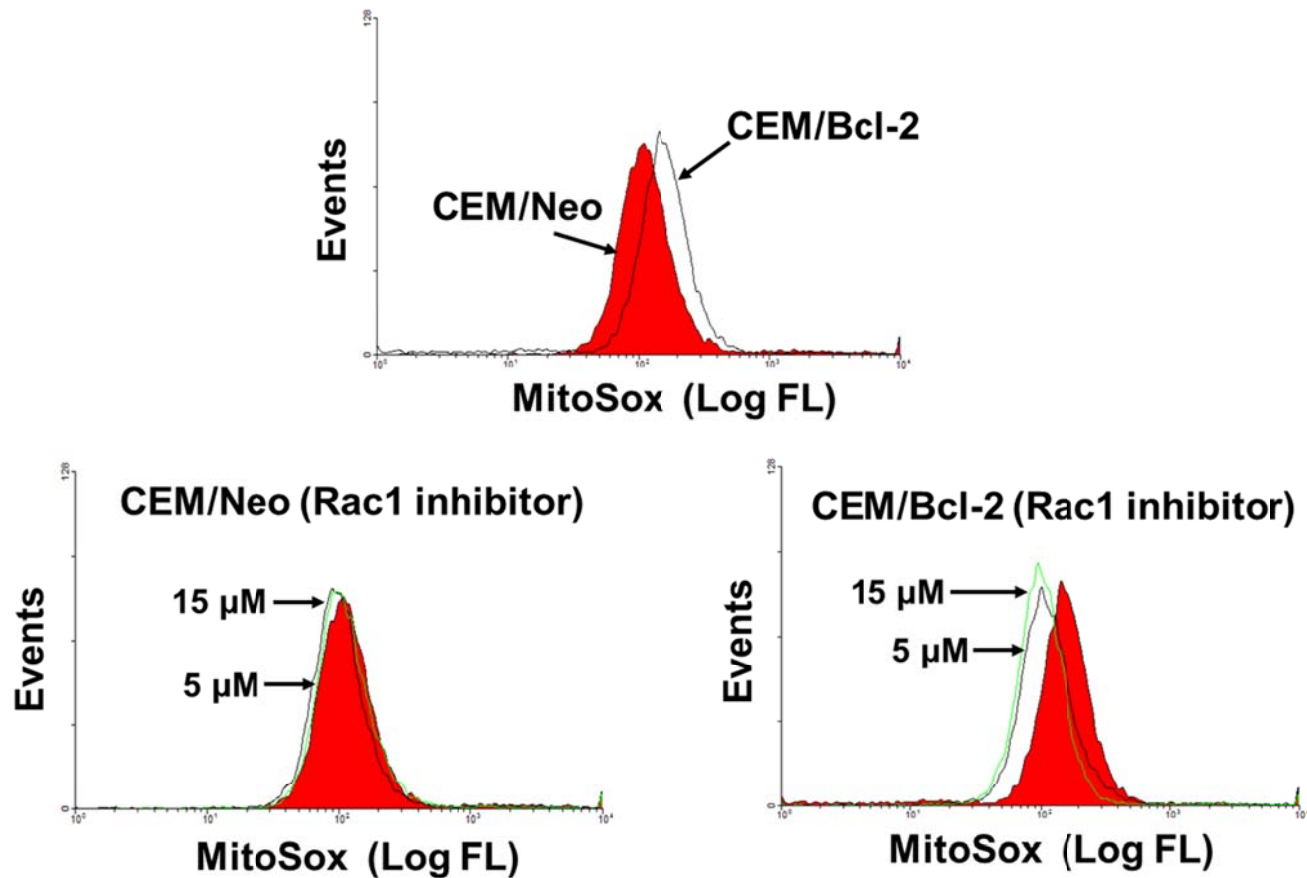
Figure 6: Pharmacological inhibition of Rac1 decreased mitochondrial O_2^- levels in Bcl-2-overexpressing cancer cells. (A) Mitochondrial O_2^- levels of human chronic myeloid leukaemia CEM cells, upon exposure to various doses of Rac1 inhibitor NSC23766 for 2 hrs, were detected by MitoSox staining and analysed through flow cytometry. At least 10,000 events were analysed by WINMDI software. Histograms shown were representative of at least three independent experiments. CEM/Bcl-2: CEM cells stably overexpressing Bcl-2; CEM/Neo: CEM cells stably overexpressing the control vector containing neomycin.

B
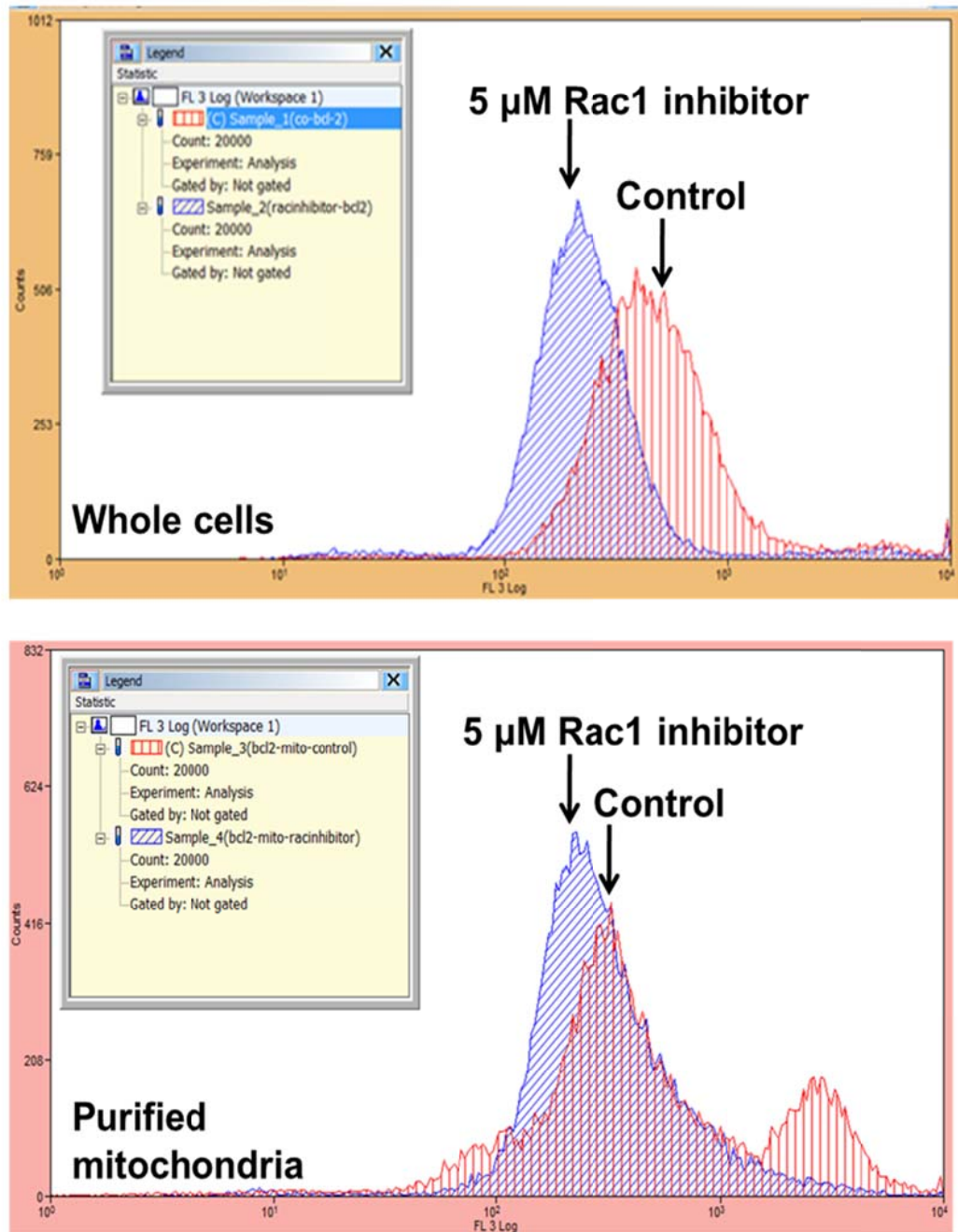
Figure 6: Pharmacological inhibition of Rac1 decreased mitochondrial O$_2^-$ levels in Bcl-2-overexpressing cancer cells. (B) Mitochondrial O$_2^-$ levels from either whole cells or the isolated mitochondria, upon exposing CEM/Bcl-2 cells to Rac1 inhibitor NSC23766 for 2 hrs, were detected by MitoSox staining and analysed through flow cytometry. At least 10,000 events were analyzed by Summit software. Histograms shown were representative of at least three experiments performed independently.
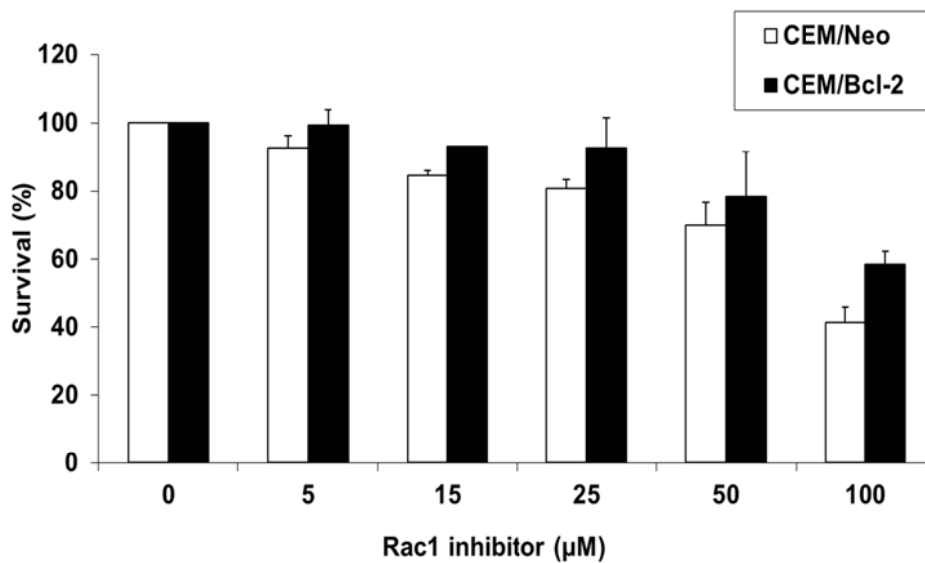
Figure 7: The pharmacological inhibitor of Rac1, NSC23766, at low doses did not significantly affect the viability of cancer cells. CEM/Neo and CEM/Bcl-2 cells were treated with various doses of Rac1 inhibitor NSC23766 for 24 hrs and cell viability was determined by the MTT assay. Cell survival was calculated as: (mean of triplicate OD values of cells incubated with Rac1 inhibitor / mean of triplicate OD values of cells incubated with control solvent) X 100%. Data shown are mean percentage of survival ± SD of at least three independent experiments performed in triplicate. CEM/Bcl-2: human chronic myeloid leukaemia CEM cells stably overexpressing Bcl-2; CEM/Neo: CEM cells stably overexpressing the control vector containing neomycin.
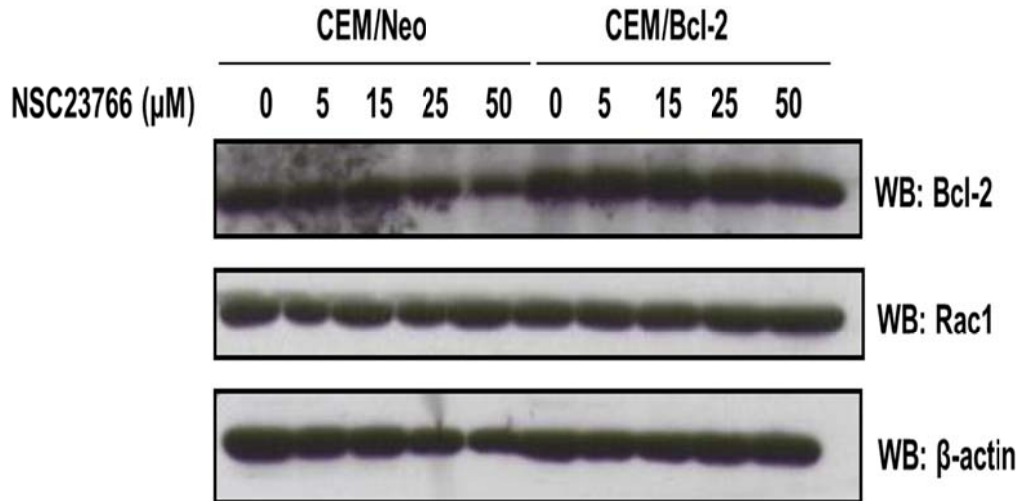
Figure 8: The pharmacological inhibitor of Rac1, NSC23766, did not affect expression levels of Rac1 and Bcl-2. Western blot analysis of Bcl-2 and Rac1 expression in CEM cells following exposure to increasing doses of Rac1 inhibitor NSC23766 for 24 hrs. β-actin was used as an internal loading control. CEM/Bcl-2: human chronic myeloid leukaemia CEM cells stably overexpressing Bcl-2; CEM/Neo: CEM cells stably overexpressing the control vector containing neomycin.

3.4. Physical Interaction of Rac1 and Bcl-2

3.4.1 mCherry-Rac1 Co-localized with GFP-Bcl-2

Results discussed in the previous sections confirmed that Bcl-2-induced pro-oxidant state in the mitochondria of cancer cells is mediated through Rac1 activation; therefore, investigation on the underlying mechanism(s) would be of great help in understanding the redox regulation in the mitochondria. Preliminary results from our laboratory indeed suggested co-localization and a physical interaction between these two proteins. In order to confirm this point, a fluorescent microscopic analysis on the subcellular localization of mCherry tagged Rac1 and GFP tagged Bcl-2 was carried out first. Both Rac1 and Bcl-2 are tagged with fluorescent proteins at the 5' end to ensure: 1) expression of the fluorophores; 2) proper subcellular targeting of the proteins of interest due to the presence of transmembrane domain at the C-terminus of Bcl-2[127] and polybasic region at the C-terminus of Rac1 that contains the nuclear localization signal (NLS) and is also important for membrane association upon geranylgeranylation[244, 245, 248]. mCherry is better off as compared to the conventional red fluorescent protein (RFP) that was used in the preliminary experiments from our laboratory in terms of photostability (thus preventing premature photobleaching) and its monomeric nature (thus revealing more accurate subcellular localization details). The obligate tetramerization of RFP *in vitro* and in living cells has been reported where RFP fusion protein chimeras formed intracellular aggregates, which raises the question as to what extent will RFP tag affect the localizations and functions of Rac1[325, 326]. In this regard, the monomeric form mCherry fused Rac1 is preferred and is co-transfected with GFP-Bcl-2 into HeLa cells and the fluorescent signals from both channels were measured under a fluorescent microscope. Control fluorescent proteins by themselves showed homogeneous overexpression all over the

cells without any specific subcellular localizations. Bcl-2, being associated primarily with membrane structures, was seen in the perinuclear regions while Rac1 is more predominantly all over the plasma membrane and cytosolic compartments. Overlay of the fluorescent signals from both the red and green channels showed yellow spots and patches mostly at the perinuclear regions suggesting co-localization of mCherry-Rac1 and GFP-Bcl-2 there, as indicated by white arrows **(Figure 9)**.
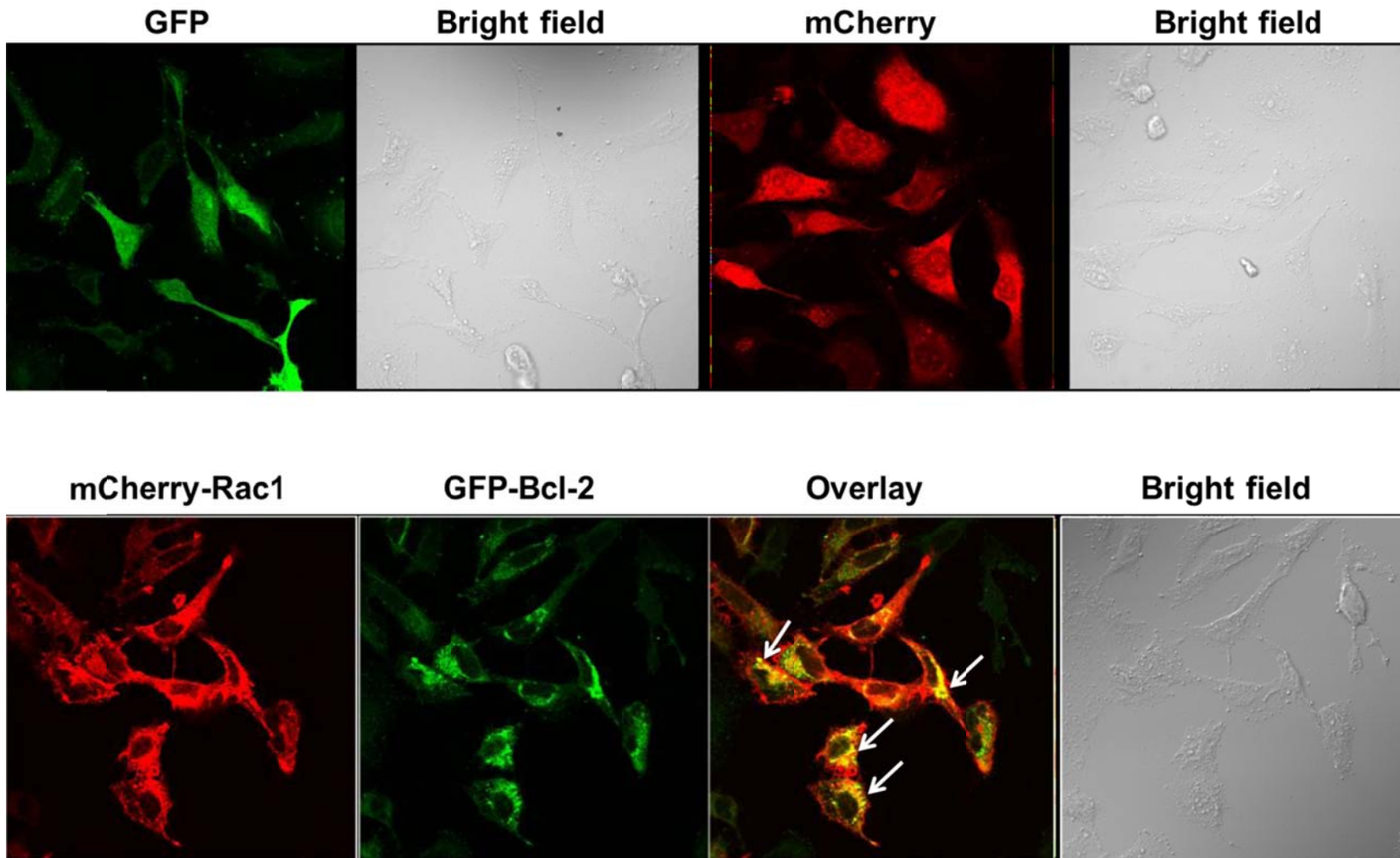
Figure 9: mCherry-Rac1 co-localized with GFP-Bcl-2. Human cervical cancer HeLa cells cultured on coverslips were transfected with either GFP (Green Fluorescent Protein)-C1 control vector, mCherry Fluorescent Protein control vector, or co-transfected with GFP-Bcl-2 and mCherry-Rac1 plasmids, respectively. Confocal microscopic analysis was performed 24 hrs post transfection for 3 or more experiments independently. The panels were merged using Olympus FluoView 2.0 software.

3.4.2   Rac1 and Bcl-2 Co-immunoprecipitated with Each Other in Cancer Cells with Higher Bcl-2 Expression Levels but not in PBMCs from Normal Healthy Volunteers

To further validate the preliminary results obtained previously from our laboratory that suggested a physical interaction between Rac1 and Bcl-2 based on *in vitro* GST pull-down assay with recombinant proteins, co-immunoprecipitation assays were performed with pull down of either anti-Rac1 and anti-Bcl-2, respectively, across four cancer cell lines with differential Bcl-2 expression levels. Indeed, Bcl-2-overexpressing HeLa (H/B) cells showed significantly enhanced association between Rac1 and Bcl-2 in both pull downs as compared to the control vector matched HeLa cells (H/N) **(Figure 10A)**. Similarly, Jurkat cells that have higher endogenous Bcl-2 expression levels as compared to Raji cells, also exhibited greater levels of association between the two proteins **(Figure 10B)**. To make sure the existence of a interaction is a cancer-specific observation, co-immunoprecipitation assay was also carried out with anti-Bcl-2 pull down in peripheral blood mononuclear cells (PBMCs) obtained from 3 healthy donors and no detectable associated Rac1 was observed since Bcl-2 is also non-detectable in these samples **(Figure 11)**. The input panels here showed the relative expression of the two interacting partners in the whole cell lysates of various cancer cell lines or samples from healthy donors, which could serve to semi-quantitate the percentage of proteins that formed complex in their whole intracellular pools. Isotype matched control IgG antibodies were used as a negative control here, which non-specifically bind to any sorts of proteins but does not specifically recognize the proteins of interest **(Figure 10 & Figure 11)**.
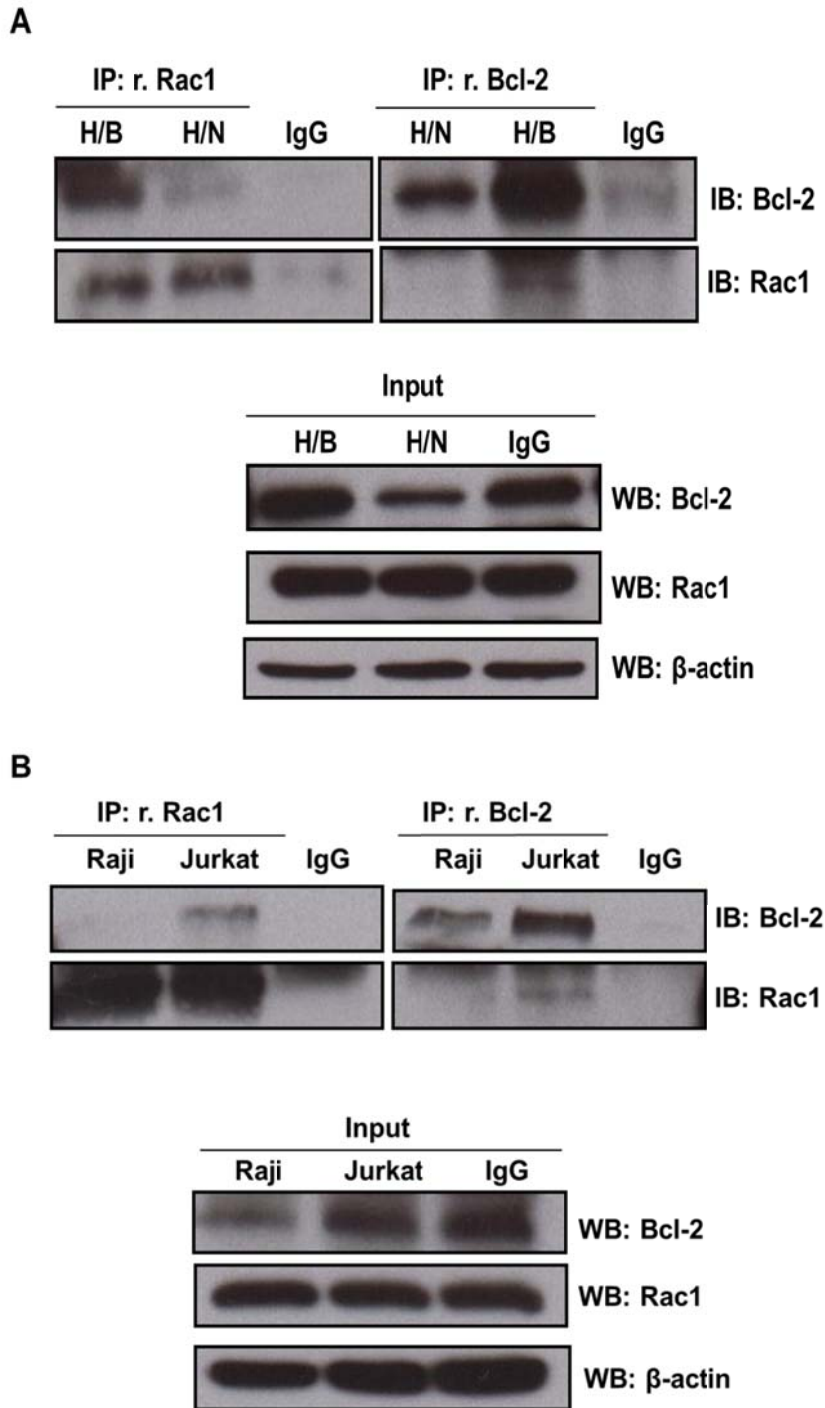
Figure 10: Rac1 and Bcl-2 co-immunoprecipitated with each other in cancer cells with higher Bcl-2 expression levels. (A) Cell lysates from HeLa stably overexpressing either control vector (H/N) or Bcl-2 plasmid (H/B) were immunoprecipitated with either anti-Rac1 or anti-Bcl-2 and probed with anti-Bcl-2 and anti-Rac1. Immunoprecipitation with control rabbit anti-IgG antibodies was used as a negative control. Whole cell lysates probed with anti-Bcl-2, anti-Rac1 and anti-β-actin are shown on the bottom panel as input. (B) Cell lysates from Raji and Jurkat were immunoprecipitated with either anti-Rac1 or anti-Bcl-2 and probed with anti-Bcl-2 and anti-Rac1. Immunoprecipitation with control rabbit anti-IgG antibodies was used as a negative control. Whole cell lysates probed with anti-Bcl-2, anti-Rac1 and anti-β-actin are shown on the bottom panel as input.
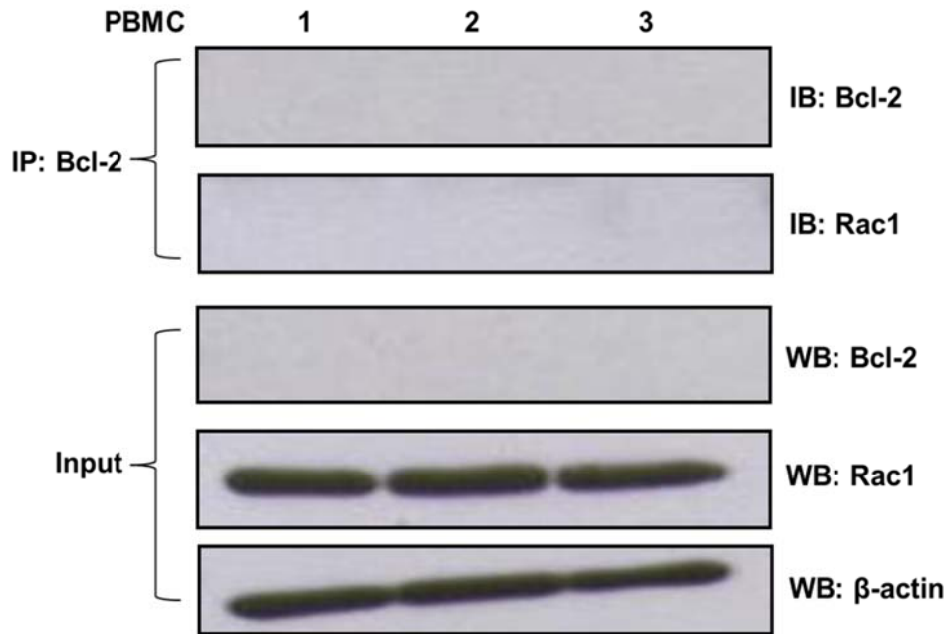
Figure 11: No interaction of Rac1 and Bcl-2 was observed in PBMCs from normal healthy volunteers. Cell lysates from peripheral blood mononuclear cells (PBMCs) obtained from 3 healthy donors were immunoprecipitated with anti-Bcl-2 and probed with anti-Bcl-2 and anti-Rac1. Whole cell lysates probed with anti-Bcl-2, anti-Rac1 and anti-β-actin are shown on the bottom panel as input.

3.5. Geranylgeranylation of Rac1 is Required for Its Mitochondria Localization and Interaction with Bcl-2

3.5.1 Mitochondrial Localization of Rac1 is Independent on Bcl-2 Expression Levels

Results discussed in the previous section based on co-immunoprecipitation analysis on the whole cell lysates from cancer cells with higher Bcl-2 expression levels confirmed a physical interaction between Rac1 and Bcl-2 **(Figure 10)**. Since Bcl-2-induced pro-oxidant state in the mitochondria is mediated through Rac1 activation, this raises the question: is this interacting complex also localized in the mitochondria so that they can take part in redox regulation? Preliminary results from our laboratory suggested that this complex is localized to the outer mitochondria membrane where Bcl-2 resides. In addition, the fluorescent microscopic analysis on subcellular distributions of the two proteins also indicated that they co-localized at the perinuclear regions **(Figure 9)**. In order to provide more evidences for the subcellular localization of this interacting complex, we checked for the mitochondrial presence of Rac1 following subcellular fractionation. Indeed, Rac1 was found to be present in the mitochondria-enriched heavy membrane (HM) fractions of both CEM/Neo and CEM/Bcl-2 cells. Although these two cell lines differ in Bcl-2 expression levels, Rac1 expression levels at mitochondria-enriched HM fractions were comparable **(Figure 12A)** indicating the localization of Rac1 to the mitochondria is probably independent on Bcl-2 expression. To further validate this point, two human fibroblast cell lines, MRC5 and IMR90, which have barely detectable Bcl-2 levels, were utilized for analyzing the mitochondria distribution of Rac1. Indeed, a significant proportion of Rac1 is still present in the HM fractions apart from light membrane (LM) and cytosolic fractions, confirming that the presence of Rac1 in the mitochondria is

independent on Bcl-2 **(Figure 12B)**. This corroborates with studies from other groups that also demonstrated the mitochondrial presence of Rac1[276-278]. Flotillin (an integral plasma membrane protein), the voltage-dependent anion channel VDAC (that is present on the outer mitochondrial membranes), and the cytosolic isoform of superoxide dismutase Cu/Zn SOD served as LM, mitochondria-enriched HM and cytosolic markers, respectively, to demonstrate that there is no cross contamination among different fractions **(Figure 12A & B)**. Although HM fractions are highly enriched in mitochondria, they do include other membrane structures such as lysosomes. Therefore, a confocal microscopic analysis was also carried out in RFP-Rac1 transfected HeLa/Neo cells followed by incubation with MitoTracker green to visualize the mitochondria. The cell-permeant MitoTracker probes would passively diffuse across the plasma membrane and get accumulated in active mitochondria due to the mildly thiol-reactive chloromethyl moiety that the probes contain. Indeed, overlay panel showed yellow membranous patches resembling typical mitochondria morphology (**Figure 12C**) indicating the mitochondrial localization of Rac1. Moreover, immunoelectron microscopy was performed to localize both Rac1 and Bcl-2 in HeLa/Neo and HeLa/Bcl-2 cells. The immunoreactivity with anti-Rac1 was detected prominently at the outer mitochondrial membranes of HeLa/Bcl-2 cells, which is also the case for Bcl-2. Negative control with just the secondary antibody was also included to rule out any non-specific binding and no immunoreactions with DAB were observed (**Figure 12D**). All these strongly supported the mitochondrial localization of Rac1.

A

HM
CEM/Neo   CEM/Bcl-2

Cytosol
CEM/Neo   CEM/Bcl-2

WB: Bcl-2

WB: Rac1

WB: VDAC

WB: Cu/Zn SOD

B

MRC5
LM   HM   S

IMR90
LM   HM   S

WB: Bcl-2

WB: Rac1

WB: Flotillin

WB: VDAC

WB: Cu/Zn SOD

C

Bright field   Green Mitotracker   RFP-Rac1   Over Lay

HeLa/Neo

RFP- Control Vector
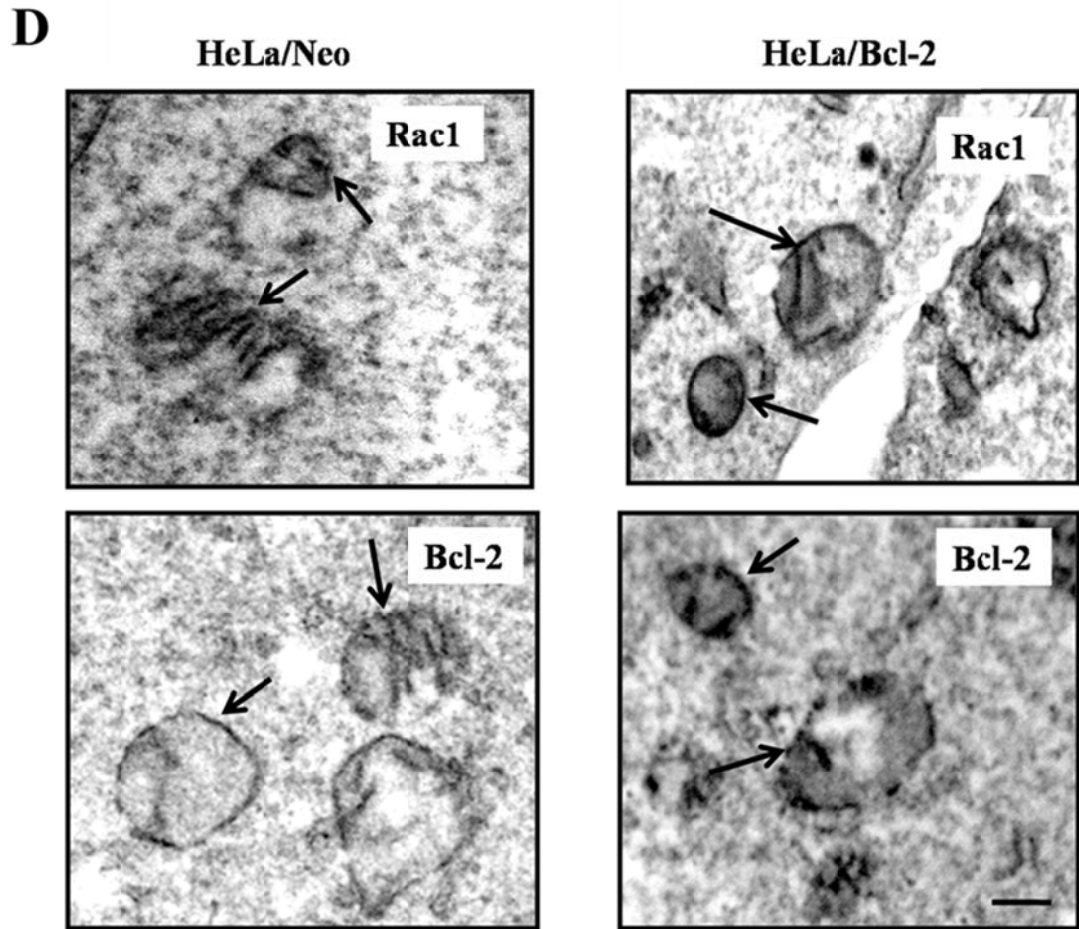
Figure 12: The mitochondrial localization of Rac1 is independent on Bcl-2 expression levels. (A) CEM/Neo and CEM/Bcl-2 cells were lysed and fractionated into purified mitochondria-enriched heavy membrane (HM) and cytosolic (S) fractions. The fractions were then probed for Bcl-2, Rac1, VDAC and Cu/Zn SOD. (B) Two human fibroblast cell lines, MRC5 and IMR90 were lysed and fractionated into purified mitochondria-enriched heavy membrane (HM), light membrane (LM) and cytosolic (S) fractions. The fraction lysates were then probed for Bcl-2, Rac1, Flotillin, VDAC and Cu/Zn SOD. (C) Human cervical cancer HeLa/Neo cells cultured on coverslips were transfected with either RFP (Red Fluorescent Protein) control vector or RFP-Rac1 plasmids. The cells were incubated with 125nM green MitoTracker for 20 mins at 37°C and fixed for confocal microscopic analysis 48 hrs post-transfection. Images shown were representative for 3 or more independent experiments. The panels were merged using Olympus FluoView 2.0 software. (D) Representative electron micrographs of HeLa/Neo and HeLa/Bcl-2 cells. The cells were stained with Rac1 and Bcl-2 antibodies. The Black arrows indicate the immunoreactive dark regions on the mitochondria showing the presence of Rac1 and Bcl-2. The scale bar = 1 μm.

3.5.2 Geranylgeranylation of Rac1 Is a Pre-requisite for Its Mitochondrial Localization

Post-translational prenylation, to be specific, geranylgeranylation at the C-terminal polybasic region of Rac1 has been shown to be required for its membrane association[248]. To check for its involvement in the mitochondrial targeting of Rac1, a pharmacological inhibitor of the geranylgeranyltransferase I, which catalyzes the addition of geranylgeranyl pyrophosphate (GGPP) to the cysteine residue, was used to block the geranylgeranylation process. Western blot analysis on the mitochondria-enriched HM fractions of Jurkat cells, following exposure to the inhibitor, revealed a dose-dependent decrease in Rac1 levels indicating that this post-translational modification is critical in targeting Rac1 to the mitochondrial membranes **(Figure 13)**, which is consistent with what others have reported[278].
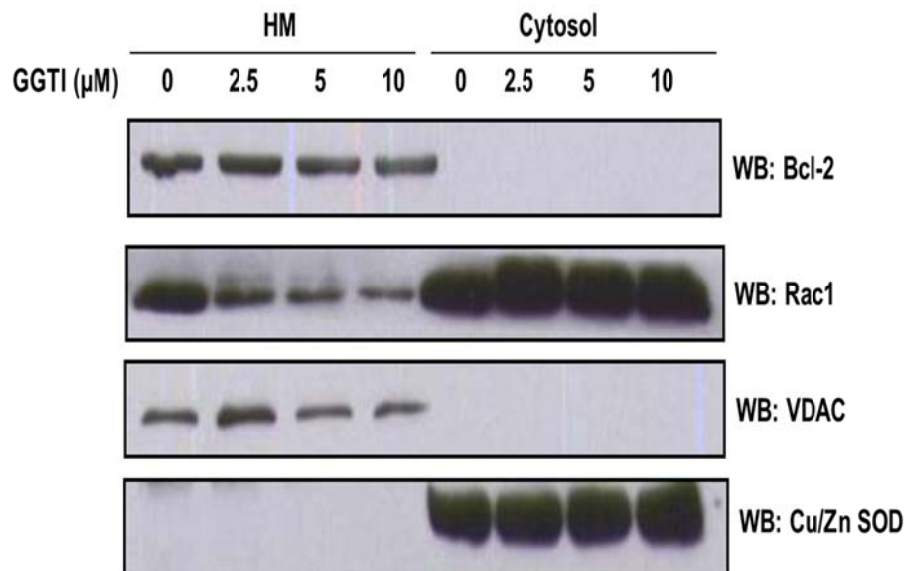
Figure 13: Geranylgeranylation of Rac1 is a pre-requisite for its mitochondrial localization. Jurkat cells treated with different doses of geranylgeranyl transferase inhibitor (GGTI) for 16 hrs were lysed and fractionated into purified mitochondria-enriched heavy membrane (HM) and cytosolic (S) fractions. The fractions were then probed for Bcl-2, Rac1, VDAC and Cu/Zn SOD.

3.5.3 Geranylgeranylation of Rac1 Is a Pre-requisite for Its Interaction with Bcl-2

Since a predominant localization for Bcl-2 is at the outer mitochondria membranes and we have also shown in the previous section that geranylgeranylation is essentially required for the mitochondrial targeting of Rac1, in order to confirm what the preliminary results have suggested in our laboratory that Rac1 interacts with Bcl-2 at the mitochondrial membranes, their interaction levels were measured through co-immunoprecipitation assay upon blocking of the geranylgeranylation process of Rac1 with GGTI. Indeed, when the mitochondrial import of Rac1 got inhibited substantially at 5 μM of GGTI **(Figure 13)**, there was also a significant reduction in the interaction levels between Rac1 and Bcl-2 and even to a non-detectable level with 10 μM of GGTI treatment observed in Jurkat cells **(Figure 14)**. The intracellular levels of Rac1 and Bcl-2 were not changed upon GGTI treatment as shown in the lower input panel **(Figure 14)** indicating that the change in the interaction levels was not due to the change in total protein levels of the two partners but rather the change of the subcellular distribution of Rac1. This confirms that it is the membrane associated Rac1 which interacts with Bcl-2.
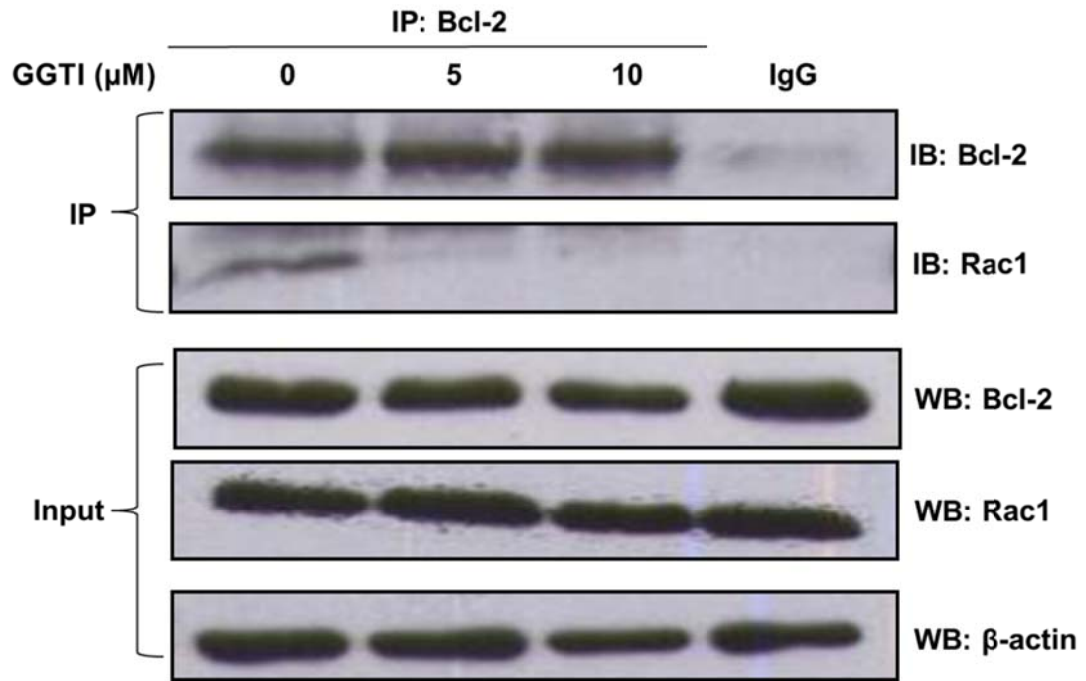
Figure 14: Geranylgeranylation of Rac1 is a pre-requisite for its interaction with Bcl-2. Jurkat cells treated with different doses of geranylgeranyl transferase inhibitor (GGTI) for 16 hrs were lysed and immunoprecipitated with anti-Bcl-2 and probed with anti-Bcl-2 and anti-Rac1. Immunoprecipitation with control rabbit anti-IgG antibodies was used as a negative control. Whole cell lysates probed with anti-Bcl-2, anti-Rac1 and anti-β-actin are shown on the bottom panel as input.
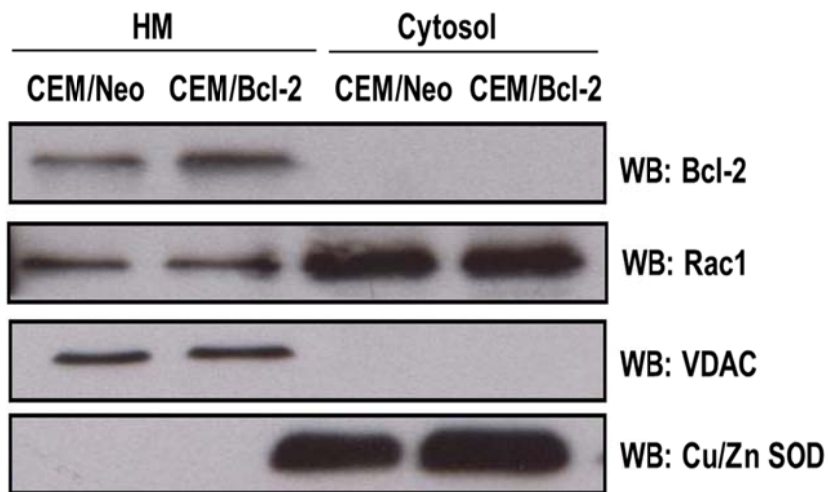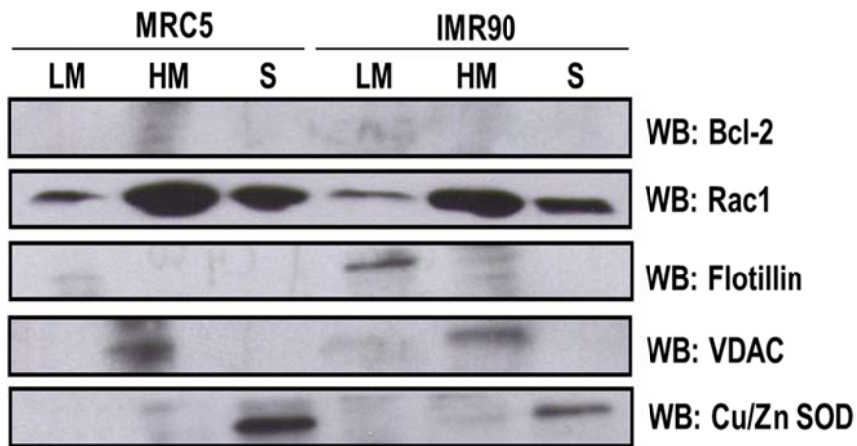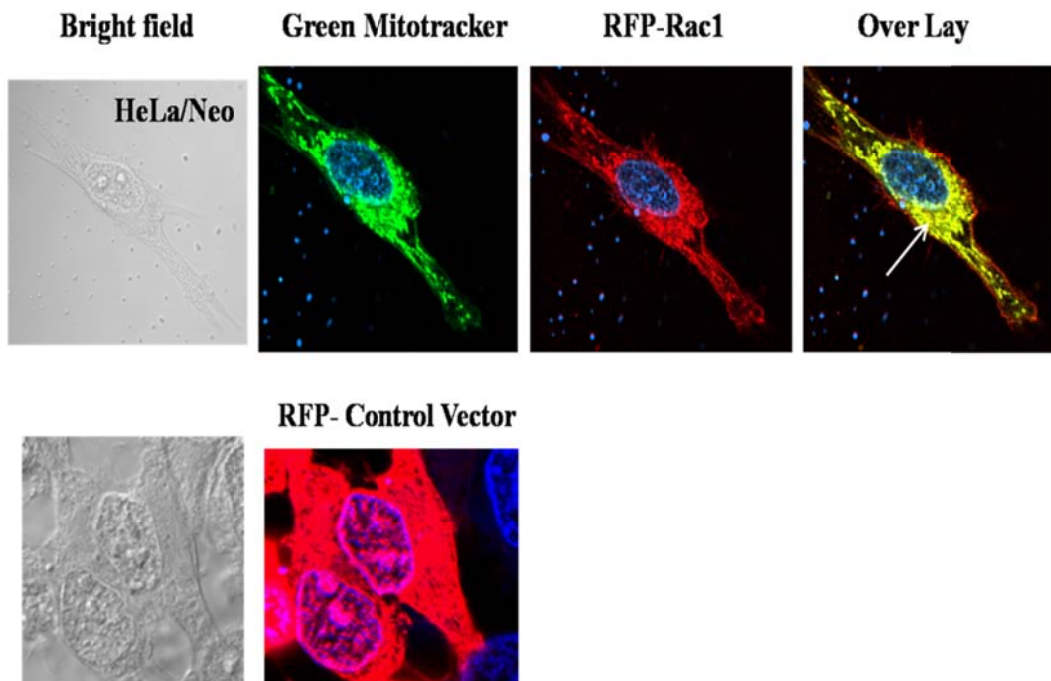
3.6. Active Rac1 Has a Higher Affinity towards Bcl-2

3.6.1 Crude Activation of GTPases by GTP-γS Loading Increased Rac1-Bcl-2 Interaction Levels while Inactivation by GDP Loading Showed the Opposite

Combining the preliminary results from our laboratory as well as the results discussed in the previous sections, Rac1 is critically involved in Bcl-2-induced pro-oxidant state in the mitochondria and this regulatory property is highly likely to be mediated through a physical interaction between the two proteins at the mitochondrial membranes. As is known, Rac1, when it is in a GTP-bound active form, can lead to activation of NADPH oxidases for O_2^- production[264-267, 272, 273]; thus it is interesting to know the nucleotide binding status for the pool of Rac1 that is associated with Bcl-2. In order to address this question, several approaches were used and the first experiment carried out utilized a crude *in vitro* manipulation of the activation levels of GTPases in general by loading excessive amount of either the non-hydrolysable GTP analog GTP-γS to lock them in constitutively active states or GDP to inactivate them. Since the nucleotides are not cell permeable, the incubation was done with whole cell lysates for 15 mins at 37°C with agitation[327]. Interestingly, in Bcl-2-overexpressing HeLa cells, those that were loaded with GTP-γS showed significantly elevated interaction levels between Bcl-2 and Rac1 as compared to control cells without any loading while those loaded with GDP showed a remarkable reduction **(Figure 15A)** indicating a direct correlation between Rac1 activation status and its interaction levels with Bcl-2. GTP- γS loading also resulted in a significant increase in the O_2^- levels of the isolated mitochondria from CEM/Bcl-2 cells (**Figure 15B**) corroborating the findings presented in section 3.3 that Rac1 regulates mitochondrial O_2^- levels of Bcl-2-overexpressing cancer cells (**Figure 5 & 6**).
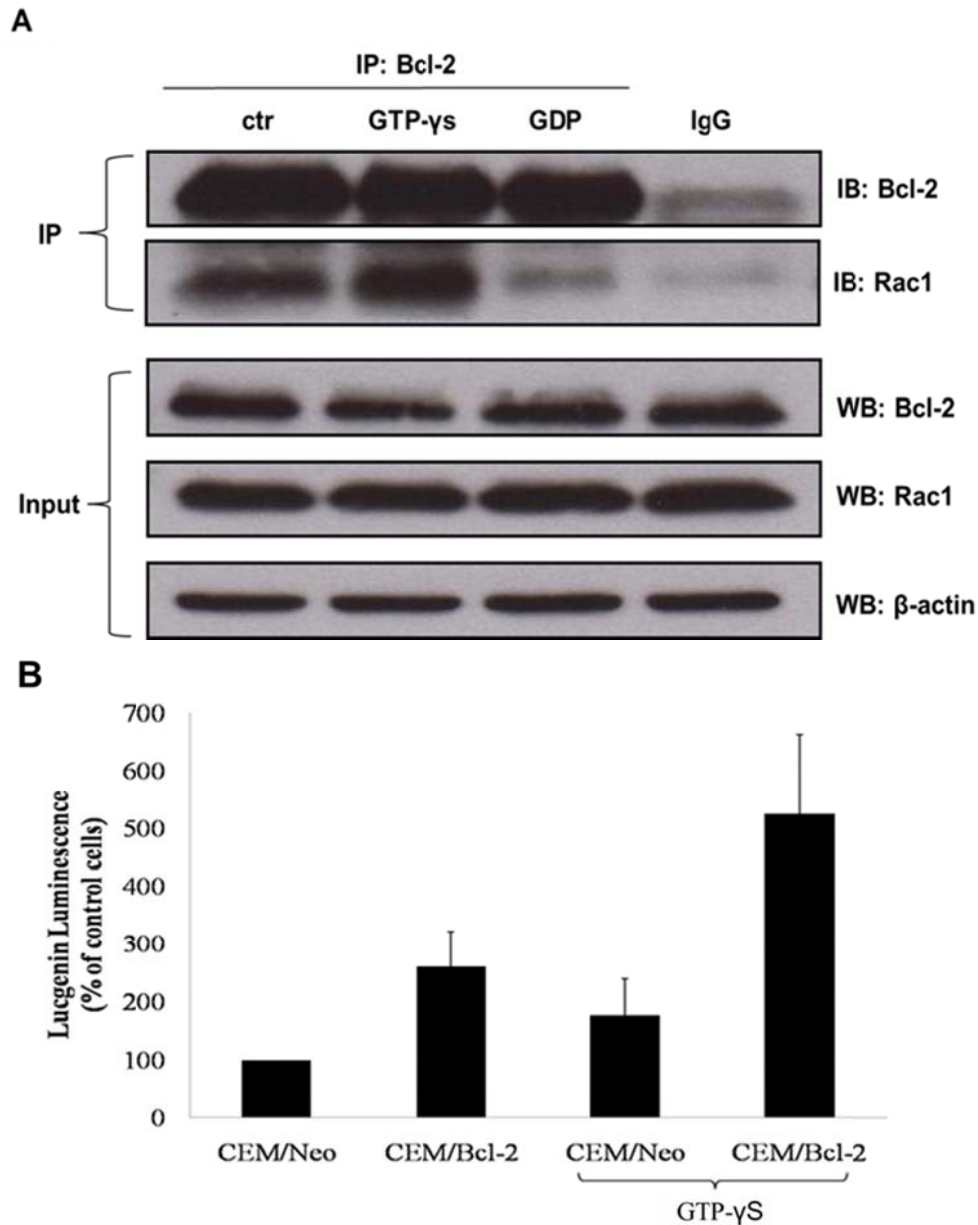
Figure 15: Crude activation of GTPases by GTP-γS loading increased Rac1-Bcl-2 interaction levels while inactivation by GDP loading decreased the interaction levels. (A) HeLa cells stably overexpressing Bcl-2 were loaded with either GTP-γS or GDP for 15 mins or without any loading (ctr) and immunoprecipitated with anti-Bcl-2 and probed with anti-Bcl-2 anti-Rac1. Immunoprecipitation with control rabbit anti-IgG antibodies was used as a negative control. Whole cell lysates probed with anti-Bcl-2, anti-Rac1 and anti-β-actin are shown on the bottom panel as input. (B) Mitochondrial O_2^- levels in isolated, GTP-γS-loaded CEM cells were measured using lucigenin-based chemiluminescence assay. The error bars represent means ± SD of at least 3 independent experiments. CEM/Bcl-2: CEM cells stably overexpressing Bcl-2; CEM/Neo: CEM cells stably overexpressing the control vector containing neomycin.

3.6.2 Transient Overexpression of a Dominant Negative Rac1 Mutant N17 Decreased Rac1-Bcl-2 Interaction Levels

Although GTP-γS loading greatly enhanced the interaction levels between Rac1 and Bcl-2 and GDP loading resulted in the opposite, this is a crude manipulation where all GTPases got activated or inactivated. In order to specifically manipulate the activation levels of Rac1, two Rac1 mutants were utilized, the constitutively active Rac1V12 and the dominant negative Rac1N17. The mutants are tagged with a polypeptide (12 amino acids long) derived from c-myc so as to differentiate with the endogenous Rac1 in the western blot analysis by about 1KDa in molecular weight. Rac1V12, with a glycine to valine substitution, is deficient in the intrinsic GTPase activity, thus the bound GTP cannot be hydrolyzed and is constitutively locked in the active state[241]. On the contrary, N17, a threonine to asparagine substitution mutant, which has essentially no affinity for GTP and reduced affinity for GDP, is constantly either in a nucleotide free form or the inactive GDP-bound form. It binds to Rac GEFs in a very high affinity therefore blocking the activation of endogenous Rac1 by these GEFs[103]. In HeLa cells that were transiently transfected with myc-tagged Rac1N17, there was a significant decrease in the interaction levels between endogenous Rac1 and Bcl-2 as compared to control vector transfected cells **(Figure 16)**. The decrease in the endogenous interaction levels could probably result from the inactivation of endogenous Rac1 due to the sequestration of Rac GEFs by the dominant negative Rac1N17 since the amount of introduced exogenous myc-tagged Rac1N17 is comparable to the endogenous levels as shown in the lower input panel **(Figure 16)**. This indicates that Rac1, when it is in the inactive GDP-bound state, loses its affinity for Bcl-2. However, due to the relatively lower transfection efficiency of the myc-tagged Rac1V12 as shown by the band right above the endogenous Rac1 in the input

panel, its interaction with endogenous Bcl-2 could not be picked up on the western blot following co-immunoprecipitation; however, there was a slightly increased interaction levels between the endogenous Rac1 and Bcl-2 upon transient introduction of exogenous Rac1V12 **(Figure 16)**.
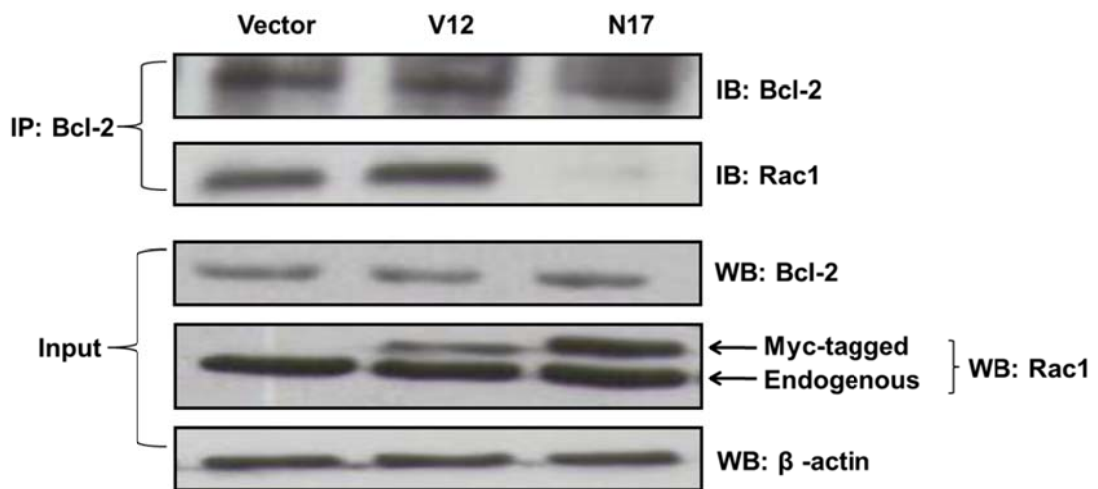
Figure 16: Transient overexpression of a constitutively active Rac1 mutant V12 increased Rac1-Bcl-2 interaction levels while overexpression of a dominant negative mutant N17 decreased the interaction levels. HeLa cells transiently transfected with either the empty pIRES vector, constitutively active Rac1 mutant V12 or dominant negative mutant N17 for 48 hrs were immunoprecipitated with anti-Bcl-2 and probed with anti-Bcl-2 and anti-Rac1. Whole cell lysates probed with anti-Bcl-2, anti-Rac1 and anti-β-actin are shown on the bottom panel as input.

3.6.3 Pharmacological Inhibition of Rac1 Activity Decreased Its Interaction Levels with Bcl-2

To further confirm that Rac1 activation status is critical in determining its binding affinity towards Bcl-2, the pharmacological inhibitor of Rac1, NSC23766 was used to block Rac1 interaction with Rac GEFs. Indeed, a significant reduction in the interaction levels between Rac1 and Bcl-2 was observed even at the lowest dose of 10 μM of NSC23766 used in HeLa cells (**Figure 17**). Since NSC23766 only blocks the interaction of Rac1 with a certain range of GEFs (including Tiam1 and TrioN) but not all (such as Vav1), a second generation pharmacological inhibitor of Rac1, EHT1864 was also used. EHT1864 binds to Rac1 in high affinity (with K_D of 40 nM) promoting dissociation of bound nucleotides therefore locking Rac1 in an inert and inactive state. EHT1864 is more potent as compared to the first generation inhibitor NSC23766 in the sense that it is expected to block all downstream effectors both *in vitro* and *in vivo*. Furthermore, EHT1864 has been shown to block a variety of downstream signaling activities even in the presence of the ectopic expression of Rac1V12 *in vivo* which couldn't be achieved with NSC23766. The IC_{50} for EHT1864 is about 2.5 μM, 20-fold more potent as compared with NSC23766 and its specificity for Rac is also demonstrated where it does not affect other members in the Rho GTPases family such as RhoA and Cdc42[243, 328]. Indeed, Bcl-2-overexpressing CEM cells, upon exposure to 5 or 10 μM EHT1864 for 2 hrs, showed dose-dependent reduction in Bcl-2-Rac1 interaction levels after normalizing against the internal control β-actin based on densitometry analysis with ImageJ **(Figure 18)** confirming once again that active Rac1 has a higher affinity towards Bcl-2.
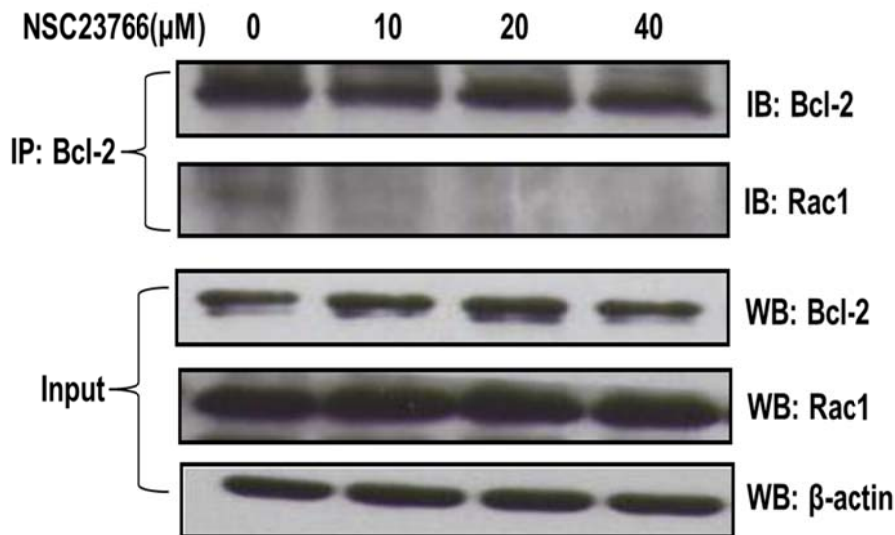
Figure 17: Pharmacological inhibition of Rac1 activity with NSC23766 decreased its interaction levels with Bcl-2. HeLa cells treated with different doses of Rac1 inhibitor NSC23766 for 24 hrs were immunoprecipitated with anti-Bcl-2 and probed with anti-Rac1. Whole cell lysates probed with anti-Bcl-2, anti-Rac1 and anti-β-actin are shown on the bottom panel as input.
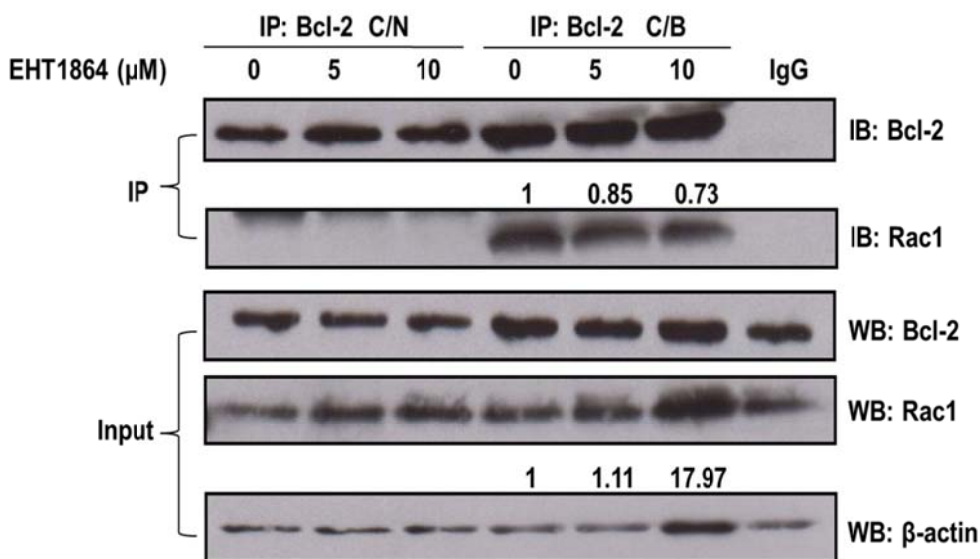
Figure 18: Pharmacological inhibition of Rac1 activity with EHT1864 decreased its interaction levels with Bcl-2. (A) CEM/Neo (C/N) and CEM/Bcl-2 (C/B) cells were treated with different doses of Rac1 inhibitor EHT1864 for 2hrs and immunoprecipitated with anti-Bcl-2 and probed with anti-Bcl-2 and anti-Rac1. Immunoprecipitation with control rabbit anti-IgG antibodies was used as a negative control. Whole cell lysates probed with anti-Bcl-2, anti-Rac1 and anti-β-actin are shown on the bottom panel as input.

3.6.4   Rac1-Bcl-2 Interaction Is Dependent on Nox Activity and Two Isoforms of

Nox Family Proteins Nox2 and Nox4 Are Present in the Mitochondria of Bcl-

2-overexpressing Cancer Cells

As discussed in the previous sections from 3.6.1 to 3.6.3, Rac1, when it is in a

GTP-bound state, has a higher affinity towards Bcl-2 and since active Rac1 is able to

activate NADPH oxidases for O_2^- production, it is interesting to investigate whether

Nox activity in turn could affect the interaction levels between Rac1 and Bcl-2. A

general inhibitor for flavin-containing enzymes, diphenyleneiodonium (DPI), was

used to block the activity of NADPH oxidases. CEM/Bcl-2 cells were subcellularly

fractionated after DPI treatment for 2 hrs followed by co-immunoprecipitation

analysis. There was a significant reduction in the interaction levels of Rac1 and Bcl-2

in mitochondria-enriched HM fractions following inhibition of NADPH oxidases

(Figure 19A) suggesting that the interaction could be redox regulated. Interestingly,

the interaction was, for the first time, observed in LM fractions as well **(Figure 19A)**

indicating that this interacting complex is possibly not restricted to mitochondrial

membranes alone. Both the interaction levels and the protein expression levels of

Rac1 in LM fractions went up after DPI treatment **(Figure 19A),** the mechanisms of

which await further investigation. Whereas for cytosolic fractions, there were no

detectable interaction levels **(Figure 19A)** since Bcl-2 is usually not a cytosolic

protein.

Intrigued by this finding that inhibition of Nox activity affected the interaction

levels in the mitochondria of Bcl-2-overexpressing cancer cells, a screen for the

presence of Nox isoforms and subunits in the mitochondria was carried out.

Preliminary results from the initial screen in different subcellular fractions of

110

CEM/Bcl-2 cells revealed that an isoform of Nox family, Nox4 was present in both the mitochondria-enriched HM fractions and LM fractions. Another isoform Nox2 (p91phox) was also detected in both fractions although to a lesser degree in HM fractions. However, the subunit common to both Nox1 and Nox2 complex, p47phox, was only detected in LM fractions but not in HM fractions **(Figure 19B)**. VDAC, Flotillin and Cu/Zn SOD were used as fraction markers to show that there was no cross contamination among different subcellular fractions **(Figure 19)**.
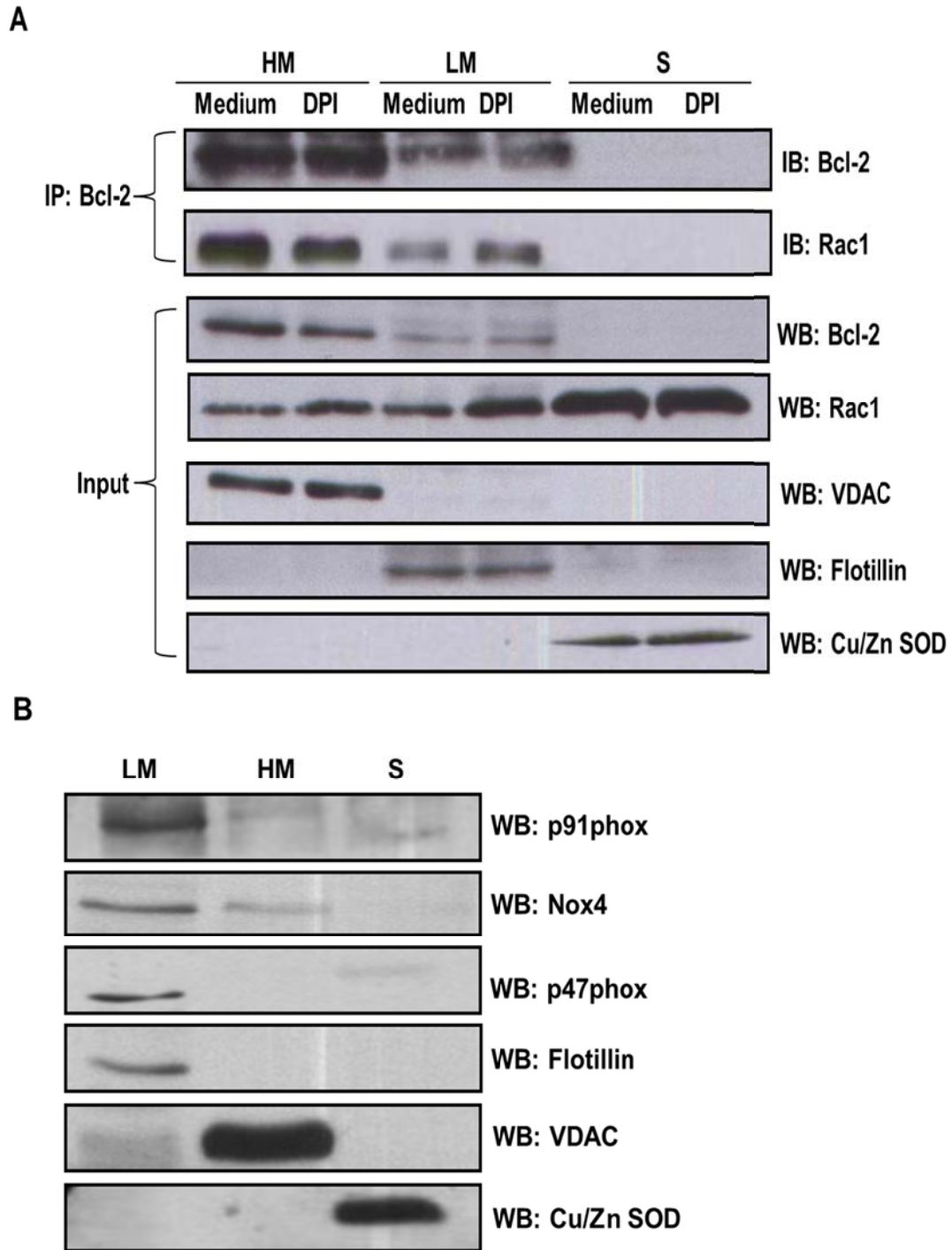
Figure 19: Rac1-Bcl-2 interaction is dependent on Nox activity. (A) CEM cells overexpressing Bcl-2 were treated with 5μM diphenyleneiodonium (DPI) or control medium for 2 hrs, lysed and fractionated into mitochondria-enriched purified heavy membrane (HM), light membrane (LM) and cytosolic (S) fractions. The fraction lysates were then immunoprecipitated with anti-Bcl-2 and probed with anti-Bcl-2 and anti-Rac1. Fraction lysates probed for Bcl-2, Rac1, VDAC, Flotillin and Cu/Zn SOD are shown on the bottom panel as input. (B) CEM cells overexpressing Bcl-2 were lysed and fractionated into mitochondria-enriched purified heavy membrane (HM), light membrane (LM) and cytosolic (S) fractions. The fractions were then probed for p91phox, Nox4, p47phox, Flotillin, VADC and Cu/Zn SOD.

3.7. Residue F37 of Rac1 Is Critical in Its Interaction with Bcl-2

In order to further characterize the exact domain(s) or even residue(s) of Rac1 involved in its interaction with Bcl-2, four point mutants currently available in our laboratory were checked for their binding ability towards Bcl-2 through co-immunoprecipitation analysis. The four mutants used were L37 (with phenylalanine substituted by leucine), H40 (with tyrosine substituted by histidine), H103 (with alanine substituted by histidine) and K166 (with glutamic acid substituted by lysine), which are all in the constitutively active V12 background. In addition, they are functional mutants as well: L37 is defective in actin cytoskeleton reorganization, H40 is defective in JNK activation, while H103 and K166 are both defective in NADPH oxidases activation[103, 329, 330]. V12 was also included serving as a positive control since active Rac1 has been shown to have a higher binding affinity towards Bcl-2 in previous sections. In order to minimize the interference coming from the fact that H40 is defective in JNK activation and Ser70 of Bcl-2 has been reported to be a phosphorylation site for JNK[171, 176, 183-185], a Bcl-2 S70E mutant was used where Ser70 is mutated to glutamic acid to mimic a phosphorylated status, instead of a wild type Bcl-2, to rule out any possible interference from phosphorylation. Furthermore, instead of Rac1 or Bcl-2 antibodies, a myc-tag specific antibody was used to pull down the transiently introduced myc-tagged Rac1 mutants to prevent any interference from the abundantly expressed endogenous Rac1. The portion of Bcl-2 that had been pulled down together with the myc-tagged Rac1 mutants was the ectopically introduced Bcl-2 S70E since HeLa has very low intracellular Bcl-2 levels as shown in the input panel **(Figure 20)**. After normalizing for the ectopic expressed Rac1 and Bc-2 levels due to variations in transfection efficiencies, preliminary screening results revealed that one of the four functional mutants, L37, had a

remarkable reduction in its interaction levels with the ectopically expressed Bcl-2 S70E **(Figure 20)**. Interestingly, residue 37 lies in the Switch 1 effector region (residues 29-40) that interacts with the magnesium ion Mg^{2+} which stabilizes the binding of guanine nucleotides and this region is also involved in Rac1's interaction with GEFs[242], suggesting that Bcl-2 interaction with Rac1 could have great impact on Rac1 activation status in return.
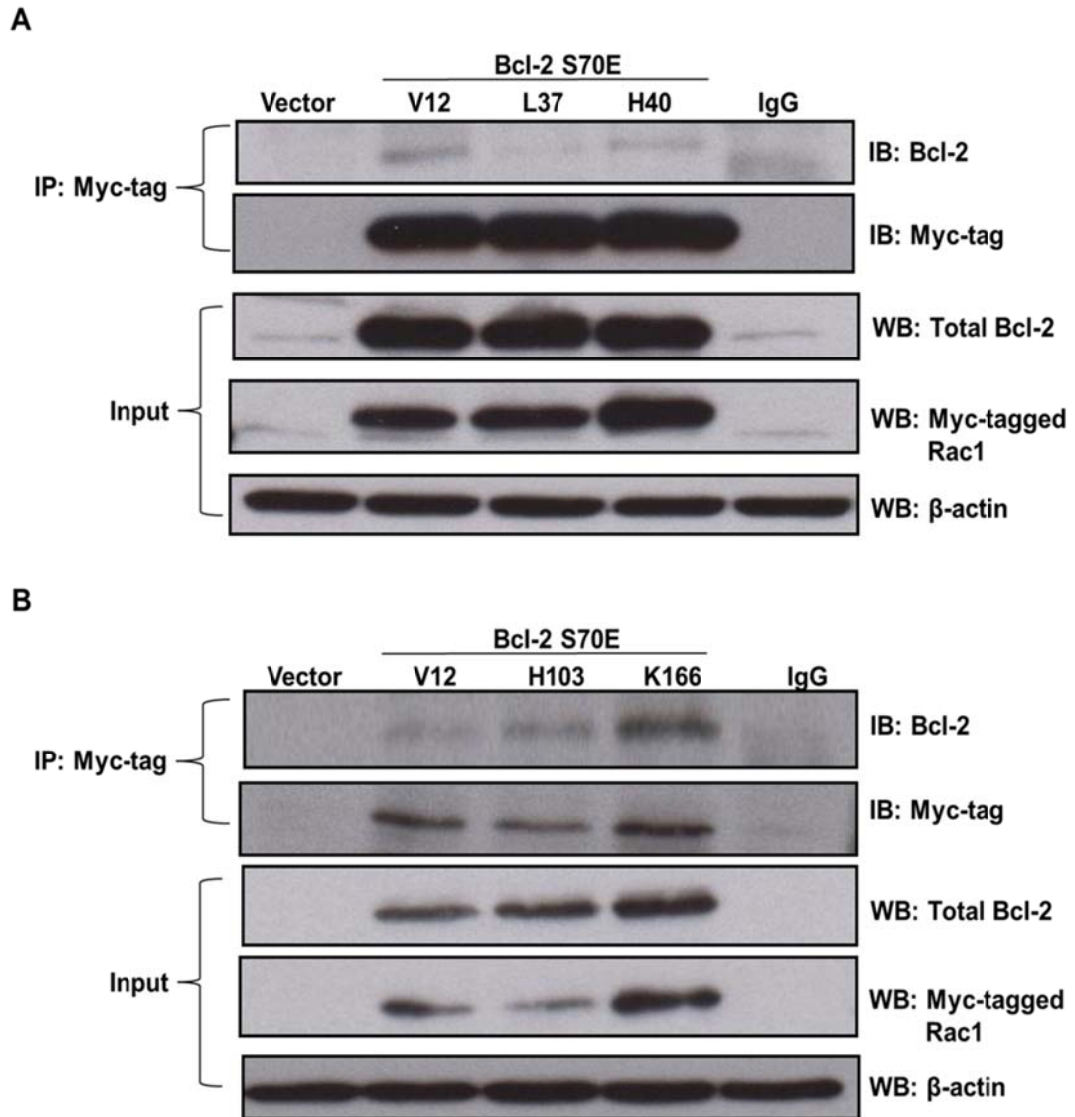
Figure 20: A functional mutant of Rac1 L37 has a significantly lower affinity for Bcl-2. (A) HeLa cells were transiently co-transfected with a Bcl-2 phosphomimetic mutant S70E and a functional Rac1 mutant (either V12 or L37 or H40) for 48 hrs and then immunoprecipitated with anti-Myc-tag and probed with anti-Bcl-2 and anti-Myc-tag. Cells co-transfected with the respective two empty vectors were used as a control. Immunoprecipitation with control rabbit IgG was used as a negative control. Whole cell lysates probed with anti-Bcl-2, anti-Myc-tag and anti-β-actin are shown on the bottom panel as input. (B) HeLa cells were transiently co-transfected with a Bcl-2 phosphomimetic mutant S70E and a functional Rac1 mutant (either V12 or H103 or K166) for 48 hrs and then immunoprecipitated with anti-Myc-tag and probed with anti-Bcl-2 and anti-Myc-tag. Cells co-transfected with the respective two empty vectors were used as a control. Immunoprecipitation with control rabbit IgG was used as a negative control. Whole cell lysates probed with anti-Bcl-2, anti-Myc-tag and anti-β-actin are shown on the bottom panel as input.

3.8. The BH3 Domain but not BH4 Domain of Bcl-2 is Required for Its Interaction with Rac1 *In Vivo*

3.8.1 Bcl-2 BH3 Peptides Disrupted Rac1 and Bcl-2 Interaction at the Mitochondria *In Vivo*

Bcl-2, as discussed earlier in the introduction, possesses four Bcl-2 homology (BH) domains[127] and preliminary *in vitro* results from our laboratory showed a BH3 domain but not BH4 domain dependency of Bcl-2 in its interaction with Rac1. To confirm this point and extend it further to *in vivo* conditions, Bcl-2-overexpressing CEM cells were incubated with a short stretch of peptides with 15 amino acids long from Bcl-2 BH3 domain **(Figure 21B)** followed by co-immunoprecipitation analysis on different subcellular fractions. To make the peptides cell permeable, an HIV TAT (Human Immunodeficiency Virus trans-activator of transcription) protein was tagged to the peptides for increasing their *in vivo* uptake[331]. Indeed, upon 2 hrs exposure of the TAT-Bcl-2 BH3 peptides which sit in and block the BH3 domain groove, there was a significant reduction in the Rac1-Bcl-2 interaction levels in the mitochondria-enriched HM fractions **(Figure 21A)** confirming the BH3 domain dependency of this interaction *in vivo*. Interestingly, similar to what was observed in **Figure 19A**, the interaction was also observed at the LM fractions **(Figure 21A)**; however, the exact functions of the interacting complex at those membrane structures remain elusive.

A

HM | LM | S
Medium BH3 | Medium BH3 | Medium BH3

IP: Bcl-2
IB: Bcl-2
IB: Rac1

Input
WB: Bcl-2
WB: Rac1
WB: VDAC
WB: Flotillin
WB: Cu/Zn SOD

B

KKKRRQRRR — PVVHLTLRQAGDDFSR — COOH

HIV-TAT
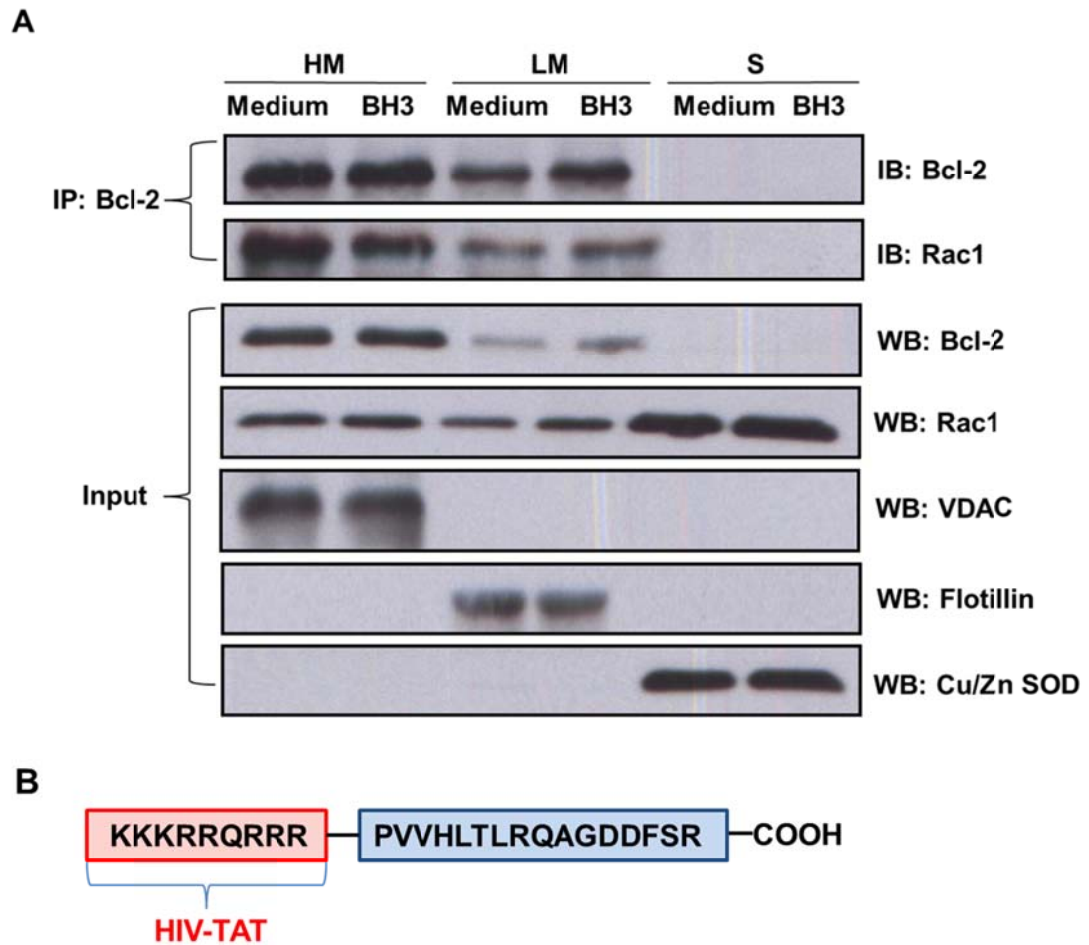
Figure 21: Bcl-2 BH3 peptides disrupted Rac1 and Bcl-2 interaction at the mitochondria-enriched heavy membranes *in vivo*. (A) CEM cells overexpressing Bcl-2 were treated with TAT-tagged Bcl-2 BH3 peptide (10μM) or control medium for 2 hrs, lysed and fractionated into mitochondria-enriched purified heavy membrane (HM), light membrane (LM) and cytosolic (S) fractions. The fraction lysates were then immunoprecipitated with anti-Bcl-2 and probed with anti-Bcl-2 and anti-Rac1. The fraction lysates probed for Bcl-2, Rac1, VDAC, Flotillin and Cu/Zn SOD are shown at the bottom panel as input. (B) Sequence of cell permeable TAT-Bcl-2 BH3 peptides.

3.8.2   Bcl-2 and Rac1 Interaction Is BH4 Domain Independent *In Vivo*

Similarly, the involvement of BH4 domain of Bcl-2 in the interacting complex was also tested by using a short stretch of peptides (24 amino acids long) from the Bcl-2 BH4 domain **(Figure 22C)**. However, contrary to what was observed with Bcl-2 BH3 domain peptides, exposure to the cell permeable TAT-Bcl-2 BH4 peptides for 2 hrs did not affect the Rac1-Bcl-2 interaction levels in the whole cell lysates of CEM/Bcl-2 cells. There was also no change in the intracellular expression levels of Rac1 and Bcl-2 **(Figure 22A)**. Since Bcl-2 is known to interact with another small GTPase Ras through its BH4 domain, this interaction was probed as a positive control where BH4 peptides significantly disrupted the interaction between Bcl-2 and pan-Ras (including all three isoforms H-Ras, K-Ras and N-Ras) even with the lowest dose of 5 μM used as shown in **Figure 22B**, consistent to what other groups have reported[194].
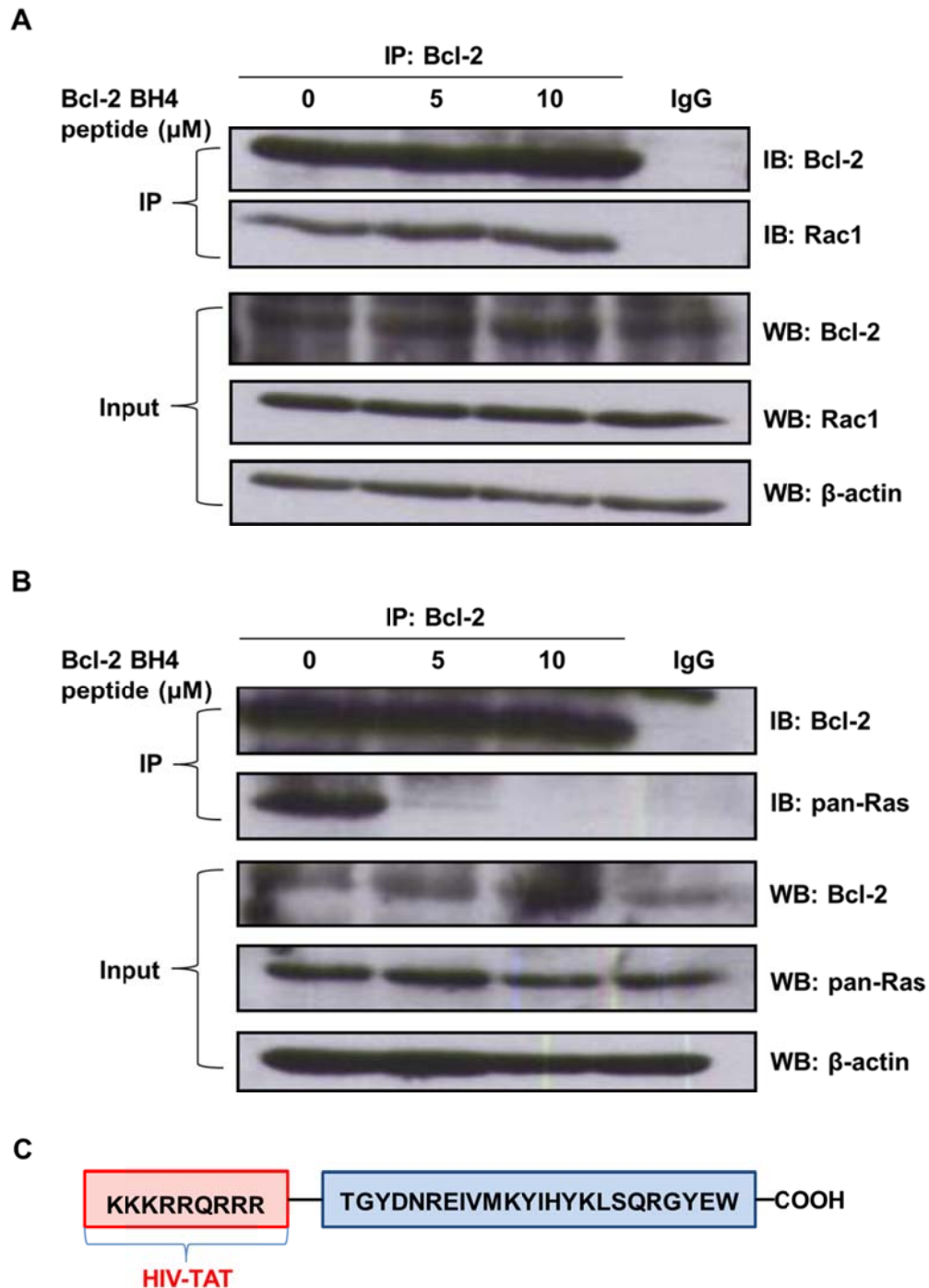
Figure 22: Bcl-2 and Rac1 interaction is BH4 domain independent *in vivo*. (A) CEM/Bcl-2 cells were incubated with various doses of TAT-tagged Bcl-2 BH4 peptides for 2 hrs and the lysates were then immunoprecipitated with anti-Bcl-2 and probed with anti-Bcl-2 and anti-Rac1. Immunoprecipitation with control rabbit IgG was used as a negative control. The whole cell lysates probed for Bcl-2, Rac1 and β-actin are shown at the bottom panel as input. (B) CEM/Bcl-2 cells were incubated with various doses of TAT-tagged Bcl-2 BH4 peptides for 2 hrs and the lysates were then immunoprecipitated with anti-Bcl-2 and probed with anti-Bcl-2 and anti-pan-Ras. Immunoprecipitation with control rabbit IgG was used as a negative control. The whole cell lysates probed for Bcl-2, pan-Ras and β-actin are shown at the bottom panel as input. (C) Sequence of cell permeable TAT-Bcl-2 BH4 peptides.

3.9. The Phosphorylation Status at the Flexible Loop Region of Bcl-2 Is Critical for Its Interaction with Rac1

3.9.1 A Non-phosphorylatable Bcl-2 Mutant T69A/S70A/S87A, When Overexpressed Transiently, Failed to Interact with Endogenous Rac1 in Cancer Cells

As discussed in the previous sections, the Bcl-2-Rac1 interaction showed a Bcl-2 BH3 domain dependency but a BH4 domain independency *in vivo*. To further characterize the binding domains of Bcl-2 involved in its interaction with Rac1, the flexible loop region, which connects BH3 and BH4 domains, was also examined with a particular focus on the phosphorylation status due to its implications on the anti-apoptotic activity of Bcl-2[131, 162, 163]. A phosphorylation deficient Bcl-2 mutant T69A/S70A/S87A (AAA) was utilized here since alanine lacks the –OH group for addition of a phosphate group thus it cannot be phosphorylated while structurally it still resembles serine/threonine (except that the –OH group is replaced with $-CH_3$ in the case of threonine). The three residues (Thr69/Ser70/Ser87) are in close proximity to BH3 domain and thus addition of a negative charge from the phosphate group could likely affect the binding affinity between Bcl-2 and Rac1. Upon 48 hrs transient transfection of this Bcl-2 AAA mutant into HeLa/Neo cells with relatively low endogenous Bcl-2 levels, co-immunoprecipitation assay was performed to analyse the binding ability of the mutant towards endogenous Rac1. The absence of a phospho-Bcl-2 band in the input panel of western blot indicated that this is a *bona fide* phosphorylation deficient mutant, as compared to the wild type (WT) Bcl-2 which showed certain levels of phosphorylation upon transient introduction into the cells **(Figure 23A)**. Interestingly, the phosphorylation levels of Bcl-2 also translated into its binding affinity towards endogenous Rac1 where the Bcl-2 AAA mutant

completely lost the affinity as compared to WT Bcl-2 **(Figure 23A)** suggesting that the phosphorylation status in one or more than one of the three residues in the flexible loop region could be important in determining Bcl-2's binding affinity towards Rac1. In addition, Bcl-2 AAA mutant was also tested for its binding affinity towards Bax, which is a well-known homologous interacting partner for Bcl-2 within the Bcl-2 family. No change in the interaction levels between Bcl-2 and Bax was observed **(Figure 23B)** indicating that although both Bax-Bcl-2 interaction and Rac1-Bcl-2 interaction show a BH3 domain dependency, their binding pocket is unlikely to be exactly the same.
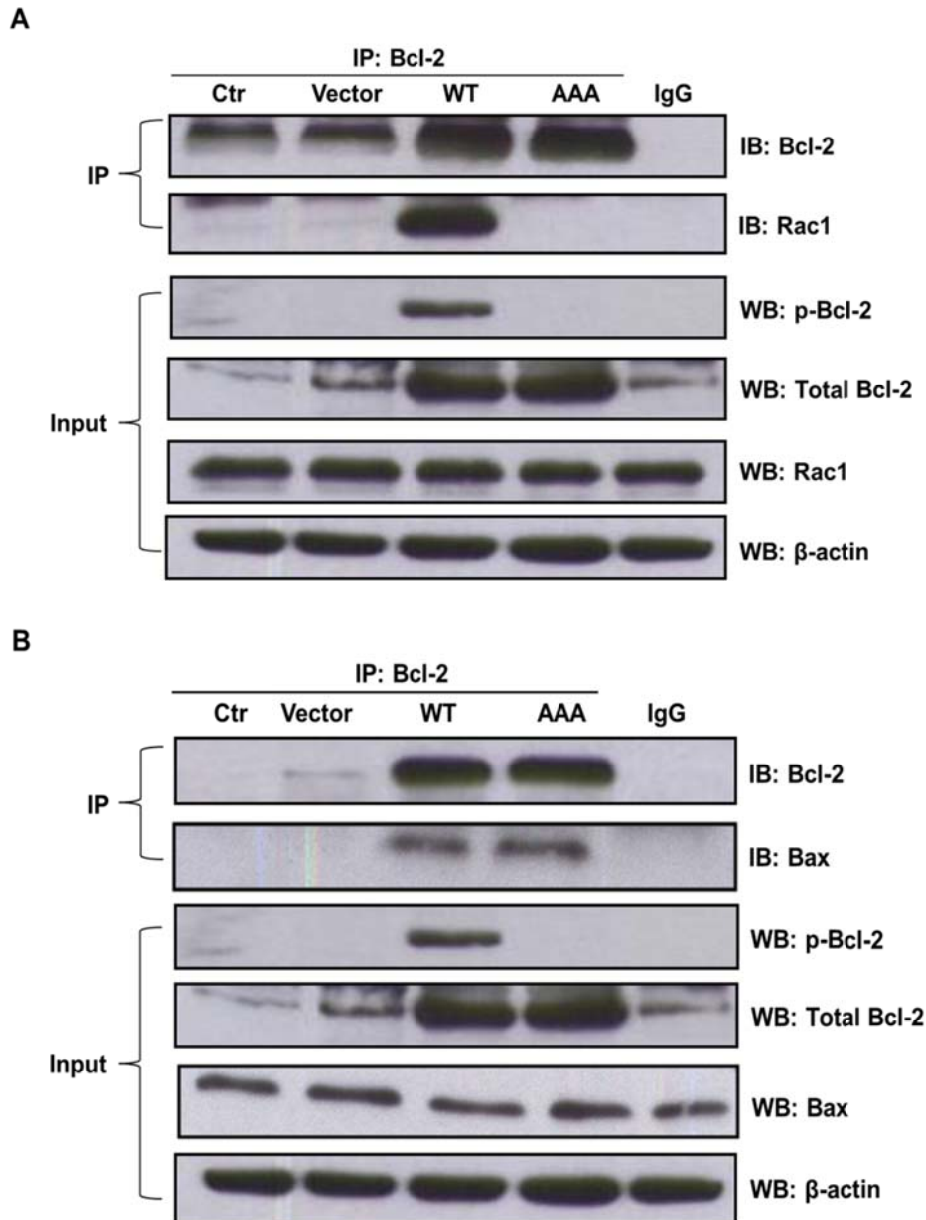
Figure 23: A non-phosphorylatable Bcl-2 mutant T69A/S70A/S87A (AAA), when overexpressed transiently, failed to interact with endogenous Rac1 in cancer cells. (A) HeLa/Neo cells were transiently transfected with control vector, Bcl-2 wild type (WT) and a non-phosphorylatable T69A/S70A/S87A (AAA) Bcl-2 mutant for 48 hrs and lysates were harvested for co-immunoprecipitation with anti-Bcl-2 and probed with anti-Bcl-2 and anti-Rac1. Immunoprecipitation with control rabbit IgG was used as a negative control. The whole cell lysates probed with anti-p-Bcl-2 (Ser70), anti-Bcl-2, anti-Rac1 and β-actin are shown at the bottom panel as input. (B) HeLa/Neo cells were transiently transfected with control vector, Bcl-2 wild type (WT) and a non-phosphorylatable T69A/S70A/S87A (AAA) Bcl-2 mutant for 48 hrs and lysates were harvested for co-immunoprecipitation with anti-Bcl-2 and probed with anti-Bcl-2 and anti-Bax. Immunoprecipitation with control rabbit IgG was used as a negative control. The whole cell lysates probed with anti-p-Bcl-2 (Ser70), anti-Bcl-2, anti-Bax and β-actin are shown at the bottom panel as input.

3.9.2 Bcl-2 Phosphorylation Status at Ser70 Is Critical for Its Interaction with Rac1

In an attempt to nail down on the exact residue(s) among the three (Thr69/Ser70/Ser87) in the flexible loop region of Bcl-2 that could be critically involved in its interaction with Rac1, both a single phosphorylation deficient mutant S70A and a single phosphomimetic mutant S70E were examined for their binding affinity towards Rac1. Glutamic acid is an effective phosphomimetic in the sense that it is basic with one negative charge and also structurally similar to phosphorylated serine. Co-immunoprecipitation analysis performed 48 hrs post-transfection of these two mutants into HeLa/Neo cells with relatively low endogenous Bcl-2 expression levels revealed that the non-phosphorylatable mutant S70A had minimal binding affinity towards endogenous Rac1 while the phosphomimetic S70E showed slightly enhanced binding affinity as compared to WT Bcl-2. The phosphorylation status of WT Bcl-2 as well as S70A and S70E mutants was shown in the input panel of the western blot analysis indicating a direct correlation between the phosphorylation status of Bcl-2 with its binding affinity towards Rac1 **(Figure 24)**.
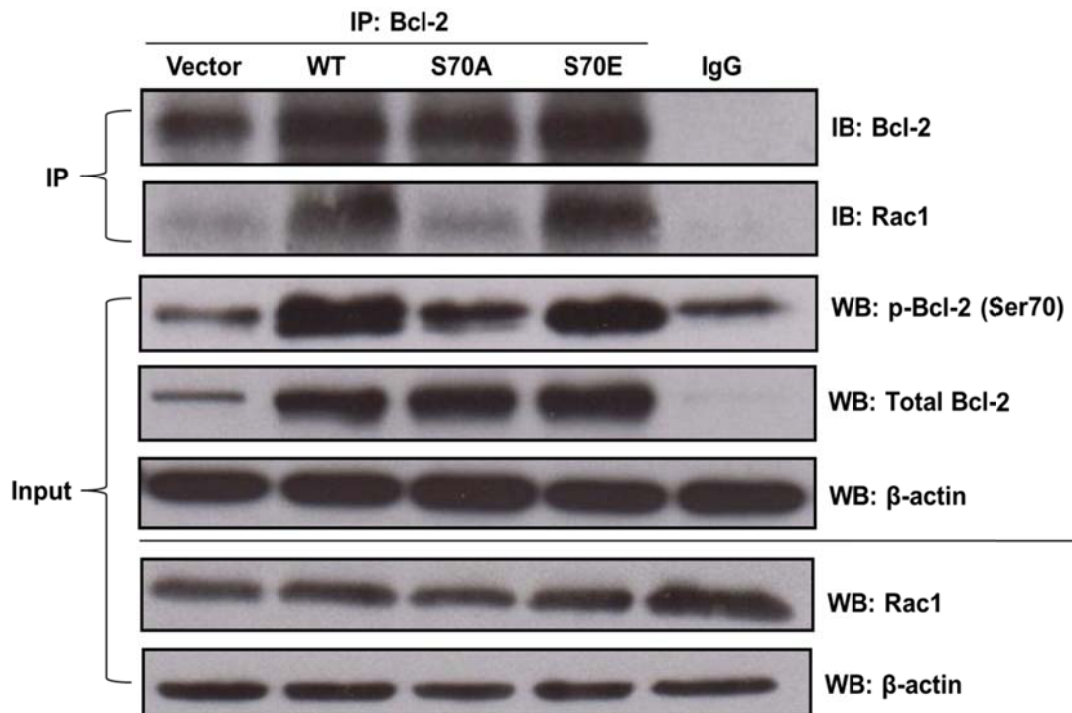
Figure 24: Bcl-2 phosphorylation status at Ser70 is critical for its interaction with Rac1. HeLa/Neo cells were transiently transfected with control vector, Bcl-2 wild type (WT), a non-phosphorylatable S70A Bcl-2 mutant and a phosphomimetic Bcl-2 mutant S70E for 48 hrs and lysates were harvested for co-immunoprecipitation with anti-Bcl-2 and probed with anti-Bcl-2 and anti-Rac1. Immunoprecipitation with control rabbit IgG was used as a negative control. Whole cell lysates probed with anti-p-Bcl-2 (Ser70), anti-Bcl-2, anti-Rac1 and anti-β-actin are shown on the bottom panel as input.

3.10. Active Rac1 Induces Phosphorylation of Bcl-2 at Ser70

3.10.1 Transient Overexpressed Bcl-2 Got Phosphorylated at Ser70 in Cancer Cells with a Constitutively Active Rac1 (V12) Background

To better characterize the two interacting partners in this complex, two functional elements that are critical for the interaction: the activation status of Rac1 and the phosphorylation status of Bcl-2, were checked to study if there is any cross talk between each other. Human melanoma M14 cells stably overexpressing either a constitutively active myc-tagged Rac1V12 or a dominant negative myc-tagged Rac1N17 and harbouring low endogenous Bcl-2 expression levels, were transiently transfected with Bcl-2. Interestingly, a significant proportion of the introduced Bcl-2 got phosphorylated at Ser70 in cells with Rac1V12 background which was not observed in control vector matched cells or cells with Rac1N17 background **(Figure 25)** suggesting a direct causal relationship between Rac1 activation and subsequent Bcl-2 phosphorylation at Ser70.
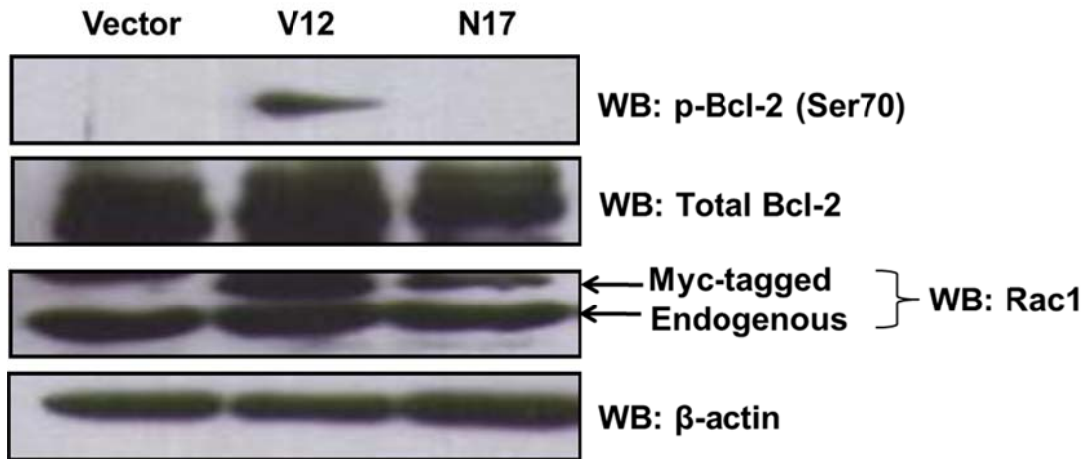
Figure 25: Transient overexpressed Bcl-2 got phosphorylated at Ser70 in cancer cells with a constitutively active Rac1 (V12) background. Human melanoma M14 cells stably overexpressing either the control vector pIRES, the constitutively active Rac1 mutant V12 or the dominant negative Rac1 mutant N17 were transiently transfected with Bcl-2 plasmid for 48 hrs. Whole cell lysates were probed with anti-p-Bcl-2 (Ser70), anti-Bcl-2, anti-Rac1 and anti-β-actin.

3.10.2 Transient Overexpression of a Dominant Negative Rac1 Mutant N17
Decreased Bcl-2 Phosphorylation Levels at Ser70

The direct causal relationship between Rac1 activation and Bcl-2 phosphorylation at Ser70 was further verified in another cancer cell line model, with a transient introduction of Rac1 mutants instead of Bcl-2. Transient introduction of the dominant negative Rac1 mutant N17 which could sequester Rac GEFs and override the effects of endogenous Rac1, significantly abolished the phosphorylation levels at Ser70 of endogenous Bcl-2 in HeLa cells while on the contrary, Rac1V12 enhanced the phosphorylation levels although to a lesser extent due to the relatively lower transfection efficiency **(Figure 26)**.
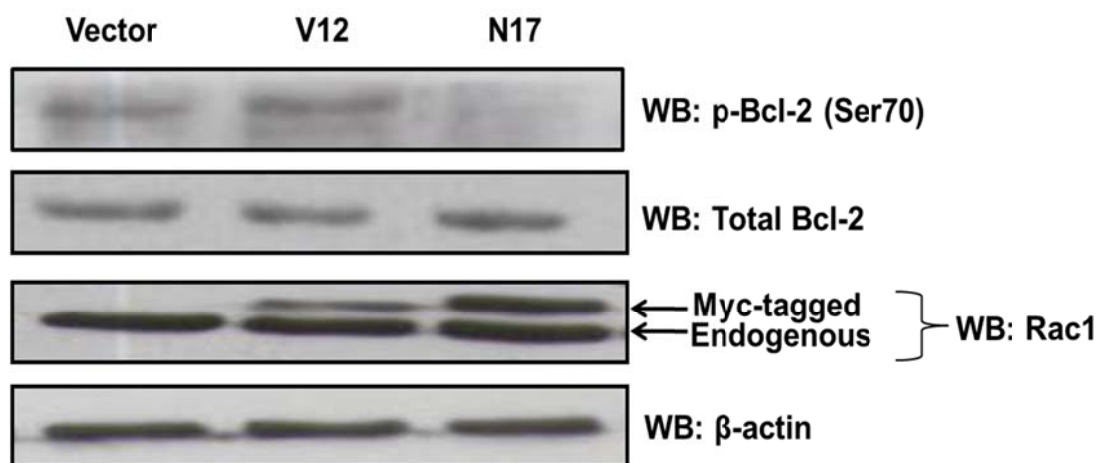
Figure 26: Transient overexpression of a dominant negative Rac1 mutant N17 decreased Bcl-2 phosphorylation levels at Ser70. HeLa cells were transiently transfected with either the control vector pIRES, the constitutively active Rac1 mutant V12 or the dominant negative Rac1 mutant N17 for 48 hrs and the lysates were probed with anti-p-Bcl-2 (Ser70), anti-Bcl-2, anti-Rac1 and anti-β-actin.

3.10.3 Pharmacological Inhibition of Rac1 Activity Decreased Bcl-2 Phosphorylation Levels at Ser70

To further confirm that there is a cross talk between Rac1 activation and Bcl-2 phosphorylation, a pharmacological inhibitor of Rac1 NSC23766 was utilized to block its activity. Indeed, upon 2 hrs exposure to increasing doses of NSC23766, a dose-dependent decrease in the endogenous phospho-Bcl-2 (Ser70) levels were observed in HeLa cells **(Figure 27)**. Taken together with the data discussed in the previous two sections, all these findings clearly point to the existence of a direct correlation between Rac1 activation levels and Bcl-2 phosphorylation status.
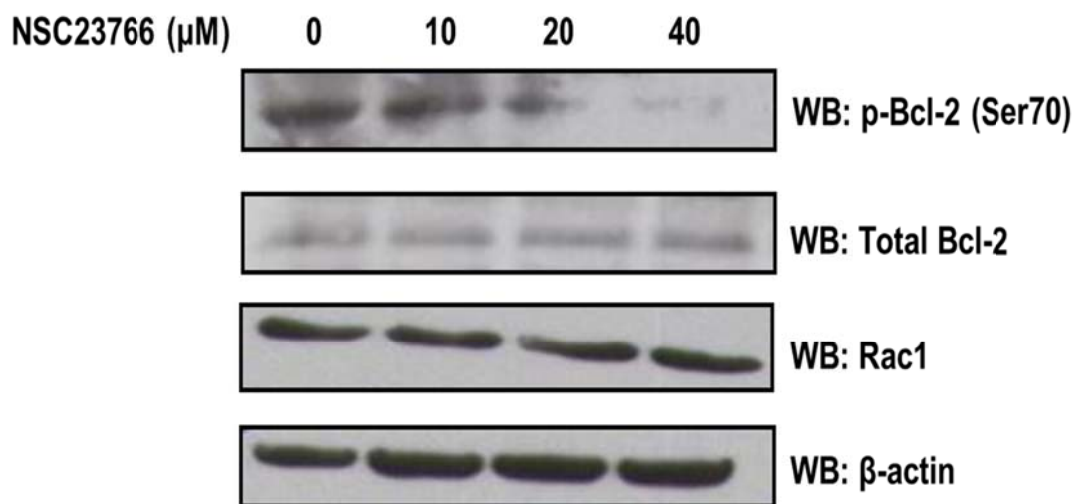
Figure 27: Pharmacological inhibition of Rac1 decreased Bcl-2 phosphorylation levels at Ser70. HeLa cells treated with different doses of Rac1 inhibitor NSC23766 for 2 hrs were lysed and probed with anti-p-Bcl-2 (Ser70), anti-Bcl-2, anti-Rac1 and anti-β-actin.

3.11. Active Rac1-induced Bcl-2 Phosphorylation at Ser70 is Mediated through JNK

3.11.1 JNK Is a Potential Upstream Kinase Responsible for Rac1V12-induced Bcl-2 Phosphorylation at Ser70

The phosphorylation status of a protein depends on the activities of both kinase(s) and phosphatase(s). In an attempt to look for the kinase(s) that is(are) responsible for active Rac1-induced Bcl-2 phosphorylation at Ser70, one group of kinases that have been pinpointed as promising candidates are the c-Jun N-terminal kinases (JNKs). JNKs belong to the mitogen-activated protein kinase (MAPK) family and as their name imply, were originally identified as kinases that phosphorylate the transcription factor c-Jun at Ser63 and Ser73 leading to downstream transcription of its target genes[332]. Rac1 activation has been shown to result in JNK activation[259, 261] and in addition, Ser70 of Bcl-2 has been demonstrated in various reports to be a target site for JNK phosphorylation[171, 176, 183-185]. To investigate on the involvement of JNKs in Rac1V12-induced Bcl-2 phosphorylation at Ser70, a general pharmacological inhibitor of JNKs (including all three isoforms JNK1, JNK2 and JNK3), SP600125, was used as a reversible ATP-competitive inhibitor with more than 20-fold selectivity towards JNKs versus other kinases and enzymes[333]. As shown in **Figure 28A**, Bcl-2, when transiently transfected into M14 cells with a constitutively active Rac1V12 background, got phosphorylated at Ser70 as compared to control vector matched cells and the phosphorylation levels went down in a dose-dependent manner upon 2 hrs exposure to SP600125 indicating that active Rac1-induced Bcl-2 phosphorylation at Ser70 was potentially mediated through JNKs. This was further verified in another cancer model of CEM/Neo cells where the 10 and 20 μM of SP600125 used effectively led to a dose-dependent reduction in the phosphorylation

levels of Bcl-2 at Ser 70 as well as a decrease in the phosphorylation status and total protein levels of the well-known JNK target c-Jun (**Figure 28B**). No changes in the total intracellular protein levels of Bcl-2 and Rac1 were observed upon inhibition of JNK activity. β-actin and GAPDH (glyceraldehyde-3-phosphate dehydrogenase) were included in the western blot analysis as internal loading controls (**Figure 28**). However, at the doses of SP600125 used, inhibition of other kinases that are reported to be involved in Bcl-2 phosphorylation at Ser70 such as PKC and MKKs (MAPK kinases) [172, 173, 180-182]couldn't be ruled out, although the inhibitory effect on those kinases would be to a much lesser extent as compared to the inhibition of JNKs[333]. Further experiments using targeted siRNA-mediated silencing of JNKs would be necessary to conclude the definite involvement of this group of kinases.
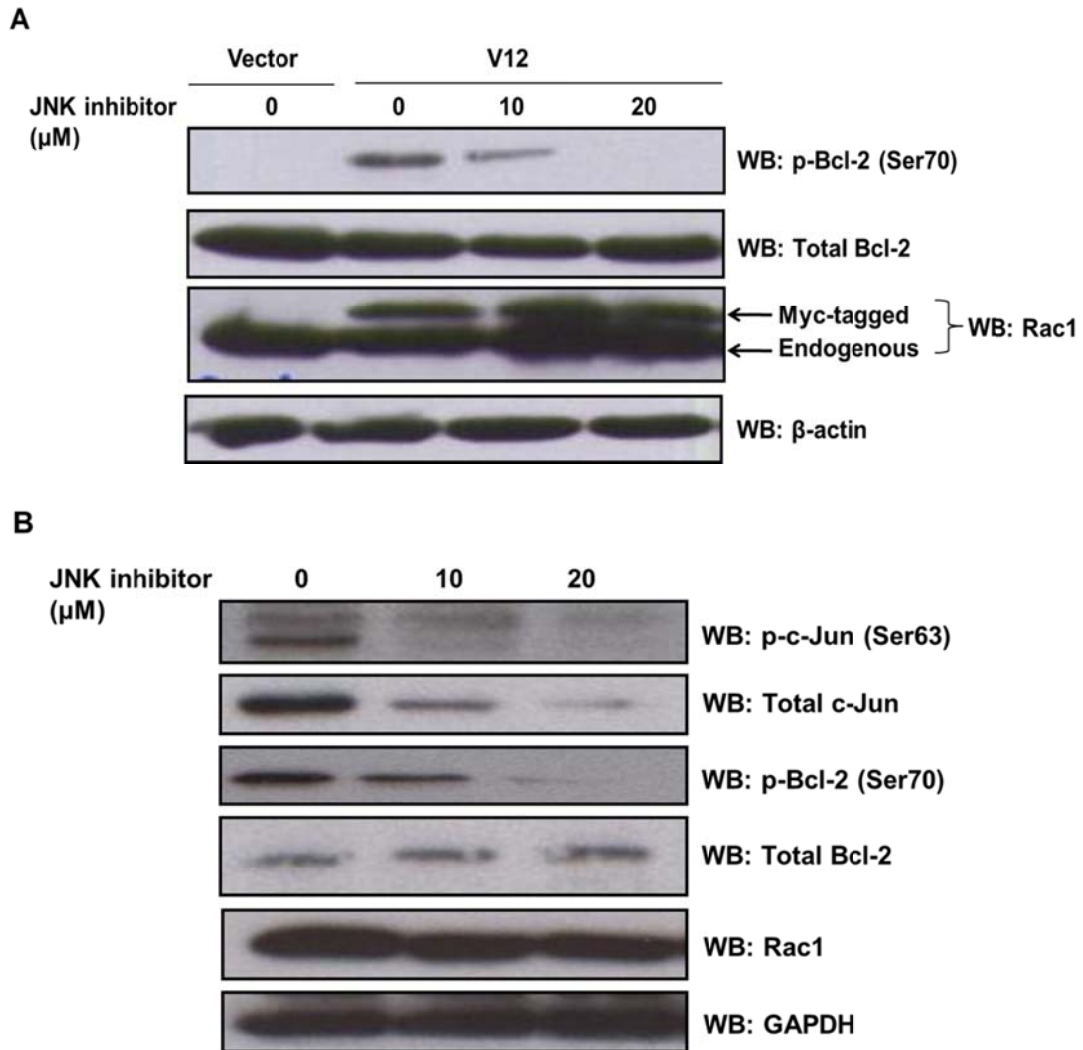
Figure 28: JNK is an upstream kinase responsible for Rac1V12-induced Bcl-2 phosphorylation at Ser70. (A) M14 cells stably overexpressing either the control vector pIRES or the constitutively active Rac1 mutant V12 were transiently transfected with Bcl-2 plasmid for 48 hrs followed by treatment of different doses of JNK inhibitor SP600125 for 2 hrs and the lysates were probed with anti-p-Bcl-2 (Ser70), anti-Bcl-2, anti-Rac1 and anti-β-actin. (B) CEM/Neo cells were treated with different doses of SP600125 for 2 hrs and the lysates were probed with anti-p-c-Jun (Ser63), anti-c-Jun, anti-p-Bcl-2 (Ser70), anti-Bcl-2, anti-Rac1 and anti-GAPDH.

3.11.2 Pharmacological Inhibition of JNK Activity Decreased Rac1-Bcl-2 Interaction Levels

Bcl-2 phosphorylation status at Ser70 has been shown to be important in Rac1-Bcl-2 interaction in the previous section 3.9. Therefore, co-immunoprecipitation analysis in two cancer cell lines, HeLa and Jurkat, was carried out upon inhibition of JNK activity that has been demonstrated earlier to result in a decrease in p-Bcl-2 (Ser70) levels (**Figure 28**). Indeed, upon increasing doses of JNK inhibitor SP600125, a dose-dependent decrease in both the Bcl-2 phosphorylation levels at Ser70 as well as the interaction levels between Rac1 and Bcl-2 were observed in both the cancer cell lines tested (**Figure 29**). This was further supported by evidence from confocal microscopic analysis on the localizations of the endogenous Rac1 and Bcl-2 in HeLa cells. Endogenous Rac1 was stained with FITC-conjugated secondary mouse IgG that recognizes anti-Rac1 while endogenous Bcl-2 was stained with rhodamine-conjugated secondary rabbit IgG that recognizes anti-Bcl-2. An overlay of the green and red fluorescent signals coming from FITC and rhodamine, respectively, revealed spots/patches of yellow at perinuclear regions indicating a co-localization of these two proteins there. However, upon exposure to increasing doses of SP600125, the overlay of yellow gradually changed to a more orangish and then to a more reddish color indicating disruption in co-localization of these two proteins (**Figure 30**).
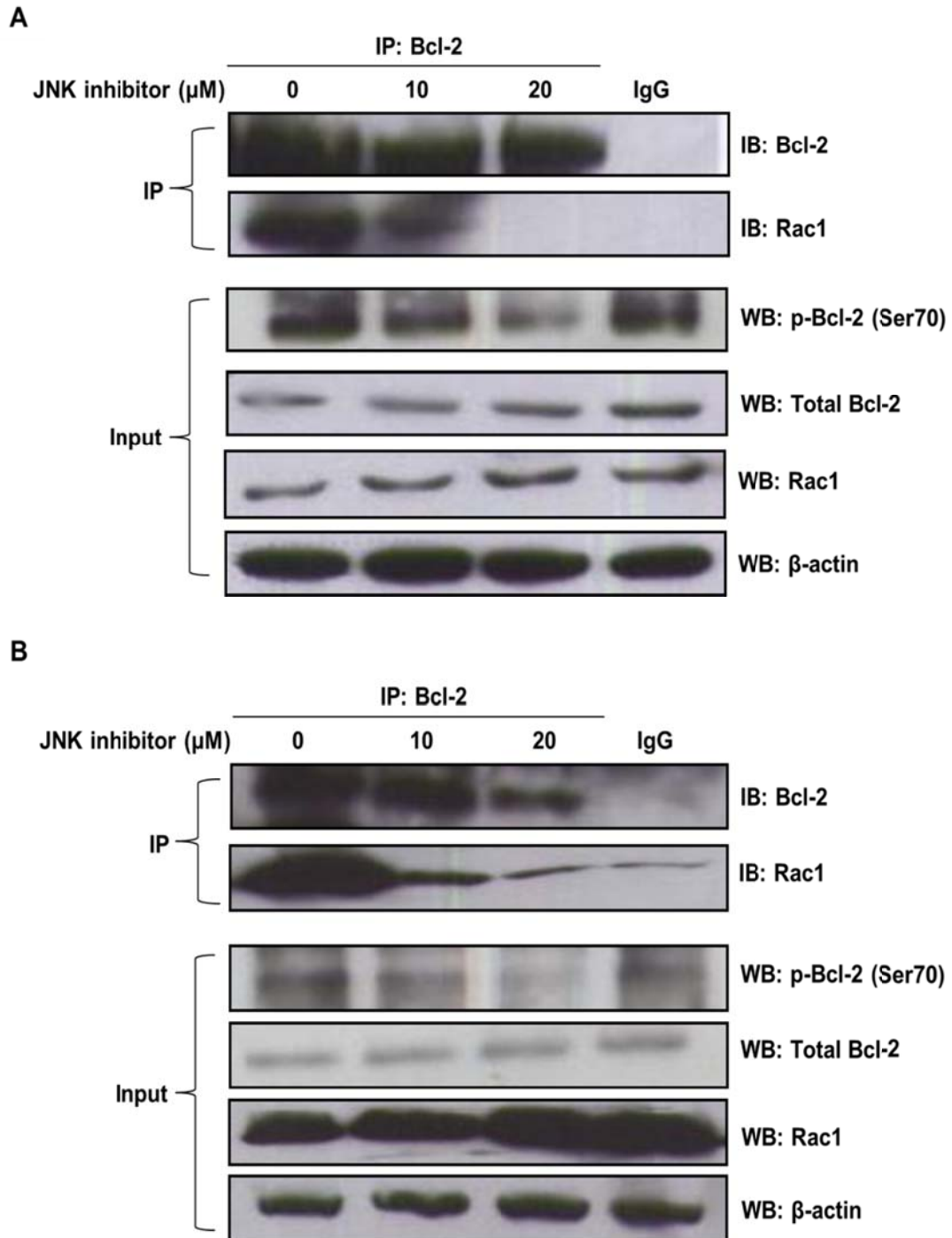
Figure 29: Pharmacological inhibition of JNK activity decreased Rac1-Bcl-2 interaction levels. (A) HeLa cells treated with different doses of JNK inhibitor SP600125 for 2 hrs were immunoprecipitated with anti-Bcl-2 and probed with anti-Bcl-2 and anti-Rac1. Immunoprecipitation with control rabbit IgG was used as a negative control. Whole cell lysates probed with anti-p-Bcl-2 (Ser70), anti-Bcl-2, anti-Rac1 and anti-β-actin are shown on the bottom panel as input. (B) Jurkat cells treated with different doses of JNK inhibitor SP600125 for 2 hrs were immunoprecipitated with anti-Bcl-2 and probed with anti-Bcl-2 and anti-Rac1. Immunoprecipitation with control rabbit IgG was used as a negative control. Whole cell lysates probed with anti-p-Bcl-2 (Ser70), anti-Bcl-2, anti-Rac1 and anti-β-actin are shown on the bottom panel as input.

133
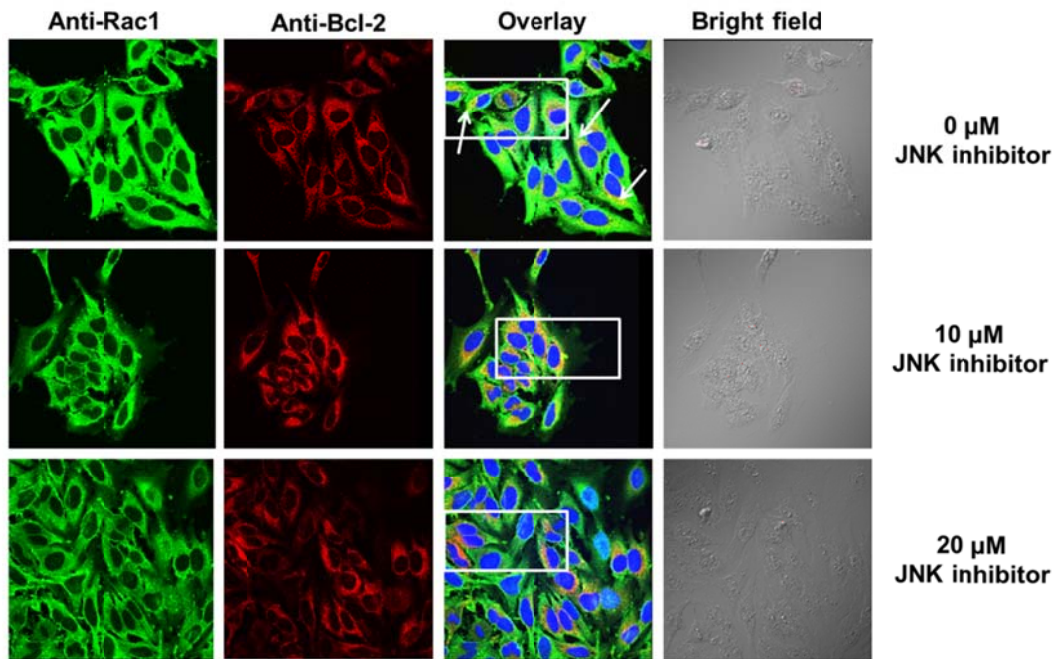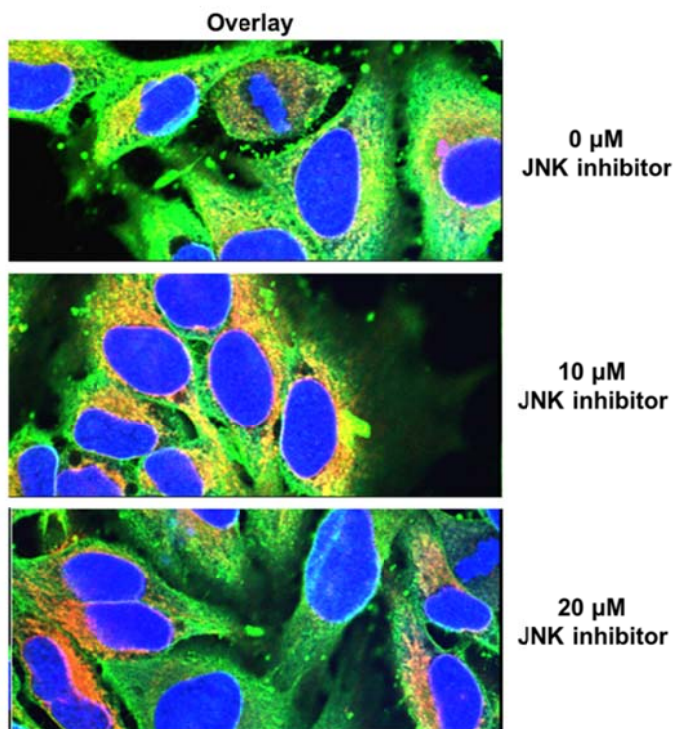
Figure 30: Pharmacological inhibition of JNK activity disrupted Rac1-Bcl-2 co-localization. (A) Representative confocal microscopic analysis of Bcl-2 and Rac1 expression in HeLa cells treated with different doses of JNK inhibitor SP600125 for 2 hrs. Rac1 was probed with anti-Rac1 and FITC-conjugated secondary mouse IgG, while Bcl-2 was probed with anti-Bcl-2 and Rhodamine-conjugated secondary rabbit IgG. The panels were merged using Olympus FluoView 2.0 software. All experiments were performed at least 3 or more times independently. (B) Enlarged views from boxed area in the overlay panel in (A).

3.12. Disruption of Rac1-Bcl-2 Interaction Leads to a Compromise of the Pro-oxidant Status of Bcl-2-overexpressing Cancer Cells

The data presented thus far have concluded that Rac1 physically interacts with Bcl-2 and the activation status of Rac1 as well as the BH3 domain of Bcl-2 are critical for the interaction. In order to gain further insight into the functional relevance of this interacting complex, with a particular focus on redox regulation in the mitochondria since Rac1 has been demonstrated in earlier sections to be involved in Bcl-2-mediated pro-oxidant status in the mitochondria. This was tested by using two approaches that could disrupt the interaction between Rac1 and Bcl-2: 1) a pharmacological inhibitor of Rac1; 2) Bcl-2 BH3 domain peptides. As shown in **Figure 6**, Bcl-2-overexpressing CEM cells, when exposed to increasing doses of the pharmacological inhibitor of Rac1 NSC23766 that could disrupt the Rac1-Bcl-2 interaction (**Figure 17**), showed a dose-dependent decrease in the mitochondrial O_2^- levels suggesting a probable redox regulatory property of this interacting complex. This was further supported by the use of TAT-Bcl-2 BH3 peptides which disrupted the interaction in the mitochondria of CEM/Bcl-2 cells (**Figure 21**). Similarly, exposure to the cell permeable BH3 peptides for 2 hrs also led to a dose-dependent decrease in the mitochondrial O_2^- levels as measured by MitoSox dye in Bcl-2-overexpressing CEM cells whereas not much change was observed in control vector matched CEM cells with relatively lower Bcl-2 expression levels (**Figure 31A**). Control peptides with scrambled sequence that does not match any region in human proteins were used as a negative control where the peptides themselves had minimal effect on mitochondrial O_2^- levels (**Figure 31B**).
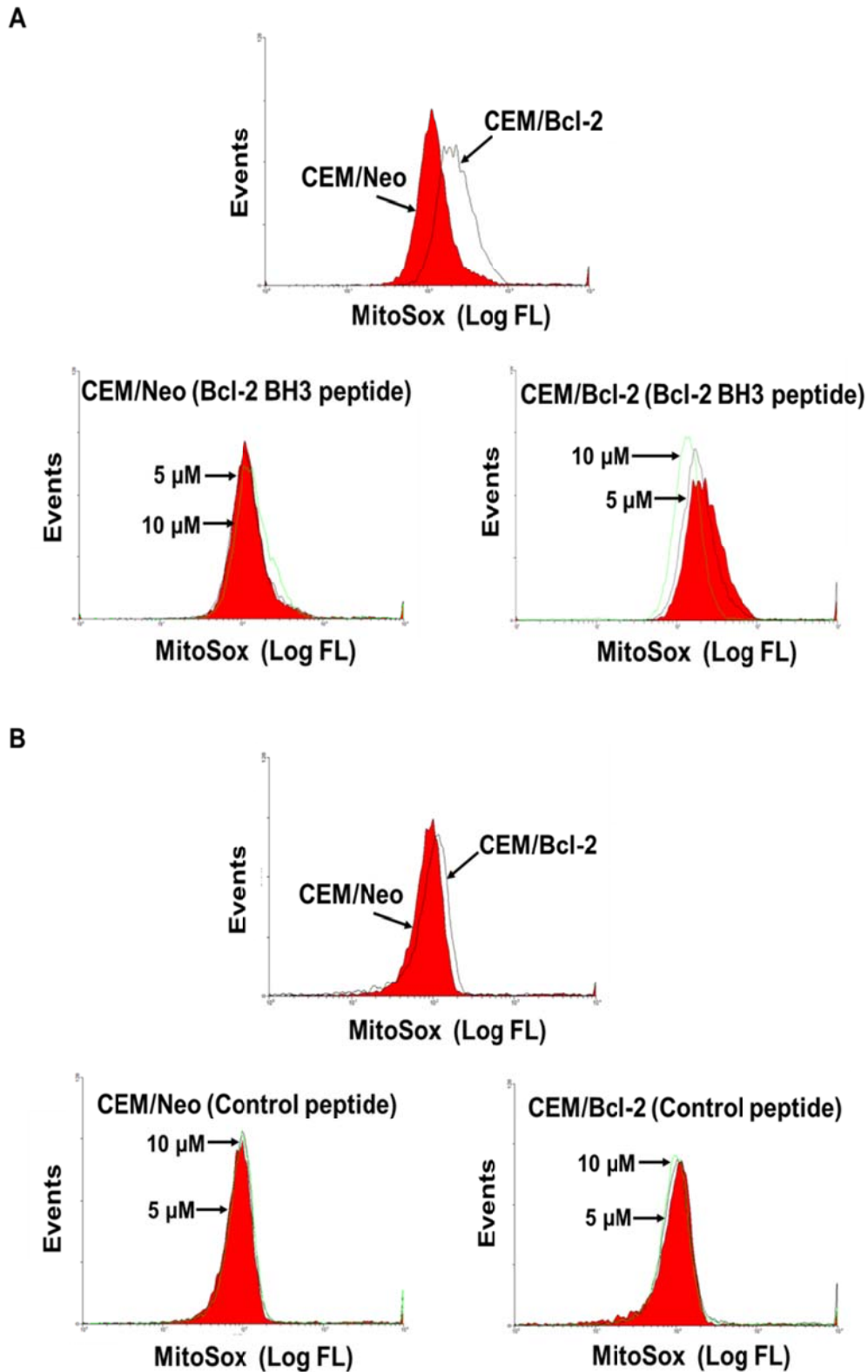
Figure 31: Bcl-2 BH3 peptides decreased mitochondrial O_2^- levels in Bcl-2-overexpressing cancer cells. Mitochondrial O_2^- levels of CEM cells, after treatment with various doses of either (A) Bcl-2 BH3 peptides or (B) control peptides for 2 hrs, were detected by MitoSox staining and analysed through flow cytometry. At least 10,000 events were analyzed by WINMDI software. Histograms shown were representative of at least three independent experiments.

3.13. Disruption of Rac1-Bcl-2 Interaction Sensitizes Bcl-2-overexpressing Cancer Cells to Chemotherapeutic Drug-induced Apoptosis

3.13.1   Bcl-2 Overexpression Confers Resistance towards Chemotherapeutic Drug Treatment

Data presented in the previous section showed that disruption of the Bcl-2-Rac1 interaction using two approaches either through pharmacological inhibition of Rac1 activity or blocking of the Bcl-2 BH3 domain resulted in a compromise of the pro-oxidant status in the mitochondria of Bcl-2-overepxressing CEM cells. As discussed in the introduction section 1.3.2 that the pro-oxidant status induced by Bcl-2 contributes towards its anti-apoptotic property, this was further investigated here to check whether the chemoresistance observed in cancer cells with Bcl-2 overexpression could be overcome through disruption of its interaction with Rac1 that compromised the pro-oxidant status. Two conventional chemotherapeutic drugs that are in routine clinical use, etoposide and vincristine, were employed here as triggers. Etoposide is a topoisomerase II inhibitor where it forms a ternary complex with DNA, which blocks re-ligation of the DNA strands causing strand breaks while vincristine is a mitotic inhibitor where it binds to tubulin dimers inhibiting the assembly of microtubule structures leading to mitotic arrest in metaphase. Both of these eventually result in mitochondria-mediated apoptosis in rapidly dividing cells[334, 335]. To establish the Bcl-2 overexpression-induced chemoresistance model, the sensitivity of CEM/Neo and CEM/Bcl-2 cells was tested against these two drugs. Indeed, both etoposide and vincristine resulted in significantly reduced cell viability in a dose-dependent manner with Bcl-2-overexpressing CEM cells showing more resistance towards these two treatments as compared to CEM/Neo cells (**Figure 32**). Since the

MTT assay used here for cell viability measurement is not a direct assessment for cell death, a pre-incubation with the cell permeable pan-caspase inhibitor Z-VAD-FMK was performed prior to drug treatment in order to confirm that the cells were dying via drug-induced apoptosis. Z-VAD-FMK blocks the activity of all caspases via the irreversible binding to the catalytic sites of caspase proteases. Indeed, inhibition of caspases through 1 hr pre-incubation of Z-VAD that prevents apoptotic execution, led to a 90% or more rescue of the cell death in both CEM/Neo and CEM/Bcl-2 cells (**Figure 33**) indicating that the reduced viability observed with etoposide and vincristine treatments was due to apoptotic cell death.
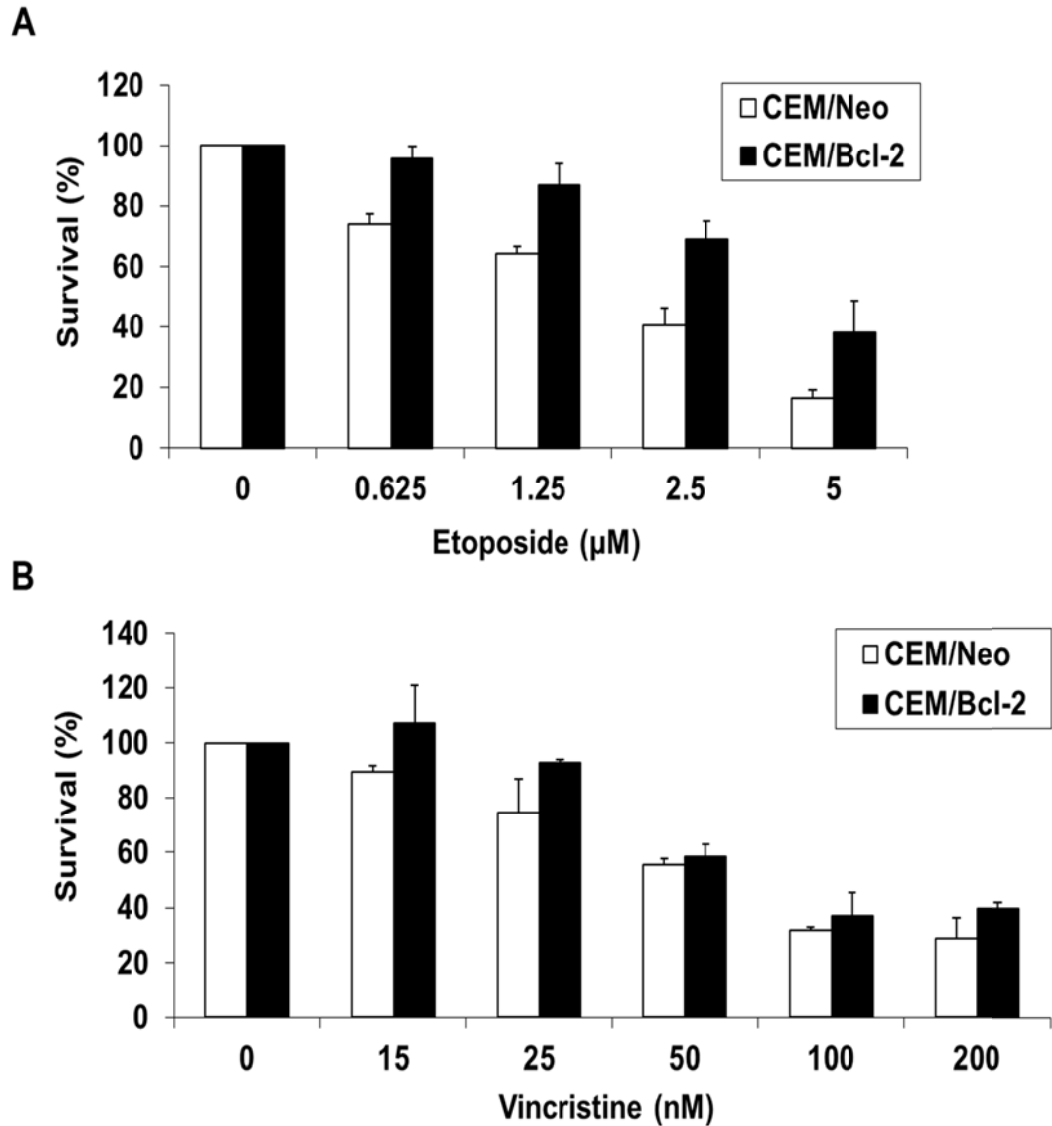
Figure 32: **Bcl-2-overexpressing cancer cells were more resistant towards treatment of chemotherapeutic drugs.** CEM/Neo and CEM/Bcl-2 cells were exposed to various doses of drugs, (A) etoposide and (B) vincristine, for 24 hrs and cell viability was determined by the MTT assay. Cell survival was calculated as: (mean of triplicate OD values of cells incubated with the respective drug / mean of triplicate OD values of cells incubated with control solvent) X 100%. Data shown are means ± SD of at least three independent experiments performed in triplicate.

A

B
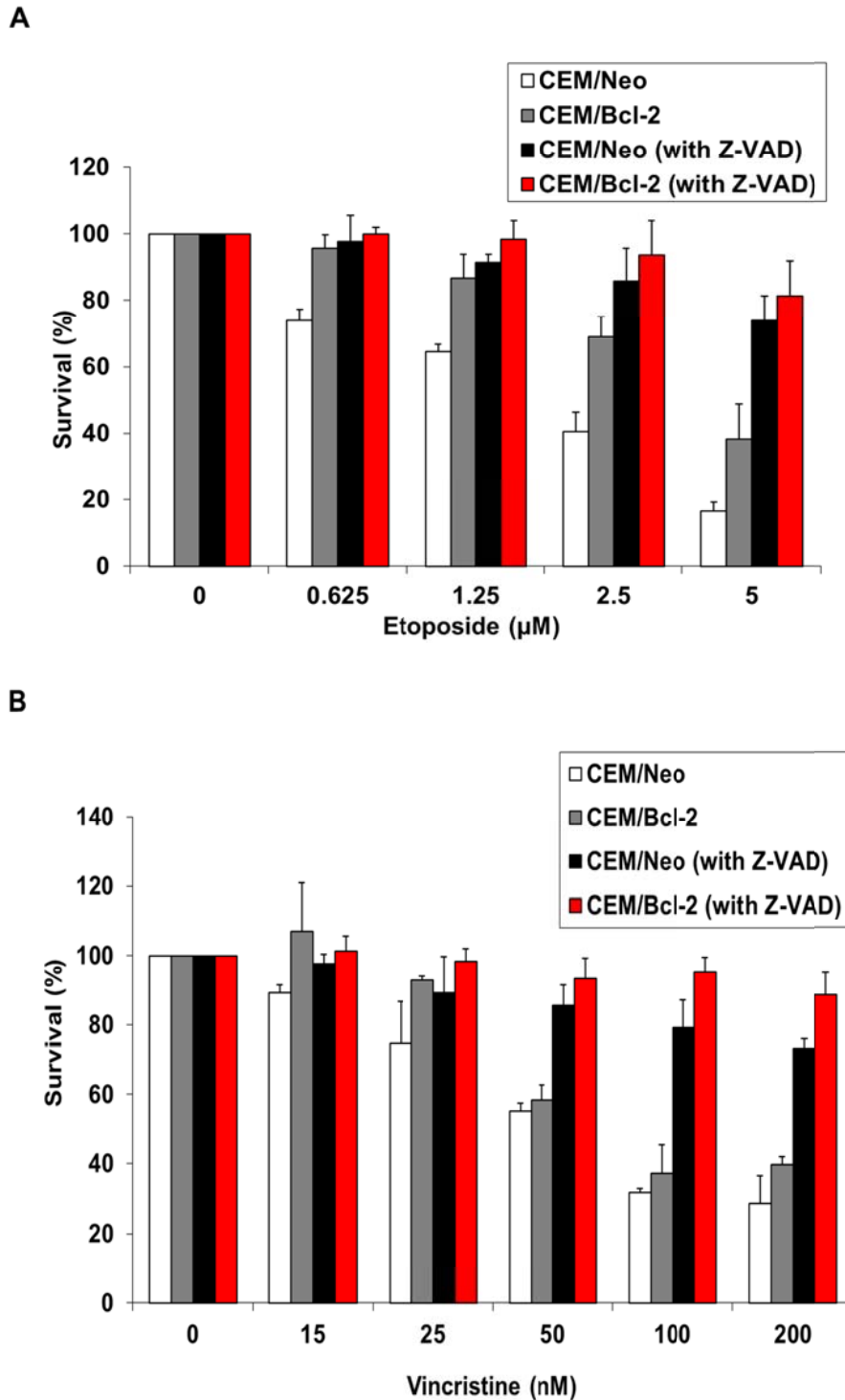
Figure 33: Pre-incubation with a pan-caspase inhibitor Z-VAD-FMK rescued human chronic myeloid leukaemia CEM cells from subsequent treatment with chemotherapeutic drugs. CEM/Neo and CEM/Bcl-2 cells were pre-incubated with pan-caspase inhibitor Z-VAD-FMK for 1 hr followed by exposure to increasing doses of (A) etoposide and (B) vincristine for 24 hrs and cell viability was determined by the MTT assay. Cell survival was calculated as: (mean of triplicate OD values of cells incubated with the respective drug / mean of triplicate OD values of cells incubated with control solvent) X 100%. Data shown are means ± SD of at least three independent experiments performed in triplicate.

3.13.2 Combination Treatment of Bcl-2 BH3 Peptides with Chemotherapeutic Drugs Greatly Jeopardized the Viability of Bcl-2-overexpressing Cancer Cells

In order to test whether disruption of the Rac1-Bcl-2 interaction could compromise the chemoresistance of Bcl-2-overexpressing cancer cells, a combination treatment including the BH3 peptides and the conventional chemotherapeutic drugs was used. The effect of Bcl-2 BH3 peptides on cell viability was checked and no significant change was observed in both CEM/Neo and CEM/Bcl-2 cells up till the dose of 20 μM used (**Figure 34**), consistent with what others have reported that Bcl-2 BH3 peptides did not induced cytochrome c release from isolated mitochondria unlike Bax BH3 or Bad BH3 peptides[302]. As such, the dose of 10 μM of Bcl-2 BH3 peptides that not only disrupted Rac1-Bcl-2 interaction as shown earlier in **Figure 21** but also had minimal effect on cell viability (**Figure 34**), was used for subsequent experiments. Meanwhile sublethal doses of the two drugs, etoposide (1.25 and 2.5 μM) and vincristine (15 and 25 nM), which caused less than 30% of cell death in CEM/Bcl-2 cells (**Figure 32**) were also chosen in order to maximize the potential synergistic effects for the combination treatment, if there are any. Indeed, the combination treatment with 1 hr pre-incubation of the Bcl-2 BH3 peptides followed by 24 hrs exposure to the drugs resulted in a statistically significant reduction in cell viability in CEM/Bcl-2 cells: around 50% more reduction with BH3 peptides and etoposide combination as compared to etoposide alone and 30-40% more reduction with BH3 peptides and vincristine combination as compared to vincristine alone, with p-values less than 0.05 (**Figure 35A & B**). Moderate synergistic effects were also observed in CEM/Neo cells, although to a less remarkable extent as compared to CEM/Bcl-2 cells (**Figure 35A & B**) indicating a better targeting for the Bcl-2 BH3 peptides to cancer cells with Bcl-2 overexpression. Control peptides with scrambled

sequence that does not match any human protein were used as a negative control where no significant change was observed upon combination treatment as compared to the drug treatment alone (**Figure 35C & D**).
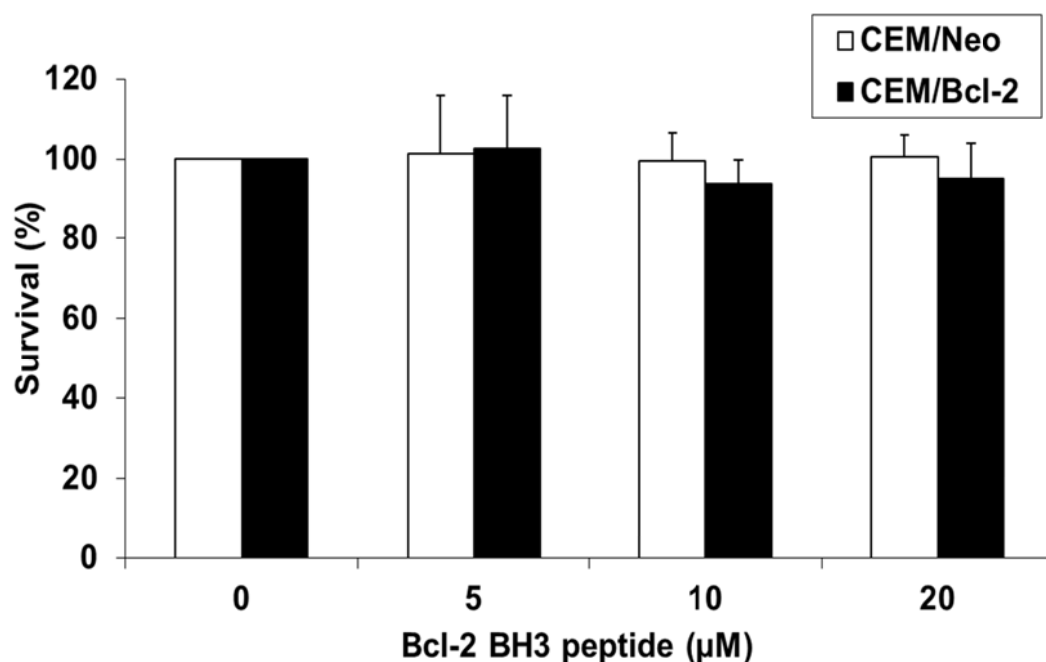
Figure 34: Low doses of Bcl-2 BH3 peptides did not affect the viability of human chronic myeloid leukaemia CEM cells. CEM/Neo and CEM/Bcl-2 cells were treated with various doses of Bcl-2 BH3 peptides for 24 hrs and cell viability was determined by the MTT assay. Cell survival was calculated as: (mean of triplicate OD values of cells incubated with the respective drug / mean of triplicate OD values of cells incubated with control solvent) X 100%. Data shown are means ± SD of at least three independent experiments performed in triplicate.

A

BH3 (μM)	-	10	-	-	10	10
Eto (μM)	-	-	1.25	2.5	1.25	2.5
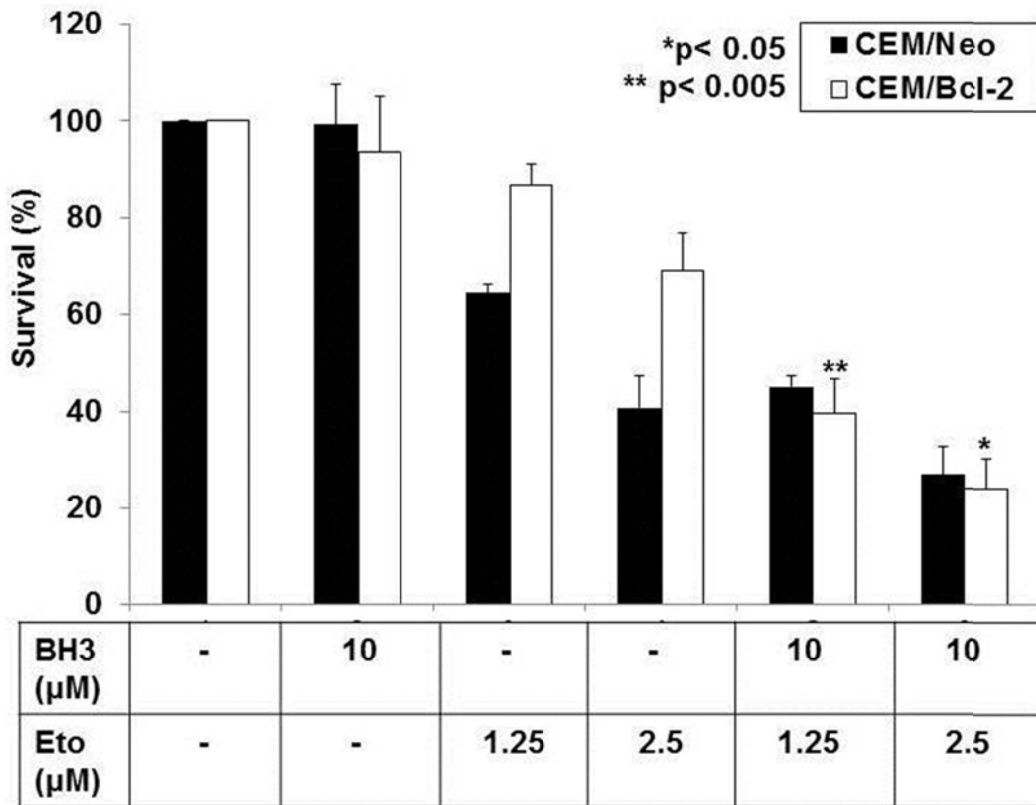
Figure 35: Combination treatment of Bcl-2 BH3 peptides with conventional chemotherapeutic drugs significantly reduced the survival of Bcl-2-overexpressing cancer cells. (A) CEM/Neo and CEM/Bcl-2 cells were pre-incubated with 10 μM Bcl-2 BH3 peptides (BH3) for 1 hr followed by exposure to increasing doses of etoposide (Eto) for 24 hrs and cell viability was assessed by the MTT assay. Cell survival was calculated as: (mean of triplicate OD values of cells incubated with the respective drug / mean of triplicate OD values of cells incubated with control solvent) X 100%. Data shown are means ± SD of at least 3 independent experiments performed in triplicate. *P<0.05, **P<0.005 when compared with the drug treatment alone. Tests were done using Student's t-test assuming equal variances.

Figure 35: Combination treatment of Bcl-2 BH3 peptides with conventional chemotherapeutic drugs significantly reduced the survival of Bcl-2-overexpressing cancer cells. (B) CEM/Neo and CEM/Bcl-2 cells were pre-incubated with 10 μM Bcl-2 BH3 peptide (BH3) for 1 hr followed by exposure to increasing doses of vincristine (Vin) for 24 hrs and cell viability was assessed by the MTT assay. Cell survival was calculated as: (mean of triplicate OD values of cells incubated with the respective drug/mean of triplicate OD values of cells incubated with control solvent) X 100%. Data shown are means ± S.D. of at least 3 independent experiments performed in triplicate. *P<0.005, **P<0.05 when compared with the drug treatment alone. Tests were done using Student's t-test assuming equal variances.

C
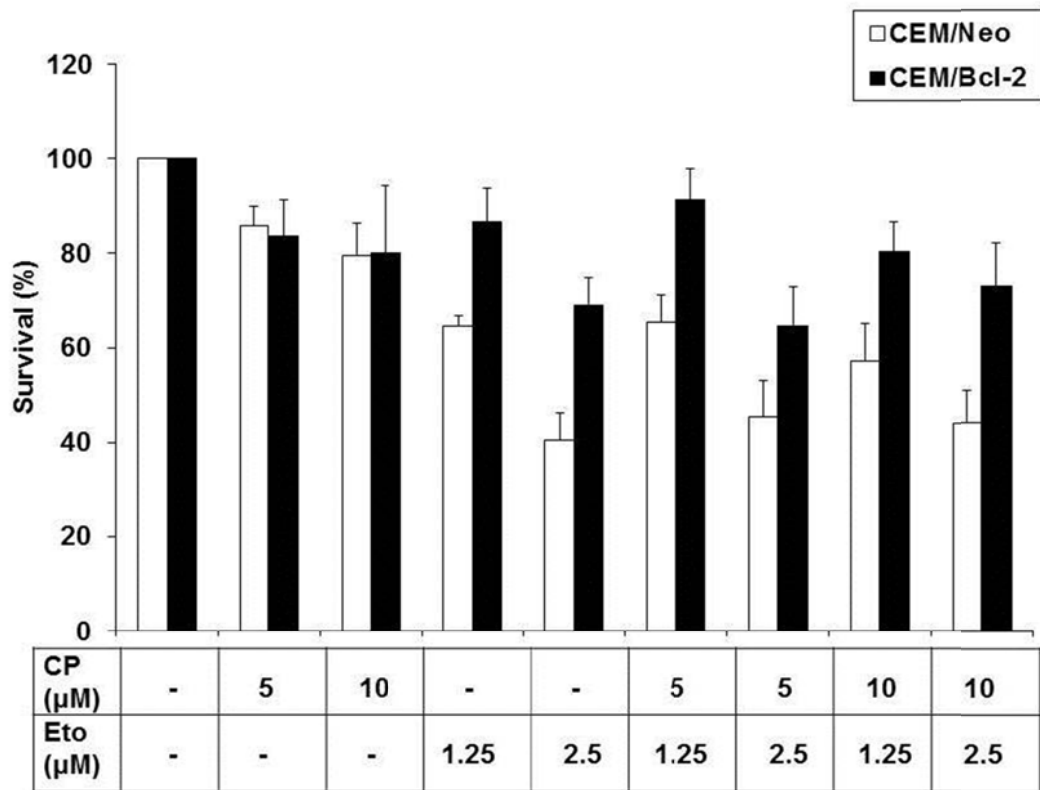
CP (μM)	-	5	10	-	-	5	5	10	10
Eto (μM)	-	-	-	1.25	2.5	1.25	2.5	1.25	2.5

Figure 35: Combination treatment of Bcl-2 BH3 peptides with conventional chemotherapeutic drugs significantly reduced the survival of Bcl-2-overexpressing cancer cells. (C) CEM/Neo and CEM/Bcl-2 cells were pre-incubated with 5 μM and 10 μM control peptides (CP) for 1 hr followed by exposure to increasing doses of etoposide (Eto) for 24 hrs and cell viability was assessed by the MTT assay. Cell survival was calculated as: (mean of triplicate OD values of cells incubated with the respective drug / mean of triplicate OD values of cells incubated with control solvent) X 100%. Data shown are means ± SD of at least 3 independent experiments performed in triplicate.

D

CP (μM)	-	5	10	-	-	5	5	10	10
Vin (nM)	-	-	-	15	25	15	25	15	25

Figure 35: Combination treatment of Bcl-2 BH3 peptides with conventional chemotherapeutic drugs significantly reduced the survival of Bcl-2-overexpressing cancer cells. (D) CEM/Neo and CEM/Bcl-2 cells were pre-incubated with 5 μM and 10 μM control peptides (CP) for 1 hr followed by exposure to increasing doses of vincristine (Vin) for 24 hrs and cell viability was assessed by the MTT assay. Cell survival was calculated as: (mean of triplicate OD values of cells incubated with the respective drug / mean of triplicate OD values of cells incubated with control solvent) X 100%. Data shown are means ± SD of at least 3 independent experiments performed in triplicate.

3.13.3 Combination Treatment of Bcl-2 BH3 Peptides with Chemotherapeutic Drugs Resulted in a Remarkably Elevated Sub-G_1 Population in Bcl-2-overexpressing Cancer Cells

In order to assess whether the reduction in cell viability observed upon combination treatment was due to cell death, a cell cycle profile analysis based on propidium iodide (PI) staining was performed. PI intercalates with DNA with a stoichiometry of one dye per 4.5 base pairs (bp); therefore, its fluorescence is a direct representation of the DNA content in a cell. In rapidly proliferating cells such as cancer cells, majority of the cells would be at G_1 phase of the cell cycle, or growth phase (since this phase takes up approximately half of the time of the whole cell cycle), where they gear up biosynthetic activities to prepare for DNA synthesis during S phase. Once entering S phase, DNA synthesis commences and at the end of S phase, all the chromosomes have been replicated resulting in double the content of DNA (4N) and the increase in the DNA content can be picked up by PI staining shown as a right shift in the histogram of flow cytometry analysis. After the completion of DNA replication, the cell then enters G_2 phase with significant biosynthesis mainly on microtubule production required for subsequent mitosis or M phase. It is not until the end of cytokinesis when the multiplied cell have divided into two daughter cells that the DNA content go back to 2N for a normal diploid cell[336]. However, for cells that are undergoing apoptosis, endonucleases will break the linkers between the nucleosomes, resulting in small fragments of DNA oligomers with about 180 bp. During the fixation and rehydration processes for PI staining, some of the lower molecular weight DNA got leached out and this will lead to a "hypodiploid" state observed with a sub-G_1 peak that is shown as a left shift to G_1 peak in the histogram of the flow cytometry analysis. For Bcl-2-overexpressing CEM cells, at resting state,

relatively low basal levels of sub-G_1 population were detected (0.64% of whole cell population as indicated on the sub-G_1 scale in the histograms) which went up to 2.45% and 5.43% with 1.25 and 2.5 μM of etoposide indicating that most probably there was a small population of cells undergoing apoptosis. Treatment with Bcl-2 BH3 peptides also did not result in much change in the sub-G_1 population. However, the sub-G_1 population went remarkably higher to 28.49% and 50.28% with combination treatment of 10 μM Bcl-2 BH3 peptides and 1.25 and 2.5 μM of etoposide, respectively. Elevated sub-G_1 population was also observed in CEM/Neo cells upon combination treatment although to a lesser extent as compared to CEM/Bcl-2 cells (**Figure 36A**). Cell cycle profile analysis was also performed for combination treatment of Bcl-2 BH3 peptides and vincristine where similar results were observed with 15- to 30-fold increase in the sub-G_1 population following combination treatment as compared to vincristine treatment alone in CEM/Bcl-2 cells (**Figure 36B**). These findings, together with the cell viability analysis through MTT assay discussed in the previous section (**Figure 35A & B**), suggested that Bcl-2 BH3 peptides significantly sensitized Bcl-2-overexpressing cancer cells to chemotherapeutic drug-induced apoptosis.

Figure 36: Combination treatment of Bcl-2 BH3 peptides with conventional chemotherapeutic drugs resulted in a significantly elevated sub-G1 population in Bcl-2-overexpressing cancer cells. (A) CEM cells were untreated (control), treated with 10 μM Bcl-2 BH3 peptides (BH3) or etoposide (Eto) for 24 hrs, or pre-incubated with Bcl-2 BH3 peptides for 1 hr followed by exposure of etoposide for another 24 hrs. Cell cycle profile analysis was done using flow cytometry after ethanol fixation and PI staining. Data was further analysed by WINMDI software and percentage of cells in the sub-G1 phase was indicated. Profile shown was representative of three independent experiments.

Figure 36: Combination treatment of Bcl-2 BH3 peptides with conventional chemotherapeutic drugs resulted in a significantly elevated sub-G1 population in Bcl-2-overexpressing cancer cells. (B) CEM cells were untreated (control), treated with 10 μM Bcl-2 BH3 peptides (BH3) or vincristine (Vin) for 24 hrs, or pre-incubated with Bcl-2 BH3 peptides for 1 hr followed by exposure of vincristine for another 24 hrs. Cell cycle profile analysis was done using flow cytometry after ethanol fixation and PI staining. Data was further analysed by WINMDI software and percentage of cells in the sub-G1 phase was indicated. Profile shown was representative of three independent experiments.

3.13.4 Combination Treatment of Functional Inhibition or siRNA mediated Silencing of Rac1 with Chemotherapeutic Drugs Greatly Jeopardized the Viability of Bcl-2-overexpressing Cancer Cells

Data presented in the previous sections showed that Bcl-2 BH3 peptides, which disrupted the interaction between Rac1 and Bcl-2, could also sensitize Bcl-2-overexpressing cancer cells to drug-induced apoptosis. To further investigate whether the chemoresistance resulted from Bcl-2 overexpression could be overcome through disruption of the interaction between Rac1 and Bcl-2, another two approaches were taken to disrupt the interaction either through pharmacological inhibition of Rac1 activity or siRNA-mediated silencing of Rac1 expression levels and the subsequent sensitization effect towards drugs would be analyzed through MTT assay and cell cycle profile analysis. Apart from the two chemotherapeutic drugs used previously, an additional drug daunorubicin was also employed here, which intercalates with DNA leading to apoptotic cell death[337]. Pre-incubation with the pharmacological inhibitor of Rac1 NSC23766 at doses (5 and 10 μM) that had minimal effect on cell viability when used alone (**Figure 7**), resulted in a remarkable reduction in the cell viability following conventional drug treatment with etoposide, vincristine or daunorubicin. The greatest sensitization effect was observed in the combination treatment of 2.5 μM, 5 μM of etoposide or 100 ng/ml of daunorubicin with 10 μM of NSC23766 in HeLa/Bcl-2 cells and 1.25 μM, 2.5 μM of etoposide or 25 nM of vincristine with 5 μM of NSC23766 in CEM/Bcl-2 cells with p-values less than 0.05 as compared to drug treatment alone (**Figure 37**).

Apart from blocking the activity of Rac1 through a pharmacological inhibitor, a smart pool of exogenous siRNAs, the small interfering RNAs, which are targeted

specifically to Rac1, were transiently introduced into HeLa/Bcl-2 cells to knock down the expression levels of Rac1. The double-stranded siRNA pool, with short stretches of sequences (20 – 25 bp) matching to different regions of Rac1, base-pair to the target sites in a single strand RNA-enzyme complex called RISC (RNA-Induced Silencing Complex) and induce cleavage of the mRNA therefore preventing the mRNA from being translated into a protein product[338]. The siRNA-mediated silencing effect was confirmed through western blot analysis where the target protein expression, Rac1, was reduced to less than 20% of that in the negative control siRNA (with scrambled sequence) transfected cells (**Figure 38A**). The sensitivity of HeLa/Bcl-2 cells towards etoposide and vincristine following siRNA-mediated silencing was assessed via MTT assay where a statistically significant reduction in cell viability was observed in this combination regime as compared to the treatment of the negative siRNA in combination with drugs (with p-value less than 0.05) (**Figure 38B**).
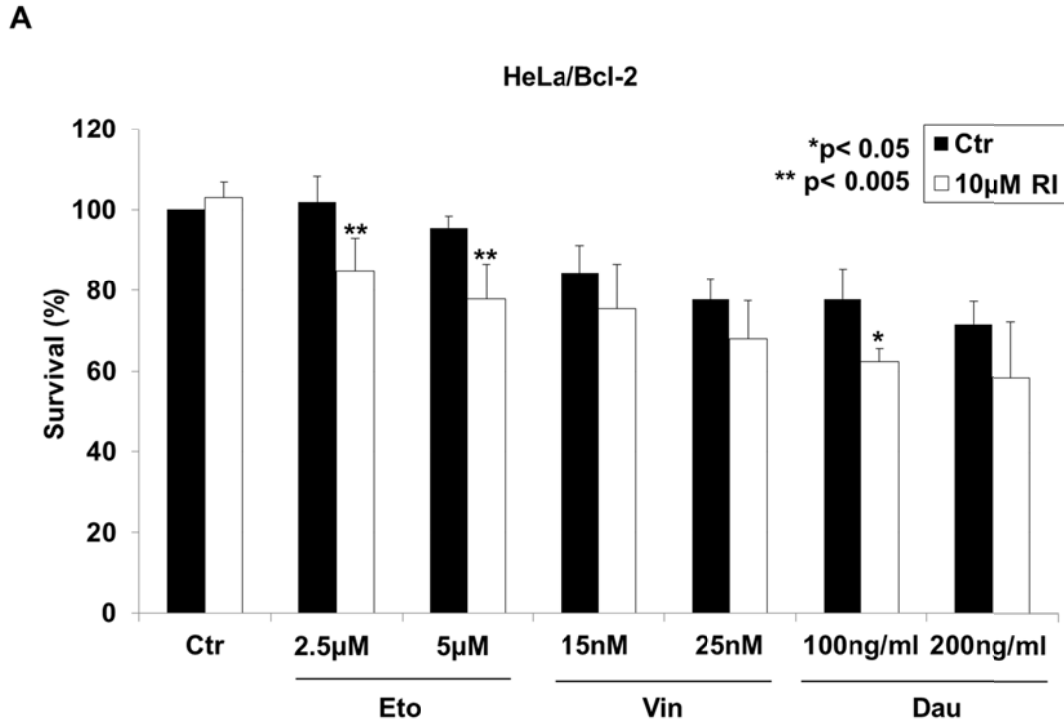
A

Figure 37: Combination treatment of a pharmacological inhibitor of Rac1 with conventional chemotherapeutic drugs significantly reduced the survival of Bcl-2-overexpressing cancer cells. (A) HeLa/Bcl-2 cells were pre-incubated with Rac1 inhibitor NSC23766 (RI) for 1hr followed by exposure to various doses of etoposide (Eto), vincristine (Vin) or daunorubicin (Dau) for 24 hrs. Cell viability was assessed by the MTT assay. Cell survival was calculated as: (mean of triplicate OD values of cells incubated with the respective drug / mean of triplicate OD values of cells incubated with control solvent) X 100%. Data shown are means ± SD of at least 3 independent experiments performed in triplicate. *P<0.05, **P<0.005 when compared with the drug treatment alone. Tests were done using Student's t-test assuming equal variances.

Figure 37: Combination treatment of a pharmacological inhibitor of Rac1 with conventional chemotherapeutic drugs significantly reduced the survival of Bcl-2-overexpressing cancer cells. (B) CEM/Bcl-2 cells were pre-incubated with Rac1 inhibitor NSC23766 (RI) for 1hr followed by exposure to various doses of etoposide (Eto) and vincristine (Vin) for 24 hrs. Cell viability was assessed by the MTT assay. Cell survival was calculated as: (mean of triplicate OD values of cells incubated with the respective drug / mean of triplicate OD values of cells incubated with control solvent) X 100%. Data shown are means ± SD of at least 3 independent experiments performed in triplicate. *P<0.05 when compared with the drug treatment alone. Tests were done using Student's t-test assuming equal variances.
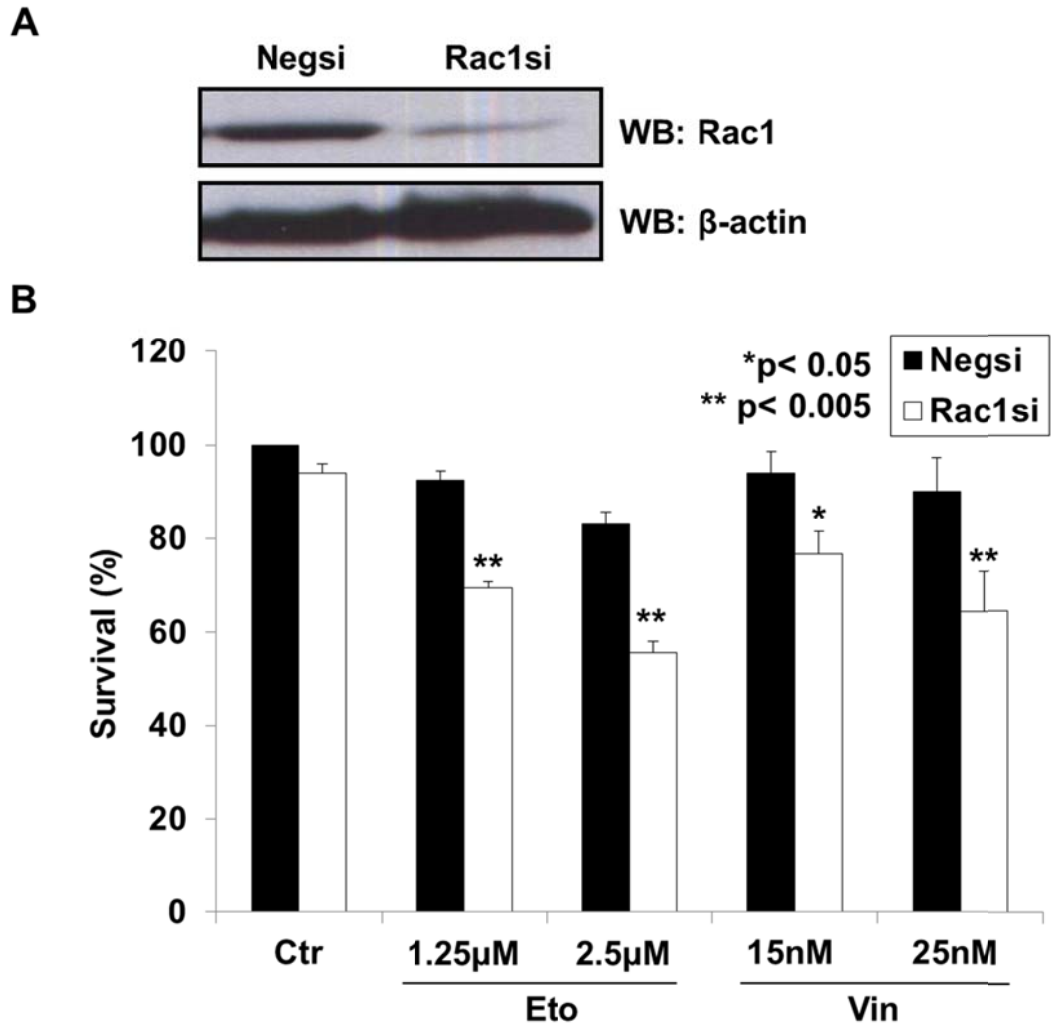
Figure 38: siRNA-mediated silencing of Rac1, in combination with conventional chemotherapeutic drugs, significantly reduced the viability of Bcl-2-overexpressing cancer cells. (A) Western blot analysis of Rac1 and β-actin expression in HeLa/Bcl-2 cells transfected with non-specific scrambled siRNA (Negsi) or siRNA specifically targeted against Rac1 (Rac1si). (B) HeLa/Bcl-2 cells transfected with non-specific scrambled siRNA (Negsi) or siRNA specifically targeted against Rac1 (Rac1si) were treated with various doses of etoposide (Eto) or vincristine (Vin) for 24 hrs. Cell viability was assessed by the crystal violet assay. Cell survival was calculated as: (mean of triplicate OD values of cells incubated with the respective drug / mean of triplicate OD values of cells incubated with control solvent) X 100%. Data shown are means ± SD of at least 3 independent experiments performed in triplicate. *P<0.05, **P<0.005 when compared with the siRNA transfected samples alone. Tests were done using Student's t-test assuming equal variances.

3.13.5   Combination Treatment of Rac1 Inhibitor with Chemotherapeutic Drugs
         Resulted in a Remarkably Elevated Sub-G1 Population in Bcl-2-
         overexpressing Cancer Cells

To further understand whether the reduced cell viability observed with the combination treatment of Rac1 inhibitor and chemotherapeutic drugs was due to either a reduction in cell proliferation or an increase in cell death, cell cycle profile analysis based on PI staining was performed. Similar to the combination treatment of Bcl-2 BH3 peptides and drugs, this combination involving Rac1 inhibitor also resulted in a significant elevation in the sub-G_1 population of CEM/Bcl-2 cells: about 10-fold increase with the combination treatment of 5 μM NSC23766 and either etoposide or vincristine as compared to drug treatment alone (**Figure 39**). Elevation in the sub-G_1 population was also observed upon combination treatment in CEM/Neo cells but to a much lesser extent (**Figure 39**) indicating that inactivation of Rac1 activity could have more profound sensitization effect in cancer cells with higher Bcl-2 expression levels.
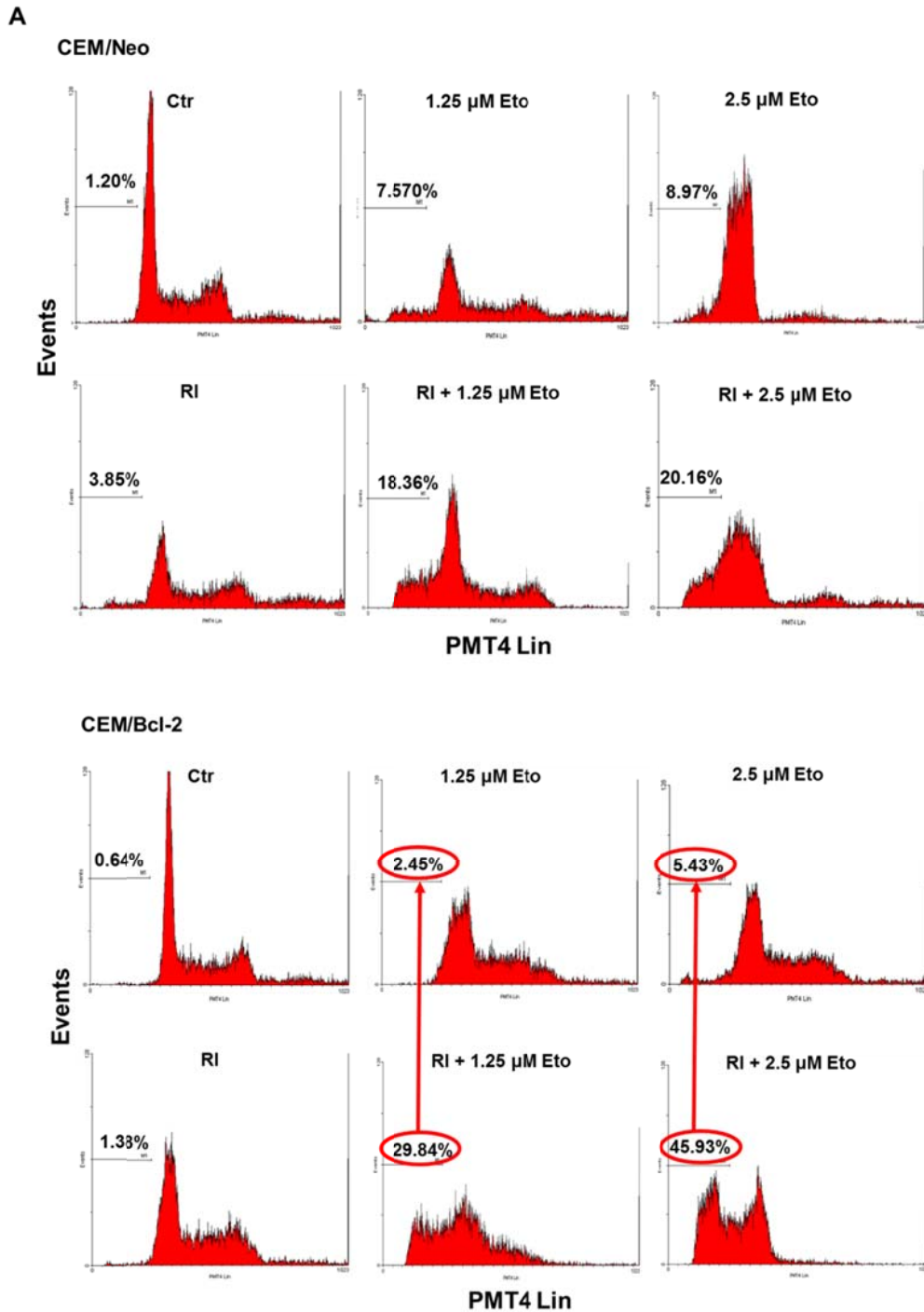
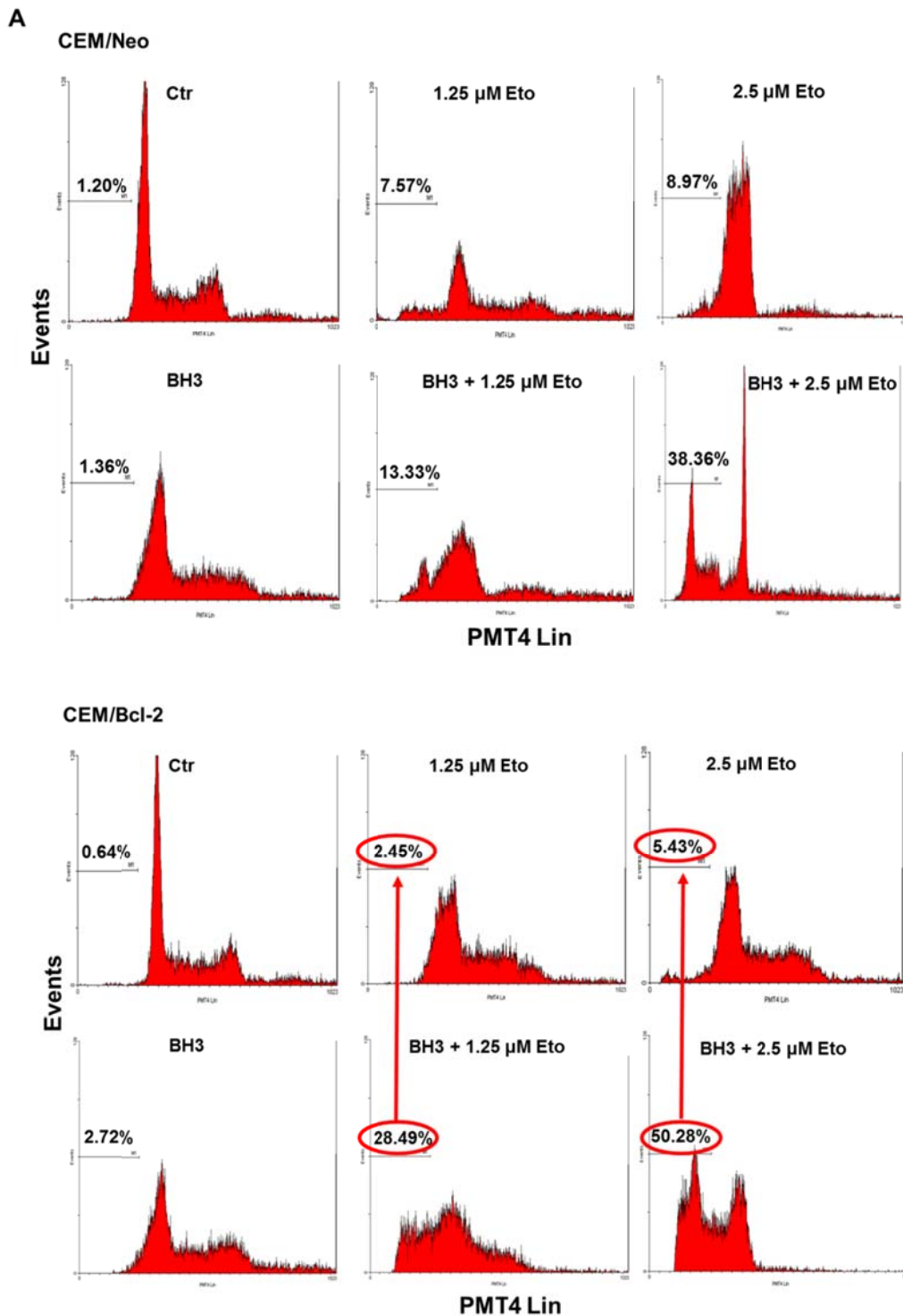**Figure 39: Combination treatment of Rac1 inhibitor with conventional chemotherapeutic drugs resulted in a significantly elevated sub-G1 population in Bcl-2-overexpressing cancer cells.** (A) CEM cells were untreated (control), treated with 5 μM Rac1 inhibitor NSC23766 (RI) or etoposide (Eto) for 24 hrs, or pre-incubated with Rac1 inhibitor for 1 hr followed by exposure of etoposide for another 24 hrs. Cell cycle profile analysis was done using flow cytometry after ethanol fixation and PI staining. Data was further analysed by WINMDI software and percentage of cells in the sub-G1 phase was indicated. Profile shown was representative of three independent experiments.
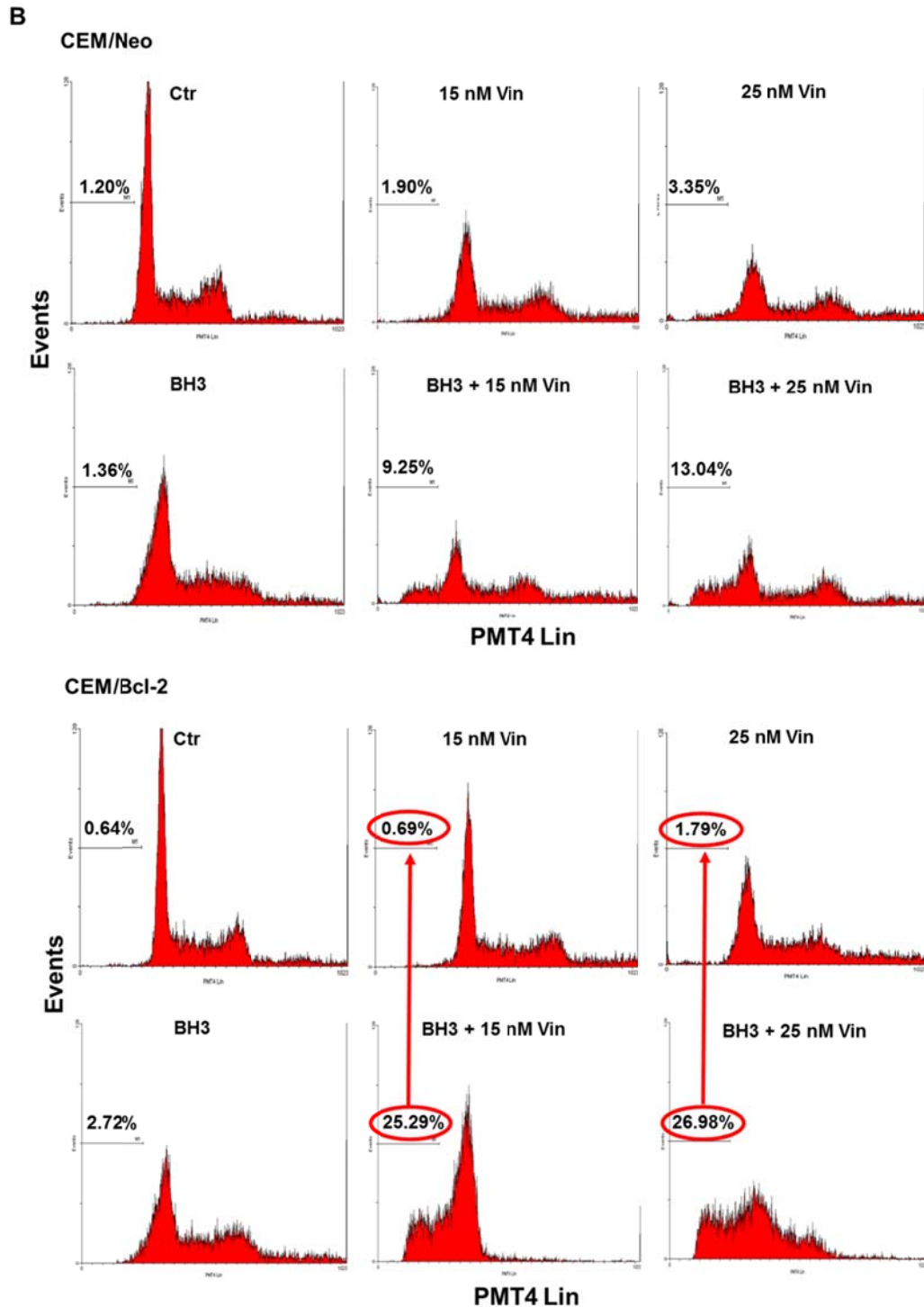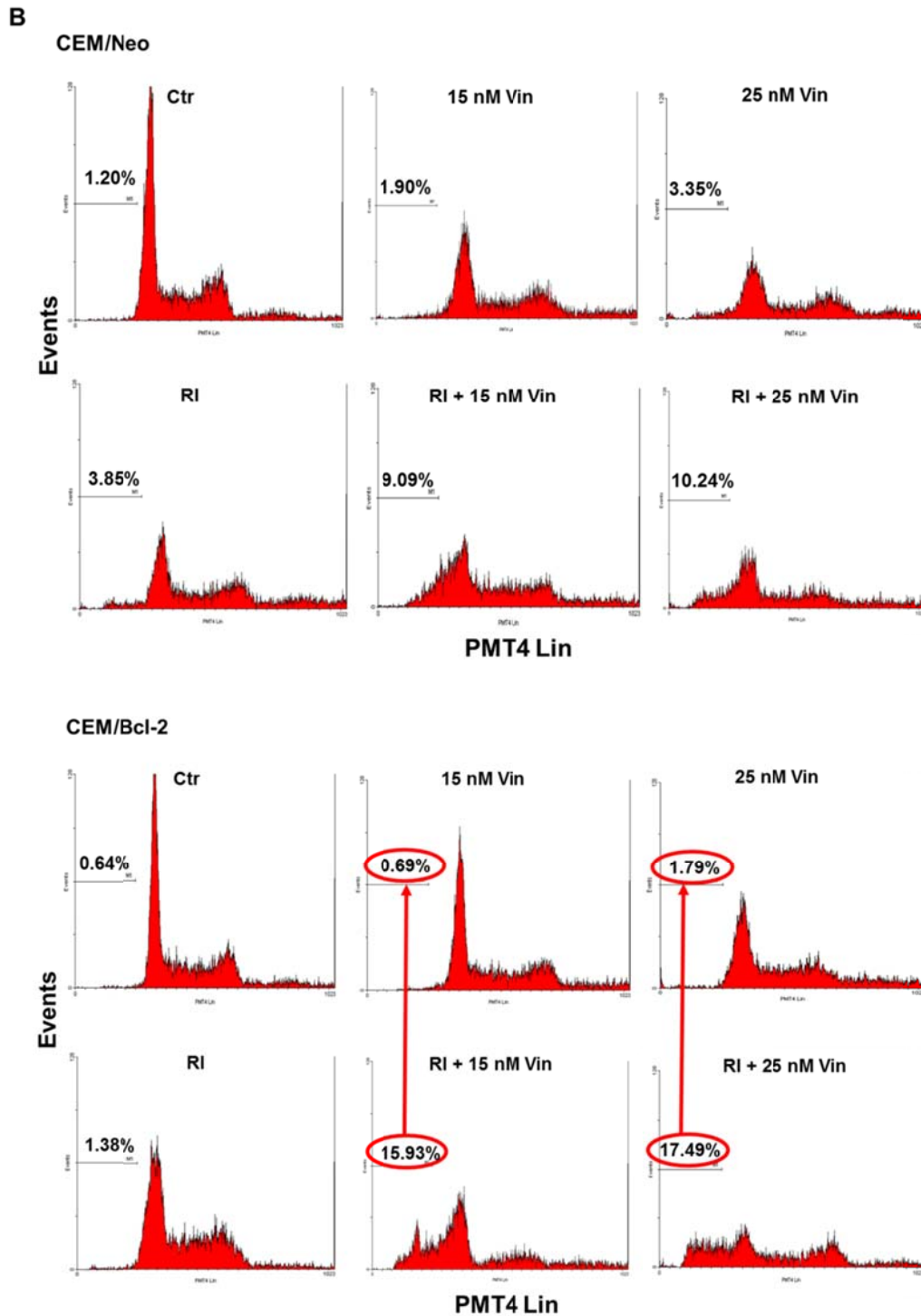
Figure 39: Combination treatment of Rac1 inhibitor and conventional chemotherapeutic drugs resulted in a significantly elevated sub-G1 population in Bcl-2-overexpressing cancer cells. (B) CEM cells were untreated (control), treated with 5 μM Rac1 inhibitor NSC23766 (RI) or vincristine (Vin) for 24 hrs, or pre-incubated with Rac1 inhibitor for 1 hr followed by exposure of vincristine for another 24 hrs. Cell cycle profile analysis was done using flow cytometry after ethanol fixation and PI staining. Data was further analysed by WINMDI software and percentage of cells in the sub-G1 phase was indicated. Profile shown was representative of three independent experiments.

3.14. ™CELLWORKS In Silico Modelling Identified STAT3 as a Potential Downstream Functional Target of the Tumorigenic Rac1-Bcl-2 Pathway

3.14.1 Rac1 and/or Bcl-2 Overexpression Greatly Enhanced Phenotypic Indices on Tumourigenesis as Predicted by ™CELLWORKS In Silico Modelling while Knocking Down of Rac1 or Bcl-2 Expression Resulted in the Opposite

To gain further insight into the functional relevance of the interaction between Rac1 and Bcl-2, computer simulation driven virtual predictive experiments based on the protein pathway dynamic network created by ™CELLWORKS Group Inc. were carried out. This is achieved by combining functional proteomics data based on various publications known to date together with engineering technologies and methodologies (such as interconnecting ordinary differential equations that describe enzyme kinetics, pathway flux distribution, *etc.*). It is a platform that mimics the human physiology system and allows the visibility into how pathways/phenotypes respond/change in a dynamic fashion upon certain stimuli/manipulation. The predictive results can be subsequently validated through wet lab experiments which greatly reduce the time and cost needed for the initial large-scale screening required otherwise[339]. With this virtual platform, it could serve as a visualization tool, in this case here, to predict the impact on tumorigenic phenotypes and pathway dynamics upon the presence or disruption of Rac1-Bcl-2 interaction in a cancer context. As such, an HCT116 human colorectal cancer cell line with K-Ras over-activation, PI3K (phosphoinositide 3-kinase) overexpression, CDKN2A (cyclin-dependent kinase inhibitor 2A) deletion and β-catenin overexpression was modeled in silico to recapitulate the major pathological system in colorectal cancer. An additional Bcl-2 overexpression was created in virtual serving as a base line and based on this a variant

cell line with Rac1 overexpression was also set up (**Figure 40A**). As shown in **Figure 40B & C**, phenotypic indices of angiogenesis, proliferation, viability, metastasis as well as tumor volume were all found to be amplified in the base and variant cell lines with Bcl-2 and/or Rac1 overexpression, as compared to the control HCT116 cells in the absence of Bcl-2 overexpression; on the contrary, upon knocking down of Rac1 or Bcl-2, these indices all went down in both the base and variant cell lines, confirming the tumorigenic effects of both proteins, in accordance with a plethora of published reports previously[126, 259-263, 279-281].

Apart from these general tumorigenic phenotypes, change in redox status, in particular the O_2^- levels, which have been well known to contribute to tumourigenesis[24, 47, 83, 84, 97, 103-110, 115], were also checked in the virtual HCT116 platform upon manipulation of Rac1 and/or Bcl-2 expression levels in silico. Indeed, overexpression of Bcl-2 in the base cell line resulted in a predicted significant elevated levels of O_2^- as compared to the control (**Figure 41**), which is consistent with what has been described by our group as well as other groups that Bcl-2 acts as a pro-oxidant intrinsically[114, 203, 218, 225-227]. Additional overexpression of Rac1 in the variant cell line resulted in double the amount of O_2^- produced as compared to the base cell line while knocking down of either Rac1 or Bcl-2 in both the base and variant cell lines led to a decrease in the O_2^- production (**Figure 41**). These predictive results are in accordance with our wet lab experimental data presented in earlier sections 3.1.1 (**Figure 1**) and 3.3 (**Figure 6**) confirming the definite involvement of both Rac1 and Bcl-2 in redox regulation.

Furthermore, a detailed look into the different apoptotic markers upon knocking down of Rac1 or Bcl-2 expression revealed that Bax, caspase 3 as well as cleaved PARP-1 (PARP-1, poly ADP ribose polymerase 1, which is involved in DNA damage repair and a substrate for activated caspase 3 protease during apoptosis[340, 341]) all went up significantly (**Figure 42**) confirming once again the pro-survival role of Rac1 and Bcl-2 as reported[126, 259, 279, 281].

A
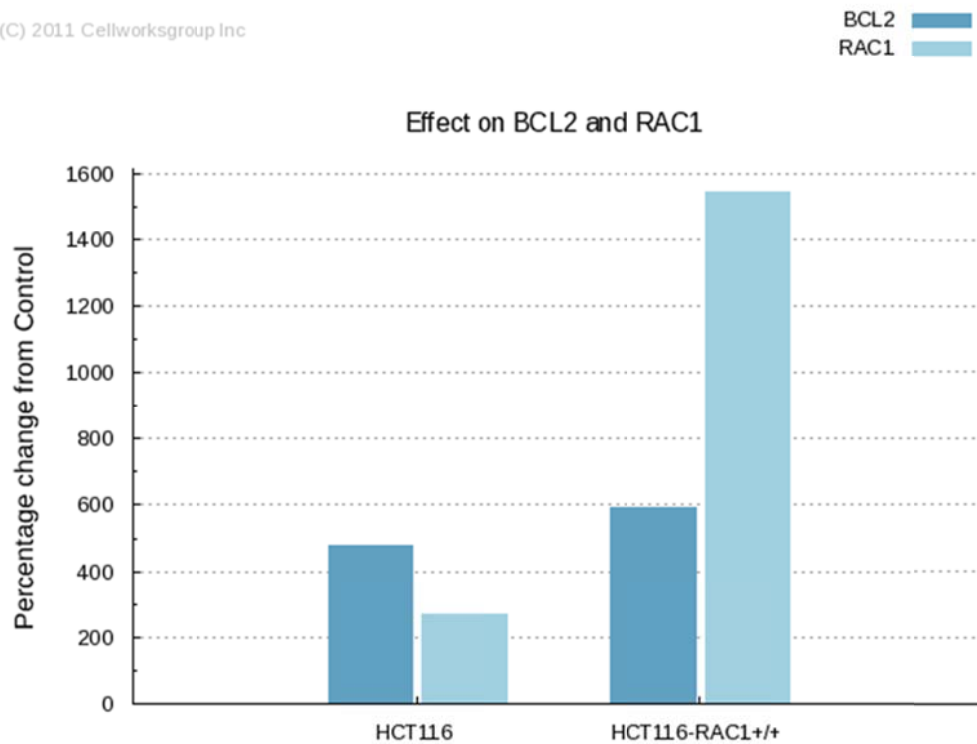
Figure 40: Rac1 and/or Bcl-2 overexpression greatly enhanced phenotypic indices on tumourigenesis as predicted by ™CELLWORKS in silico modelling while knocking down of Rac1 or Bcl-2 expression resulted in the opposite. Computer simulation driven virtual predictive experiments based on the protein pathway dynamic network created by ™CELLWORKS Group Inc. were carried out to study the functional implication(s) of Rac1-Bcl-2 interaction. The base line used was a K-Ras over-activated, PI3K overexpressed, CDKN2A deleted, β-catenin overexpressed and Bcl-2 overexpressed system aligned to HCT116 human colorectal cancer cell line and a variant of the above base line was created with Rac1 levels overexpressed by 3-fold. (A) The histograms show the percentage change in the virtual expression levels of Rac1 and Bcl-2 in the base and variant cell lines as compared to a control HCT116 cell line without Bcl-2 overexpression.
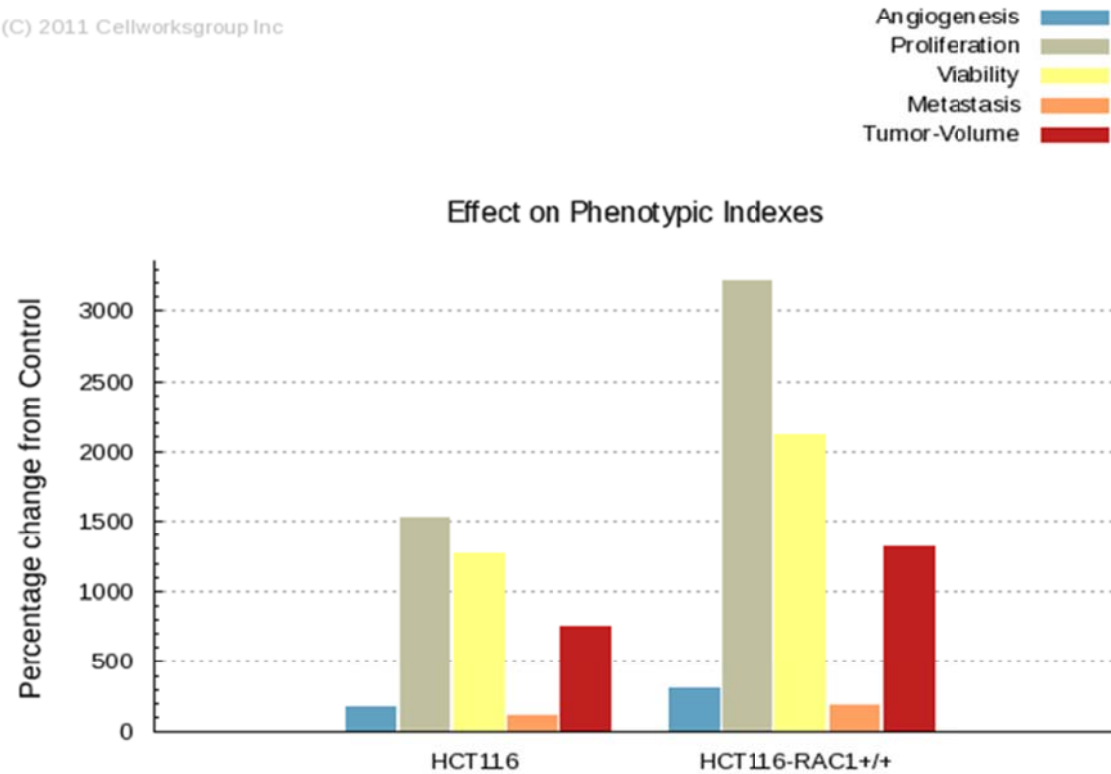
Figure 40: Rac1 and/or Bcl-2 overexpression greatly enhanced phenotypic indices on tumourigenesis as predicted by ™CELLWORKS in silico modelling while knocking down of Rac1 or Bcl-2 expression resulted in the opposite. (B) Percentage changes on key biomarkers and phenotypic indices including angiogenesis, proliferation, viability, metastasis and tumour volume were predicted in both the base and variant cell lines as compared to the control HCT116 cell line without Bcl-2 overexpression.
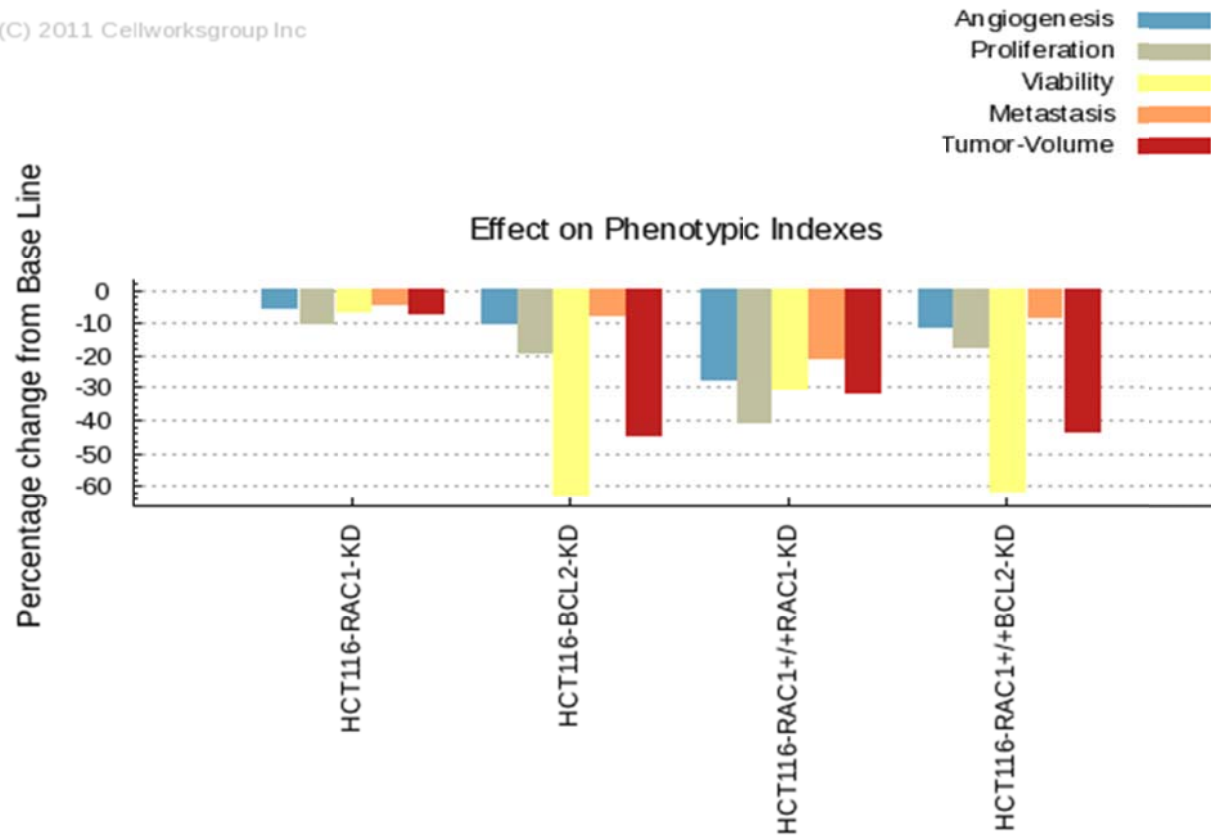
Figure 40: Rac1 and/or Bcl-2 overexpression greatly enhanced phenotypic indices on tumourigenesis as predicted by ™CELLWORKS in silico modelling while knocking down of Rac1 or Bcl-2 expression resulted in the opposite. (C) Percentage changes on key biomarkers and phenotypic indices were predicted upon knocking down the expression of Rac1 (target inhibition by 70%) or Bcl-2 (target inhibition by 70%) in both the base and variant cell lines as compared to the base cell line.

A

Figure 41: Rac1 and/or Bcl-2 overexpression greatly enhanced intracellular O_2^- levels as predicted by ™CELLWORKS in silico modelling while knocking down of Rac1 or Bcl-2 expression resulted in the opposite. Computer simulation driven virtual predictive experiments based on the protein pathway dynamic network created by ™CELLWORKS Group Inc. were carried out. The base line used was a K-Ras over-activated, PI3K overexpressed, CDKN2A deleted, β-catenin overexpressed and Bcl-2 overexpressed system aligned to HCT116 human colorectal cancer cell line and a variant of the above base line was created with Rac1 levels overexpressed by 3-fold. (A) Percentage changes on intracellular O_2^- levels were predicted in both the base and variant cell lines as compared to the control HCT116 cell line without Bcl-2 overexpression.

Figure 41: Rac1 and/or Bcl-2 overexpression greatly enhanced intracellular O_2^- levels as predicted by ™CELLWORKS in silico modelling while knocking down of Rac1 or Bcl-2 expression resulted in the opposite. (B) Percentage changes on intracellular O_2^- levels were predicted upon knocking down the expression of Rac1 (target inhibition by 70%) or Bcl-2 (target inhibition by 70%) in both the base and variant cell lines as compared to the base cell line.

Figure 42: Knocking down of Rac1 or Bcl-2 expression greatly elevated the levels of apoptotic markers as predicted by ™CELLWORKS in silico modelling. Computer simulation driven virtual predictive experiments based on the protein pathway dynamic network created by ™CELLWORKS Group Inc. were carried out. The base line used was a K-Ras over-activated, PI3K overexpressed, CDKN2A deleted, β-catenin overexpressed and Bcl-2 overexpressed system aligned to HCT116 human colorectal cancer cell line and a variant of the above base line was created with Rac1 levels overexpressed by 3-fold. Percentage changes on Bax, caspase 3 and cleaved PARP-1 levels were predicted in both the base and variant cell lines upon knocking down the expression of Rac1 (target inhibition by 70%) or Bcl-2 (target inhibition by 70%) as compared to the base cell line.

3.14.2 Rac1 and/or Bcl-2 Overexpression Greatly Amplified STAT3 Protein Levels as Predicted by ™CELLWORKS In Silico Modelling while Knocking Down of Rac1 or Bcl-2 Expression Resulted in the Opposite

In an attempt to identify the potential downstream targets that could mediate the pro-survival effects of Rac1 and Bcl-2, a large-scale in silico screening was performed on all the proteins that have been documented so far to be involved in tumorigenic signaling. Bcl-2 overexpression in the base HCT116 cell line resulted in a significant amplification in the protein levels of STAT3 and β-catenin and an additional Rac1 overexpression in the variant cell line led to a further enhancement in the expression levels of these two proteins (**Figure 43A**). On the contrary, knocking down on the expression levels of Rac1 or Bcl-2 in both the base and variant cell lines affected the expression levels of four proteins including STAT3 and β-catenin which are also the targets in the overexpression models as mentioned above as well as AGER and NF-κB1(**Figure 43B**). AGER, the Receptor for Advanced Glycation End-products, is involved in innate immunity[342] while NF- κB1, nuclear factor κ-light-chain-enhancer of activated B cells p105 subunit, is a Rel (the Class II NF-κB transcription factors) protein-specific transcription inhibitor involved in a wide variety of cellular functions including proliferation and survival[343]. Apparently, the two proteins that are consistently in direct correlation with the changes in the expression levels of both Rac1 and Bcl-2 are STAT3 and β-catenin (**Figure 43**). Subsequent follow-up studies to validate these in silico predictive results were carried out through web lab experiments, with a specific focus on STAT3 in this thesis due to its documented involvement in mitochondrial respiration, ROS signaling and Rac1 pathways[87, 89, 344, 345]. However validation for β-catenin, a subunit of the cadherin protein complex involved in Wnt signaling pathway that has been implicated

in oncogenesis[346], is beyond the scope of this thesis and will be carried out by other members in our laboratory.

STAT3 belongs to the family of proteins named as signal transducers and activators of transcription. Upon receiving signals from upstream activated cytokine and growth factor receptors, STAT3 gets phosphorylated at Tyr705, homodimerizes and translocates to the nucleus modulating the transcription of downstream responsive genes[347-352]. It has been demonstrated by various groups that STAT3 is critically involved in the initiation, progression and maintenance of different types of cancers[348, 350-353]. Elevated levels of active STAT3 have been found in most of the major human malignancies, including leukaemia, lymphoma, multiple myeloma, melanoma, cervical squamous-cell carcinoma, osteosarcoma, head and neck squamous cell carcinoma, breast cancer, non-small-cell lung cancer, gastric carcinoma, hepatocellular carcinoma, pancreatic adenocarcinoma, cholangiocarcinoma, colorectal cancer, renal cell carcinoma, ovarian carcinoma and prostate carcinoma[348, 350, 352-354]. STAT3-activated genes not only promote cell proliferation and survival, angiogenesis and metastasis but also inhibit apoptosis, differentiation and anti-tumor immune responses[348, 350-353, 355], therefore elevated levels of active STAT3 are usually associated with poor prognosis in many cancers[348, 350, 351, 353, 354, 356]. In addition, a constitutively active form of STAT3 has been shown to be sufficient in transforming normal epithelial and immortalized fibroblasts derived from prostate and breast tissues[357]. Active STAT3 is also required in the viral oncogene v-src-induced cellular transformation[348, 353, 354, 357-359]. The oncogene addiction phenotype of these cancer cells that require continued STAT3 activation render it as a good candidate for anti-cancer therapy. Indeed, various studies have shown that

disruption in STAT3 signalling results in growth inhibition and apoptosis in cancer cell lines as well as tumor growth inhibition in mouse xenograft cancer models including myeloproliferative neoplasms, acute lymphoblastic leukaemia, glioblastoma, head and neck squamous cell carcinoma, breast cancer, lung adenocarcinoma and renal cell carcinoma[348, 351-353, 358, 360-366].

Apart from being a transcription factor for many genes that are of tumorigenic nature such as Bcl-2[357], what makes STAT3 an appealing candidate to follow up based on the predictive screening results is its involvement in mitochondrial respiration, ROS signaling and most importantly its physical interaction with Rac1 and implications in Rac1 pathways[87, 89, 344, 345]. STAT3 has been found in the mitochondria, where it regulates cellular respiration. A loss of mitochondrial STAT3 results in a decrease in the activity of both Complex I and II in the ETC leading to a decrease in the oxygen consumption rate. This function of STAT3 has been demonstrated to be independent on its transcriptional activity but rather dependent on the phosphorylation status of Ser727. However, the precise mechanism on how STAT3 regulates the activity of Complex I and II remains elusive[344]. It has also been shown that Rac1, when in an active form, can directly bind, through its effector domain, to STAT3. Moreover, STAT3 phosphorylation on both Tyr705 and Ser727 can be stimulated with active Rac1, whereas dominant negative Rac1 inhibits STAT3 activation induced by growth factors[345]. Furthermore, it is well known that Rac1 is involved in ROS production[264, 272, 273] and ROS have been demonstrated to activate Jak2 (Janus kinase 2) and TYK2 (tyrosine kinase 2) [87] that phosphorylate STAT3 while inhibiting low molecular weight-protein tyrosine phosphatase (LMW-PTP that dephosphorylates Jak2) through oxidation[89], therefore it would be of great

interest to examine whether there is a functional link between STAT3 activation and redox changes mediated by the Rac1-Bcl-2 interaction in our model.
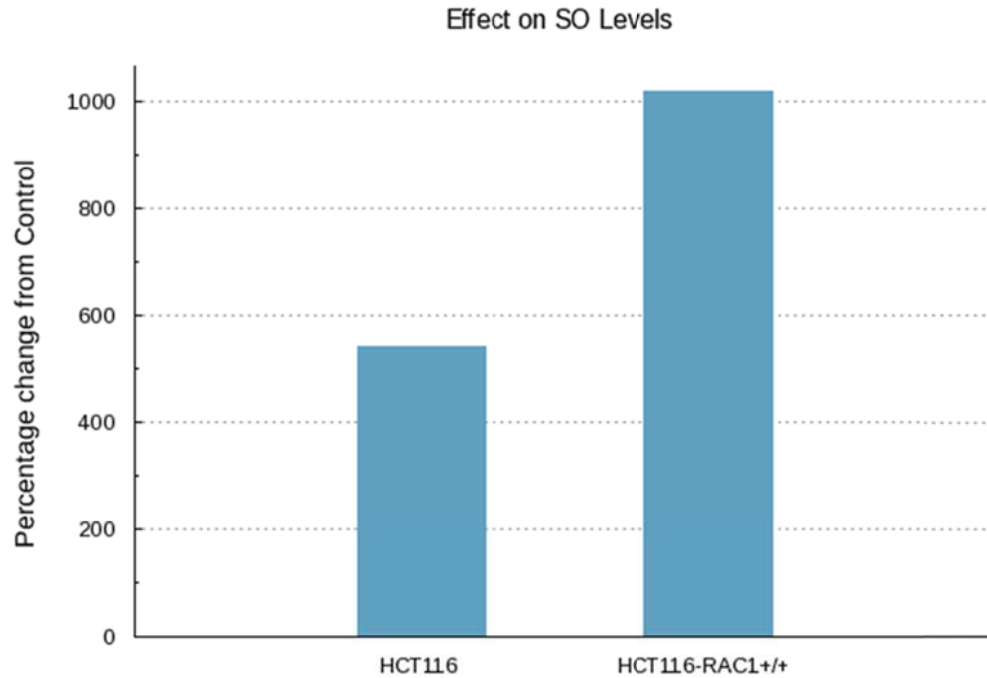

Figure 43: Rac1 and/or Bcl-2 overexpression greatly amplified STAT3 protein levels as predicted by ™CELLWORKS in silico modelling while knocking down of Rac1 or Bcl-2 expression resulted in the opposite. Computer simulation driven virtual predictive experiments based on the protein pathway dynamic network created by ™CELLWORKS Group Inc. were carried out. The base line used was a K-Ras over-activated, PI3K overexpressed, CDKN2A deleted, β-catenin overexpressed and Bcl-2 overexpressed system aligned to HCT116 human colorectal cancer cell line and a variant of the above base line was created with Rac1 levels overexpressed by 3-fold. (A) Percentage changes on protein levels of β-catenin and STAT3 were predicted in both the base and variant cell lines as compared to the control HCT116 cell line.
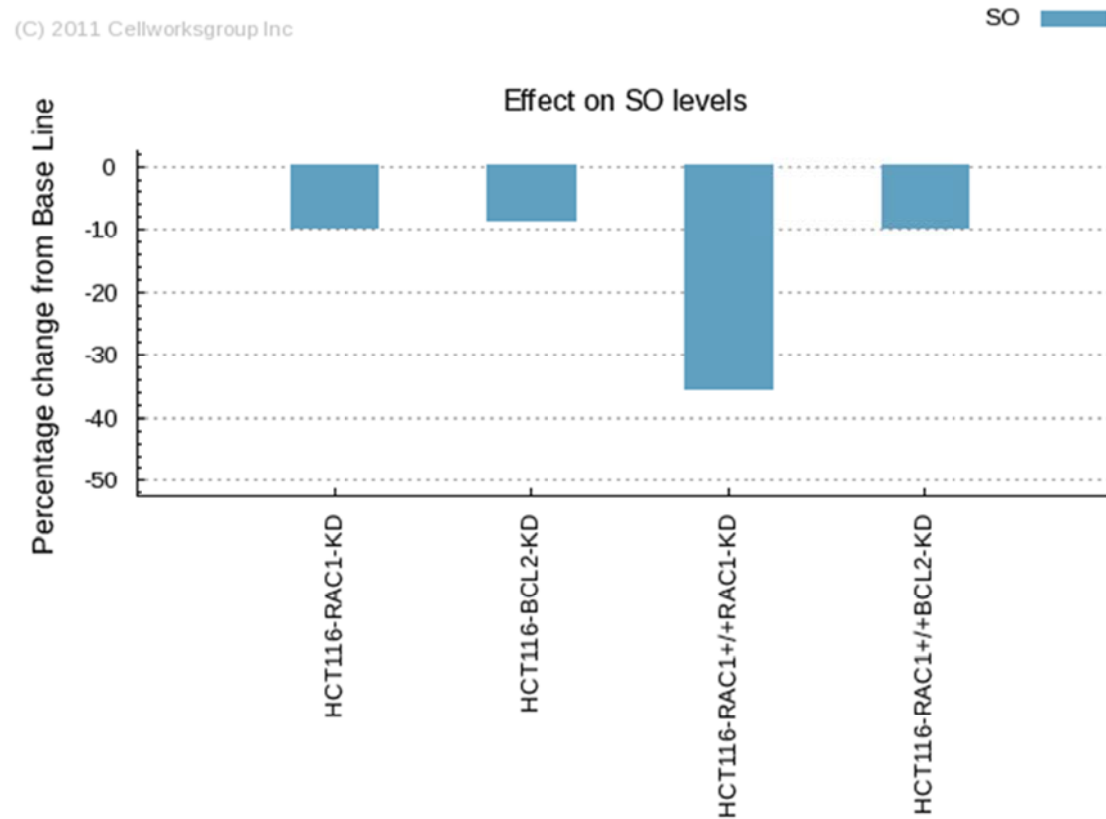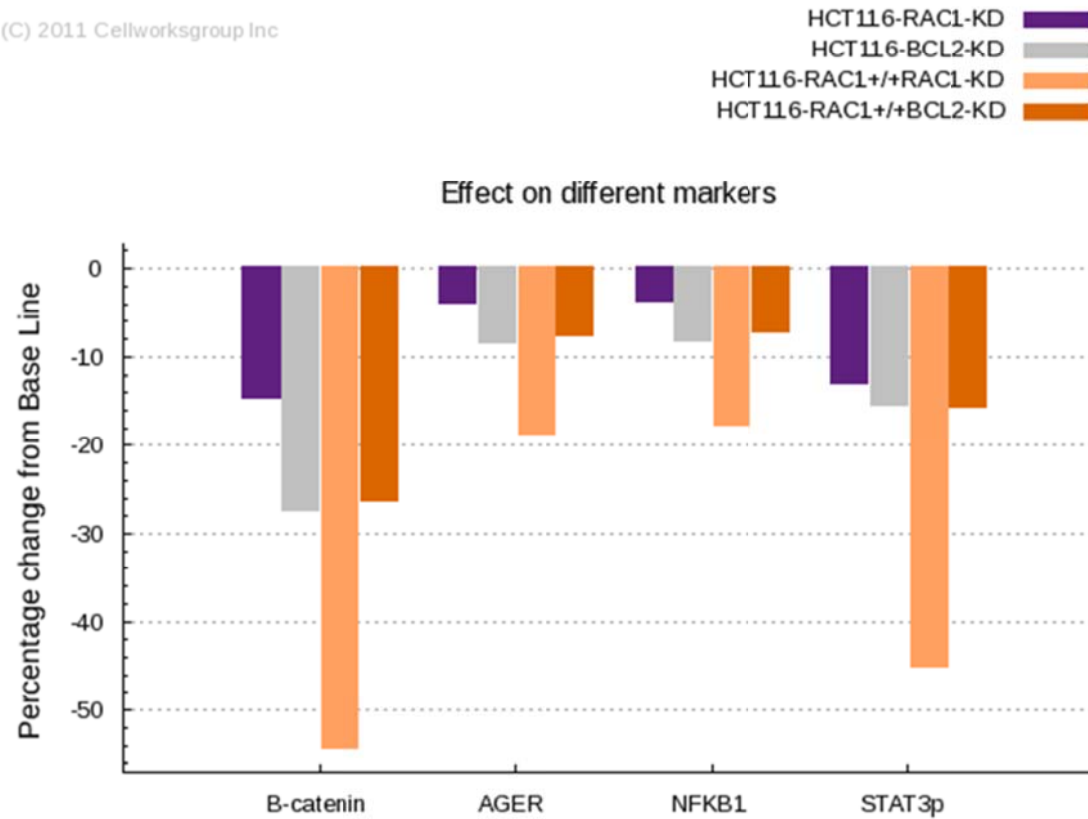
Figure 43: Rac1 and/or Bcl-2 overexpression greatly amplified STAT3 protein levels as predicted by ™CELLWORKS in silico modelling while knocking down of Rac1 or Bcl-2 expression resulted in the opposite. (B) Percentage changes on protein levels of β-catenin, AGER, NF-κB1 and STAT3 were predicted upon knocking down of the expression of Rac1 (target inhibition by 70%) or Bcl-2 (target inhibition by 70%) in both the base and variant cell lines as compared to the base cell line.
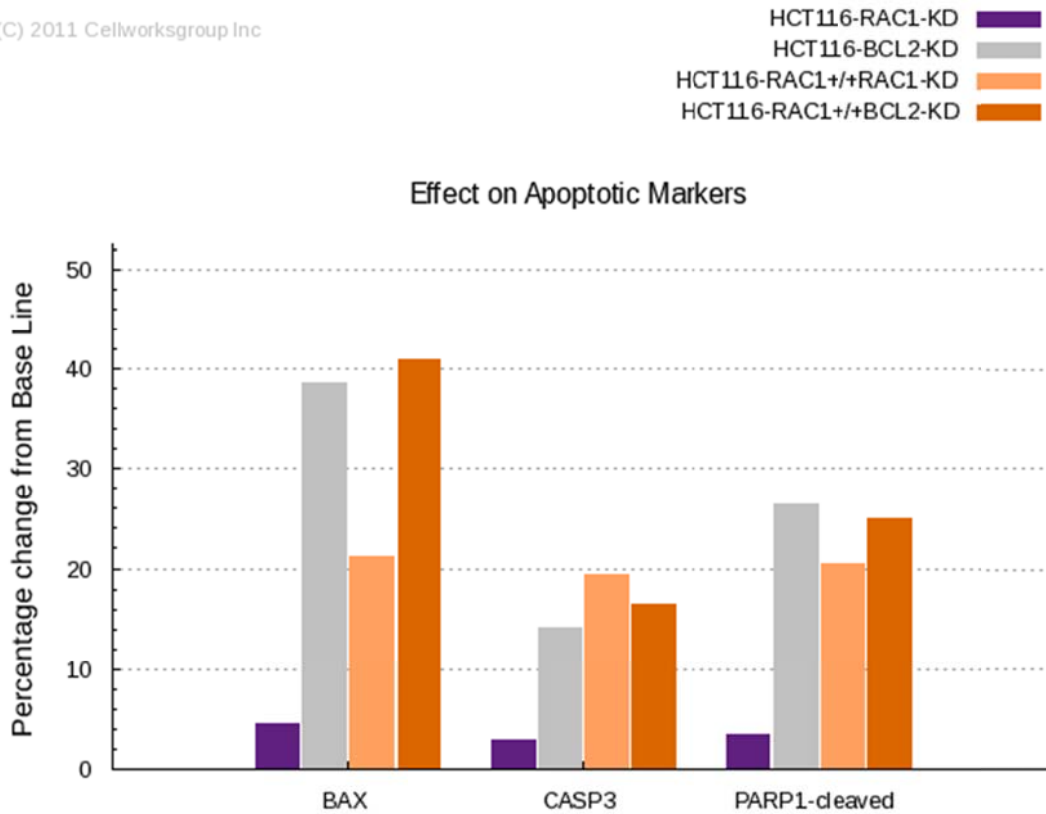
3.14.3 Bcl-2-overexpressing Cancer Cells Harbour Higher Activation Levels of Mitochondrial STAT3

Being intrigued by the in silico predictive results and the documented involvement of STAT3 in ROS signaling and Rac1 pathways[87, 89, 344, 345], a set of wet lab experiments were carried out in a sequential order to validate whether STAT3 is functionally relevant in the Rac1-Bcl-2 pathways. First of all, the localization of STAT3 was examined through western blot analysis following subcellular fractionation and indeed, STAT3 was found both in the cytosolic as well as mitochondria-enriched HM fractions, where the latter is the resident place for the Rac1-Bcl-2 interacting complex. The mitochondrial distribution of STAT3 is also in consistence with reports from other groups[344]. Interestingly, although the protein levels of STAT3 in the HM fractions were comparable in both CEM/Neo and CEM/Bcl-2 cells, its phosphorylation status at Tyr705, which marked the activation levels, differed remarkably with Bcl-2-overrexpressing cells harbouring a higher phosphorylated levels of STAT3 (**Figure 44**). The phosphorylation levels of Bcl-2 at Ser70 were also higher in CEM/Bcl-2 cells apparently due to the higher total protein levels of Bcl-2. VDAC and Cu/Zn SOD were used as markers for HM and cytosolic fractions, respectively, to show that there was no cross contamination between different subcellular fractions (**Figure 44**).
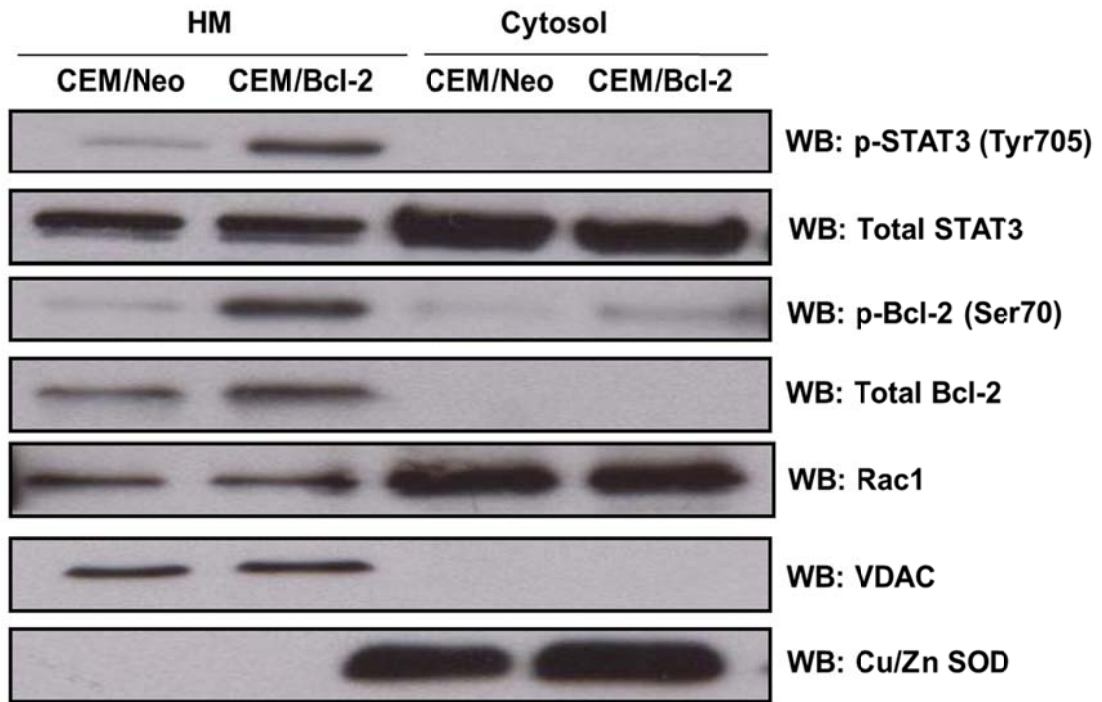
Figure 44: Bcl-2-overexpressing cancer cells have higher phosphorylation levels of mitochondrial STAT3 at Tyr705. Human chronic myeloid leukaemia CEM cells overexpressing Bcl-2 were lysed and fractionated into mitochondria-enriched purified heavy membrane (HM) and cytosolic (S) fractions. The fractions were then probed for p-STAT3 (Tyr705), total STAT3, p-Bcl-2 (Ser70), total Bcl-2, Rac1, VDAC and Cu/Zn SOD.

3.14.4 Bcl-2-induced STAT3 Activation is Mediated through Rac1 Activation and ROS Production

In order to gain further insight into the relationship between STAT3 activation and Bcl-2 expression levels, Bcl-2 was transiently overexpressed in HeLa cells and the activation levels of STAT3 as marked by its phosphorylation levels at Tyr705 were monitored through western blot analysis. Indeed, a clear causal relationship was observed where transient overexpression of Bcl-2 induced a significant increase in STAT3 phosphorylation levels at Tyr705 as compared to the empty vector transfected control cells (**Figure 45**).

Since data presented in the section 3.2 showed that Bcl-2 overexpression induced Rac1 activation in cancer cells (**Figure 3-4**) and it has also been reported that STAT3 phosphorylation on both Tyr705 and Ser727 can be stimulated with active Rac1 whereas dominant negative Rac1 inhibits STAT3 activation induced by growth factors[345], the pharmacological inhibitor of Rac1 EHT1864 was utilized to investigate whether Bcl-2-induced STAT3 activation could be mediated through Rac1 activation. HeLa cells that stably overexpress Bcl-2 showed constitutively higher activation levels of STAT3 as marked by phospho-Tyr705 as compared to empty vector matched control HeLa/Neo cells. Interestingly indeed, a dose-dependent decrease in the phospho-STAT3 levels at Tyr705 was observed with increasing doses of EHT1864 (**Figure 46**) that locked Rac1 in an inactive state indicating that Rac1 activation was required for Bcl-2-induced activation of STAT3. A dose-dependent decrease in the phosphorylation levels of Bcl-2 at Ser70 was also observed with EHT1864 corroborating with previous discussed data in the section 3.10 that active Rac1 induced phosphorylation of Bcl-2 at Ser70 (**Figure 25-27**).

Furthermore, it is well known that Rac1 is involved in ROS production[264, 272, 273] and ROS have been demonstrated to activate STAT3 through either activating corresponding kinases[87] and/or inhibiting the phosphatase[89], therefore examination on whether active Rac1-induced STAT3 activation is mediated through redox changes would be beneficial in understanding the Rac1-STAT3 pathway. DPI, a general pharmacological inhibitor of Nox, was used to block the production of O_2^- downstream of Rac1 activation. Exposure to the increasing doses of DPI resulted in a decrease in the STAT3 phosphorylation levels at Tyr705 in HeLa/Bcl-2 cells (**Figure 47**) suggesting a probable regulatory role for ROS in Bcl-2-induced STAT3 activation model here. Similarly, phosphorylation levels of Bcl-2 at Ser70 were also decreased with DPI treatment (**Figure 47**) indicating that it could also be redox regulated.
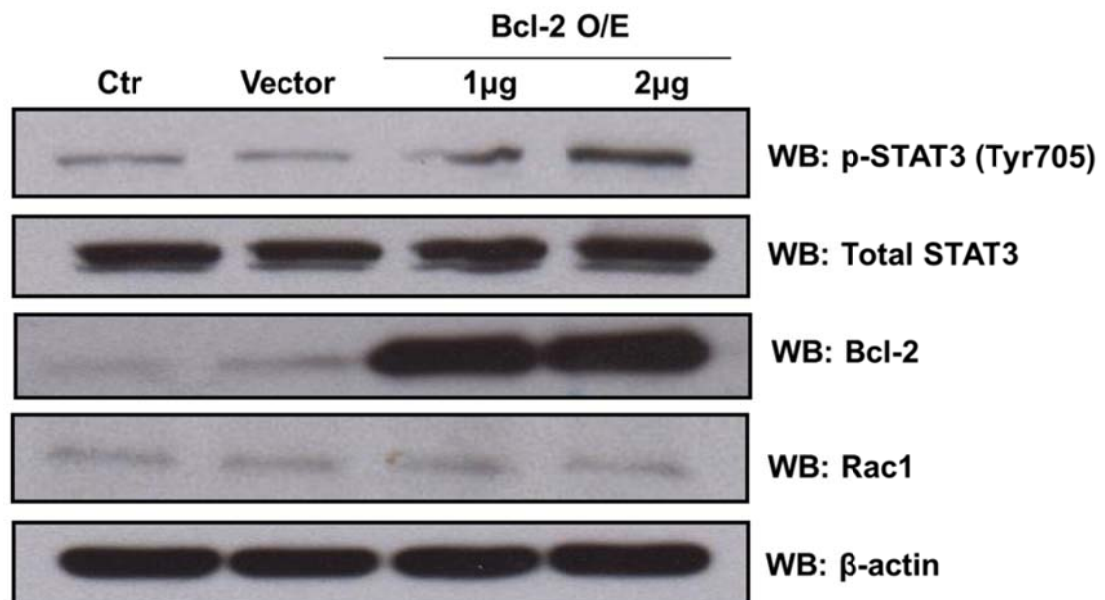
Figure 45: Transient overexpression of Bcl-2 induced STAT3 phosphorylation at Tyr705. Lysates from control HeLa cells or cells transiently transfected with either the empty vector or Bcl-2 wild type (with increasing amount of plasmids) for 48 hrs were probed for p-STAT3 (Tyr705), total STAT3, Bcl-2, Rac1 and β-actin.
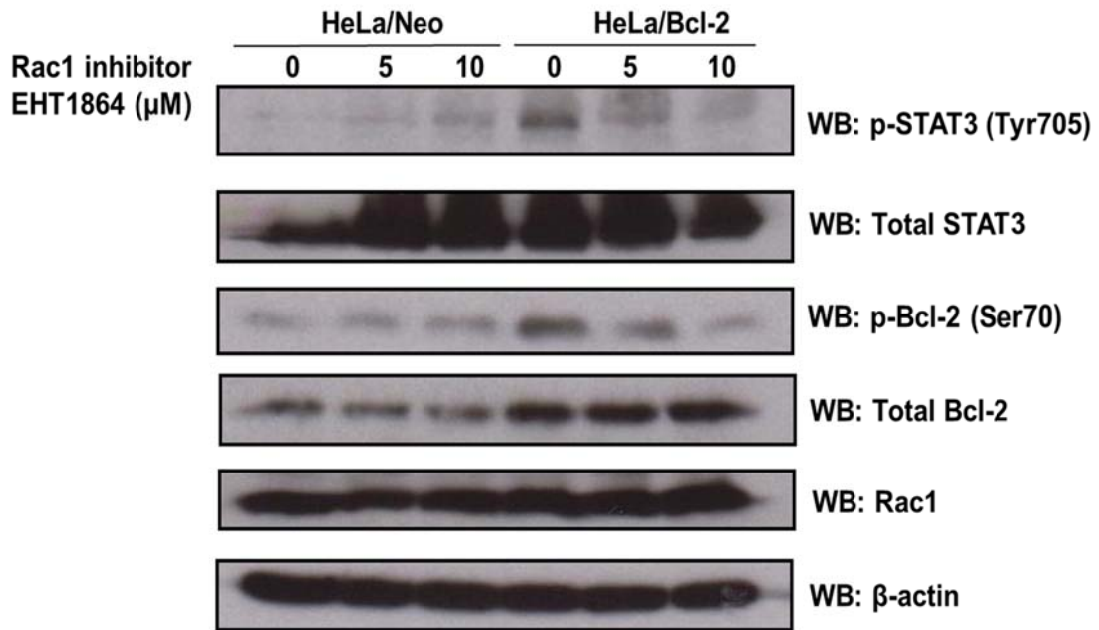
Figure 46: Pharmacological inhibition of Rac1 activity decreased STAT3 phosphorylation levels at Tyr705 in Bcl-2-overexpressing cancer cells. HeLa cells stably overexpressing either the control vector (HeLa/Neo) or Bcl-2 (HeLa/Bcl-2) were treated with different doses of Rac1 inhibitor EHT1864 and the lysates were probed for p-STAT3 (Tyr705), total STAT3, p-Bcl-2 (Ser70), total Bcl-2, Rac1 and β-actin.
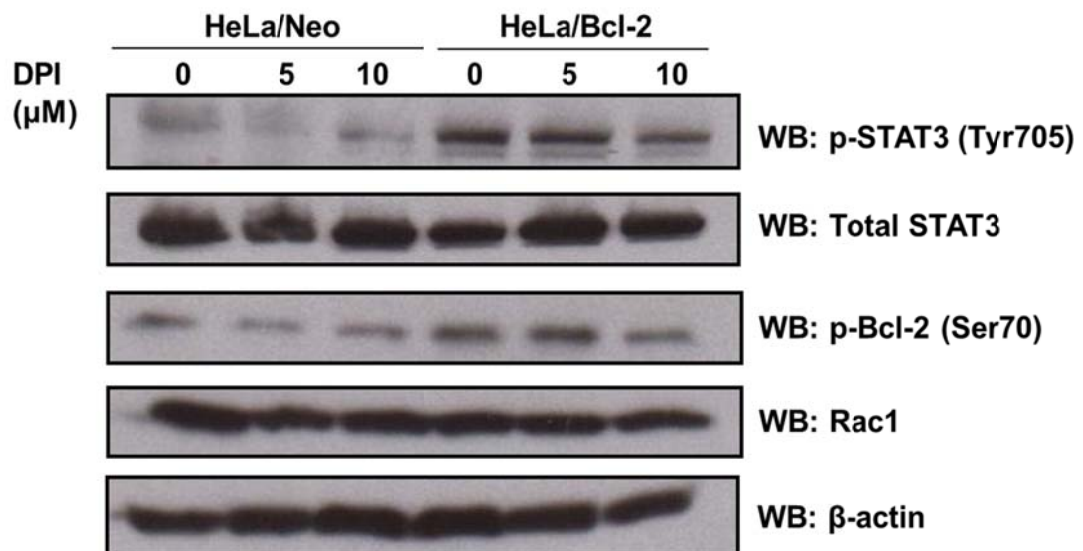
Figure 47: Pharmacological inhibition of NADPH oxidase activity decreased STAT3 phosphorylation levels at Tyr705 in Bcl-2-overexpressing cancer cells. HeLa cells stably overexpressing either the control vector (HeLa/Neo) or Bcl-2 (HeLa/Bcl-2) were treated with different doses of the Nox inhibitor DPI and the lysates were probed for p-STAT3 (Tyr705), total STAT3, p-Bcl-2 (Ser70), Rac1 and β-actin.

3.14.5 Rac1, Bcl-2 and STAT3 Co-immunoprecipitated with Each Other in Cancer Cells with Higher Bcl-2 Expression Levels

Data presented thus far revealed that Bcl-2-induced STAT3 activation was mediated through Rac1 activation and ROS production. Interestingly, these three proteins are functionally linked through physical interactions between Rac1 and Bcl-2 as presented in the previous sections of this thesis (**Figure 10**) as well as between Rac1 and STAT3 as described by other groups[345]. Intrigued by these findings, co-immunoprecipitation analysis was performed in different cancer cell lines with varying amount of Bcl-2 expression by pulling down each of these three proteins and probing for the rest two. Apart from the physical interactions known between Rac1 and Bcl-2 as well as between Rac1 and STAT3, a novel physical interaction was observed between Bcl-2 and STAT3. All the three interactions (Rac1-Bcl-2, Rac1-STAT3 as well as Bcl-2-STAT3) showed a Bcl-2 expression dependency where higher interaction levels were observed in cell lines with higher Bcl-2 expression levels such as Jurkat and HeLa/Bcl-2 (**Figure 48**). However, whether the activation of STAT3 could be a direct functional readout for its interaction with Rac1 or Bcl-2 awaits further exploration. Of a particular note are the expression levels of STAT3, which seem to correlate with Bcl-2 expression levels as well in this case where Jurkat and HeLa/Bcl-2 had higher STAT3 protein levels as compared to Raji and HeLa/Neo, respectively, corroborating the in silico prediction (**Figure 43**).
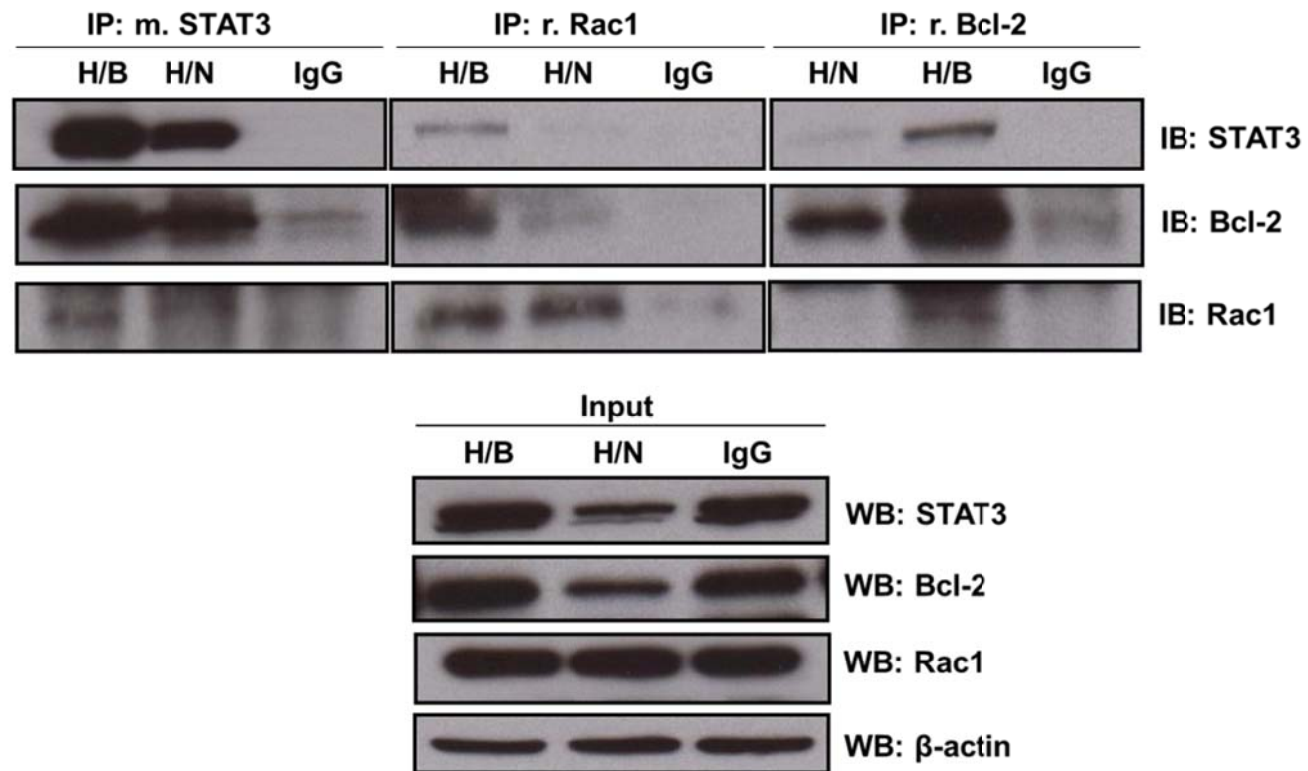
Figure 48: Rac1, Bcl-2 and STAT3 co-immunoprecipitated with each other in Bcl-2-overexpressing cancer cells. (A) Cell lysates from HeLa cells stably overexpressing either the control vector (H/N) or Bcl-2 plasmid (H/B) were immunoprecipitated with either anti-STAT3, anti-Rac1 or anti-Bcl-2 and probed with anti-STAT3, anti-Bcl-2 and anti-Rac1. Immunoprecipitation with control matching anti-IgG antibodies was used as a negative control. Whole cell lysates probed with anti-STAT3, anti-Bcl-2, anti-Rac1 and anti-β-actin are shown on the bottom panel as input.

B
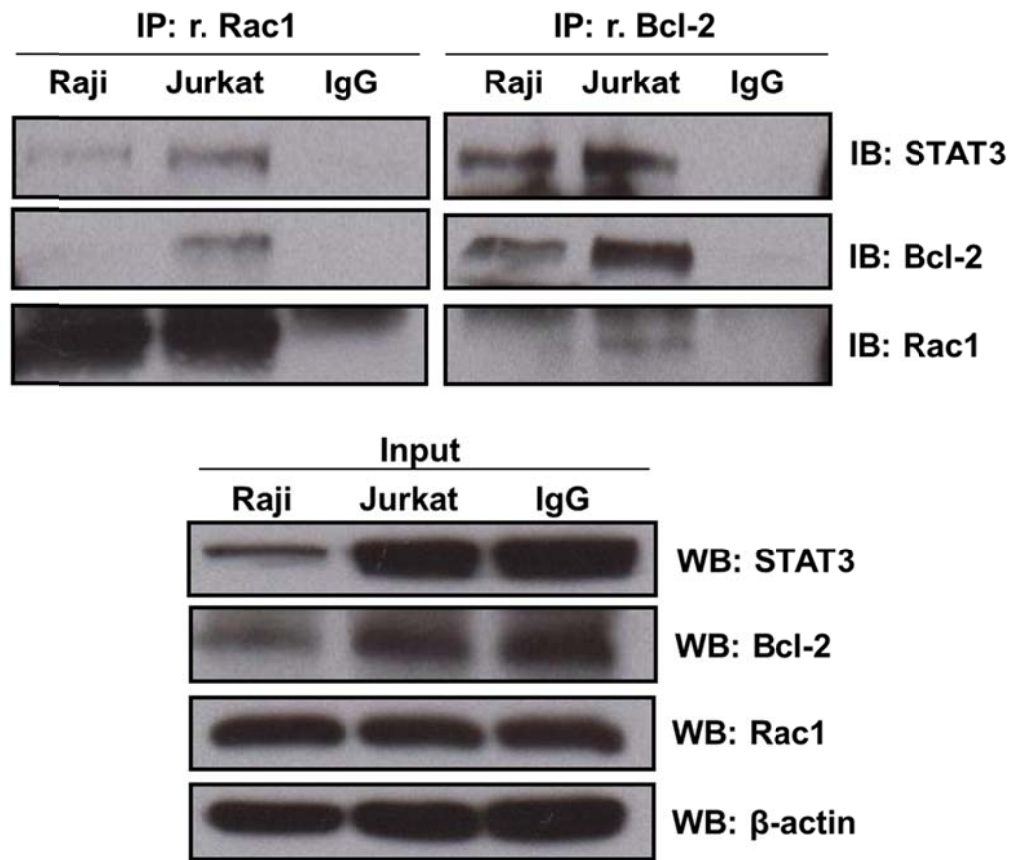
Figure 48: Rac1, Bcl-2 and STAT3 co-immunoprecipitate with each other in Bcl-2-overexpressing cancer cells. (B) Cell lysates from Raji and Jurkat cells were immunoprecipitated with either anti-Rac1 or anti-Bcl-2 and probed with anti-STAT3, anti-Bcl-2 and anti-Rac1. Immunoprecipitation with control matching anti-IgG antibodies was used as a negative control. Whole cell lysates probed with anti-STAT3, anti-Bcl-2, anti-Rac1 and anti-β-actin are shown on the bottom panel as input.

CHAPTER 4: DISCUSSION

4.1. Pro-oxidant vs. Reductive Intracellular Milieu in Cancers

One common denominator for all cancers is the dysregulated or defective ratio between cell proliferation and cell death. Our group as well as others have hypothesized that reactive oxygen species (ROS) are one of the major underlying culprit signals, which has been supported by abundant evidences over the past couple of years[2, 24-32, 47, 82-110, 112-117, 120-122]. Unlike their universal detrimental effects at high concentrations among all reactive members of ROS, the exact proliferative and/or pro-survival roles ROS play at low doses depend very much on the ratio of respective species involved, to be specific, the ratio between O_2^- and H_2O_2. It is now well established that, as compared to their normal counterparts, a number of cancers exhibit a constitutively elevated levels of O_2^- which creates a pro-oxidant intracellular milieu favouring proliferation as well as survival (indirectly through inhibition of apoptosis). On the contrary, a reductive milieu is created when the ratio tilts in favour of H_2O_2, which is permissive for apoptotic execution[24, 47, 103-110]. In this regard, identifying potential intracellular targets responsible for maintaining the redox-mediated proliferative and/or pro-survival signals could have invaluable impact for cancer therapeutics and this has always been the interest of many researchers including our group. One of the targets that has surfaced and will remain as the prime focus of this thesis is the anti-apoptotic protein Bcl-2.

4.2.   Bcl-2-induced Chemoresistance Could be Mediated through Redox Regulation: A Non-canonical Perspective

4.2.1   Bcl-2 as a Culprit for Inducing the Pro-oxidant Intracellular Milieu in Cancer Cells

During the course in search for potential druggable targets that could be utilized to manipulate cellular redox status for therapeutic purpose, the anti-apoptotic protein Bcl-2 has come to our notice for its non-canonical role as a redox regulator[70, 123, 203, 204]. It has been well established that Bcl-2 acts as an oncogene by virtue of its ability to guard the integrity of the mitochondrial membranes, for example through sequestration of the pro-apoptotic and/or BH3 only proteins of the Bcl-2 family members[124, 126, 137, 152, 155, 156]. This has been linked to the lack of efficacy of chemotherapy regimens in hematopoietic and other malignancies where Bcl-2 overexpression is observed, be it intrinsic or acquired[123, 282-289]. However, it has not been clearly studied on other alternative paradigms that Bcl-2 relies on for apoptotic evasion. Being intrigued by the facts that ROS being the underlying signals for numerous tumorigenic events and Bcl-2 being localized at the sites of ROS generation, i.e. mitochondria, endoplasmic reticulum (ER) and nucleus, we began to explore the possibility of Bcl-2 being a redox regulator. Interestingly, the initial reports that linked Bcl-2 and ROS dated back as early as 1993 where Bcl-2 was described to protect against ROS-induced apoptosis decreasing ROS production and preventing oxidants-induced lipid peroxidation[112, 206]. Although subsequent studies suggested Bcl-2's protective capacity against ROS triggers could be due to its function as an antioxidant, this was soon challenged by the findings that Bcl-2 itself possesses no intrinsic antioxidant property[215]. In 1995, a study done by Steinmann's group revealed that on the contrary, Bcl-2 is inducing a basal oxidative

stress which led to the subsequent enhancement in the antioxidant capacity observed providing the first evidence that Bcl-2 is functioning as a pro-oxidant[225]. In that light, our laboratory observed in 2003 that in chronic myeloid leukaemia (CEM) cells, overexpression of Bcl-2 resulted in a mild but constitutive elevation in the intracellular O_2^- levels creating a pro-oxidant milieu and this is demonstrated, for the first time, to contribute towards Bcl-2-mediated chemoresistance of those cells[114]. Similarly, we showed in this thesis as well that CEM cells stably overexpressing Bcl-2 exhibited enhanced O_2^- levels in the mitochondria (**Figure 1**) which confirms a definite pro-oxidant nature of Bcl-2 corroborating earlier findings from our group and others[114, 203, 218, 226, 227]. However, despite sharing homologous sequence and structure, another pro-survival member of the Bcl-2 family, Bcl-xL, could not function as a pro-oxidant by inducing an increase in the O_2^- levels *per se* (**Figure 2**) indicating that the redox regulatory property, specific for Bcl-2, is very likely not related to its conventional role in preventing MOMP (mitochondrial outer membrane permeabilization). Being intrigued by this notion, we set off to explore the underlying mechanism(s) for this new facet of Bcl-2 biology in redox regulation.

4.2.2   Mechanisms Employed by Bcl-2 in Inducing the Pro-oxidant State: Involvement of COX, Nox and Rac1

4.2.2.1 Engaging the mitochondrial respiration through COX

Bcl-2, being largely localized to the mitochondria[127], its connection with the mitochondrial respiration, a major source of intracellular ROS production[34], was first studied. A greater basal oxygen consumption rate and COX activity (cytochrome c oxidase or Complex IV, which is the rate-limiting step of the electron

transport chain (ETC)) was observed in Bcl-2-overexpressing cancer cells, which could explain, at least in part, to the elevated mitochondrial O_2^- produced. More importantly, the impact of Bcl-2 on mitochondrial respiration is bidirectional where Bcl-2 can modulate the activity of COX and thus oxygen consumption upon "sensing" overt oxidative stress maintaining the ROS levels at an optimal threshold promoting survival of cancer cells. This is achieved through a physical interaction with the Va subunit of COX[203, 204].

4.2.2.2 Involvement of Nox

Other than the mitochondrial respiration, the connection between Bcl-2 and another major intracellular source for ROS production, the Nox family proteins[43, 72, 73], is also being studied in our laboratory. The first piece of evidence came from the observation that introduction of a general pharmacological inhibitor of Nox, DPI, led to a decrease in the intracellular O_2^- levels in Bcl-2-overexpressing cancer cells[114]. Interestingly, here we showed that a preliminary screening of different Nox complex subunits in these cancer cells revealed the presence of 2 isoforms of Nox at the mitochondrial membranes, predominantly Nox4 and to a lesser extent Nox2 (**Figure 19B**). Although the mitochondrial localization of Nox4 and its regulation on mitochondrial O_2^- levels have been reported earlier in cultured mesangial cells, kidney cortex and cardiac myocytes[67-69], its particular involvement in the Bcl-2-mediated pro-oxidant model awaits further exploration.

4.2.2.3 Preliminary findings: Activity of Rac1 is critical in Bcl-2-mediated pro-oxidant state in cancer cells

Another piece of evidence suggesting the involvement of Nox complex in Bcl-2-mediated pro-oxidant status is from the report where our group showed that transient introduction of a dominant negative mutant of the small GTPase Rac1, a subunit of Nox complex which is required in a GTP-bound active form for the assembly and activation of Nox1, Nox2 and Nox3 complexes[59, 60, 273], led to a decrease in the intracellular O_2^- levels of Bcl-2-overexpressing cells[114] indicating a functional involvement of Rac1 in Bcl-2-mediated pro-oxidant milieu. However, the use of dominant negative mutant Rac1N17 is confounding since it sequesters endogenous GEFs (guanine nucleotide exchange factors) shared by GTPases other than Rac1 as well[367], for example, its expression has been shown to interfere with the activation of RhoA by the Dbl GEF[368]. The problem on lack of specificity was later solved by using siRNA-mediated silencing targeted specifically at Rac1 and indeed knocking down the expression of Rac1 reduced the O_2^- levels both intracellularly and intra-mitochondrially[70]. This is confirmed again in this thesis using a pharmacological inhibitor of Rac1, NSC23766, which disrupts the interaction between Rac1 and Rac specific GEFs such as TrioN and Tiam1[243]. Here we report that upon blocking of Rac1 activation (**Figure 5**), there was a significant drop in the O_2^- levels in the mitochondria of Bcl-2-overexpressing cancer cells (**Figure 6**). Of particular note is the different extent in the decrease of Rac1 activation levels upon NSC23766 treatment in CEM cells with varying Bcl-2 expression levels where the inhibition of Rac1 activity was more prominent in Bcl-2-overexpressing CEM cells (CEM/Bcl-2) with higher basal activation levels to begin with as compared to the control vector matched CEM/Neo cells (**Figure 5**). The extent in the decrease of Rac1

activity is reflected in the degree of reduction in mitochondrial O_2^- levels (**Figure 6**) indicating a direct correlation between these two. The functional involvement of Rac1 in Bcl-2-mediated pro-oxidant state was further supported by the observations that Bcl-2 expression levels are directly correlated with GTP loading of Rac1 (**Figure 3**) and moreover activation of Rac1 can be induced upon Bcl-2 overexpression (**Figure 4**). However, the exact mechanism for Bcl-2-induced Rac1 activation is currently still under investigation. Interestingly, it has been reported that similar to small GTPases, Bcl-2 has GTP binding property although the GTP loading mechanism has not been studied in details[369]. Intriguingly, the viral homologue of Bcl-2, BNIP-2, has been shown to bind to one of the Rho GTPases, Cdc42 and the corresponding Cdc42GAP (GTPase activating protein) as well stimulating the intrinsic GTPase activity of Cdc42. The association between BNIP-2 and Cdc42GAP is mediated through the homology between the catalytic domain of BNIP-2 with the noncatalytic domain of Cdc42GAP[370, 371]. These findings raise the possibility of Bcl-2 interacting with Rac1 or its corresponding GAP(s) or GEF(s) either directly or indirectly and modulating their activities leading to an induced Rac1 activation.

4.2.2.3.1   Studies from other groups on the role of Rac1 in mitochondrial redox regulation

The role of Rac1 in regulating O_2^- production has been well established in phagocytes through activation of Nox2 complex as well as in non-phagocytic cells through activation of other isoforms such as Nox1 and Nox3[59, 60, 273]. However, most of the studies centre on Rac1 at the plasma membrane where Nox complexes are commonly known to be assembled and activated. Less is known about the role of Rac1 in the mitochondrial redox homeostasis except only a handful of reports. It has

186

been reported that Rac1 was enriched in the mitochondrial fractions as early as 1995[276] and this is supported by another two reports in 2003 and 2012 [277, 278]. Indeed, the presence of Rac1 in mitochondria was also demonstrated by our group in 2011[70] and it is further confirmed here in this thesis in a number of cell lines including not only cancerous but also normal immortalized human fibroblasts (**Figure 12**). Up to date, there are only four reports that described a link between Rac1 and mitochondrial ROS production. Werner and group showed in 2002 that Rac1 activation was induced upon integrin engagement in fibroblasts changing the mitochondrial membrane potential and leading to production of mitochondrial ROS, which was insensitive to Nox inhibition by DPI. Interestingly, the ROS production could be inhibited by Bcl-2 suggesting an indirect association of Bcl-2 in Rac1's ability to modulate mitochondrial redox status[372]. Another report by Irani and group in 2003 also described that introduction of a constitutively active mutant Rac1V12 resulted in mitochondrial oxidative stress in human vascular endothelial cells leading to senescence of those cells. The production of mitochondrial ROS could be inhibited with the Complex I inhibitor rotenone but not with the Nox inhibitor apocynin and this was attributed to Rac1's ability in generating intracellular ceramide which is known to disrupt mitochondrial ETC[373]. In addition, Nieto and group reported in 2005 that Rac1b, the splice variant of Rac1, through disruption of the mitochondrial transmembrane potential, was able to induce mitochondrial oxidative stress as well and this led to oxidative damage and genomic instability enhancing the invasiveness of the breast cancer cells[374]. More recently Carter and group showed that Rac1 localizes in mitochondria and can increase mitochondrial H_2O_2 production in alveolar macrophages of asbestosis patients, through direct electron transfer from cytochrome c[278]. These four reports indicated the involvement of Rac1 in

modulating mitochondrial redox status which is critical in oncogenesis or aging or other pathological states such as pulmonary fibrosis. Intrigued by these findings and our own observations that Rac1 is involved in Bcl-2-mediated pro-oxidant state both intracellularly[70] and intra-mitochondrially (**Figure 6**), we went ahead to investigate the underlying mechanism(s) and hypothesize a direct association between Bcl-2 and Rac1 since Bcl-2 is known to interact with other small GTPases including Ras[194], RalA and Cdc42[70] as well. Indeed we identified for the first time, a physical interaction between Rac1 and Bcl-2 at the mitochondrial level[70].

4.3. Identification of the Small GTPase Rac1 as a Novel Binding Partner for Bcl-2 and Characterization of the Binding Domains/Residues

4.3.1 Existence of a Physical Interaction between Bcl-2 and Rac1 in Cancers with Bcl-2 Overexpression

Previous results from our laboratory identified a direct association between Rac1 and Bcl-2 at the mitochondria both *in vitro* with cell free system and *in vivo* with cancer cell lines and lymphoma patient samples. Here we confirmed once again on the existence of this physical interaction through co-immunoprecipitation assays (**Figure 10**) as well as co-localization between these two proteins through fluorescent microscopic analysis (**Figure 9**). The interaction is specific for cancerous cells, higher the Bcl-2 expression levels, higher the interaction levels (**Figure 10**) while no interaction was observed in peripheral blood mononuclear cells (PBMCs) obtained from healthy donors (**Figure 11**) corroborating with our previous findings[70].

Interestingly, despite sharing sequence and structural homology, the interaction with Rac1 is specific to Bcl-2 but not other Bcl-2 family members such as Bcl-xL and Bax[70] raising the possibility that the interaction could potentially involve regions that are less conserved (e.g. the flexible loop region that links BH3 and BH4 domains of the pro-survival members) or structurally dissimilar (e.g. a wider hydrophobic BH3 domain groove in Bcl-2 as compared to Bcl-xL)[129-134, 375]. These differences would affect the topology and electrostatic status of Bcl-2, which could probably explain its unique interacting property with Rac1. This intrigued us to go on to characterize the binding domains/residues involved which could have great impact not only on understanding the structural biology of Bcl-2 family members but also on future therapeutic design targeting specifically at malignancies with Bcl-2 overexpression.

4.3.2 Characterization of the Essential Binding Domains/Residues Required for the Rac1-Bcl-2 Interaction

4.3.2.1 Geranylgeranylation at the C-terminus of Rac1 is required for its membrane localization and interaction with Bcl-2

The trafficking of Rac1 to different membrane compartments is dependent on a post-translational modification named as geranylgeranylation, i.e. covalent attachment of a geranylgeranyl pyrophosphate (GGPP) group, to the C-terminal cysteine residue (CAAX motif) of Rac1. The GGPP moiety is then recognized by Rho GDI (guanine nucleotide dissociation inhibitor) to keep Rac1 in a soluble state in cytosol for subsequent shuttling to various membrane compartments[248]. Here we report that this post-translational modification is indeed essential in the mitochondrial

targeting of Rac1 where pharmacological inhibition of the geranylgeranyltransferase I resulted in a dose-dependent decrease in the protein levels of Rac1 at mitochondria (**Figure 13**). Similarly, another group also described recently that Rac1 localizes to the mitochondria in the alveolar macrophages of asbestosis patients, which is dependent on the geranylgeranylation of Cys189 at the C-terminus[278]. More importantly, we observed that upon inhibition of the enzyme that resulted in the failure of Rac1 to be targeted to mitochondria, there was a corresponding significant decrease in the interaction levels between Rac1 and Bcl-2 in the whole cell lysates (**Figure 14**) indicating that the mitochondrial localization, or at least the membrane localization of Rac1, is essential for its interaction with Bcl-2. Indeed, previous results from our laboratory confirmed that Rac1 interacts with Bcl-2 at the outer mitochondrial membranes based on electron microscopic and confocal microscopic analysis, co-immunoprecipitation and GST pull-down assays on different subcellular fractions[70].

Interestingly, Bcl-2 has been shown to interact with another small GTPase Ras and a similar post-translational modification, i.e. farnesylation at the C-terminal CAAX motif (which differs from geranylgeranylation in the non-sterol isoprenoid that is added)[376], is essential for the association in the mitochondria[194]. Raf-1, the serine/threonine kinase downstream of the Ras subfamily of membrane associated small GTPases, has also been reported to associate with Bcl-2 and this helps in the targeting of Raf-1 to the mitochondrial membranes allowing phosphorylation of its targets there, e.g. the BH3 only protein Bad[195]. In addition, another report suggested that Bcl-2 is able to target the serine/threonine phosphatase PP1α to its substrate Bad via a tripartite interaction as well[377]. These findings lead us to

speculate whether the Rac1-Bcl-2 interaction that we reported could aid in the mitochondrial targeting of Rac1 in a similar fashion. However, although the expression levels of Rac1 in the total mitochondrial membranes seem to be independent on Bcl-2 expression (**Figure 12**), the presence of Nox isoforms in the mitochondria (**Figure 19B**), in particular Nox2 since Rac1 is known to be a subunit of the Nox2 complex, still raises the possibility that the microdomain(s) within the mitochondrial membranes where Rac1 resides could be affected via interaction with Bcl-2 thus allowing micro-targeting of Rac1 to site(s) of biological importance so that it could potentially mediate the assembly and activation of Nox complex(es) for O_2^- production. Indeed, previous results from our laboratory (results not published) showed that proteinase K treatment that proteolytically depleted Bcl-2 from the outer mitochondrial membranes also decreased the mitochondrial levels of Rac1 although not completely suggesting that Bcl-2 could have a function in the sequestration of Rac1 in the outer mitochondrial membranes thus changing its localization within the mitochondria.

4.3.2.2 The GTP-bound active form of Rac1 has a greater affinity for Bcl-2

The nucleotide bound status of Rac1 is the second parameter that we have examined when investigating the requirements for its interaction with Bcl-2. Being a small GTPase that acts as a molecular switch, the GTP/GDP cycling of Rac1 is essential in carrying the upstream signals downwards. Based on a variety of methods to manipulate the activation levels of endogenous Rac1 including crude *in vitro* GTP-γS/GDP loading (**Figure 15A**), transient introduction of the dominant negative Rac1N17 mutant (**Figure 16**) as well as the pharmacological inhibition of Rac1 activity with either the 1st generation inhibitor NSC23766 (**Figure 17**) or the 2nd

generation inhibitor EHT1864 (**Figure 18**), we identified that the GTP-bound form of Rac1 that is active, has a significantly higher affinity towards Bcl-2 while the GDP bound inactive form of Rac1 has a minimal affinity. Interestingly, the interaction of Bcl-2 with Ras at the mitochondria, as mentioned in the previous section, also requires an activated GTPase[194].

This finding that active Rac1 has a higher affinity towards Bcl-2 is intriguing since first of all, Rac1, when it is activated, is known to aid in the assembly and activation of the Nox complexes for O_2^- production[59, 60, 273] and this sheds light on the possibility that the Bcl-2-induced pro-oxidant state in the mitochondria could be mediated through its interaction with an activated Rac1. The further observation that the interaction between Rac1 and Bcl-2 is dependent on Nox activity (**Figure 19A**) lends more weight to this hypothesis. Secondly, the essential requirement in the GTP loading for the interaction highlights that the nucleotide binding pocket of Rac1 could be a potential contact site between the two interacting partners, which consists of 1) the two guanine recognition loops (residues 116-119 and residues 158-160); 2) the two phosphate-binding loops (residues 10-17 named as the P-loop, and residues 57-61 including part of the Switch 2); 3) the Switch 1 effector loop region (residues 29-40) that interacts with the ribose and the magnesium ion Mg^{2+}. Moreover, the remarkable reduction in the Rac1-Bcl-2 interaction levels observed in cancer cells exposed to the 1st generation Rac1 inhibitor (that disrupts its interaction with Rac GEFs) also stresses the importance of the groove formed by Switch 1, Switch 2 and β1- β3 strands where the GEFs bind[242, 243].

4.3.2.3 The effector loop region of Rac1, in particular residue 37, is implicated as a

potential binding site with Bcl-2

In an attempt to nail down on the domains/residues of Rac1 involved in its interaction with Bcl-2, we performed a preliminary screening on four point mutants of Rac1, L37F, H40Y, H103A and K166E and all these four mutants are in a constitutively active V12 background. In addition, they are functional mutants as well where L37 is defective in actin cytoskeleton reorganization, H40 is defective in JNK activation, H103 and K166 are both defective in NADPH oxidase activation[103, 329, 330]. Co-immunoprecipitation analysis revealed that L37 mutant had a significantly reduced affinity towards ectopically introduced Bcl-2 in human cervical cancer HeLa cells while the rest three mutants had more or less comparable affinity as compared to Rac1V12 mutant after normalizing for different transfection efficiency (**Figure 20**). This indicates that the benzene ring present in the phenylalanine residue in the wild type Rac1 but lost when mutated to leucine could be somehow essential for the interaction. Interestingly, residue 37 lies in the Switch 1 effector loop region (residues 29-40) that interacts with the magnesium ion Mg^{2+} which stabilizes the binding of guanine nucleotides corroborating our observation discussed in the previous section that GTP-loaded Rac1 had a greater affinity towards Bcl-2 (**Figure 15A-18**). In addition, the groove where Rac1 interacts with Rac GEFs also involves this region[242] and thus it is tempting to speculate that Bcl-2-induced Rac1 activation as we observed (**Figure 3-5**) could be mediated through a more efficient GEF(s) recruitment as a result of the Rac1-Bcl-2 interaction. Furthermore, the docking sites where the pharmacological inhibitor NSC23766 binds on Rac1 that could disrupt its interaction with Bcl-2 (**Figure 17**) include Asp38 and Asn39[243] which are right beside residue 37. All these suggest that the Switch 1 effector region of Rac1 could be

a potential contact site in its interaction with Bcl-2, which awaits further deletional mutation analysis for confirmation. The flexibility of the Switch 1 effector loop is probably important for specificity towards different GEFs to signal distinct downstream functions; therefore, interaction with other proteins at this region[242, 243], in our case with Bcl-2, could potentially in turn alters the conformation of Rac1 and modulates its activity, opening doors to further exploration.

4.3.2.4 The Rac1-Bcl-2 interaction shows a Bcl-2 BH3 domain dependency

After identification of the three critical parameters in Rac1 that are essentially required for its interaction with Bcl-2, namely the geranylgeranylation modification, activation status as well as the Switch 1 effector loop region of Rac1 (**Figure 14-18 & 20**), we went on to characterize the domains/residues in Bcl-2 that are critical for the interaction. Structurally, Bcl-2 possesses four Bcl-2 homology (BH) domains, namely BH1, BH2, BH3 and BH4 domains as well as a carboxyl terminal hydrophobic transmembrane domain (TM) responsible for its membrane localization. The hydrophobic groove present on the surface of the protein that is formed by BH1, BH2 and BH3 domains has been reported to be mostly essential in heterodimerization of Bcl-2 with BH3 domain containing pro-apoptotic family members[128]. However, there are also interesting reports showing that the BH3 domain binding groove of Bcl-2 can interact with non-familial proteins such as Beclin-1 for initiation of autophagy as well as GSH for redox regulation at the mitochondria[223, 378]. On the other hand, the BH4 domain is mostly involved in the interaction of Bcl-2 with other non-homologous proteins including Ras[194], Raf-1[196] and PP2A[186], *etc*. As such, we started off by examining the involvement of BH3 and BH4 domains of Bcl-2 in its interaction with Rac1 using a peptide walking approach. Peptide walking was first

194

utilized to map the functional binding domains between Rac1 and NADPH oxidase, which is a useful tool to study the activity of an interacting complex[271]. Synthetic BH3 domain peptides that are able to sit in the hydrophobic groove of Bcl-2 pro-survival family members and dislodge their pro-apoptotic binding partners, have been widely used to study the homodimerization and heterodimerization within the family and their subsequent effects on apoptosis[155, 158, 304].

Exposure to short stretches of amino acids corresponding to the BH3 domain of Bcl-2 with cell permeable tags resulted in a remarkable disruption in the interaction levels at mitochondrial membranes *in vivo* (**Figure 21**) indicating a BH3 domain dependency for Rac1-Bcl-2 interaction corroborating our previous results using BH3 peptides *in vitro* as well as small-molecule BH3 mimetics *in vivo*[70]. Although the cell permeable Bcl-2 BH4 peptides successfully disrupted the interaction between Bcl-2 and Ras as described by others that Ras-Bcl-2 interaction is BH4 domain dependent[194], there was no change in the Rac1-Bcl-2 interaction observed *in vivo*(**Figure 22**) which is in consistency with our previous results *in vitro*[70] indicating that Bcl-2 BH4 domain is most likely not involved in its interaction with Rac1. Despite the homology between Rac1 and Ras which both fall under the Ras superfamily of small GTPases, the presence of an additional insert region in Rac1 (residues 124-135) distinct from Ras[379] could be a highly probable contributing factor in the domain-specific interaction between Bcl-2 and Ras family GTPases.

4.3.2.5 Phosphorylation status at the flexible loop region of Bcl-2, in particular the

residue Ser70, is critical for its interaction with Rac1

The finding discussed in the previous section that Rac1-Bcl-2 interaction showed a BH3 domain dependency raises the question whether Rac1 would compete with the pro-apoptotic Bcl-2 family proteins, which also bind to the BH3 domain groove of Bcl-2[128]. In our quest to figure out whether or not there is an existence of a competitive binding which could have profound effects for apoptotic signalling, we examined the adjacent region that lies in between BH3 and BH4 domains of Bcl-2, namely the flexible loop region[129]. Based on X-ray crystallographic and nuclear magnetic resonance (NMR) spectroscopic studies on Bcl-xL[129], a putative unstructured loop is also present in Bcl-2 between the first and second helix[128]. In addition, specific residues within that flexible loop, to be specific Thr56, Thr69, Thr74, Ser70 as well as Ser87, are subjective to phosphorylation in response to a variety of stimuli[130-134]. Although the significance of Bcl-2 phosphorylation in the flexible loop region on its anti-apoptotic activity has been controversial, a closer examination on the specific residues being phosphorylated reveals that generally speaking, single site phosphorylation on Ser70 enhances Bcl-2's anti-apoptotic function while multi-site phosphorylation on Thr69, Ser70 and Ser87 leads to both activation/inactivation of Bcl-2 depending on the cellular context[171-174].

As such, we first made use of a triple Bcl-2 mutant T69A/S70A/S87A (AAA) where the respective serines or threonine are replaced by alanines thus it cannot be phosphorylated. Interestingly, the transiently introduced non-phosphorylatable Bcl-2 mutant AAA completely lost its ability to interact with endogenous Rac1 while it still retained the ability to bind endogenous Bax (**Figure 23**). This suggests that although

both Rac1 and Bax associate with the BH3 domain groove of Bcl-2, Rac1 is probably associating with the region of BH3 groove that is closer to the flexible loop region (since phosphorylation status of Thr69, Ser70 and Ser87 are critically required for the interaction) thus it is highly likely that the region where Bax associates with Bcl-2 remain largely unaffected when Rac1 binds Bcl-2. Subsequent experiments attempting to nail down on the exact residue(s) involved revealed that the phosphorylation deficient mutant of Ser70, S70A had a similarly minimal binding affinity towards Bcl-2 while the phosphomimetic mutant S70E had the opposite effect (**Figure 24**) indicating that the phosphorylation status at Ser70 alone is positively correlating with the interaction levels between Bcl-2 and Rac1. These findings are intriguing since single site phosphorylation on Ser70 has been reported to enhance the anti-apoptotic activity of Bcl-2[172, 174] and this leads us to speculate that it could be mediated through its interaction with Rac1, at least partially. Interestingly, studies from other groups have also shown the importance of the phosphorylation status in the loop region of Bcl-2 on its interaction with other proteins such as p53[201] and FKBP38[197-199] leading to modulation of the anti-apoptotic activity of Bcl-2.

4.3.2.6 Crosstalk between Rac1 activation and Bcl-2 phosphorylation at Ser70:

Involvement of the kinase JNK and ROS production

So far we have identified five critical parameters that are required in Rac1-Bcl-2 interaction, namely the geranylgeranylation of Rac1 (**Figure 14**), the activation of Rac1 (**Figure 15A-18**), the Switch 1 effector loop region (in particular residue 37) of Rac1 (**Figure 20**) as well as the BH3 domain groove of Bcl-2 (**Figure 21**) and the phosphorylation of the flexible loop region (in particular Ser70) of Bcl-2 (**Figure 23 & 24**). In order to investigate if there is any cross talk between these parameters, we

started off by checking the link between Rac1 activation and Bcl-2 phosphorylation since one group of the kinases responsible for phosphorylating Bcl-2 at Ser70, JNKs[171, 176, 183-185], are also known to function downstream of Rac1 activation[259, 261]. Indeed, the existence of cross talk between Rac1 and Bcl-2 was identified where active Rac1 can induce the phosphorylation of Bcl-2 at Ser70 and this was confirmed via manipulation of Rac1 activity either through introduction of Rac1V12 or Rac1N17 mutants both transiently (**Figure 26**) and stably (**Figure 25**) or through the pharmacological inhibition of Rac1 (**Figure 27**). A preliminary screening on the kinase involved revealed that pharmacological inhibition of JNK activity resulted in a dose-dependent decrease in the constitutively active Rac1V12-induced Bcl-2 phosphorylation at Ser70 (**Figure 28**), which led to the subsequent disruption of Rac1-Bcl-2 interaction (**Figure 29-30**) emphasizing again on the importance of the phosphorylation status at Ser70 of Bcl-2 for its interaction with Rac1. Together with the results discussed in earlier sections that Bcl-2 overexpression led to Rac1 activation, the identification of the crosstalks between these three parameters, Bcl-2 overexpression, Rac1 activation and Bcl-2 phosphorylation at Ser70, suggest the possibility of the existence of a positive feedback loop in cancer cells with Bcl-2 overexpression which establishes an enhanced interaction between Rac1 and Bcl-2.

Interestingly, phosphorylation levels of Bcl-2 at Ser70 were also decreased with DPI treatment (**Figure 47**) indicating that it could also be redox regulated. The ROS could be coming from Rac1 activation-induced Nox complex activation, which either affect the corresponding kinase(s) or the phosphatase(s). It is well established that JNKs, being among the oxidation-reduction-sensitive mitogen-activated protein kinase (MAPK) members, can be activated through redox changes such as elevated

levels of O_2^- as well as H_2O_2[380-385]. On the other hand, the activity of the serine/threonine protein phosphatase, PP2A (where Ser70 of Bcl-2 is one of its substrates[186-189]), has also been shown to be susceptible to redox changes[386-392]. Indeed, unpublished results from our laboratory provide evidence that PP2A is inactivated through S-nitrosylation mediated by the production of peroxynitrite from O_2^- and No . Taken together, the activation of JNKs and inactivation of PP2A under the pro-oxidant state induced by Bcl-2 could explain the constitutively elevated phosphorylation levels at Ser70 of Bcl-2 itself enhancing its affinity towards Rac1. This also corroborates with the observation that inhibition of Nox activity by DPI resulted in a decrease in the Rac1-Bcl-2 interaction at mitochondrial membranes (**Figure 19A**).

4.4. Functional Implications of the Rac1-Bcl-2 Interaction in Redox Regulation: Clinical Relevance for Targeted Cancer Therapy

4.4.1 Disruption of the Rac1-Bcl-2 Interaction Compromises Bcl-2-induced Pro-oxidant Milieu in Cancer Cells

As discussed earlier, it is well established that Bcl-2 functions as a pro-oxidant[70, 123, 203, 204] and we demonstrated here once again that overexpression of this protein could indeed induce a mild but constitutive elevation in the mitochondrial O_2^- levels in cancer cells (**Figure 1**). On the other hand, the small GTPase Rac1 is also known to be involved in O_2^- production through activating Nox complexes[59, 60, 273]. The fact that there is a physical interaction between these two proteins at the mitochondrial membranes[70] which is confirmed in this thesis as well (**Figure 10 & 14**) makes it tempting to hypothesize that Bcl-2-induced pro-oxidant

state, particularly at the mitochondria, could be mediated through its interaction with Rac1. Indeed, GTP-γS loading that resulted in a dramatic increase in Rac1-Bcl-2 interaction levels (**Figure 15A**) led to a prominent increase in O_2^- levels in the mitochondria of CEM/Bcl-2 cells (**Figure 15B**). Moreover, two approaches that disrupted the interaction between Rac1 and Bcl-2, either through the use of the pharmacological inhibitor of Rac1 NSC23766 (**Figure 17**) or the Bcl-2 BH3 domain peptides (**Figure 21**), both resulted in a significant drop in the mitochondrial O_2^- levels in Bcl-2-overexpressing CEM cells (**Figure 6 & 31**) suggesting that disruption of the interaction led to a compromise in the pro-oxidant state of those cancer cells. Similarly, we have previously reported that transient introduction of the dominant negative Rac1N17, which not only had minimal affinity towards Bcl-2 itself but also remarkably abolished the interaction between endogenous Rac1 and Bcl-2 as shown in **Figure 16**, led to the same compromising effect on the pro-oxidant milieu as well[114]. Whether inhibition of the post-translational geranylgeranylation process by GGTI, that resulted in a significant reduction in Rac1-Bcl-2 interaction (**Figure 14**), also would lead to a compromise in Bcl-2-induced pro-oxidant state remains to be explored. Nonetheless, the suppressing effect of GGTI on O_2^- production by NADPH oxidase was reported. It has also been demonstrated by another group that a reduction in O_2^- production stimulated by constitutively active mutant H-Ras or PDGF or IL-1β was observed following GGTI exposure in pulmonary vascular smooth muscle[393]. In addition, inhibitory effect of GGTI on O_2^- production in LPS-stimulated microglial cells was reported as well[394]. All these findings make it tempting to speculate a similar effect of GGTI on the pro-oxidant state in Bcl-2-overexpressing cancer cells. However, further evidences based on point mutants of either Rac1 (such as L37) or Bcl-2 (such as S70A) with minimal interacting affinity

are still needed to confirm the redox regulatory property of Rac1-Bcl-2 interaction. Nonetheless, the importance of Bcl-2 BH3 domain and the activation status of Rac1 in Bcl-2-mediated pro-oxidant state in cancer cells cannot be overestimated. Interestingly, transient introduction of another pro-survival Bcl-2 family member Bcl-xL (**Figure 2**), which does not interact with Rac1[70], did not alter the intracellular O_2^- levels providing further evidence in favour of our hypothesis.

4.4.2   Overcoming Bcl-2-mediated Chemoresistance in Cancers: Cellular Redox
         Status as a Novel Target

Overexpression of Bcl-2 has been well known as one of the mechanisms for chemoresistance in cancers, be it intrinsic or acquired, which has been associated with poor disease prognosis[123]. This is mainly observed in hematologic malignancies[282]; however recently the list of examples in solid tumours is on the increase as well[283-289]. The failure of conventional chemotherapeutic drugs to induce apoptosis in Bcl-2-overexpressing cancers has urged the need to develop targeted therapy for Bcl-2 specifically in the clinical settings. With regards to this, the emerging role of Bcl-2 as a redox regulator[70, 123, 203, 204] as well as the significance of ROS in cell fate decision[2, 24-32, 47, 82-110, 112-117, 120-122] discussed in previous sections of this thesis, have highlighted the potential of a novel approach that combines the targeting of pro-oxidant Bcl-2 with conventional therapies[123, 290]. To that end, we have utilized treatment regimes that combine sublethal doses of chemotherapeutic drugs currently available in the clinics with the different agents that have all been demonstrated to compromise the pro-oxidant state in Bcl-2-overexpressing cancer cells including the Bcl-2 BH3 domain peptides (**Figure 31**), the pharmacological inhibitor of Rac1 (**Figure 6**) as well as siRNA

targeted specifically at Rac1 to knock down its expression levels[70]. Since both the anti-apoptotic activity of Bcl-2 as well as Rac1 activation are essentially required for survival, in order to observe the synergistic effects, if there are any, we picked up doses of the Bcl-2 BH3 peptides and Rac1 inhibitor to be on the lower end which manifested the blocking effect on mitochondrial O_2^- levels (**Figure 6 & 31A**) but yet had minimal killing effect for the cancer cells (**Figure 7 & 34**). Altogether there were three main combination regimes tested in Bcl-2-overexpressing cells (both in CEM and HeLa): 1) Bcl-2 BH3 peptides with either etoposide or vincristine; 2) Rac1 inhibitor with either etoposide or vincristine or daunorubicin; 3) siRNA targeted at Rac1 with either etoposide or vincristine. Most of these combination therapies resulted in statistically significant reduction in the cell viability (p-values less than 0.05) as compared to drug treatment alone (**Figure 35, 37 & 38**). Peptides with sequence not matching any existing human proteins were also included as a negative control and no change in the cellular response to drugs was observed (**Figure 35C & D**). These findings indicate the existence of synergism when combining conventional DNA damaging (etoposide and daunorubicin)[335, 337] or mitotic inhibiting (vincristine)[334] chemotherapeutic drugs with agents that targeted to compromise Bcl-2's pro-oxidant property. In addition, significant elevation in the sub-G1 population was observed in the BH3 peptides and Rac1 inhibitor combination regimens (**Figure 36 & 39**) indicating that the cancer cells were probably dying through apoptosis as a result of destabilization of the anti-apoptotic activity of Bcl-2 via blocking its pro-oxidant property.

These novel findings shed light on the potential development of combination treatment for cancers that include both the conventional drugs and the targeted

therapies that could manipulate the cellular redox status and in our case here, through blocking the pro-oxidant property of the anti-apoptotic protein Bcl-2. Furthermore, the identification of Rac1-Bcl-2 interaction in patients diagnosed with diffuse B-cell lymphoma, follicular lymphoma and chronic lymphocytic leukaemia[70] but not in noncancerous PBMCs (peripheral blood mononuclear cells) (**Figure 11**) demonstrated the translational relevance of targeting this redox regulating complex for future cancer therapeutics design without incurring much toxicity to normal tissues. Among the five parameters that we have identified to be essential for the Rac1-Bcl-2 interaction as reported in this thesis, the geranylgeranylation of Rac1, the activation status of Rac1 and the BH3 domain of Bcl-2 are all promising targets that could be exploited as means to disrupt the interaction to achieve potential therapeutic outcome. Indeed, one of the BH3 mimetics, ABT-737, which binds to the BH3 domain groove of Bcl-2, is currently in phase II clinical trial[311] and its modified version, ABT-263, with higher oral availability, is now in phase I/II clinical trials as well for the management of various human malignancies including chronic lymphocytic leukaemia (CLL), non-Hodgkin's lymphoma (NHL) and small cell lung cancer[311, 317-319]. The inhibitor for the geranylgeranylation process, GGTI-2418, has also demonstrated promising results both *in vitro* and in animal models and is currently in phase I clinical trial for patients with refractory solid tumours[395]. Although GGTI-2418 is originally developed mainly to treat cancers that are addicted to mutant Ras (where K-Ras and N-Ras undergo alternative geranylgeranylation when farnesylation is inhibited) and the downstream small GTPases in the Ras pathway[395], it would be interesting to investigate its potential usage in Bcl-2-overexpressing cancers vis-a`-vis the effect mediated through Rac1.

4.5. A Computational Approach Based on the Virtual Cancer Platform from ™CELLWORKS Identified Potential Therapeutic Targets for Further Exploration in Human Malignancies with Bcl-2 Overexpression

4.5.1 ™CELLWORKS In Silico Modelling Confirmed the Tumorigenic Nature of Rac1-Bcl-2 Pathway

We have discussed thus far that Bcl-2-induced pro-oxidant state, which contributes towards chemoresistance, could be mediated through its interaction with Rac1. To further assess the functional relevance of this interaction in the cancer context, we carried out computer simulation driven predictive experiments in collaboration with ™CELLWORKS Group Inc.. This is achieved through a virtual platform that mimics the human physiology system which serves as a visualization tool to predict the impact on phenotypes and pathway dynamics upon certain stimuli[339], which in this case here would be the presence or blockage of Rac1-Bcl-2 interaction through manipulating their expression levels. The cell line used is a modelled HCT116 which recapitulates the relevant genetic abnormalities in human colorectal carcinoma. An additional Bcl-2 amplification was created to mimic malignances with Bcl-2 overexpression and this is treated as a base line and a variant cell line with Rac1 overexpression based on the base line was also created (**Figure 40A**). In consistency with the literature findings on the tumorigenic nature of both Rac1 and Bcl-2[126, 259-263, 279-281], it was reflected in the predictive results that the phenotypic indices of angiogenesis, proliferation, viability, metastasis as well as tumor volume are all positively correlated with Bcl-2 and/or Rac1 expression levels (**Figure 40B & C**). Moreover, the pro-oxidant nature of Bcl-2 in inducing an elevated O_2^- levels and the functional involvement of Rac1 in the pro-oxidant intracellular

milieu of Bcl-2-overexpressing cancer cells were also confirmed in the simulated model (**Figure 41**) corroborating our wet lab findings (**Figure 1 & 6**)[70]. Knowing that slightly elevated O_2^- levels have been well demonstrated to contribute to tumourigenesis[24, 47, 83, 84, 97, 103-110, 115], these computer simulated predictions lend further weight to our hypothesis that the pro-oxidant state observed in malignancies with Bcl-2 overexpression could be attributed to its interaction with Rac1 leading to chemoresistance and tumour progression.

4.5.2 STAT3: A Potential Functional Readout for Rac1-Bcl-2 Interaction?

Being inspired by the findings shown earlier that disruption of the Rac1-Bcl-2 interaction, through the pharmacological inhibitor of Rac1, siRNA-mediated silencing of Rac1 or the Bcl-2 BH3 domain peptides, led to sensitization of Bcl-2-overexpressing cancer cells to conventional chemotherapeutic drugs (**Figure 35-39**), we continue to search for potential druggable targets that lie downstream of Rac1-Bcl-2 interaction. A large scale of in silico screening was performed and two potential targets with high hit score for positive correlation to Rac1 and/or Bcl-2 expression levels were identified, which are STAT3, signal transducers and activators of transcription 3, and β-catenin, a subunit of the cadherin protein complex involved in Wnt signaling pathway (**Figure 43**). STAT3 is chosen for the follow-up validation wet lab experiments here not only because STAT3-activated genes are known to promote cell proliferation, survival, angiogenesis and metastasis[348, 350-353, 355] but more importantly due to its documented involvement in mitochondrial respiration, ROS signaling and Rac1 pathways as discussed earlier[87, 89, 344, 345]. Indeed, consistent with what other groups have reported[344], STAT3 was found in the mitochondria (**Figure 44**), where the Rac1-Bcl-2 interacting complex resides. More

intriguingly, the activation levels of mitochondrial STAT3, as marked by the phosphorylation status of Tyr705, were significantly higher in Bcl-2-overrexpressing cancer cells (**Figure 44**) and this Bcl-2-induced STAT3 activation (**Figure 45**) was shown to be mediated through both Rac1 and Nox activities (**Figure 46 & 47**). Knowing that 1) Bcl-2 overexpression could induce Rac1 activation in cancer cells (**Figure 3-4**); 2) STAT3 phosphorylation on Tyr705 can be stimulated with active Rac1 whereas dominant negative Rac1 inhibits STAT3 activation induced by growth factors[345]; 3) ROS have been demonstrated to activate STAT3 through either activating the corresponding kinases[87] and/or inhibiting the phosphatase[89]; it is therefore tempting to hypothesize that in human malignancies with Bcl-2 overexpression, there is a stimulated Rac1 activation and interaction between the two at the mitochondria leading to elevated production of O_2^- that results in STAT3 activation which initiates the downstream transcription of target genes involved in proliferation and survival. Subsequent identification of the existence of physical interactions between each of these three proteins, Rac1, Bcl-2 and STAT3 in Bcl-2-overexpressing cancer cells (**Figure 48**) raised the possibility of a potential tripartite interacting complex involved in translating the signals from intra-mitochondrial redox changes to the transcription of target genes involved in tumourigenesis. However, Rac1, when it is in an active form, has been described to associate with STAT3 via the residue 37 in the Switch 1 effector loop[345], which is also implicated in the Rac1-Bcl-2 interaction (**Figure 20A**). It is unlikely that the two proteins Bcl-2 and STAT3 will bind to the same spot of Rac1 at the same time; thus alternatively, it could be possible that in cancers with Bcl-2 overexpression, the induced GTP loading onto Rac1 causes it to interact with STAT3 and leads to the activation of the latter probably as a result of redox changes or induced conformational change. With regard

to the Bcl-2-STAT3 interaction, whether it has any functional relevance in the whole Rac1-Bcl-2 pathway on redox regulation and chemoresistance requires further exploration.

However, discrepancy between ™CELLWORKS in silico prediction results and wet lab experimental data does exist where the latter demonstrate a correlation between expression levels of Bcl-2 and phosphorylation levels of STAT3 (Tyr705) instead of the total protein levels as predicted through modeling. This could probably be explained by the different cell line models utilized by the virtual prediction and wet lab experiments with the former being HCT116 human colorectal carcinoma cells and the latter being CEM human chronic myeloid leukemia and HeLa human cervical cancer cells. The limitations of modeling on signaling pathways are conceivable by virtual of the heterogenous nature of cancer as a disease and the complexities of biological signaling system. Indeed, based on the feedback from the wet lab experimental data presented in this thesis, optimization of the ™CELLWORKS virtual cancer platform is currently being carried out to incorporate phosphorylation/dephosphorylation pathways for a better representation of the physiological signaling system. Nonethelss, the identification of STAT3 as a potential downstream functional player in Rac1-Bcl-2 pathway through in silico modeling by ™CELLWORKS highlighted a way to screen for targets that have been addicted to in cancers with Bcl-2 overexpression, in a faster and more economical manner. Potential targets that have positive correlation with Bcl-2 are found through in silico simulation and subsequently the effects on cell viability upon inhibition of the identified targets in Bcl-2-overexpressing modelled cell line can be checked in the virtual platform via apoptotic indicators including cleaved active caspases and cleaved PARP (where

PARP is a substrate for active caspase 3)[118, 340, 341]. This is conceptually similar to "synthetic lethality screen". For a given mutation A, if there is an existence of another mutation B which is lethal to the organism when mutation A is present, mutation B is considered as synthetic lethal with mutation A[396]. In our case here, mutation A would be the overexpression of Bcl-2 resulting from the chromosomal translocation and gene fusion[125] and B is the target that we are trying to identify which cancer cells with Bcl-2 mutation are addicted to for survival. The mutation B does not necessary have to be a genetic mutation but instead it could be an inhibition of the protein function with a drug-like small molecule[397]. This approach has been adopted by various studies where they identified small molecules that are selectively synthetic lethal for cancers harbouring a specific oncogenic aberration[398-405].

Furthermore, the identification of STAT3 as a downstream target in Rac1-Bcl-2 interaction in silico followed by the wet lab experimental validation of the association between STAT3 activation and Bcl-2 overexpression (mediated through the activity of Rac1 and Nox) opens up another possible avenue to overcome Bcl-2-induced chemoresistance by targeting STAT3, in addition to the previously suggested BH3 mimetics and geranylgeranyl transferase I inhibitor that are out in clinical trials. Indeed, a dual inhibitor of NF-κB and STAT3, RTA 402, is currently undergoing phase II clinical trial in patients with solid tumours and lymphoid malignancies and another STAT3 inhibitor, OPB-31121, has just entered phase I clinical trial for advanced solid tumours. It would be then interesting to look at their efficacy vis-a`-vis cancers with Bcl-2 overexpression. Further investigation on the potential network among the following three parameters: Bcl-2 overexpression, Rac1 activation and STAT3 activation, in relation to the disease severity and chemoresistance of cancers

would be beneficial in stratifying malignancies where Bcl-2 overexpression presents a great challenge in disease management, which could have tremendous prognostic and therapeutic implications.

CHAPTER 5: CONCLUSION AND FUTURE PERSPECTIVES

Overexpression of the anti-apoptotic protein Bcl-2, is a major hindrance in the therapeutic management of a number of hematopoietic malignancies[282], and recently the list of examples in solid tumours is on the increase as well[283-289]. Both the canonical mechanism of Bcl-2 to prevent the outer mitochondrial membrane permeabilization[124, 126, 137, 152, 155, 156] as well as its non-canonical property as a redox regulator[70, 123, 203, 204], contribute towards chemoresistance[123, 282-289]. The failure of conventional chemotherapeutic drugs to induce apoptosis in Bcl-2-overexpressing cancers has urged the need to develop targeted therapy for Bcl-2 specifically in the clinical settings. Bearing in mind the heterogeneity and complexity of the disease, a strategy that is aimed at targeting the critical circuit that is common and essential would be a better choice. With regards to this, the emerging role of Bcl-2 as a redox regulator[70, 123, 203, 204] as well as the significance of ROS in cell fate decision inevitably observed across a plethora of cancers[2, 24-32, 47, 82-110, 112-117, 120-122], have highlighted the potential of a novel approach that combines the targeting of pro-oxidant Bcl-2 with conventional therapies[123, 290]. To that end, a better understanding on the molecular mechanisms that govern the role of Bcl-2 in inducing a pro-oxidant state will aid in the future therapeutic design.

Here in this study, we demonstrated that Bcl-2-induced pro-oxidant state in the mitochondria of cancer cells is mediated through the activation of the small GTPase Rac1. Subsequently, a physical interaction between these two proteins at the mitochondrial membranes is confirmed and the essential binding domains/residues are characterized, namely 1) the geranylgeranylation of Rac1 at the C-terminal cysteine

residue, which is important for its membrane localization; 2) the GTP loading of Rac1, which turns it on to an active state; 3) the Switch 1 effector loop region (in particular the residue 37), which is critical for the interaction of Rac1 with Rac GEFs for activation; 4) the BH3 domain groove of Bcl-2; 5) the phosphorylation of the flexible loop region (in particular at the residue Ser70) adjacent to BH3 domain, which has been reported to stabilize the anti-apoptotic activity of Bcl-2[172-174]. In addition, the crosstalk between these parameters where Bcl-2 overexpression is capable of inducing Rac1 activation that in turn leads to Bcl-2 phosphorylation at Ser70 through JNK and redox changes, suggests a possible positive feedback loop in enhancing the interaction levels in human malignancies with aberrant Bcl-2. That this interaction is contributing towards Bcl-2-mediated pro-oxidant state and chemoresistance was demonstrated later in the follow-up tests on combination therapies aimed at disrupting the interaction between Bcl-2 and Rac1 together with conventional drugs. Either the pharmacological inhibitor of Rac1 or siRNA-mediated silencing of Rac1 as well as the synthetic Bcl-2 BH3 domain peptides successfully compromised the pro-oxidant state and sensitized Bcl-2-overexpressing cancer cells to routine chemotherapeutic agents including etoposide, vincristine and daunorubicin in chronic myeloid leukaemia and cervical cancer models. To further assess the functional relevance of this interaction in the cancer context, computer simulation driven predictive experiments, in collaboration with ™CELLWORKS Group Inc., confirmed the tumorigenic nature of Rac1-Bcl-2 pathway as reflected by enhanced phenotypic indices of angiogenesis, proliferation, viability, metastasis and tumor volume as well as the pro-oxidant intracellular milieu as indicated by a mild but constitutive elevation in the O_2^- levels upon Bcl-2 and/or Rac1 overexpression, corroborating our wet lab experimental data. Interestingly, the signal transducers and activators of transcription

3, STAT3, was identified in a large scale computer simulation screening to positively correlate with the expression levels of Rac1 and Bcl-2. Indeed, subsequent preliminary wet lab experiments hinted that STAT3 activation could be a functional readout for Rac1-Bcl-2 interaction leading to transcription of downstream target genes involved in proliferation and survival. Our findings that STAT3 activation, as marked by phosphorylation at Tyr705, could be induced by Bcl-2-overexpression (mediated through Rac1 activation and O_2^- production), have opened doors for future exploration on STAT3 as a therapeutic target to overcome Bcl-2-mediated chemoresistance, in addition to inhibition of Rac1 activity and blockage of Bcl-2 BH3 domain groove. The schematic diagram of the working model is shown in Figure 49.

Unlike the conventional chemotherapies that have evolved for more than half a century[6], the development of targeted therapies is still in its infant stage[2]. Our data presented here in the pilot study, revealed for the first time, that the physical interaction between Rac1 and Bcl-2 is the culprit in inducing a pro-oxidant and chemoresistant milieu in human malignancies with Bcl-2-overexpression. We also provided evidence that by disrupting the interaction, the apoptotic execution machinery could be re-activated in those cancer cells upon triggers from clinically available chemotherapeutic agents. These novel findings pave the way for future therapeutic development that combines targeted therapy with conventional drugs, aiming at eradication of cancers harbouring oncogenic Bcl-2.
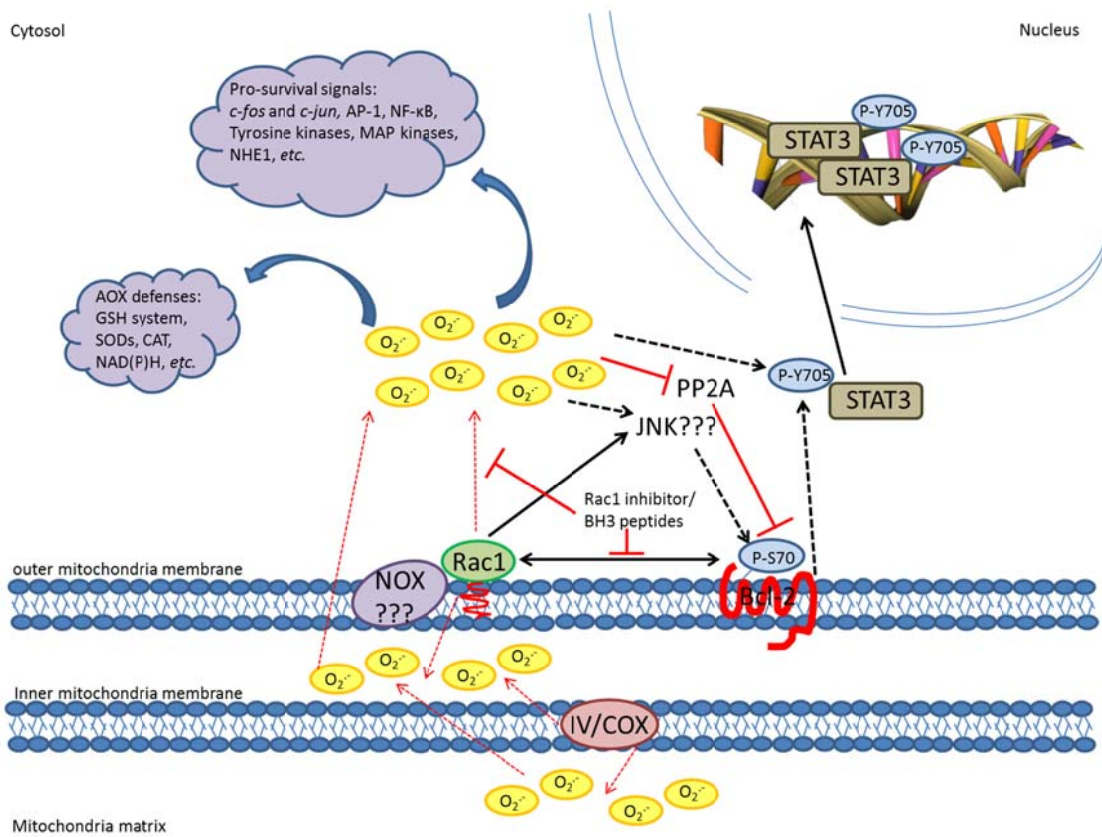
Figure 49: Schematic representation of the working model.

CHAPTER 6: BIBLIOGRAPHY

1. Lim, G.H., K.Y. Chow, and H.P. Lee, *Singapore cancer trends in the last decade.* Singapore medical journal, 2012. **53**(1): p. 3-10.
2. Pervaiz, S., *Anti-cancer drugs of today and tomorrow: are we close to making the turn from treating to curing cancer?* Current pharmaceutical design, 2002. **8**(19): p. 1723-34.
3. Hanahan, D. and R.A. Weinberg, *The hallmarks of cancer.* Cell, 2000. **100**(1): p. 57-70.
4. Iorio, M.V. and C.M. Croce, *MicroRNA dysregulation in cancer: diagnostics, monitoring and therapeutics. A comprehensive review.* EMBO molecular medicine, 2012.
5. Evan, G.I. and K.H. Vousden, *Proliferation, cell cycle and apoptosis in cancer.* Nature, 2001. **411**(6835): p. 342-8.
6. Griswold, D.P., Jr. and S.D. Harrison, Jr., *Tumor models in drug development.* Cancer metastasis reviews, 1991. **10**(3): p. 255-61.
7. Schwartsmann, G. and R.A. Bender, *Vinca alkaloids.* Cancer chemotherapy and biological response modifiers, 1988. **10**: p. 50-6.
8. Rowinsky, E.K., *Current developments in antitumor antibiotics, epipodophyllotoxins, and vinca alkaloids.* Current opinion in oncology, 1991. **3**(6): p. 1060-9.
9. Huizing, M.T., et al., *Taxanes: a new class of antitumor agents.* Cancer investigation, 1995. **13**(4): p. 381-404.
10. Sackett, D.L. and T. Fojo, *Taxanes and other microtubule stabilizing agents.* Cancer chemotherapy and biological response modifiers, 1999. **18**: p. 59-80.
11. Rosowsky, A., *Chemistry and biological activity of antifolates.* Progress in medicinal chemistry, 1989. **26**: p. 1-252.
12. Gready, J.E., *Dihydrofolate reductase: binding of substrates and inhibitors and catalytic mechanism.* Advances in pharmacology and chemotherapy, 1980. **17**: p. 37-102.
13. Hatse, S., E. De Clercq, and J. Balzarini, *Role of antimetabolites of purine and pyrimidine nucleotide metabolism in tumor cell differentiation.* Biochemical pharmacology, 1999. **58**(4): p. 539-55.
14. Reiter, A., et al., *AraC-based pharmacotherapy of chronic myeloid leukaemia.* Expert opinion on pharmacotherapy, 2001. **2**(7): p. 1129-35.
15. Fujita, K. and A. Munakata, *Concentration of 5-fluorouracil in renal cells from cancer patients administered a mixture of 1-(2-tetrahydrofuryl)-5-fluorouracil and uracil.* International journal of clinical pharmacology research, 1991. **11**(4): p. 171-4.
16. Gordaliza, M., et al., *Podophyllotoxin: distribution, sources, applications and new cytotoxic derivatives.* Toxicon : official journal of the International Society on Toxinology, 2004. **44**(4): p. 441-59.
17. Johnson, I.S., et al., *The Vinca Alkaloids: A New Class of Oncolytic Agents.* Cancer research, 1963. **23**: p. 1390-427.
18. Himes, R.H., *Interactions of the catharanthus (Vinca) alkaloids with tubulin and microtubules.* Pharmacology & therapeutics, 1991. **51**(2): p. 257-67.
19. Tan, C., et al., *Daunomycin, an antitumor antibiotic, in the treatment of neoplastic disease. Clinical evaluation with special reference to childhood leukemia.* Cancer, 1967. **20**(3): p. 333-53.

20. Ben-Ishay, Z. and V. Barak, *Bone marrow stromal dysfunction in mice administered cytosine arabinoside.* European journal of haematology, 2001. **66**(4): p. 230-7.

21. Lobert, S., *Neurotoxicity in cancer chemotherapy: vinca alkaloids.* Critical care nurse, 1997. **17**(4): p. 71-9.

22. Moscow, J.A. and K.H. Cowan, *Multidrug resistance.* Journal of the National Cancer Institute, 1988. **80**(1): p. 14-20.

23. Ludwig, W.D., *[Possibilities and limitations of stratified medicine based on biomarkers and targeted therapies in oncology].* Zeitschrift fur Evidenz, Fortbildung und Qualitat im Gesundheitswesen, 2012. **106**(1): p. 11-22.

24. Pervaiz, S. and M.V. Clement, *A permissive apoptotic environment: function of a decrease in intracellular superoxide anion and cytosolic acidification.* Biochemical and biophysical research communications, 2002. **290**(4): p. 1145-50.

25. Ahmad, K.A., et al., *Hydrogen peroxide-mediated cytosolic acidification is a signal for mitochondrial translocation of Bax during drug-induced apoptosis of tumor cells.* Cancer research, 2004. **64**(21): p. 7867-78.

26. Chen, Z.X., R. Velaithan, and S. Pervaiz, *mitoEnergetics and cancer cell fate.* Biochimica et biophysica acta, 2009. **1787**(5): p. 462-7.

27. Pervaiz, S., *Pro-oxidant milieu blunts scissors: insight into tumor progression, drug resistance, and novel druggable targets.* Current pharmaceutical design, 2006. **12**(34): p. 4469-77.

28. Clement, M.V. and S. Pervaiz, *Reactive oxygen intermediates regulate cellular response to apoptotic stimuli: an hypothesis.* Free radical research, 1999. **30**(4): p. 247-52.

29. Pervaiz, S. and M.V. Clement, *Superoxide anion: oncogenic reactive oxygen species?* The international journal of biochemistry & cell biology, 2007. **39**(7-8): p. 1297-304.

30. Pervaiz, S. and M.V. Clement, *Tumor intracellular redox status and drug resistance--serendipity or a causal relationship?* Current pharmaceutical design, 2004. **10**(16): p. 1969-77.

31. Fogg, V.C., N.J. Lanning, and J.P. Mackeigan, *Mitochondria in cancer: at the crossroads of life and death.* Chinese journal of cancer, 2011. **30**(8): p. 526-39.

32. Ray, P.D., B.W. Huang, and Y. Tsuji, *Reactive oxygen species (ROS) homeostasis and redox regulation in cellular signaling.* Cellular signalling, 2012. **24**(5): p. 981-90.

33. Morgan, M.J. and Z.G. Liu, *Crosstalk of reactive oxygen species and NF-kappaB signaling.* Cell research, 2011. **21**(1): p. 103-15.

34. Boveris, A. and B. Chance, *The mitochondrial generation of hydrogen peroxide. General properties and effect of hyperbaric oxygen.* The Biochemical journal, 1973. **134**(3): p. 707-16.

35. Hamanaka, R.B. and N.S. Chandel, *Mitochondrial reactive oxygen species regulate cellular signaling and dictate biological outcomes.* Trends in biochemical sciences, 2010. **35**(9): p. 505-13.

36. Fridovich, I., *The biology of oxygen radicals.* Science, 1978. **201**(4359): p. 875-80.

37. Beckman, J.S. and W.H. Koppenol, *Nitric oxide, superoxide, and peroxynitrite: the good, the bad, and ugly.* The American journal of physiology, 1996. **271**(5 Pt 1): p. C1424-37.

38. Cadenas, E., et al., *Production of superoxide radicals and hydrogen peroxide by NADH-ubiquinone reductase and ubiquinol-cytochrome c reductase from beef-heart mitochondria.* Archives of biochemistry and biophysics, 1977. **180**(2): p. 248-57.

39. Han, D., E. Williams, and E. Cadenas, *Mitochondrial respiratory chain-dependent generation of superoxide anion and its release into the intermembrane space.* The Biochemical journal, 2001. **353**(Pt 2): p. 411-6.

40. St-Pierre, J., et al., *Topology of superoxide production from different sites in the mitochondrial electron transport chain.* The Journal of biological chemistry, 2002. **277**(47): p. 44784-90.

41. Tahara, E.B., F.D. Navarete, and A.J. Kowaltowski, *Tissue-, substrate-, and site-specific characteristics of mitochondrial reactive oxygen species generation.* Free radical biology & medicine, 2009. **46**(9): p. 1283-97.

42. Piskernik, C., et al., *Antimycin A and lipopolysaccharide cause the leakage of superoxide radicals from rat liver mitochondria.* Biochimica et biophysica acta, 2008. **1782**(4): p. 280-5.

43. Brand, M.D., *The sites and topology of mitochondrial superoxide production.* Experimental gerontology, 2010. **45**(7-8): p. 466-72.

44. Starkov, A.A., et al., *Mitochondrial alpha-ketoglutarate dehydrogenase complex generates reactive oxygen species.* The Journal of neuroscience : the official journal of the Society for Neuroscience, 2004. **24**(36): p. 7779-88.

45. Fang, H., et al., *Imaging superoxide flash and metabolism-coupled mitochondrial permeability transition in living animals.* Cell research, 2011. **21**(9): p. 1295-304.

46. Wang, W., et al., *Superoxide flashes in single mitochondria.* Cell, 2008. **134**(2): p. 279-90.

47. Suh, Y.A., et al., *Cell transformation by the superoxide-generating oxidase Mox1.* Nature, 1999. **401**(6748): p. 79-82.

48. Banfi, B., et al., *A mammalian H+ channel generated through alternative splicing of the NADPH oxidase homolog NOH-1.* Science, 2000. **287**(5450): p. 138-42.

49. Kikuchi, H., et al., *NADPH oxidase subunit, gp91(phox) homologue, preferentially expressed in human colon epithelial cells.* Gene, 2000. **254**(1-2): p. 237-43.

50. Banfi, B., et al., *NOX3, a superoxide-generating NADPH oxidase of the inner ear.* The Journal of biological chemistry, 2004. **279**(44): p. 46065-72.

51. Geiszt, M., et al., *Identification of renox, an NAD(P)H oxidase in kidney.* Proceedings of the National Academy of Sciences of the United States of America, 2000. **97**(14): p. 8010-4.

52. Shiose, A., et al., *A novel superoxide-producing NAD(P)H oxidase in kidney.* The Journal of biological chemistry, 2001. **276**(2): p. 1417-23.

53. Yang, S., et al., *A new superoxide-generating oxidase in murine osteoclasts.* The Journal of biological chemistry, 2001. **276**(8): p. 5452-8.

54. Banfi, B., et al., *A Ca(2+)-activated NADPH oxidase in testis, spleen, and lymph nodes.* The Journal of biological chemistry, 2001. **276**(40): p. 37594-601.

55. Cheng, G., et al., *Homologs of gp91phox: cloning and tissue expression of Nox3, Nox4, and Nox5.* Gene, 2001. **269**(1-2): p. 131-40.

56.   Dupuy, C., et al., *Solubilization and characteristics of the thyroid NADPH-dependent H2O2 generating system.* Biochemical and biophysical research communications, 1986. **141**(2): p. 839-46.

57.   De Deken, X., et al., *Cloning of two human thyroid cDNAs encoding new members of the NADPH oxidase family.* The Journal of biological chemistry, 2000. **275**(30): p. 23227-33.

58.   Dupuy, C., et al., *Purification of a novel flavoprotein involved in the thyroid NADPH oxidase. Cloning of the porcine and human cdnas.* The Journal of biological chemistry, 1999. **274**(52): p. 37265-9.

59.   Brown, D.I. and K.K. Griendling, *Nox proteins in signal transduction.* Free radical biology & medicine, 2009. **47**(9): p. 1239-53.

60.   Lambeth, J.D., *NOX enzymes and the biology of reactive oxygen.* Nature reviews. Immunology, 2004. **4**(3): p. 181-9.

61.   Leto, T.L. and M. Geiszt, *Role of Nox family NADPH oxidases in host defense.* Antioxidants & redox signaling, 2006. **8**(9-10): p. 1549-61.

62.   Oakley, F.D., et al., *Signaling components of redox active endosomes: the redoxosomes.* Antioxidants & redox signaling, 2009. **11**(6): p. 1313-33.

63.   Ushio-Fukai, M., *Localizing NADPH oxidase-derived ROS.* Science's STKE : signal transduction knowledge environment, 2006. **2006**(349): p. re8.

64.   Mumbengegwi, D.R., et al., *Evidence for a superoxide permeability pathway in endosomal membranes.* Molecular and cellular biology, 2008. **28**(11): p. 3700-12.

65.   Kuroda, J., et al., *The superoxide-producing NAD(P)H oxidase Nox4 in the nucleus of human vascular endothelial cells.* Genes to cells : devoted to molecular & cellular mechanisms, 2005. **10**(12): p. 1139-51.

66.   Ambasta, R.K., et al., *Direct interaction of the novel Nox proteins with p22phox is required for the formation of a functionally active NADPH oxidase.* The Journal of biological chemistry, 2004. **279**(44): p. 45935-41.

67.   Block, K., Y. Gorin, and H.E. Abboud, *Subcellular localization of Nox4 and regulation in diabetes.* Proceedings of the National Academy of Sciences of the United States of America, 2009. **106**(34): p. 14385-90.

68.   Kuroda, J., et al., *NADPH oxidase 4 (Nox4) is a major source of oxidative stress in the failing heart.* Proceedings of the National Academy of Sciences of the United States of America, 2010. **107**(35): p. 15565-70.

69.   Ago, T., et al., *Upregulation of Nox4 by hypertrophic stimuli promotes apoptosis and mitochondrial dysfunction in cardiac myocytes.* Circulation research, 2010. **106**(7): p. 1253-64.

70.   Velaithan, R., et al., *The small GTPase Rac1 is a novel binding partner of Bcl-2 and stabilizes its antiapoptotic activity.* Blood, 2011. **117**(23): p. 6214-26.

71.   Hilenski, L.L., et al., *Distinct subcellular localizations of Nox1 and Nox4 in vascular smooth muscle cells.* Arteriosclerosis, thrombosis, and vascular biology, 2004. **24**(4): p. 677-83.

72.   Jezek, P. and L. Hlavata, *Mitochondria in homeostasis of reactive oxygen species in cell, tissues, and organism.* The international journal of biochemistry & cell biology, 2005. **37**(12): p. 2478-503.

73.   Li, J.M. and A.M. Shah, *ROS generation by nonphagocytic NADPH oxidase: potential relevance in diabetic nephropathy.* Journal of the American Society of Nephrology : JASN, 2003. **14**(8 Suppl 3): p. S221-6.

74. Duchen, M.R., *Mitochondria in health and disease: perspectives on a new mitochondrial biology.* Molecular aspects of medicine, 2004. **25**(4): p. 365-451.

75. Patenaude, A., M.R. Ven Murthy, and M.E. Mirault, *Mitochondrial thioredoxin system: effects of TrxR2 overexpression on redox balance, cell growth, and apoptosis.* The Journal of biological chemistry, 2004. **279**(26): p. 27302-14.

76. Ahsan, M.K., et al., *Redox regulation of cell survival by the thioredoxin superfamily: an implication of redox gene therapy in the heart.* Antioxidants & redox signaling, 2009. **11**(11): p. 2741-58.

77. He, C., et al., *Mitochondrial Cu,Zn-superoxide dismutase mediates pulmonary fibrosis by augmenting H2O2 generation.* The Journal of biological chemistry, 2011. **286**(17): p. 15597-607.

78. Kira, Y., E.F. Sato, and M. Inoue, *Association of Cu,Zn-type superoxide dismutase with mitochondria and peroxisomes.* Archives of biochemistry and biophysics, 2002. **399**(1): p. 96-102.

79. Naik, E. and V.M. Dixit, *Mitochondrial reactive oxygen species drive proinflammatory cytokine production.* The Journal of experimental medicine, 2011. **208**(3): p. 417-20.

80. Hwang, A.B. and S.J. Lee, *Regulation of life span by mitochondrial respiration: the HIF-1 and ROS connection.* Aging, 2011. **3**(3): p. 304-10.

81. Wallace, D.C., *Mitochondria and cancer: Warburg addressed.* Cold Spring Harbor symposia on quantitative biology, 2005. **70**: p. 363-74.

82. Burdon, R.H., V. Gill, and C. Rice-Evans, *Cell proliferation and oxidative stress.* Free radical research communications, 1989. **7**(3-6): p. 149-59.

83. Burdon, R.H., *Control of cell proliferation by reactive oxygen species.* Biochemical Society transactions, 1996. **24**(4): p. 1028-32.

84. Burdon, R.H., *Superoxide and hydrogen peroxide in relation to mammalian cell proliferation.* Free radical biology & medicine, 1995. **18**(4): p. 775-94.

85. Sauer, H., M. Wartenberg, and J. Hescheler, *Reactive oxygen species as intracellular messengers during cell growth and differentiation.* Cellular physiology and biochemistry : international journal of experimental cellular physiology, biochemistry, and pharmacology, 2001. **11**(4): p. 173-86.

86. Heffetz, D., et al., *The insulinomimetic agents H2O2 and vanadate stimulate protein tyrosine phosphorylation in intact cells.* The Journal of biological chemistry, 1990. **265**(5): p. 2896-902.

87. Simon, A.R., et al., *Activation of the JAK-STAT pathway by reactive oxygen species.* The American journal of physiology, 1998. **275**(6 Pt 1): p. C1640-52.

88. Qin, S. and P.B. Chock, *Implication of phosphatidylinositol 3-kinase membrane recruitment in hydrogen peroxide-induced activation of PI3K and Akt.* Biochemistry, 2003. **42**(10): p. 2995-3003.

89. Lee, J.K., et al., *NADPH oxidase promotes pancreatic cancer cell survival via inhibiting JAK2 dephosphorylation by tyrosine phosphatases.* Gastroenterology, 2007. **133**(5): p. 1637-48.

90. Droge, W., *Free radicals in the physiological control of cell function.* Physiological reviews, 2002. **82**(1): p. 47-95.

91. Kretz-Remy, C., et al., *Inhibition of I kappa B-alpha phosphorylation and degradation and subsequent NF-kappa B activation by glutathione peroxidase overexpression.* The Journal of cell biology, 1996. **133**(5): p. 1083-93.

92. Kretz-Remy, C., E.E. Bates, and A.P. Arrigo, *Amino acid analogs activate NF-kappaB through redox-dependent IkappaB-alpha degradation by the proteasome without apparent IkappaB-alpha phosphorylation. Consequence on HIV-1 long terminal repeat activation.* The Journal of biological chemistry, 1998. **273**(6): p. 3180-91.

93. Barrett, W.C., et al., *Regulation of PTP1B via glutathionylation of the active site cysteine 215.* Biochemistry, 1999. **38**(20): p. 6699-705.

94. Xu, D., Rovira, II, and T. Finkel, *Oxidants painting the cysteine chapel: redox regulation of PTPs.* Developmental cell, 2002. **2**(3): p. 251-2.

95. Shibanuma, M., T. Kuroki, and K. Nose, *Superoxide as a signal for increase in intracellular pH.* Journal of cellular physiology, 1988. **136**(2): p. 379-83.

96. Cerutti, P.A., *Prooxidant states and tumor promotion.* Science, 1985. **227**(4685): p. 375-81.

97. Kumar, B., et al., *Oxidative stress is inherent in prostate cancer cells and is required for aggressive phenotype.* Cancer research, 2008. **68**(6): p. 1777-85.

98. Weydert, C., et al., *Suppression of the malignant phenotype in human pancreatic cancer cells by the overexpression of manganese superoxide dismutase.* Molecular cancer therapeutics, 2003. **2**(4): p. 361-9.

99. Cullen, J.J., et al., *The role of manganese superoxide dismutase in the growth of pancreatic adenocarcinoma.* Cancer research, 2003. **63**(6): p. 1297-303.

100. Zhao, Y., et al., *Overexpression of manganese superoxide dismutase suppresses tumor formation by modulation of activator protein-1 signaling in a multistage skin carcinogenesis model.* Cancer research, 2001. **61**(16): p. 6082-8.

101. Oberley, L.W., *Anticancer therapy by overexpression of superoxide dismutase.* Antioxidants & redox signaling, 2001. **3**(3): p. 461-72.

102. Darby Weydert, C.J., et al., *Inhibition of oral cancer cell growth by adenovirusMnSOD plus BCNU treatment.* Free radical biology & medicine, 2003. **34**(3): p. 316-29.

103. Pervaiz, S., et al., *Activation of the RacGTPase inhibits apoptosis in human tumor cells.* Oncogene, 2001. **20**(43): p. 6263-8.

104. Clement, M.V. and I. Stamenkovic, *Superoxide anion is a natural inhibitor of FAS-mediated cell death.* The EMBO journal, 1996. **15**(2): p. 216-25.

105. Hampton, M.B. and S. Orrenius, *Dual regulation of caspase activity by hydrogen peroxide: implications for apoptosis.* FEBS letters, 1997. **414**(3): p. 552-6.

106. Mannick, J.B., X.Q. Miao, and J.S. Stamler, *Nitric oxide inhibits Fas-induced apoptosis.* The Journal of biological chemistry, 1997. **272**(39): p. 24125-8.

107. Pervaiz, S., et al., *Superoxide anion inhibits drug-induced tumor cell death.* FEBS letters, 1999. **459**(3): p. 343-8.

108. Clement, M.V., S. Sivarajah, and S. Pervaiz, *Production of intracellular superoxide mediates dithiothreitol-dependent inhibition of apoptotic cell death.* Antioxidants & redox signaling, 2005. **7**(3-4): p. 456-64.

109. Clement, M.V., A. Ponton, and S. Pervaiz, *Apoptosis induced by hydrogen peroxide is mediated by decreased superoxide anion concentration and reduction of intracellular milieu.* FEBS letters, 1998. **440**(1-2): p. 13-8.

110. Clement, M.V. and S. Pervaiz, *Intracellular superoxide and hydrogen peroxide concentrations: a critical balance that determines survival or death.* Redox report : communications in free radical research, 2001. **6**(4): p. 211-4.

111. Dixon, S.J., et al., *Ferroptosis: an iron-dependent form of nonapoptotic cell death.* Cell, 2012. **149**(5): p. 1060-72.

112. Hockenbery, D.M., et al., *Bcl-2 functions in an antioxidant pathway to prevent apoptosis.* Cell, 1993. **75**(2): p. 241-51.

113. Hampton, M.B., B. Fadeel, and S. Orrenius, *Redox regulation of the caspases during apoptosis.* Annals of the New York Academy of Sciences, 1998. **854**: p. 328-35.

114. Clement, M.V., J.L. Hirpara, and S. Pervaiz, *Decrease in intracellular superoxide sensitizes Bcl-2-overexpressing tumor cells to receptor and drug-induced apoptosis independent of the mitochondria.* Cell death and differentiation, 2003. **10**(11): p. 1273-85.

115. Lin, K.I., et al., *Decreased intracellular superoxide levels activate Sindbis virus-induced apoptosis.* The Journal of biological chemistry, 1999. **274**(19): p. 13650-5.

116. Sen, C.K., *Cellular thiols and redox-regulated signal transduction.* Current topics in cellular regulation, 2000. **36**: p. 1-30.

117. Nicholson, D.W., et al., *Identification and inhibition of the ICE/CED-3 protease necessary for mammalian apoptosis.* Nature, 1995. **376**(6535): p. 37-43.

118. Thornberry, N.A., *Caspases: key mediators of apoptosis.* Chemistry & biology, 1998. **5**(5): p. R97-103.

119. Thornberry, N.A., *Interleukin-1 beta converting enzyme.* Methods in enzymology, 1994. **244**: p. 615-31.

120. Yamakawa, H., et al., *Activation of caspase-9 and -3 during H2O2-induced apoptosis of PC12 cells independent of ceramide formation.* Neurological research, 2000. **22**(6): p. 556-64.

121. Akram, S., et al., *Reactive oxygen species-mediated regulation of the Na+-H+ exchanger 1 gene expression connects intracellular redox status with cells' sensitivity to death triggers.* Cell death and differentiation, 2006. **13**(4): p. 628-41.

122. Kumar, A.P., et al., *Oxidative repression of NHE1 gene expression involves iron-mediated caspase activity.* Cell death and differentiation, 2007. **14**(10): p. 1733-46.

123. Low, I.C., J. Kang, and S. Pervaiz, *Bcl-2: a prime regulator of mitochondrial redox metabolism in cancer cells.* Antioxidants & redox signaling, 2011. **15**(12): p. 2975-87.

124. Tsujimoto, Y., et al., *Involvement of the bcl-2 gene in human follicular lymphoma.* Science, 1985. **228**(4706): p. 1440-3.

125. Cleary, M.L., S.D. Smith, and J. Sklar, *Cloning and structural analysis of cDNAs for bcl-2 and a hybrid bcl-2/immunoglobulin transcript resulting from the t(14;18) translocation.* Cell, 1986. **47**(1): p. 19-28.

126. Reed, J.C., et al., *Oncogenic potential of bcl-2 demonstrated by gene transfer.* Nature, 1988. **336**(6196): p. 259-61.

127. Krajewski, S., et al., *Investigation of the subcellular distribution of the bcl-2 oncoprotein: residence in the nuclear envelope, endoplasmic reticulum, and outer mitochondrial membranes.* Cancer research, 1993. **53**(19): p. 4701-14.

128. Petros, A.M., et al., *Solution structure of the antiapoptotic protein bcl-2.* Proceedings of the National Academy of Sciences of the United States of America, 2001. **98**(6): p. 3012-7.

129. Muchmore, S.W., et al., *X-ray and NMR structure of human Bcl-xL, an inhibitor of programmed cell death.* Nature, 1996. **381**(6580): p. 335-41.

130. Bassik, M.C., et al., *Phosphorylation of BCL-2 regulates ER Ca2+ homeostasis and apoptosis.* The EMBO journal, 2004. **23**(5): p. 1207-16.

131. Basu, A., G. DuBois, and S. Haldar, *Posttranslational modifications of Bcl2 family members--a potential therapeutic target for human malignancy.* Frontiers in bioscience : a journal and virtual library, 2006. **11**: p. 1508-21.

132. Breitschopf, K., et al., *Posttranslational modification of Bcl-2 facilitates its proteasome-dependent degradation: molecular characterization of the involved signaling pathway.* Molecular and cellular biology, 2000. **20**(5): p. 1886-96.

133. Chang, B.S., et al., *Identification of a novel regulatory domain in Bcl-X(L) and Bcl-2.* The EMBO journal, 1997. **16**(5): p. 968-77.

134. Pattingre, S., et al., *Role of JNK1-dependent Bcl-2 phosphorylation in ceramide-induced macroautophagy.* The Journal of biological chemistry, 2009. **284**(5): p. 2719-28.

135. Strasser, A., *The role of BH3-only proteins in the immune system.* Nature reviews. Immunology, 2005. **5**(3): p. 189-200.

136. Youle, R.J. and A. Strasser, *The BCL-2 protein family: opposing activities that mediate cell death.* Nature reviews. Molecular cell biology, 2008. **9**(1): p. 47-59.

137. Johnstone, R.W., A.A. Ruefli, and S.W. Lowe, *Apoptosis: a link between cancer genetics and chemotherapy.* Cell, 2002. **108**(2): p. 153-64.

138. Antonsson, B., et al., *Inhibition of Bax channel-forming activity by Bcl-2.* Science, 1997. **277**(5324): p. 370-2.

139. Minn, A.J., et al., *Bcl-x(L) forms an ion channel in synthetic lipid membranes.* Nature, 1997. **385**(6614): p. 353-7.

140. Schendel, S.L., et al., *Channel formation by antiapoptotic protein Bcl-2.* Proceedings of the National Academy of Sciences of the United States of America, 1997. **94**(10): p. 5113-8.

141. Sattler, M., et al., *Structure of Bcl-xL-Bak peptide complex: recognition between regulators of apoptosis.* Science, 1997. **275**(5302): p. 983-6.

142. Wei, M.C., et al., *Proapoptotic BAX and BAK: a requisite gateway to mitochondrial dysfunction and death.* Science, 2001. **292**(5517): p. 727-30.

143. Brenner, C., et al., *Bcl-2 and Bax regulate the channel activity of the mitochondrial adenine nucleotide translocator.* Oncogene, 2000. **19**(3): p. 329-36.

144. Zamzami, N. and G. Kroemer, *The mitochondrion in apoptosis: how Pandora's box opens.* Nature reviews. Molecular cell biology, 2001. **2**(1): p. 67-71.

145. Shi, Y., et al., *Identification of the protein-protein contact site and interaction mode of human VDAC1 with Bcl-2 family proteins.* Biochemical and biophysical research communications, 2003. **305**(4): p. 989-96.

146. Vander Heiden, M.G. and C.B. Thompson, *Bcl-2 proteins: regulators of apoptosis or of mitochondrial homeostasis?* Nature cell biology, 1999. **1**(8): p. E209-16.

147. Shimizu, S., M. Narita, and Y. Tsujimoto, *Bcl-2 family proteins regulate the release of apoptogenic cytochrome c by the mitochondrial channel VDAC.* Nature, 1999. **399**(6735): p. 483-7.

148. Vander Heiden, M.G., et al., *Bcl-xL promotes the open configuration of the voltage-dependent anion channel and metabolite passage through the outer mitochondrial membrane.* The Journal of biological chemistry, 2001. **276**(22): p. 19414-9.

149. Zong, W.X., et al., *BH3-only proteins that bind pro-survival Bcl-2 family members fail to induce apoptosis in the absence of Bax and Bak.* Genes & development, 2001. **15**(12): p. 1481-6.

150. Oda, E., et al., *Noxa, a BH3-only member of the Bcl-2 family and candidate mediator of p53-induced apoptosis.* Science, 2000. **288**(5468): p. 1053-8.

151. Nakano, K. and K.H. Vousden, *PUMA, a novel proapoptotic gene, is induced by p53.* Molecular cell, 2001. **7**(3): p. 683-94.

152. Zha, J., et al., *Serine phosphorylation of death agonist BAD in response to survival factor results in binding to 14-3-3 not BCL-X(L).* Cell, 1996. **87**(4): p. 619-28.

153. Puthalakath, H., et al., *Bmf: a proapoptotic BH3-only protein regulated by interaction with the myosin V actin motor complex, activated by anoikis.* Science, 2001. **293**(5536): p. 1829-32.

154. Puthalakath, H., et al., *The proapoptotic activity of the Bcl-2 family member Bim is regulated by interaction with the dynein motor complex.* Molecular cell, 1999. **3**(3): p. 287-96.

155. Letai, A., et al., *Distinct BH3 domains either sensitize or activate mitochondrial apoptosis, serving as prototype cancer therapeutics.* Cancer cell, 2002. **2**(3): p. 183-92.

156. Kuwana, T., et al., *BH3 domains of BH3-only proteins differentially regulate Bax-mediated mitochondrial membrane permeabilization both directly and indirectly.* Molecular cell, 2005. **17**(4): p. 525-35.

157. Zhu, Y., et al., *Constitutive association of the proapoptotic protein Bim with Bcl-2-related proteins on mitochondria in T cells.* Proceedings of the National Academy of Sciences of the United States of America, 2004. **101**(20): p. 7681-6.

158. Willis, S.N., et al., *Apoptosis initiated when BH3 ligands engage multiple Bcl-2 homologs, not Bax or Bak.* Science, 2007. **315**(5813): p. 856-9.

159. Willis, S.N. and J.M. Adams, *Life in the balance: how BH3-only proteins induce apoptosis.* Current opinion in cell biology, 2005. **17**(6): p. 617-25.

160. Walsh, G. and R. Jefferis, *Post-translational modifications in the context of therapeutic proteins.* Nature biotechnology, 2006. **24**(10): p. 1241-52.

161. Kutuk, O. and A. Letai, *Regulation of Bcl-2 family proteins by posttranslational modifications.* Current molecular medicine, 2008. **8**(2): p. 102-18.

162. Blagosklonny, M.V., *Unwinding the loop of Bcl-2 phosphorylation.* Leukemia : official journal of the Leukemia Society of America, Leukemia Research Fund, U.K, 2001. **15**(6): p. 869-74.

163. Matsuyoshi, S., et al., *Bcl-2 phosphorylation has pathological significance in human breast cancer.* Pathobiology : journal of immunopathology, molecular and cellular biology, 2006. **73**(4): p. 205-12.

164. Jordan, M.A. and L. Wilson, *Microtubules and actin filaments: dynamic targets for cancer chemotherapy.* Current opinion in cell biology, 1998. **10**(1): p. 123-30.

165. Scatena, C.D., et al., *Mitotic phosphorylation of Bcl-2 during normal cell cycle progression and Taxol-induced growth arrest.* The Journal of biological chemistry, 1998. **273**(46): p. 30777-84.

166. Blagosklonny, M.V., et al., *Taxol-induced apoptosis and phosphorylation of Bcl-2 protein involves c-Raf-1 and represents a novel c-Raf-1 signal transduction pathway.* Cancer research, 1996. **56**(8): p. 1851-4.

167. Blagosklonny, M.V., et al., *Raf-1/bcl-2 phosphorylation: a step from microtubule damage to cell death.* Cancer research, 1997. **57**(1): p. 130-5.

168. Haldar, S., A. Basu, and C.M. Croce, *Bcl2 is the guardian of microtubule integrity.* Cancer research, 1997. **57**(2): p. 229-33.

169. Barboule, N., I. Truchet, and A. Valette, *Localization of phosphorylated forms of Bcl-2 in mitosis: co-localization with Ki-67 and nucleolin in nuclear structures and on mitotic chromosomes.* Cell cycle, 2005. **4**(4): p. 590-6.

170. Ling, Y.H., C. Tornos, and R. Perez-Soler, *Phosphorylation of Bcl-2 is a marker of M phase events and not a determinant of apoptosis.* The Journal of biological chemistry, 1998. **273**(30): p. 18984-91.

171. Yamamoto, K., H. Ichijo, and S.J. Korsmeyer, *BCL-2 is phosphorylated and inactivated by an ASK1/Jun N-terminal protein kinase pathway normally activated at G(2)/M.* Molecular and cellular biology, 1999. **19**(12): p. 8469-78.

172. Ito, T., et al., *Bcl-2 phosphorylation required for anti-apoptosis function.* The Journal of biological chemistry, 1997. **272**(18): p. 11671-3.

173. May, W.S., et al., *Interleukin-3 and bryostatin-1 mediate hyperphosphorylation of BCL2 alpha in association with suppression of apoptosis.* The Journal of biological chemistry, 1994. **269**(43): p. 26865-70.

174. Deng, X., et al., *Mono- and multisite phosphorylation enhances Bcl2's antiapoptotic function and inhibition of cell cycle entry functions.* Proceedings of the National Academy of Sciences of the United States of America, 2004. **101**(1): p. 153-8.

175. Pathan, N., et al., *Microtubule-targeting drugs induce bcl-2 phosphorylation and association with Pin1.* Neoplasia, 2001. **3**(6): p. 550-9.

176. Fan, M., et al., *Vinblastine-induced phosphorylation of Bcl-2 and Bcl-XL is mediated by JNK and occurs in parallel with inactivation of the Raf-1/MEK/ERK cascade.* The Journal of biological chemistry, 2000. **275**(39): p. 29980-5.

177. Calastretti, A., et al., *Damaged microtubules can inactivate BCL-2 by means of the mTOR kinase.* Oncogene, 2001. **20**(43): p. 6172-80.

178. Srivastava, R.K., et al., *Involvement of microtubules in the regulation of Bcl2 phosphorylation and apoptosis through cyclic AMP-dependent protein kinase.* Molecular and cellular biology, 1998. **18**(6): p. 3509-17.

179. Deng, X., et al., *Survival function of ERK1/2 as IL-3-activated, staurosporine-resistant Bcl2 kinases.* Proceedings of the National Academy of Sciences of the United States of America, 2000. **97**(4): p. 1578-83.

180. Deng, X., et al., *Regulation of Bcl2 phosphorylation and potential significance for leukemic cell chemoresistance.* Journal of the National Cancer Institute. Monographs, 2001(28): p. 30-7.

181. Ruvolo, P.P., X. Deng, and W.S. May, *Phosphorylation of Bcl2 and regulation of apoptosis.* Leukemia : official journal of the Leukemia Society of America, Leukemia Research Fund, U.K, 2001. **15**(4): p. 515-22.

182. Ruvolo, P.P., et al., *A functional role for mitochondrial protein kinase Calpha in Bcl2 phosphorylation and suppression of apoptosis.* The Journal of biological chemistry, 1998. **273**(39): p. 25436-42.

183. Maundrell, K., et al., *Bcl-2 undergoes phosphorylation by c-Jun N-terminal kinase/stress-activated protein kinases in the presence of the constitutively active GTP-binding protein Rac1.* The Journal of biological chemistry, 1997. **272**(40): p. 25238-42.

184. Wang, T.H., et al., *Microtubule-interfering agents activate c-Jun N-terminal kinase/stress-activated protein kinase through both Ras and apoptosis signal-regulating kinase pathways.* The Journal of biological chemistry, 1998. **273**(9): p. 4928-36.

185. Thomas, A., T. Giesler, and E. White, *p53 mediates bcl-2 phosphorylation and apoptosis via activation of the Cdc42/JNK1 pathway.* Oncogene, 2000. **19**(46): p. 5259-69.

186. Deng, X., F. Gao, and W.S. May, *Protein phosphatase 2A inactivates Bcl2's antiapoptotic function by dephosphorylation and up-regulation of Bcl2-p53 binding.* Blood, 2009. **113**(2): p. 422-8.

187. Ruvolo, P.P., et al., *Ceramide induces Bcl2 dephosphorylation via a mechanism involving mitochondrial PP2A.* The Journal of biological chemistry, 1999. **274**(29): p. 20296-300.

188. Deng, X., et al., *Reversible phosphorylation of Bcl2 following interleukin 3 or bryostatin 1 is mediated by direct interaction with protein phosphatase 2A.* The Journal of biological chemistry, 1998. **273**(51): p. 34157-63.

189. Ray, R.M., S. Bhattacharya, and L.R. Johnson, *Protein phosphatase 2A regulates apoptosis in intestinal epithelial cells.* The Journal of biological chemistry, 2005. **280**(35): p. 31091-100.

190. Brichese, L., G. Cazettes, and A. Valette, *JNK is associated with Bcl-2 and PP1 in mitochondria: paclitaxel induces its activation and its association with the phosphorylated form of Bcl-2.* Cell cycle, 2004. **3**(10): p. 1312-9.

191. Poommipanit, P.B., B. Chen, and Z.N. Oltvai, *Interleukin-3 induces the phosphorylation of a distinct fraction of bcl-2.* The Journal of biological chemistry, 1999. **274**(2): p. 1033-9.

192. Bos, J.L., *ras oncogenes in human cancer: a review.* Cancer research, 1989. **49**(17): p. 4682-9.

193. Downward, J., *Ras signalling and apoptosis.* Current opinion in genetics & development, 1998. **8**(1): p. 49-54.

194. Denis, G.V., et al., *Bcl-2, via its BH4 domain, blocks apoptotic signaling mediated by mitochondrial Ras.* The Journal of biological chemistry, 2003. **278**(8): p. 5775-85.

195. Wang, H.G., U.R. Rapp, and J.C. Reed, *Bcl-2 targets the protein kinase Raf-1 to mitochondria.* Cell, 1996. **87**(4): p. 629-38.

196. Jin, S., et al., *p21-activated Kinase 1 (Pak1)-dependent phosphorylation of Raf-1 regulates its mitochondrial localization, phosphorylation of BAD, and Bcl-2 association.* The Journal of biological chemistry, 2005. **280**(26): p. 24698-705.

197. Shirane, M. and K.I. Nakayama, *Inherent calcineurin inhibitor FKBP38 targets Bcl-2 to mitochondria and inhibits apoptosis.* Nature cell biology, 2003. **5**(1): p. 28-37.

198. Kang, C.B., et al., *Molecular characterization of FK-506 binding protein 38 and its potential regulatory role on the anti-apoptotic protein Bcl-2.* Biochemical and biophysical research communications, 2005. **337**(1): p. 30-8.

199. Kang, C.B., et al., *The flexible loop of Bcl-2 is required for molecular interaction with immunosuppressant FK-506 binding protein 38 (FKBP38).* FEBS letters, 2005. **579**(6): p. 1469-76.

200. Marchenko, N.D., A. Zaika, and U.M. Moll, *Death signal-induced localization of p53 protein to mitochondria. A potential role in apoptotic signaling.* The Journal of biological chemistry, 2000. **275**(21): p. 16202-12.

201. Deng, X., et al., *Bcl2's flexible loop domain regulates p53 binding and survival.* Molecular and cellular biology, 2006. **26**(12): p. 4421-34.

202. Lin, B., et al., *Conversion of Bcl-2 from protector to killer by interaction with nuclear orphan receptor Nur77/TR3.* Cell, 2004. **116**(4): p. 527-40.

203. Chen, Z.X. and S. Pervaiz, *Bcl-2 induces pro-oxidant state by engaging mitochondrial respiration in tumor cells.* Cell death and differentiation, 2007. **14**(9): p. 1617-27.

204. Chen, Z.X. and S. Pervaiz, *Involvement of cytochrome c oxidase subunits Va and Vb in the regulation of cancer cell metabolism by Bcl-2.* Cell death and differentiation, 2010. **17**(3): p. 408-20.

205. Chen, S.R., D.D. Dunigan, and M.B. Dickman, *Bcl-2 family members inhibit oxidative stress-induced programmed cell death in Saccharomyces cerevisiae.* Free radical biology & medicine, 2003. **34**(10): p. 1315-25.

206. Kane, D.J., et al., *Bcl-2 inhibition of neural death: decreased generation of reactive oxygen species.* Science, 1993. **262**(5137): p. 1274-7.

207. Mirkovic, N., et al., *Resistance to radiation-induced apoptosis in Bcl-2-expressing cells is reversed by depleting cellular thiols.* Oncogene, 1997. **15**(12): p. 1461-70.

208. Myers, K.M., et al., *Bcl-2 protects neural cells from cyanide/aglycemia-induced lipid oxidation, mitochondrial injury, and loss of viability.* Journal of neurochemistry, 1995. **65**(6): p. 2432-40.

209. Zamzami, N., et al., *The thiol crosslinking agent diamide overcomes the apoptosis-inhibitory effect of Bcl-2 by enforcing mitochondrial permeability transition.* Oncogene, 1998. **16**(8): p. 1055-63.

210. Tyurina, Y.Y., et al., *Direct evidence for antioxidant effect of Bcl-2 in PC12 rat pheochromocytoma cells.* Archives of biochemistry and biophysics, 1997. **344**(2): p. 413-23.

211. Bruce-Keller, A.J., et al., *Bcl-2 protects isolated plasma and mitochondrial membranes against lipid peroxidation induced by hydrogen peroxide and amyloid beta-peptide.* Journal of neurochemistry, 1998. **70**(1): p. 31-9.

212. Lee, M., et al., *Effect of overexpression of wild-type and mutant Cu/Zn-superoxide dismutases on oxidative stress and cell death induced by hydrogen peroxide, 4-hydroxynonenal or serum deprivation: potentiation of injury by ALS-related mutant superoxide dismutases and protection by Bcl-2.* Journal of neurochemistry, 2001. **78**(2): p. 209-20.

213. Hochman, A., et al., *Enhanced oxidative stress and altered antioxidants in brains of Bcl-2-deficient mice.* Journal of neurochemistry, 1998. **71**(2): p. 741-8.

214. Hochman, A., et al., *Developmental changes in antioxidant enzymes and oxidative damage in kidneys, liver and brain of bcl-2 knockout mice.* Cellular and molecular biology, 2000. **46**(1): p. 41-52.

215. Lee, M., et al., *Effect of overexpression of BCL-2 on cellular oxidative damage, nitric oxide production, antioxidant defenses, and the proteasome.* Free radical biology & medicine, 2001. **31**(12): p. 1550-9.

216. Chen, Z.X. and S. Pervaiz, *BCL-2: pro-or anti-oxidant?* Frontiers in bioscience, 2009. **1**: p. 263-8.

217. Ellerby, L.M., et al., *Shift of the cellular oxidation-reduction potential in neural cells expressing Bcl-2.* Journal of neurochemistry, 1996. **67**(3): p. 1259-67.

218. Kowaltowski, A.J. and G. Fiskum, *Redox mechanisms of cytoprotection by Bcl-2.* Antioxidants & redox signaling, 2005. **7**(3-4): p. 508-14.

219. Kowaltowski, A.J., A.E. Vercesi, and G. Fiskum, *Bcl-2 prevents mitochondrial permeability transition and cytochrome c release via maintenance of reduced pyridine nucleotides.* Cell death and differentiation, 2000. **7**(10): p. 903-10.

220. Papadopoulos, M.C., et al., *Potentiation of murine astrocyte antioxidant defence by bcl-2: protection in part reflects elevated glutathione levels.* The European journal of neuroscience, 1998. **10**(4): p. 1252-60.

221. Rudin, C.M., et al., *Inhibition of glutathione synthesis reverses Bcl-2-mediated cisplatin resistance.* Cancer research, 2003. **63**(2): p. 312-8.

222. Jang, J.H. and Y.J. Surh, *Potentiation of cellular antioxidant capacity by Bcl-2: implications for its antiapoptotic function.* Biochemical pharmacology, 2003. **66**(8): p. 1371-9.

223. Zimmermann, A.K., et al., *Glutathione binding to the Bcl-2 homology-3 domain groove: a molecular basis for Bcl-2 antioxidant function at mitochondria.* The Journal of biological chemistry, 2007. **282**(40): p. 29296-304.

224. Vieira, H.L., et al., *Permeabilization of the mitochondrial inner membrane during apoptosis: impact of the adenine nucleotide translocator.* Cell death and differentiation, 2000. **7**(12): p. 1146-54.

225. Steinman, H.M., *The Bcl-2 oncoprotein functions as a pro-oxidant.* The Journal of biological chemistry, 1995. **270**(8): p. 3487-90.

226. Armstrong, J.S. and D.P. Jones, *Glutathione depletion enforces the mitochondrial permeability transition and causes cell death in Bcl-2 overexpressing HL60 cells.* FASEB journal : official publication of the Federation of American Societies for Experimental Biology, 2002. **16**(10): p. 1263-5.

227. Esposti, M.D., et al., *Bcl-2 and mitochondrial oxygen radicals. New approaches with reactive oxygen species-sensitive probes.* The Journal of biological chemistry, 1999. **274**(42): p. 29831-7.

228. Kowaltowski, A.J., et al., *Effect of Bcl-2 overexpression on mitochondrial structure and function.* The Journal of biological chemistry, 2002. **277**(45): p. 42802-7.

229. Low, I.C., Z.X. Chen, and S. Pervaiz, *Bcl-2 modulates resveratrol-induced ROS production by regulating mitochondrial respiration in tumor cells.* Antioxidants & redox signaling, 2010. **13**(6): p. 807-19.

230. Campian, J.L., et al., *Cytochrome C oxidase activity and oxygen tolerance.* The Journal of biological chemistry, 2007. **282**(17): p. 12430-8.

231. Lambert, A.J. and M.D. Brand, *Inhibitors of the quinone-binding site allow rapid superoxide production from mitochondrial NADH:ubiquinone*

oxidoreductase (complex I). The Journal of biological chemistry, 2004. **279**(38): p. 39414-20.

232. Takai, Y., T. Sasaki, and T. Matozaki, *Small GTP-binding proteins.* Physiological reviews, 2001. **81**(1): p. 153-208.

233. Wennerberg, K. and C.J. Der, *Rho-family GTPases: it's not only Rac and Rho (and I like it).* Journal of cell science, 2004. **117**(Pt 8): p. 1301-12.

234. Van Aelst, L. and C. D'Souza-Schorey, *Rho GTPases and signaling networks.* Genes & development, 1997. **11**(18): p. 2295-322.

235. Nobes, C.D. and A. Hall, *Rho, rac, and cdc42 GTPases regulate the assembly of multimolecular focal complexes associated with actin stress fibers, lamellipodia, and filopodia.* Cell, 1995. **81**(1): p. 53-62.

236. Ridley, A.J., *Rho family proteins: coordinating cell responses.* Trends in cell biology, 2001. **11**(12): p. 471-7.

237. Didsbury, J., et al., *rac, a novel ras-related family of proteins that are botulinum toxin substrates.* The Journal of biological chemistry, 1989. **264**(28): p. 16378-82.

238. Chan, A.Y., et al., *Roles of the Rac1 and Rac3 GTPases in human tumor cell invasion.* Oncogene, 2005. **24**(53): p. 7821-9.

239. Haataja, L., J. Groffen, and N. Heisterkamp, *Characterization of RAC3, a novel member of the Rho family.* The Journal of biological chemistry, 1997. **272**(33): p. 20384-8.

240. Jordan, P., et al., *Cloning of a novel human Rac1b splice variant with increased expression in colorectal tumors.* Oncogene, 1999. **18**(48): p. 6835-9.

241. Schnelzer, A., et al., *Rac1 in human breast cancer: overexpression, mutation analysis, and characterization of a new isoform, Rac1b.* Oncogene, 2000. **19**(26): p. 3013-20.

242. Hirshberg, M., et al., *The crystal structure of human rac1, a member of the rho-family complexed with a GTP analogue.* Nature structural biology, 1997. **4**(2): p. 147-52.

243. Nassar, N., et al., *Structure-function based design of small molecule inhibitors targeting Rho family GTPases.* Current topics in medicinal chemistry, 2006. **6**(11): p. 1109-16.

244. Lanning, C.C., et al., *The Rac1 C-terminal polybasic region regulates the nuclear localization and protein degradation of Rac1.* The Journal of biological chemistry, 2004. **279**(42): p. 44197-210.

245. Williams, C.L., *The polybasic region of Ras and Rho family small GTPases: a regulator of protein interactions and membrane association and a site of nuclear localization signal sequences.* Cellular signalling, 2003. **15**(12): p. 1071-80.

246. Kreck, M.L., et al., *Membrane association of Rac is required for high activity of the respiratory burst oxidase.* Biochemistry, 1996. **35**(49): p. 15683-92.

247. Del Pozo, M.A., et al., *Integrins regulate GTP-Rac localized effector interactions through dissociation of Rho-GDI.* Nature cell biology, 2002. **4**(3): p. 232-9.

248. Konstantinopoulos, P.A., M.V. Karamouzis, and A.G. Papavassiliou, *Post-translational modifications and regulation of the RAS superfamily of GTPases as anticancer targets.* Nature reviews. Drug discovery, 2007. **6**(7): p. 541-55.

249. Navarro-Lerida, I., et al., *A palmitoylation switch mechanism regulates Rac1 function and membrane organization.* The EMBO journal, 2012. **31**(3): p. 534-51.

250. Welch, H.C., et al., *Phosphoinositide 3-kinase-dependent activation of Rac.* FEBS letters, 2003. **546**(1): p. 93-7.

251. Etienne-Manneville, S. and A. Hall, *Rho GTPases in cell biology.* Nature, 2002. **420**(6916): p. 629-35.

252. Rossman, K.L., C.J. Der, and J. Sondek, *GEF means go: turning on RHO GTPases with guanine nucleotide-exchange factors.* Nature reviews. Molecular cell biology, 2005. **6**(2): p. 167-80.

253. Bishop, A.L. and A. Hall, *Rho GTPases and their effector proteins.* The Biochemical journal, 2000. **348 Pt 2**: p. 241-55.

254. Hordijk, P.L., et al., *Inhibition of invasion of epithelial cells by Tiam1-Rac signaling.* Science, 1997. **278**(5342): p. 1464-6.

255. Han, J., et al., *Lck regulates Vav activation of members of the Rho family of GTPases.* Molecular and cellular biology, 1997. **17**(3): p. 1346-53.

256. Worthylake, D.K., K.L. Rossman, and J. Sondek, *Crystal structure of Rac1 in complex with the guanine nucleotide exchange region of Tiam1.* Nature, 2000. **408**(6813): p. 682-8.

257. Gao, Y., et al., *Trp(56) of rac1 specifies interaction with a subset of guanine nucleotide exchange factors.* The Journal of biological chemistry, 2001. **276**(50): p. 47530-41.

258. Karnoub, A.E., et al., *Molecular basis for Rac1 recognition by guanine nucleotide exchange factors.* Nature structural biology, 2001. **8**(12): p. 1037-41.

259. Aznar, S. and J.C. Lacal, *Rho signals to cell growth and apoptosis.* Cancer letters, 2001. **165**(1): p. 1-10.

260. Evers, E.E., et al., *Rho-like GTPases in tumor cell invasion.* Methods in enzymology, 2000. **325**: p. 403-15.

261. Kwei, K.A., et al., *The role of Rac1 in maintaining malignant phenotype of mouse skin tumor cells.* Cancer letters, 2006. **231**(2): p. 326-38.

262. Irani, K., et al., *Mitogenic signaling mediated by oxidants in Ras-transformed fibroblasts.* Science, 1997. **275**(5306): p. 1649-52.

263. Irani, K. and P.J. Goldschmidt-Clermont, *Ras, superoxide and signal transduction.* Biochemical pharmacology, 1998. **55**(9): p. 1339-46.

264. Diekmann, D., et al., *Interaction of Rac with p67phox and regulation of phagocytic NADPH oxidase activity.* Science, 1994. **265**(5171): p. 531-3.

265. Babior, B.M., *NADPH oxidase: an update.* Blood, 1999. **93**(5): p. 1464-76.

266. Groemping, Y. and K. Rittinger, *Activation and assembly of the NADPH oxidase: a structural perspective.* The Biochemical journal, 2005. **386**(Pt 3): p. 401-16.

267. Dinauer, M.C., *Regulation of neutrophil function by Rac GTPases.* Current opinion in hematology, 2003. **10**(1): p. 8-15.

268. Nisimoto, Y., et al., *The p67(phox) activation domain regulates electron flow from NADPH to flavin in flavocytochrome b(558).* The Journal of biological chemistry, 1999. **274**(33): p. 22999-3005.

269. Freeman, J.L., A. Abo, and J.D. Lambeth, *Rac "insert region" is a novel effector region that is implicated in the activation of NADPH oxidase, but not PAK65.* The Journal of biological chemistry, 1996. **271**(33): p. 19794-801.

270. Kwong, C.H., et al., *Regulation of the human neutrophil NADPH oxidase by rho-related G-proteins.* Biochemistry, 1993. **32**(21): p. 5711-7.

271. Joseph, G. and E. Pick, *"Peptide walking" is a novel method for mapping functional domains in proteins. Its application to the Rac1-dependent*

activation of NADPH oxidase. The Journal of biological chemistry, 1995. **270**(49): p. 29079-82.

272. Sundaresan, M., et al., *Regulation of reactive-oxygen-species generation in fibroblasts by Rac1.* The Biochemical journal, 1996. **318 (Pt 2)**: p. 379-82.

273. Ueyama, T., M. Geiszt, and T.L. Leto, *Involvement of Rac1 in activation of multicomponent Nox1- and Nox3-based NADPH oxidases.* Molecular and cellular biology, 2006. **26**(6): p. 2160-74.

274. Cheng, G. and J.D. Lambeth, *NOXO1, regulation of lipid binding, localization, and activation of Nox1 by the Phox homology (PX) domain.* The Journal of biological chemistry, 2004. **279**(6): p. 4737-42.

275. Bokoch, G.M. and B.A. Diebold, *Current molecular models for NADPH oxidase regulation by Rac GTPase.* Blood, 2002. **100**(8): p. 2692-6.

276. Boivin, D. and R. Beliveau, *Subcellular distribution and membrane association of Rho-related small GTP-binding proteins in kidney cortex.* The American journal of physiology, 1995. **269**(2 Pt 2): p. F180-9.

277. Kowluru, A., H.Q. Chen, and M. Tannous, *Novel roles for the rho subfamily of GTP-binding proteins in succinate-induced insulin secretion from betaTC3 cells: further evidence in support of the succinate mechanism of insulin release.* Endocrine research, 2003. **29**(3): p. 363-76.

278. Osborn-Heaford, H.L., et al., *Mitochondrial Rac1 GTPase import and electron transfer from cytochrome c are required for pulmonary fibrosis.* The Journal of biological chemistry, 2012. **287**(5): p. 3301-12.

279. McDonnell, T.J., et al., *bcl-2-immunoglobulin transgenic mice demonstrate extended B cell survival and follicular lymphoproliferation.* Cell, 1989. **57**(1): p. 79-88.

280. Sentman, C.L., et al., *bcl-2 inhibits multiple forms of apoptosis but not negative selection in thymocytes.* Cell, 1991. **67**(5): p. 879-88.

281. Cox, A.G. and M.B. Hampton, *Bcl-2 over-expression promotes genomic instability by inhibiting apoptosis of cells exposed to hydrogen peroxide.* Carcinogenesis, 2007. **28**(10): p. 2166-71.

282. Kitada, S., et al., *Dysregulation of apoptosis genes in hematopoietic malignancies.* Oncogene, 2002. **21**(21): p. 3459-74.

283. Tang, L., et al., *Expression of apoptosis regulators in cutaneous malignant melanoma.* Clinical cancer research : an official journal of the American Association for Cancer Research, 1998. **4**(8): p. 1865-71.

284. Du, J., et al., *Resistance to apoptosis of HPV 16-infected laryngeal cancer cells is associated with decreased Bak and increased Bcl-2 expression.* Cancer letters, 2004. **205**(1): p. 81-8.

285. Beenken, S.W. and K.I. Bland, *Biomarkers for breast cancer.* Minerva chirurgica, 2002. **57**(4): p. 437-48.

286. Mitsudomi, T. and T. Takahashi, *[Genetic abnormalities in lung cancer and their prognostic implications].* Gan to kagaku ryoho. Cancer & chemotherapy, 1996. **23**(8): p. 990-6.

287. Ghaneh, P., et al., *Molecular prognostic markers in pancreatic cancer.* Journal of hepato-biliary-pancreatic surgery, 2002. **9**(1): p. 1-11.

288. Reed, J.C., *Mechanisms of Bcl-2 family protein function and dysfunction in health and disease.* Behring Institute Mitteilungen, 1996(97): p. 72-100.

289. McDonnell, T.J., et al., *Expression of the protooncogene bcl-2 in the prostate and its association with emergence of androgen-independent prostate cancer.* Cancer research, 1992. **52**(24): p. 6940-4.

290. Hartman, M.L. and M. Czyz, *Pro-apoptotic Activity of BH3-only Proteins and BH3 Mimetics: from Theory to Potential Cancer Therapy.* Anti-cancer agents in medicinal chemistry, 2012.

291. Chi, K.C., et al., *Effects of Bcl-2 modulation with G3139 antisense oligonucleotide on human breast cancer cells are independent of inherent Bcl-2 protein expression.* Breast cancer research and treatment, 2000. **63**(3): p. 199-212.

292. Ramanarayanan, J., et al., *Pro-apoptotic therapy with the oligonucleotide Genasense (oblimersen sodium) targeting Bcl-2 protein expression enhances the biological anti-tumour activity of rituximab.* British journal of haematology, 2004. **127**(5): p. 519-30.

293. O'Connor, O.A., et al., *The combination of the proteasome inhibitor bortezomib and the bcl-2 antisense molecule oblimersen sensitizes human B-cell lymphomas to cyclophosphamide.* Clinical cancer research : an official journal of the American Association for Cancer Research, 2006. **12**(9): p. 2902-11.

294. Waters, J.S., et al., *Phase I clinical and pharmacokinetic study of bcl-2 antisense oligonucleotide therapy in patients with non-Hodgkin's lymphoma.* Journal of clinical oncology : official journal of the American Society of Clinical Oncology, 2000. **18**(9): p. 1812-23.

295. Rudin, C.M., et al., *Phase I study of G3139, a bcl-2 antisense oligonucleotide, combined with carboplatin and etoposide in patients with small-cell lung cancer.* Journal of clinical oncology : official journal of the American Society of Clinical Oncology, 2004. **22**(6): p. 1110-7.

296. Tolcher, A.W., *Targeting Bcl-2 protein expression in solid tumors and hematologic malignancies with antisense oligonucleotides.* Clinical advances in hematology & oncology : H&O, 2005. **3**(8): p. 635-42, 662.

297. Pro, B., et al., *Phase II multicenter study of oblimersen sodium, a Bcl-2 antisense oligonucleotide, in combination with rituximab in patients with recurrent B-cell non-Hodgkin lymphoma.* British journal of haematology, 2008. **143**(3): p. 355-60.

298. O'Brien, S., et al., *Randomized phase III trial of fludarabine plus cyclophosphamide with or without oblimersen sodium (Bcl-2 antisense) in patients with relapsed or refractory chronic lymphocytic leukemia.* Journal of clinical oncology : official journal of the American Society of Clinical Oncology, 2007. **25**(9): p. 1114-20.

299. Bedikian, A.Y., et al., *Bcl-2 antisense (oblimersen sodium) plus dacarbazine in patients with advanced melanoma: the Oblimersen Melanoma Study Group.* Journal of clinical oncology : official journal of the American Society of Clinical Oncology, 2006. **24**(29): p. 4738-45.

300. Gjertsen, B.T., et al., *Bcl-2 antisense in the treatment of human malignancies: a delusion in targeted therapy.* Current pharmaceutical biotechnology, 2007. **8**(6): p. 373-81.

301. Neuzil, J., et al., *Induction of cancer cell apoptosis by alpha-tocopheryl succinate: molecular pathways and structural requirements.* FASEB journal : official publication of the Federation of American Societies for Experimental Biology, 2001. **15**(2): p. 403-15.

302. Shangary, S. and D.E. Johnson, *Peptides derived from BH3 domains of Bcl-2 family members: a comparative analysis of inhibition of Bcl-2, Bcl-x(L) and*

Bax oligomerization, induction of cytochrome c release, and activation of cell death. Biochemistry, 2002. **41**(30): p. 9485-95.

303. Walensky, L.D., et al., *Activation of apoptosis in vivo by a hydrocarbon-stapled BH3 helix.* Science, 2004. **305**(5689): p. 1466-70.

304. Vieira, H.L., et al., *Cell permeable BH3-peptides overcome the cytoprotective effect of Bcl-2 and Bcl-X(L).* Oncogene, 2002. **21**(13): p. 1963-77.

305. Goldsmith, K.C., et al., *BH3 peptidomimetics potently activate apoptosis and demonstrate single agent efficacy in neuroblastoma.* Oncogene, 2006. **25**(33): p. 4525-33.

306. Li, R., et al., *Targeting antiapoptotic Bcl-2 family members with cell-permeable BH3 peptides induces apoptosis signaling and death in head and neck squamous cell carcinoma cells.* Neoplasia, 2007. **9**(10): p. 801-11.

307. Verhaegen, M., et al., *A novel BH3 mimetic reveals a mitogen-activated protein kinase-dependent mechanism of melanoma cell death controlled by p53 and reactive oxygen species.* Cancer research, 2006. **66**(23): p. 11348-59.

308. Mohammad, R.M., et al., *Preclinical studies of TW-37, a new nonpeptidic small-molecule inhibitor of Bcl-2, in diffuse large cell lymphoma xenograft model reveal drug action on both Bcl-2 and Mcl-1.* Clinical cancer research : an official journal of the American Association for Cancer Research, 2007. **13**(7): p. 2226-35.

309. Al-Katib, A.M., et al., *SMI of Bcl-2 TW-37 is active across a spectrum of B-cell tumors irrespective of their proliferative and differentiation status.* Journal of hematology & oncology, 2009. **2**: p. 8.

310. Wang, Z., et al., *TW-37, a small-molecule inhibitor of Bcl-2, inhibits cell growth and invasion in pancreatic cancer.* International journal of cancer. Journal international du cancer, 2008. **123**(4): p. 958-66.

311. Azmi, A.S. and R.M. Mohammad, *Non-peptidic small molecule inhibitors against Bcl-2 for cancer therapy.* Journal of cellular physiology, 2009. **218**(1): p. 13-21.

312. van Delft, M.F., et al., *The BH3 mimetic ABT-737 targets selective Bcl-2 proteins and efficiently induces apoptosis via Bak/Bax if Mcl-1 is neutralized.* Cancer cell, 2006. **10**(5): p. 389-99.

313. Vogler, M., et al., *A novel paradigm for rapid ABT-737-induced apoptosis involving outer mitochondrial membrane rupture in primary leukemia and lymphoma cells.* Cell death and differentiation, 2008. **15**(5): p. 820-30.

314. Konopleva, M., et al., *Mechanisms of apoptosis sensitivity and resistance to the BH3 mimetic ABT-737 in acute myeloid leukemia.* Cancer cell, 2006. **10**(5): p. 375-88.

315. Del Gaizo Moore, V., et al., *BCL-2 dependence and ABT-737 sensitivity in acute lymphoblastic leukemia.* Blood, 2008. **111**(4): p. 2300-9.

316. Del Gaizo Moore, V., et al., *Chronic lymphocytic leukemia requires BCL2 to sequester prodeath BIM, explaining sensitivity to BCL2 antagonist ABT-737.* The Journal of clinical investigation, 2007. **117**(1): p. 112-21.

317. Roberts, A.W., et al., *Substantial susceptibility of chronic lymphocytic leukemia to BCL2 inhibition: results of a phase I study of navitoclax in patients with relapsed or refractory disease.* Journal of clinical oncology : official journal of the American Society of Clinical Oncology, 2012. **30**(5): p. 488-96.

318. Gandhi, L., et al., *Phase I study of Navitoclax (ABT-263), a novel Bcl-2 family inhibitor, in patients with small-cell lung cancer and other solid tumors.*

Journal of clinical oncology : official journal of the American Society of Clinical Oncology, 2011. **29**(7): p. 909-16.

319. Wilson, W.H., et al., *Navitoclax, a targeted high-affinity inhibitor of BCL-2, in lymphoid malignancies: a phase 1 dose-escalation study of safety, pharmacokinetics, pharmacodynamics, and antitumour activity.* The lancet oncology, 2010. **11**(12): p. 1149-59.

320. Chonghaile, T.N. and A. Letai, *Mimicking the BH3 domain to kill cancer cells.* Oncogene, 2008. **27 Suppl 1**: p. S149-57.

321. Howard, A.N., et al., *ABT-737, a BH3 mimetic, induces glutathione depletion and oxidative stress.* Cancer chemotherapy and pharmacology, 2009. **65**(1): p. 41-54.

322. Chen, Z.X. and S. Pervaiz, *Bcl-2 induces pro-oxidant state by engaging mitochondrial respiration in tumor cells.* Cell death and differentiation, 2012. **19**(3): p. 551.

323. Li, Y., et al., *Validation of lucigenin (bis-N-methylacridinium) as a chemilumigenic probe for detecting superoxide anion radical production by enzymatic and cellular systems.* The Journal of biological chemistry, 1998. **273**(4): p. 2015-23.

324. Mosmann, T., *Rapid colorimetric assay for cellular growth and survival: application to proliferation and cytotoxicity assays.* Journal of immunological methods, 1983. **65**(1-2): p. 55-63.

325. Wiedenmann, J., F. Oswald, and G.U. Nienhaus, *Fluorescent proteins for live cell imaging: opportunities, limitations, and challenges.* IUBMB life, 2009. **61**(11): p. 1029-42.

326. Campbell, R.E., et al., *A monomeric red fluorescent protein.* Proceedings of the National Academy of Sciences of the United States of America, 2002. **99**(12): p. 7877-82.

327. Pellegrin, S. and H. Mellor, *Rho GTPase activation assays.* Current protocols in cell biology / editorial board, Juan S. Bonifacino ... [et al.], 2008. **Chapter 14**: p. Unit 14 8.

328. Shutes, A., et al., *Specificity and mechanism of action of EHT 1864, a novel small molecule inhibitor of Rac family small GTPases.* The Journal of biological chemistry, 2007. **282**(49): p. 35666-78.

329. Joneson, T. and D. Bar-Sagi, *A Rac1 effector site controlling mitogenesis through superoxide production.* The Journal of biological chemistry, 1998. **273**(29): p. 17991-4.

330. Toporik, A., et al., *Mutational analysis of novel effector domains in Rac1 involved in the activation of nicotinamide adenine dinucleotide phosphate (reduced) oxidase.* Biochemistry, 1998. **37**(20): p. 7147-56.

331. Denicourt, C. and S.F. Dowdy, *Medicine. Targeting apoptotic pathways in cancer cells.* Science, 2004. **305**(5689): p. 1411-3.

332. Musti, A.M., M. Treier, and D. Bohmann, *Reduced ubiquitin-dependent degradation of c-Jun after phosphorylation by MAP kinases.* Science, 1997. **275**(5298): p. 400-2.

333. Bennett, B.L., et al., *SP600125, an anthrapyrazolone inhibitor of Jun N-terminal kinase.* Proceedings of the National Academy of Sciences of the United States of America, 2001. **98**(24): p. 13681-6.

334. Groninger, E., et al., *Vincristine induced apoptosis in acute lymphoblastic leukaemia cells: a mitochondrial controlled pathway regulated by reactive oxygen species?* International journal of oncology, 2002. **21**(6): p. 1339-45.

335. Karpinich, N.O., et al., *The course of etoposide-induced apoptosis from damage to DNA and p53 activation to mitochondrial release of cytochrome c.* The Journal of biological chemistry, 2002. **277**(19): p. 16547-52.

336. De Souza, C.P. and S.A. Osmani, *Mitosis, not just open or closed.* Eukaryotic cell, 2007. **6**(9): p. 1521-7.

337. Laurent, G. and J.P. Jaffrezou, *Signaling pathways activated by daunorubicin.* Blood, 2001. **98**(4): p. 913-24.

338. Hamilton, A.J. and D.C. Baulcombe, *A species of small antisense RNA in posttranscriptional gene silencing in plants.* Science, 1999. **286**(5441): p. 950-2.

339. Barve, A., et al., *A kinetic platform for in silico modeling of the metabolic dynamics in Escherichia coli.* Advances and applications in bioinformatics and chemistry : AABC, 2010. **3**: p. 97-110.

340. Ha, H.C. and S.H. Snyder, *Poly(ADP-ribose) polymerase-1 in the nervous system.* Neurobiology of disease, 2000. **7**(4): p. 225-39.

341. Godon, C., et al., *PARP inhibition versus PARP-1 silencing: different outcomes in terms of single-strand break repair and radiation susceptibility.* Nucleic acids research, 2008. **36**(13): p. 4454-64.

342. Neeper, M., et al., *Cloning and expression of a cell surface receptor for advanced glycosylation end products of proteins.* The Journal of biological chemistry, 1992. **267**(21): p. 14998-5004.

343. Gilmore, T.D., *Introduction to NF-kappaB: players, pathways, perspectives.* Oncogene, 2006. **25**(51): p. 6680-4.

344. Wegrzyn, J., et al., *Function of mitochondrial Stat3 in cellular respiration.* Science, 2009. **323**(5915): p. 793-7.

345. Simon, A.R., et al., *Regulation of STAT3 by direct binding to the Rac1 GTPase.* Science, 2000. **290**(5489): p. 144-7.

346. MacDonald, B.T., K. Tamai, and X. He, *Wnt/beta-catenin signaling: components, mechanisms, and diseases.* Developmental cell, 2009. **17**(1): p. 9-26.

347. Heinrich, P.C., et al., *Interleukin-6-type cytokine signalling through the gp130/Jak/STAT pathway.* The Biochemical journal, 1998. **334 (Pt 2)**: p. 297-314.

348. Leeman, R.J., V.W. Lui, and J.R. Grandis, *STAT3 as a therapeutic target in head and neck cancer.* Expert opinion on biological therapy, 2006. **6**(3): p. 231-41.

349. Quesnelle, K.M., A.L. Boehm, and J.R. Grandis, *STAT-mediated EGFR signaling in cancer.* Journal of cellular biochemistry, 2007. **102**(2): p. 311-9.

350. Frank, D.A., *STAT3 as a central mediator of neoplastic cellular transformation.* Cancer letters, 2007. **251**(2): p. 199-210.

351. Germain, D. and D.A. Frank, *Targeting the cytoplasmic and nuclear functions of signal transducers and activators of transcription 3 for cancer therapy.* Clinical cancer research : an official journal of the American Association for Cancer Research, 2007. **13**(19): p. 5665-9.

352. Jing, N. and D.J. Tweardy, *Targeting Stat3 in cancer therapy.* Anti-cancer drugs, 2005. **16**(6): p. 601-7.

353. Johnston, P.A. and J.R. Grandis, *STAT3 signaling: anticancer strategies and challenges.* Molecular interventions, 2011. **11**(1): p. 18-26.

354. Aggarwal, B.B., et al., *Signal transducer and activator of transcription-3, inflammation, and cancer: how intimate is the relationship?* Annals of the New York Academy of Sciences, 2009. **1171**: p. 59-76.

355. Regis, G., et al., *Ups and downs: the STAT1:STAT3 seesaw of Interferon and gp130 receptor signalling.* Seminars in cell & developmental biology, 2008. **19**(4): p. 351-9.

356. Seethala, R.R., et al., *Immunohistochemical analysis of phosphotyrosine signal transducer and activator of transcription 3 and epidermal growth factor receptor autocrine signaling pathways in head and neck cancers and metastatic lymph nodes.* Clinical cancer research : an official journal of the American Association for Cancer Research, 2008. **14**(5): p. 1303-9.

357. Bromberg, J.F., et al., *Stat3 as an oncogene.* Cell, 1999. **98**(3): p. 295-303.

358. Egloff, A.M. and J.R. Grandis, *Improving Response Rates to EGFR-Targeted Therapies for Head and Neck Squamous Cell Carcinoma: Candidate Predictive Biomarkers and Combination Treatment with Src Inhibitors.* Journal of oncology, 2009. **2009**: p. 896407.

359. Silva, C.M., *Role of STATs as downstream signal transducers in Src family kinase-mediated tumorigenesis.* Oncogene, 2004. **23**(48): p. 8017-23.

360. Boehm, A.L., et al., *Combined targeting of epidermal growth factor receptor, signal transducer and activator of transcription-3, and Bcl-X(L) enhances antitumor effects in squamous cell carcinoma of the head and neck.* Molecular pharmacology, 2008. **73**(6): p. 1632-42.

361. Fletcher, S., et al., *Molecular disruption of oncogenic signal transducer and activator of transcription 3 (STAT3) protein.* Biochemistry and cell biology = Biochimie et biologie cellulaire, 2009. **87**(6): p. 825-33.

362. Leeman-Neill, R.J., et al., *Guggulsterone enhances head and neck cancer therapies via inhibition of signal transducer and activator of transcription-3.* Carcinogenesis, 2009. **30**(11): p. 1848-56.

363. Leeman-Neill, R.J., et al., *Honokiol inhibits epidermal growth factor receptor signaling and enhances the antitumor effects of epidermal growth factor receptor inhibitors.* Clinical cancer research : an official journal of the American Association for Cancer Research, 2010. **16**(9): p. 2571-9.

364. Lui, V.W., et al., *Antiproliferative mechanisms of a transcription factor decoy targeting signal transducer and activator of transcription (STAT) 3: the role of STAT1.* Molecular pharmacology, 2007. **71**(5): p. 1435-43.

365. Zhang, C., et al., *Curcumin selectively induces apoptosis in cutaneous T-cell lymphoma cell lines and patients' PBMCs: potential role for STAT-3 and NF-kappaB signaling.* The Journal of investigative dermatology, 2010. **130**(8): p. 2110-9.

366. Zhang, X., et al., *Therapeutic effects of STAT3 decoy oligodeoxynucleotide on human lung cancer in xenograft mice.* BMC cancer, 2007. **7**: p. 149.

367. Zheng, Y., *Dbl family guanine nucleotide exchange factors.* Trends in biochemical sciences, 2001. **26**(12): p. 724-32.

368. Debreceni, B., et al., *Mechanisms of guanine nucleotide exchange and Rac-mediated signaling revealed by a dominant negative trio mutant.* The Journal of biological chemistry, 2004. **279**(5): p. 3777-86.

369. Haldar, S., et al., *The bcl-2 gene encodes a novel G protein.* Nature, 1989. **342**(6246): p. 195-8.

370. Low, B.C., et al., *Tyrosine phosphorylation of the Bcl-2-associated protein BNIP-2 by fibroblast growth factor receptor-1 prevents its binding to*

Cdc42GAP and Cdc42. The Journal of biological chemistry, 1999. **274**(46): p. 33123-30.

371. Low, B.C., K.T. Seow, and G.R. Guy, *The BNIP-2 and Cdc42GAP homology domain of BNIP-2 mediates its homophilic association and heterophilic interaction with Cdc42GAP.* The Journal of biological chemistry, 2000. **275**(48): p. 37742-51.

372. Werner, E. and Z. Werb, *Integrins engage mitochondrial function for signal transduction by a mechanism dependent on Rho GTPases.* The Journal of cell biology, 2002. **158**(2): p. 357-68.

373. Deshpande, S.S., et al., *Constitutive activation of rac1 results in mitochondrial oxidative stress and induces premature endothelial cell senescence.* Arteriosclerosis, thrombosis, and vascular biology, 2003. **23**(1): p. e1-6.

374. Radisky, D.C., et al., *Rac1b and reactive oxygen species mediate MMP-3-induced EMT and genomic instability.* Nature, 2005. **436**(7047): p. 123-7.

375. Suzuki, M., R.J. Youle, and N. Tjandra, *Structure of Bax: coregulation of dimer formation and intracellular localization.* Cell, 2000. **103**(4): p. 645-54.

376. Caponigro, F., M. Casale, and J. Bryce, *Farnesyl transferase inhibitors in clinical development.* Expert opinion on investigational drugs, 2003. **12**(6): p. 943-54.

377. Ayllon, V., et al., *Bcl-2 targets protein phosphatase 1 alpha to Bad.* Journal of immunology, 2001. **166**(12): p. 7345-52.

378. Maiuri, M.C., et al., *Functional and physical interaction between Bcl-X(L) and a BH3-like domain in Beclin-1.* The EMBO journal, 2007. **26**(10): p. 2527-39.

379. Hakoshima, T., T. Shimizu, and R. Maesaki, *Structural basis of the Rho GTPase signaling.* Journal of biochemistry, 2003. **134**(3): p. 327-31.

380. Torres, M. and H.J. Forman, *Redox signaling and the MAP kinase pathways.* BioFactors, 2003. **17**(1-4): p. 287-96.

381. Lu, G.D., et al., *Critical role of oxidative stress and sustained JNK activation in aloe-emodin-mediated apoptotic cell death in human hepatoma cells.* Carcinogenesis, 2007. **28**(9): p. 1937-45.

382. Pechtelidou, A., I. Beis, and C. Gaitanaki, *Transient and sustained oxidative stress differentially activate the JNK1/2 pathway and apoptotic phenotype in H9c2 cells.* Molecular and cellular biochemistry, 2008. **309**(1-2): p. 177-89.

383. Conde de la Rosa, L., et al., *Superoxide anions and hydrogen peroxide induce hepatocyte death by different mechanisms: involvement of JNK and ERK MAP kinases.* Journal of hepatology, 2006. **44**(5): p. 918-29.

384. Liu, S.L., et al., *Reactive oxygen species stimulated human hepatoma cell proliferation via cross-talk between PI3-K/PKB and JNK signaling pathways.* Archives of biochemistry and biophysics, 2002. **406**(2): p. 173-82.

385. Kanterewicz, B.I., L.T. Knapp, and E. Klann, *Stimulation of p42 and p44 mitogen-activated protein kinases by reactive oxygen species and nitric oxide in hippocampus.* Journal of neurochemistry, 1998. **70**(3): p. 1009-16.

386. Foley, T.D., et al., *Phenylarsine oxide binding reveals redox-active and potential regulatory vicinal thiols on the catalytic subunit of protein phosphatase 2A.* Neurochemical research, 2011. **36**(2): p. 232-40.

387. Nemani, R. and E.Y. Lee, *Reactivity of sulfhydryl groups of the catalytic subunits of rabbit skeletal muscle protein phosphatases 1 and 2A.* Archives of biochemistry and biophysics, 1993. **300**(1): p. 24-9.

388. Codreanu, S.G., et al., *Inhibition of protein phosphatase 2A activity by selective electrophile alkylation damage.* Biochemistry, 2006. **45**(33): p. 10020-9.

389. Whisler, R.L., et al., *Sublethal levels of oxidant stress stimulate multiple serine/threonine kinases and suppress protein phosphatases in Jurkat T cells.* Archives of biochemistry and biophysics, 1995. **319**(1): p. 23-35.

390. Rao, R.K. and L.W. Clayton, *Regulation of protein phosphatase 2A by hydrogen peroxide and glutathionylation.* Biochemical and biophysical research communications, 2002. **293**(1): p. 610-6.

391. Foley, T.D., J.J. Armstrong, and B.R. Kupchak, *Identification and H2O2 sensitivity of the major constitutive MAPK phosphatase from rat brain.* Biochemical and biophysical research communications, 2004. **315**(3): p. 568-74.

392. Foley, T.D., et al., *Oxidative inhibition of protein phosphatase 2A activity: role of catalytic subunit disulfides.* Neurochemical research, 2007. **32**(11): p. 1957-64.

393. Boota, A., et al., *Prenyltransferase inhibitors block superoxide production by pulmonary vascular smooth muscle.* American journal of physiology. Lung cellular and molecular physiology, 2000. **278**(2): p. L329-34.

394. Roy, A., et al., *Sodium phenylbutyrate controls neuroinflammatory and antioxidant activities and protects dopaminergic neurons in mouse models of Parkinson's disease.* PloS one, 2012. **7**(6): p. e38113.

395. Berndt, N., A.D. Hamilton, and S.M. Sebti, *Targeting protein prenylation for cancer therapy.* Nature reviews. Cancer, 2011. **11**(11): p. 775-91.

396. Hartwell, L.H., et al., *Integrating genetic approaches into the discovery of anticancer drugs.* Science, 1997. **278**(5340): p. 1064-8.

397. Stockwell, B.R., *Chemical genetics: ligand-based discovery of gene function.* Nature reviews. Genetics, 2000. **1**(2): p. 116-25.

398. Yang, W.S. and B.R. Stockwell, *Synthetic lethal screening identifies compounds activating iron-dependent, nonapoptotic cell death in oncogenic-RAS-harboring cancer cells.* Chemistry & biology, 2008. **15**(3): p. 234-45.

399. Weiwer, M., et al., *Development of small-molecule probes that selectively kill cells induced to express mutant RAS.* Bioorganic & medicinal chemistry letters, 2012. **22**(4): p. 1822-6.

400. Bittker, J.A., et al., *Screen for RAS-Selective Lethal Compounds and VDAC Ligands - Probe 1*, in *Probe Reports from the NIH Molecular Libraries Program*2010: Bethesda (MD).

401. Toledo, L.I., et al., *A cell-based screen identifies ATR inhibitors with synthetic lethal properties for cancer-associated mutations.* Nature structural & molecular biology, 2011. **18**(6): p. 721-7.

402. Kim, Y.W., et al., *Identification of novel synergistic targets for rational drug combinations with PI3 kinase inhibitors using siRNA synthetic lethality screening against GBM.* Neuro-oncology, 2011. **13**(4): p. 367-75.

403. Azorsa, D.O., et al., *Synthetic lethal RNAi screening identifies sensitizing targets for gemcitabine therapy in pancreatic cancer.* Journal of translational medicine, 2009. **7**: p. 43.

404. Ji, Z., et al., *Chemical genetic screening of KRAS-based synthetic lethal inhibitors for pancreatic cancer.* Frontiers in bioscience : a journal and virtual library, 2009. **14**: p. 2904-10.

405.	Whitehurst, A.W., et al., *Synthetic lethal screen identification of chemosensitizer loci in cancer cells.* Nature, 2007. **446**(7137): p. 815-9.

APPENDICES

LIST OF PUBLICATIONS

1. Rathiga Velaithan[*], **Jia Kang**[*], Jayshree L. Hirpara, Thomas Loh, Boon Cher Goh, Morgane Le Bras, Catherine Brenner, Marie-Veronique Clément and Shazib Pervaiz, *The small GTPase Rac1 is a novel binding partner of Bcl-2 and stabilizes its anti-apoptotic activity.* Blood, 2011. **117**: p. 6214-26.

   [*]**Both authors contributed equally to this study.**

2. Ivan Cherh Chiet Low, **Jia Kang** and Shazib Pervaiz, *Bcl-2: A prime regulator of mitochondrial redox metabolism in cancer cells.* Antioxidants & Redox Signalling, 2011. **15**: p. 2975-87.

3. **Jia Kang** and Shazib Pervaiz, *Mitochondria: redox metabolism and dysfunction.* Biochemistry Research International, 2012. **Epub Apr 24**.

LIST OF CONFERENCE ORAL & POSTER PRESENTATIONS

1. **Jia Kang**, Rathiga Velaithan, Jayshree L. Hirpara, Thomas Loh, Marie-V. Clément, Catherine Brenner and Shazib Pervaiz. *Identification of interaction of anti-apoptotic protein Bcl-2 with the small GTPase Rac1: A possible BH3 domain-mediated binding and regulation at the mitochondria.* **(Poster presentation)**

   17th Euroconference on Apoptosis (ECDO): Destruction, degradation and death. Cell death control in cancer and neurodegeneration. September 23rd-26th, 2009. Institut Pasteur, Paris, France.

2. **Jia Kang**, Rathiga Velaithan, Jayshree L. Hirpara, Thomas Loh, Catherine Brenner, Marie-Veronique Clément and Shazib Pervaiz. *Rac1 is a novel binding partner of the anti-apoptotic protein Bcl-2.* **(Poster presentation)**
   American Association for Cancer Research (AACR) 101st Annual Meeting. April 17th-21st, 2010. Walter E. Washington Convention Centre, Washington, D.C., United States of America.

3. **Jia Kang**, Rathiga Velaithan, Jayshree L. Hirpara, Thomas Loh, Boon Cher Goh, Morgane Le Bras, Catherine Brenner, Marie-Veronique Clément and Shazib Pervaiz. *The small GTPase Rac1 is a novel binding partner of Bcl-2 and stabilizes its anti-apoptotic activity.* **(Poster Presentation)**
   Gordon Research Conference: Mechanisms on Cell Signalling. July 31st-August 5th, 2011. Bates College, Lewiston, Maine, United States of America.

4. **Jia Kang**, Rathiga Velaithan, Jayshree L. Hirpara, Thomas Loh, Boon Cher Goh, Morgane Le Bras, Catherine Brenner, Marie-Veronique Clément and Shazib Pervaiz. *The small GTPase Rac1 is a novel binding partner of Bcl-2 and stabilizes its anti-apoptotic activity.* **(Oral Presentation)**

   2nd Mitochondria, Apoptosis and Cancer Conference. October 27th-29th, 2011. University Hall, National University of Singapore, Singapore.

5. **Jia Kang**, Shireen Vali, Shweta Kapoor, Taher Abbasi and Shazib Pervaiz. *STAT3 is a critical mediator of the pro-survival effect of Bcl-2-Rac1 interaction in human cancer cells.* **(Poster Presentation)**

   American Association for Cancer Research (AACR) 103rd Annual Meeting. March 31st- April 4th, 2012. McCormick Place, Chicago, Illinois, United States of America.